UNIVERSITY OF BIRMINGHAM

Project 1: Investigating the control of genetic crossover formation during meiosis in *Arabidopsis thaliana.*

and

Project 2: Investigating the regulatory effects of *N*-acyl-homoserine lactones and hormone networks on spore germination in the model bryophyte *Physcomitrella patens*.

by

Amy Whitbread

A combined research thesis submitted to The University of Birmingham as part requirement for the degree of Master of Research in Molecular and Cellular Biology.

University of Birmingham

School of Biosciences

August 2014

Summary

The following combined thesis consists of two research projects, carried out at the University of Birmingham. The first project analysed the control of meiotic crossovers in *Arabidopsis thaliana*. Recombinant proteins were produced for two key meiotic proteins, AtSHOC1 and AtASY1, for use in antibody-based immunological studies. Additionally, protein interactions were analysed between AtPCH2 and a number of axis-associated proteins, via yeast two-hybrid analysis. AtPCH2 was found to self-interact and interact with the AtSPO11-accessory protein, PRD3, as seen with the rice homologues. AtPCH2 did not interact with AtASY1, even following disrupted ATP hydrolytic activity by mutagenesis, as was reported for the orthologues in budding yeast. The results of this study therefore suggest that either the function of AtPCH2 may differ in *Arabidopsis* to that observed in yeast, or that AtASY1 may require phosphorylation or additional proteins to interact. This project contributes to understanding the control of meiotic recombination in plants, and ultimately contributes to efforts to ensuring food security.

The second project involved investigating the control of spore germination in *Physcomitrella patens.* The quorum-sensing signal molecules, *N*-acyl-homoserine lactones, were found to effect germination rates, with unsubstituted, long chain variants having more potent increasing effects overall. Additionally, increased germination rates in a DELLA-deficient mutant line, lacking the negative regulator of the gibberellin signalling pathway, were observed. This project thus provides novel data suggesting the presence of a DELLA-mediated GA signalling pathway in moss, controlling developmental processes, suggesting an earlier acquisition of this pathway during land plant evolution, than was previously believed.

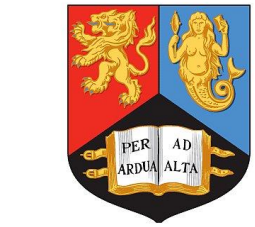

UNIVERSITY OF
BIRMINGHAM

Investigating the control of genetic crossover formation during meiosis in *Arabidopsis thaliana.*

by

Amy Whitbread

A thesis submitted to The University of Birmingham as part requirement for the degree of Master of Research in Molecular and Cellular Biology

School of Biosciences

University of Birmingham

Abstract

Homologous recombination results in the formation of novel combinations of alleles, during meiosis. AtSHOC1 is an XPF endonuclease related protein essential for the formation of class I crossovers. This study involves the generation of recombinant proteins for both AtSHOC1 and the axis-associated protein, AtASY1, for use in antibody-based immunological analyses. PCH2 is an ATPase thought to have a functional role in the regulation of meiotic crossover outcomes, however little is known regarding the molecular mechanisms of Pch2 function. In yeast, Pch2 binds and remodels Hop1, the AtASY1 orthologue, regulating Hop1 localisation. In this study, yeast two-hybrid analyses were carried out between AtPCH2 and key axis proteins. AtPCH2 was found to self-interact and interact with the AtSPO11-accessory protein, PRD3. AtPCH2 did not interact with AtASY1, even following disrupted ATP hydrolytic activity, shown to increase Pch2 and Hop1 interactions, in yeast. AtPCH2 may therefore perform an alternative function compared to that in yeast, or AtASY1 may require modification or additional proteins to interact. Understanding the control of recombination is of huge significance due to the beneficial impact this potentially has on increasing genetic variation available to plant breeders, contributing to efforts to ensure food security.

Acknowledgements

I would like to thank everyone that has helped me throughout the process of carrying out this project.

Firstly, I would like to express my gratitude to Professor Chris Franklin, for his exceptional supervision, continued support and for providing me with the opportunity to carry out such a profound research project, as part of an established research team.

Furthermore, I wish to thank Allan West and Christophe Lambing, for whom without, completion of this project would not have been possible due to their excellent supervision and patience, and for helping me gain confidence as a scientific researcher.

Additionally, I would like to thank Kim Osman and Ruth Perry for their support and guidance throughout completion of this project.

Table of Contents

List of Tables and Figures

Appendix 3.

List of Abbreviations

AD Vector	Plasmid encoding a fusion of the Gal4 activation domain
Ade	Adenine
AE	Axial element
ASY1	Asynaptic 1
At	*Arabidopsis thaliana*
AMP	Adenosine mono-phosphate
ATP	Adenosine tri-phosphate
BLAST	Basic Local Alignment Search Tool
BSA	Bovine Serum Albumin
CRC1	Central Region Component 1
CO	Crossover
C-terminal	Carboxyl-terminal
ddH_2O	Double deionized water
D-loop	Displacement loop
DMC1	Disruption of meiotic control 1
DMSO	Dimethyl sulfoxide
DNA	Deoxyribonucleic Acid
DNA-BD Vector	Plasmid encoding a fusion of the Gal4 DNA-binding domain
dNTP	Deoxynucleotide Triphosphate
DDO	Double Dropout
dHj	Double Holliday junction
DSB	Double-strand break
ECL	Enhanced chemiluminescence
GST	Glutathione S-Transferase
H2AX	Histone variant H2AX
His	Histidine
Hop1	Homologue pairing 1
HORMA	Common structural domain found in Hop1p, Rev7p and MAD2
IPTG	Isopropyl β-D-1-thiogalactopyranoside
LB	Lysogeny Broth
Leu	Leucine
LE	Lateral Element

MLH1	MutL homologue 1
MLH3	MutL homologue 3
MSH4	MutS homolog 4
MSH5	MutS homolog 5
MUS81	MMS and UV sensitive 81
NCBI	National Centre for Biotechnology Information
NCO	Non-crossover
NEB	New England Biolabs
N-terminal	Amino-terminal
O/N	Overnight
PAIR1	Homologous Pairing Aberration in Rice Meiosis 1
PBS	Phosphate buffered saline
PCR	Polymerase Chain Reaction
PTD	ParTing Dancer
QDO	Quadruple Dropout
RBR	Retinoblastoma Protein
RMI1	RecQ mediated genome instability 1
RPA	Replication protein A
rpm	Revolutions per minute
SEI	Single-end invasion
SC	Synaptonemal complex
SCC	Sister-chromatid cohesion
SD	Synthetically defined
SDSA	Synthesis-dependent strand annealing
SDS-PAGE	Sodium-dodecyl-sulfate polyacrylamide gel electrophoresis
SDW	Sterile Distilled Water
SHOC1	Shortage in Chiasma 1
SMC	Structural Maintenance of Chromosome
S-phase	Synthesis-phase
SPO11	Sporulation specific protein 11
ssDNA	Single stranded DNA
T-DNA	Transfer DNA
TDO	Triple Dropout
TF	Transverse filament
Trp	Tryptophan

Y2H	Yeast Two-Hybrid
YPDA	Yeast extract, peptone, glucose, adenine hemisulfate
ZYP1	Synaptonemal complex protein 1

Introduction

The global population is estimated to increase by 2 billion by 2050, highlighting the need to enhance food production to ensure increasing food demand is met. Arable land and space is limited, owing to the importance to generate sustained improvements in crop yield. Moreover, inevitable adverse effects associated with climate change have further heightened the importance of improving crop yields (reviewed in Chakraborty & Newton 2011). As a result, ensuring food security has emerged as a crucial target for the 21st century whereby considerable efforts are being made.

One such effort of crop improvement is that regarding classical breeding. Genetic variation permits adaptation to changing environments and emerging pressures via natural selection. Therefore, plant breeding efforts whereby artificial selection is harnessed to produce beneficial varieties, plays a crucial part regarding food security. An example of this can be seen with the attempts to establish a method by which breeders could select sugar beet (*Beta vulgaris* L.) lines with increased drought tolerance (Ober *et al.* 2005). The amount and distribution of rainfall presents a limiting factor on sugar beet yield in the UK, which is predicted to have an increased impact following estimated climate change models. Hence, the utilisation of genetic variation to generate sugar beet with drought-tolerance would prove invaluable to ensuring sustained productivity, thus contributing to food security efforts.

Homologous recombination during meiosis allows for the generation of genetic variation by the production of novel combinations of alleles which confer new

phenotypes. Such phenotypes could prove advantageous to crop breeders by allowing for enhanced performance and increased yield. Consequently, an important contribution to ensure food security includes fundamental research in an attempt to understand the molecular control mechanisms underlying homologous recombination during meiosis, in plants. An understanding of the control of meiotic recombination could potentially provide breeders with increased genetic variation, via the modification of recombination in crops.

Developments in microscopy techniques have permitted direct observations of the segregation of chromosomes during meiosis in a number of organisms, providing beneficial insights into chromosome behaviour and organisation during meiotic events. Nevertheless, an understanding of the molecular mechanisms underpinning the control of meiotic recombination has only recently emerged, with studies in *Saccharomyces cerevisiae* (budding yeast) playing a prominent role. These along with studies in a diverse range of eukaryotes, have provided insights into meiosis, particularly with regards to the formation of meiotic crossovers (COs) (reviewed in Osman *et al*. 2011).

Introduction to Meiosis

Meiosis is a specialised type of cell division that forms the basis of sexual reproduction within eukaryotic organisms. Meiosis is comprised of chromosome duplication, via a single round of DNA replication, followed by meiosis I and meiosis II, two sequential nuclear divisions, which subsequently result in the formation of four recombined haploid gametes (Fig.1). Meiosis I and meiosis II, referred to as the reductional and equational divisions respectively, are essential in the restoration of zygote chromosome number, enabling stable chromosome complements over generations (Hochwagen 2008).

Meiosis I and meiosis II are divided into four cytogenetically distinct stages – prophase, metaphase, anaphase and telophase. Meiosis I consists of the separation of homologous chromosomes, resulting in a reductional division whereby chromosome number is halved. Furthermore, homologous recombination and thus the formation of new combinations of alleles, occurs during prophase I of meiosis I, following the reciprocal exchange of genetic information between two homologous chromosomes.

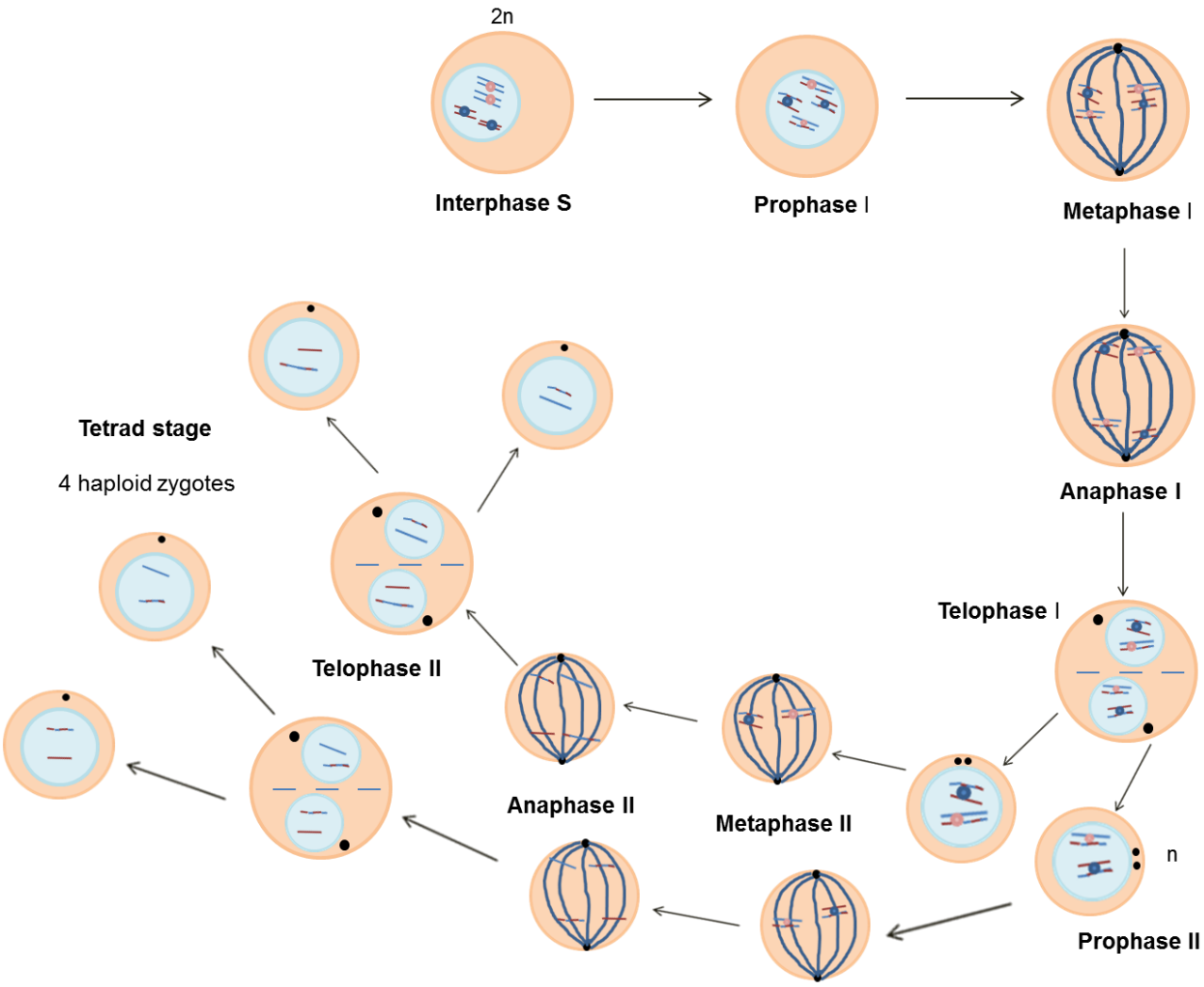

Figure 1. Schematic representation of meiosis. Prior to meiosis, DNA replication occurs. Prophase I of meiosis I consists of pairing between homologous chromosomes and subsequent synapsis. Homologous recombination occurs between homologue pairs producing reciprocal exchange of genetic information. During metaphase 1, the homologous chromosomes remain associated at the chiasma sites and align on the metaphase plate, with their separation taking place during anaphase I. Telophase I involves the dyad stage where two haploid cells with attached sister chromatids are formed. Meiosis I is followed by an equational division in meiosis II whereby separation of the sister chromatids occurs to form the tetrad stage of four recombined haploid gametes.

The Meiotic Pathway

S-phase: sister chromatid cohesion

The synthesis-phase (S-phase) constitutes to the period of DNA replication that occurs at the same time or shortly after the initiation of meiosis. An integral aspect of this phase is the establishment of cohesion between newly synthesised sister chromatids (Uhlmann & Nasmyth 1998). Sister-chromatid cohesion is an essential prerequisite for accurate chromosome segregation by allowing for the biorientation of chromosomes on the meiotic spindle (Nasmyth 2001).

Homologous kinetochores attach to microtubules emanating from opposite poles. Cohesion maintains the association between homologous chromosomes, despite forces attempting to pull them apart (Reider & Salmon 1998; Klein *et al.* 1999). The tension generated as a result of these counteracting forces provides the signal that homologous kinetochores are biorientated (Haering *et al.* 2002). Cohesion between sister chromatids is removed following two individual events (Reider & Cole 1999; van Heemst & Heyting 2000; Page & Hawley 2003; Petronczki *et al*. 2003). Cohesion along the chromosome arms is removed during the metaphase-anaphase transition during meiosis I, allowing for the disjunction of homologous chromosomes during anaphase I. During anaphase II, the centromeric cohesion between sister chromatids is removed resulting in their segregation towards opposite poles of the cell (Lee & Orr-Weaver 2001).

Sister-chromatid cohesion is generated by the action of at least four highly conserved proteins, which form the meiotic cohesin complex, REC8, STAG3, SMC1 and SMC3

(Molnar *et al.* 1995; Prieto *et al*. 2001; Gruber *et al*. 2003). In *Arabidopsis*, AtSYN1 and ATSCC3 have been identified as the cohesins required for sister-chromatid cohesion (Bai *et al.* 1999; Cai *et al*. 2003; Chelysheva *et al.* 2005). Assembly and disassembly of cohesin, and therefore the regulation of this complex, is achieved via the action of numerous accessory proteins. Loading of cohesin onto chromatin involves the action of the adherin, AtSCC2, in *Arabidopsis* (Sebastian *et al.* 2009). AtSGO1 is the shugoshin homologue essential for maintaining cohesion at the centromeres, preventing premature sister chromatid separation during meiosis I (Zamariola *et al.* 2013).

Defects regarding sister-chromatid cohesion result in aneuploidy and therefore subsequent improper reproductive growth, seen via cytological analysis of *A.thaliana syn1* (*rec8* homologue) mutants, highlighting the importance of cohesion and correct segregation (Bai *et al*. 1999).

G2: proteinaceous axis formation

The elaboration of a proteinaceous axial structure occurs during the latter stages of interphase in G2 (Kleckner 1999). The structure is formed along the chromatids, from which chromatin loops emanate, forming a loop-array organisation (Fig.2) (Kleckner 1999). This structure, known as the axial element (AE), possibly persists until mid-prophase I, enabling subsequent steps to take place (Kleckner 2006).

Meiosis I: the reductional division

Prophase I is divided into five cytologically prominent substages: leptotene, zygotene, pachytene, diplotene and diakinesis. Prophase I is the longest stage of meiosis, with studies showing it takes 30h in *A.thaliana,* with the whole of meiosis being completed within 33h (Armstrong *et al.* 2003), although this varies between species.

Pairing and movement of homologous chromosomes.

Pairing between homologous chromosomes is imperative, during early prophase I, in order for correct chromosome segregation (Tiang *et al*. 2012). In eukaryotes, chromosomes are arranged in the RabI-orientation, prior to meiosis. This configuration consists of centromere clustering near one pole of the nucleus, with the chromosomes arms extending towards the opposite pole, arranged in parallel (Tiang *et al.* 2012). Progression into prophase I is accompanied by chromosome movements leading to the formation of the characteristic ‘bouquet’ configuration. This arrangement of chromosomes is observed in a range of organisms (Loidl 1990; Zicker & Kleckner 1999; Scherthan 2001) and is characterised via the formation of a polarized organisation with chromosomes bundled at their telomeres (Ding *et al.* 2004). The bouquet arrangement is thought to facilitate homologous pairing of chromosomes by bringing the pairs of homologous chromosomes into close proximity (Bass *et al.* 2000). Due to the significant changes in telomere organisation within the nucleus, telomeres are thought to play an important role in homologous chromosome pairing (Link *et al.* 2014).

Studies in *Schizosaccharomyces pombe* (fission yeast) have led to the proposed model in which chromosomes are aligned along their length, with their telomeres clustered beneath the nuclear envelope near the microtubule organizing centre (MTOC). Subsequent nuclear oscillations enable chromosomal movements which allow for homologue search and recognition and thus homologue pairing (Ding *et al.* 2004). This model has been supported by numerous studies (Shimanuki *et al*. 1997; Cooper *et al*. 1998; Nimmo *et al*. 1998; Yamamoto *et al*. 1999; Chikashige & Hiraoka 2001; Kanoh & Ishikawa 2001), providing evidence that telomere clustering and nuclear movements facilitate pairing of homologous chromosomes, highlighting its importance for homologous recombination.

Telomere clustering has been demonstrated to be a ubiquitous aspect of chromosome behaviour during meiosis, however the degree and timing of this phenomenon is known to vary between species. An example of this can be seen in *A.thaliana*, whereby the classical bouquet configuration of telomeres is replaced by nucleolus-associated clustering that is established prior to meiosis and remains through to early-mid leptotene. Consequently, the pairing of telomeres and thus homologue pairing is initiated earlier in *A.thaliana* than in other eukaryotic species, due to the utilisation of a pre-existing arrangement (Armstrong *et al.* 2001).

Although observed early in some species, such as onion (Church & Moens 1976), centromere pairing is not evident in *A.thaliana* until zygotene (Armstrong *et al.* 2001). This led to the proposal that centromeric pairing may aid in the removal of unwanted chromosomal connections via rapid telomere-led chromosome movements that occur during midprophase (Lee *et al*. 2012).

In *Caenorhabditis elegans,* pairing centres (PCs) located at subtelomeric regions on each chromosome, comprised of heterochromatic repeats, have been implicated in homologous chromosome recognition (MacQueen *et al.* 2005). PCs are attached to the nuclear envelope via a nuclear membrane spanning complex of SUN/KASH proteins, indirectly linking PCs to cytoskeletal microtubules (Hiraoka & Dernburg 2009). Interactions with the dynein motor protein, via the KASH protein ZYG-12, aid in the separation of non-homologous pairing, thus promoting homologous chromosome pairing (discussed in Osman *et al.* 2011). SUN domain orthologues have been identified in *A.thaliana* (Graumann *et al*. 2009), implicating a similar mechanism for the telomere-led chromosome movements observed.

Synapsis of Homologous Chromosomes

Homologous chromosomes are juxtaposed in an intimate association following homologous pairing, enabling the formation of the synaptonemal complex (SC) along the entire chromosome lengths (Moses 1968; von Wettstein *et al*.1984). The SC is a highly conserved proteinaceous structure assembled during zygotene, owing to the stabilisation of homologue pairing and hence facilitating recombination events that are concurrently taking place (reviewed in Page & Hawley 2004).

DNA double-strand breaks (DSBs) are generated within the chromatin loops during the G2/leptotene transition, following association of the loops with the axes.

A minority of these inter-axis bridges mature into axial associations, during leptotene (Albini & Jones 1987; Rockmill *et al*. 1995; Tesse *et al*. 2003). These subsequently nucleate and denote the formation of the SC and thus synapsis of homologous

chromosomes, during zygotene. Axial elements are hence incorporated into the SC tripartite structure as a component of the paired homologous lateral elements (LEs) that are cross-linked by transverse filaments (TFs) spanning the central region (Fig.2) (Heyting 1996; Zickler & Kleckner 1999). Assembly of the SC progresses throughout zygotene, occurring in a zipper-like manner, with fully synapsed bivalents being prevalent by pachytene.

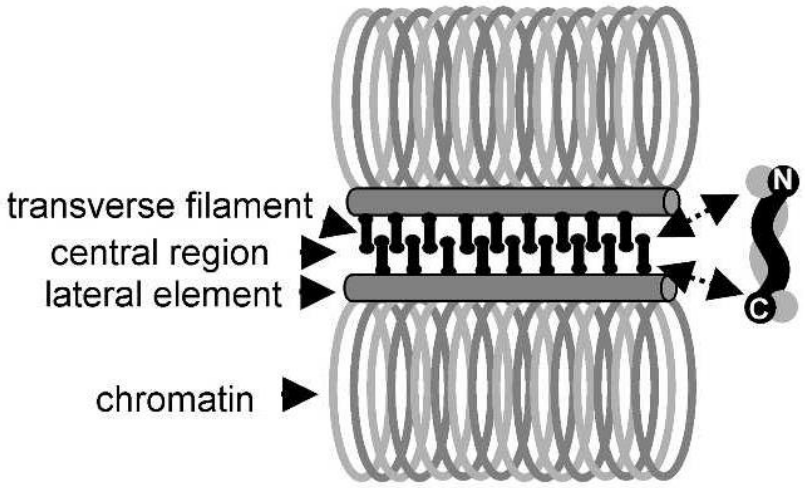

Figure 2. [Reproduced from Higgins *et al.* (2005)]. Dual loop organization and the structure of the synaptonemal complex. Schematic representation of the dual-loop organization of sister chromatids, whereby parallel sets of loops are aligned and anchored along a linear proteinaceous axis. Model also shows the structure of the SC, depicting the organization of the TFs, with their C termini associated with the LEs and the opposing dimers' N termini overlapping in the central region, forming parallel homodimers.

In a number of organisms, genes encoding components of the SC have been identified, implicated in SC formation. The ZMM protein, Zip1, in budding yeast, has been identified as the TF component of the SC that polymerizes along aligned LEs during zygotene (Sym *et al*. 1993). This coiled-coil protein localizes along the entire

length of synapsed homologous chromosomes during pachytene. Furthermore, *zip1* mutants were shown to be defective in synapsis, although homologous pairing and AE formation still took place (Sym *et al.* 1993). In the absence of DSBs, a proportion of Zip1 associates with the centromeres (Tsubouchi & Roeder 2005), hence suggesting homolog pairing is dependent upon this centromeric interaction. ZYP1a and ZYP1b are two partially redundant proteins, collectively referred to as ZYP1, which were identified as the Zip1 orthologues in *A.thaliana* (Higgins *et al.* 2005). ZYP1 localisation during the leptotene/zygotene transition has been shown to depend on the formation of DSBs. This coincides with previous studies which indicated that centromeres were not required for homolog pairing in *Arabidopsis*, which is telomere-led (Armstrong *et al.* 2001).

Hop1 is a DNA-binding protein that contains a HORMA domain that associates with the chromosome axes in budding yeast, and is therefore an integral component of the SC (Hollingsworth & Byers 1989). ASY1 was identified as the functional *A.thaliana* homologue of Hop1, with this protein being required for the synapsis of homologous chromosomes (Caryl *et al*. 2000). This is evident by the asynaptic phenotype displayed by *asy1* mutants (Ross *et al*. 1997). Prior to chromosome axis formation, AtASY1 is shown to associate with chromatin. With the progression into leptotene, and therefore the formation of the axes, ASY1 localises to the chromatin loop in which is in close proximity to the AEs (Armstrong *et al*. 2002).

Following the completion of homologous recombination during pachytene, desynapsis of the paired homologous chromosomes occurs during late prophase I (diplotene), with the SC being fully disassembled by diakinesis (Heyting 1996).

There is much discrepancy regarding the real functional role of the SC, however this evolutionarily conserved structure is proposed to be fundamental for the homologous recombination events that take place during meiosis.

Meiotic Recombination: Meiotic DNA Double-Strand Break Formation

Studies in budding yeast have provided much insight into the mechanisms that underpin meiotic recombination in meiosis. The formation of DSBs, during leptotene, denotes the onset of meiotic recombination. SPO11, a conserved topoisomerase II-related transesterase, catalyses programmed-DSB formation and remains covalently attached to the 5'-ends on either side of each DSB site (Keeney *et al*. 1997). In *Arabidopsis,* three paralogues of SPO11 have been identified, AtSPO11-1, AtSPO11-2 and AtSPO11-3 (Grelon *et al.* 2001; Hartung & Puchta 2001), although only AtSPO11-1 and AtSPO11-2 are required for DSB formation, thought to act non-redundantly as a heterodimer (Grelon *et al.* 2001; Stacey *et al.* 2006; Sanchez-Moran *et al.* 2007). In budding yeast, a number of accessory proteins have been identified as essential for the initiation of meiotic recombination (reviewed in Cole *et al*. 2010), however, functional homologues of these proteins have yet to be identified in *Arabidopsis* (Keeney *et al.* 1997). Nevertheless, DSB formation in *Arabidopsis* has been found to require the activity of the three proteins AtPRD1, AtPRD2 and AtPRD3 (De Muyt *et al.* 2007; De Muyt *et al.* 2009). AtPRD2 directly binds to chromosomes to promote DSB formation, whilst AtPRD1 has been shown to interact directly with AtSPO11, suggesting it functions in partnership with the DSB formation catalyst (reviewed in Osman *et al*. 2011). AtPRD3, on the other hand, has been shown to link break complexes to the axis via interaction with AtASY1 (Osman *et al*. 2011).

Meiotic Recombination: Double-Strand Break Processing

Following DSB formation, a DNA repair process is initiated which is facilitated by the phosphorylation of the histone variant, H2AX, over regions surrounding DSBs (Fernandez-Capetillo *et al*. 2003; Shroff *et al.* 2004). SPO11 remains covalently attached to the 5'-DNA end on either side of the DSB. Subsequently, strand resection of the 5' ends occurs, alongside SPO11 removal, resulting in the formation of 3' single stranded DNA (ssDNA). This process is mediated by the MRE11-RAD50-XRS2/NBS1 complex acting in conjuction with COM1/SAE2 in budding yeast (Mimitou & Symington 2009). SPO11 is released from the DSB ends following endonucleolytic cleavage on either side of the DSB site (Neale *et al*. 2005). AtMRE11 and AtRAD50 interact *in-vitro* (Daoudal-Cotterell *et al.* 2002) and are involved in DNA repair in *Arabidopsis*, therefore owing to the conservation of the MRX/N complex in end processing (Gallego *et al*.2001; Bundock & Hooykaas 2002; Bleuyard *et al.* 2004; Puizina *et al.* 2004). In addition to this, NBS1 (Akutsu *et al.* 2007; Waterworth *et al*. 2007) and COM1 orthologues have been identified in the *Arabidopsis* genome (Uanschou *et al.* 2007). Although the precise mechanisms of DSB processing have not been fully resolved, it is thought that both MRE11 and COM1/SAE2 are required for sufficient endonuclease cleavage to permit strand resection and therefore homologous recombination (reviewed in Osman *et al*. 2011).

Meiotic Recombination: Strand Invasion and Exchange

The RecA-related recombinases, RAD51 and DMC1, form nucleoprotein presynaptic filaments on 3'ssDNA tails. Following homology searches, single end invasion occurs resulting in the formation of joint molecules, implemented in the initiation of strand

exchange (Bishop & Zickler 2004). An *A.thaliana* DMC1 orthologue has been identified, along with six RAD51 paralogues, of which only three have been shown to be essential for meiotic recombination: AtRAD51, AtRAD51C and AtXRRC3 (reviewed in Osman *et al*. 2011). *Atrad51* mutant is infertile due to a lack of AtSPO11-induced DSB repair ability (Li *et al*. 2004), with RAD51 being shown to repair DSBs using the sister chromatid as a template (Siaud *et al*. 2004). On the other hand, random segregation of univalents at anaphase I was observed in *Atdmc1* mutants, demonstrating the role of this protein in inter-homologue recombination (Couteau *et al*. 1999). It has been proposed that RAD51 and DMC1 coordinate their functions as a means to promote inter-homologue recombination, thus ensuring genetic variation (Bishop 1994), with RAD51 possibly acting to catalyse the activity of DMC1 (Cloud *et al*. 2012). Immunolocalisation studies in *A.thaliana* early prophase I chromosome spreads indicated that AtRAD51 and AtDMC1 form doublets which were seen to co-localise with γH2AX foci. Therefore, it can be said that nucleoprotein filaments comprised of either AtRAD51 or AtDMC1 flank DSBs. Furthermore, DSB repair carried out by AtDMC1-coated nucleoprotein filaments is thought to be mediated by the axis protein AtASY1, in order to promote inter-homologue recombination over the use of the sister-chromatid as a template (Sanchez-Moran *et al.* 2007; Kurzbauer *et al*. 2012).

A number of accessory proteins are thought to mediate strand exchange protein assembly in budding yeast. One such accessory protein is Replication Protein A (RPA), which is essential for the formation of nucleofilaments via its ability to remove secondary structures within the DNA allowing for the assembly of RAD51 onto the 3'-ended ssDNA. Incorrect RAD51-mediated strand exchange is proposed to be

prevented following the coating of ssDNA by RPA (discussed in San Filippo *et al.* 2008). Strand invasion has also been shown to be promoted by the MND1/HOP2 complex (Chi *et al*. 2007), that is known to interact with both RAD51 and DMC1 in *A.thaliana* in immunoprecipitation studies (Kerzendorder 2006; Vignard *et al*. 2007). This complex is thought to enable homology searching and subsequent strand invasion, coinciding with RAD51 and DMC1 activity (Tsubouchi & Roeder 2002), stabilising the presynaptic filament whilst also promoting DNA duplex capture (reviewed in Osman *et al*. 2011).

Single-end invasion of the RAD51/DMC1-containing nucleoprotein filament occurs following a homology search, whereby the filament invades the intact duplex, displacing complementary ssDNA from the donor strand. Polymerisation of the invading strand occurs, causing the formation of a recombination intermediate structure known as the 'displacement loop' (D-loop) (reviewed in Bishop & Zickler 2004), the fate of which results in either a crossover (CO) or non-crossover (NCO) event.

Meiotic Recombination: Pathways to Crossover Formation

In a vast majority of species, including plants, ~5% of DSBs result in the formation of genetic COs, thus resulting in the reciprocal exchange of genetic information. However, a large proportion of single-end invasions are repaired via DNA synthesis mechanisms, resulting in a NCO event (Barakate *et al.* 2014). This repair pathway is referred to as synthesis-dependent strand annealing (SDSA) (Fig.3) (Allers & Lichten 2001).

Following strand invasion, the stable intermediate single end invasion (SEI) is formed as a result of the invading strand in the D-loop interacting with the intact duplex. Association of the second invading strand with the donor duplex occurs resulting in DNA synthesis allowing for the joining of the newly synthesised 3'end DNA with the resected 5' ends. As a result of this, a stable DNA intermediate is formed known as the double Holliday junction (dHJ) (Holliday 1964), the resolution of which leads to CO formation (reviewed in Bishop & Zickler 2004).

Chiasmata are the physical manifestations of the reciprocal exchange of genetic information and thus the result of COs. Therefore, in addition to increasing genetic diversity, COs ensure accurate chromosome disjunction by allowing for the vital physical connection between homologous chromosomes, owing to the importance of CO events in meiosis (Jones & Franklin 2006). CO assurance has been observed in most species, whereby at least one obligate CO per chromosome pair is ensured (Jones 1984; Jones & Franklin 2006; Shinohara *et al.* 2008). CO homeostasis is carried out in order to ensure an obligate CO, by the maintenance of COs being favoured at the expense of NCOs (Martini *et al.* 2006). The control of CO events is therefore tightly regulated in many species, including *A.thaliana,* where it has been observed that each of the 5 chromosome pairs always receives an obligate CO, with wild-type showing 8-12 chiasmata per nucleus (Higgins *et al*. 2004).

Studies in budding yeast led to the development of the early decision model of meiotic recombination, suggesting an early time point for the CO/NCO decision (reviewed in Osman *et al.* 2011). It is proposed that prior to the establishment of a stable SEI intermediate, the fate of individual DSBs to proceed via the CO/NCO route

is determined, with the imposition of this fate coordinating with SC formation (Barakate *et al.* 2014).

Two alternative CO formation pathways coexist in most eukaryotes, resulting in class I and class II COs (Fig.3) (Börner *et al.* 2004).

Pathways to Crossover formation: Class I Crossovers

The Class I crossover pathway is the major pathway accounting for ~85% of the total number of meiotic COs in *A.thaliana.* The formation of Class I COs is dependent upon a series of recombination proteins, collectively referred to as ZMMs (the zipper proteins: ZIP1, ZIP2, ZIP3 and ZIP4, MER3 (Meiotic Recombination 3) and the MutS homologoues: MSH4 and MSH5) and on the MLH1-MLH3 heteroduplex, first identified in budding yeast (Börner *et al.* 2004; discussed in Lynn *et al.* 2007). These proteins are conserved in a wide range of eukaryotes, with putative homologues also identified in *Arabidopsis* (reviewed in Osman *et al.* 2011). MSH4 and MSH5 have a fundamental role regarding the promotion of CO formation (Ross-MacDonald & Roeder 1994; Zalevsky *et al*. 1999). These proteins have been shown to form a dimer which binds to the cores of dHJs and other recombination DNA intermediates, such as D-loops, stabilising single-end invasion via a sliding clamp mechanism. Conversion of intermediates into dHJs and subsequent resolution of dHJs by nucleases is therefore promoted by the embracing of duplex DNA by the dimer (Snowden *et al.* 2004). In yeast, the *msh5* mutant phenotype supported the role of this protein, as no apparent dHJs or COs were observed (Börner *et al.* 2004). MSH4 and MSH5 orthologues have been found to be encoded by the *A.thaliana* genome (Higgins *et al*. 2004; Higgins *et al.* 2008a). Immunolocalisation studies revealed a

significant decrease in AtMSH5 foci localisation to chromosomes from zygotene to pachytene, possibly indicating recombination intermediates carry out additional functions as well as CO formation (Higgins *et al*. 2008b). On the other hand, the retinoblastoma protein, RBR, whose mutant phenotype displays a reduction in CO formation, is thought to be required for normal localisation of AtMSH4 (Chen *et al*. 2011). The Class I CO formation pathway is sometimes referred to as the MSH4-dependent pathway.

The TF protein, Zip1, known to play a fundamental role in SC formation, has also been shown to be involved in CO formation in budding yeast, as a ZMM (Storlazzi *et al.* 1996; Borner *et al.* 2004). A reduction of CO formation observed in *zip1* mutants in budding yeast, *Arabidopsis* and Barley (Börner *et al*. 2004; Higgins *et al.* 2005; Barakate *et al.* 2014), along with the fact that the appearance of AtZYP1 foci coincides with that of AtMSH4/AtMSH5, prior to SC formation, led to the suggestion that Zip1 is involved in the control of CO formation.

Shortage in Chiasmata 1 (SHOC1) is an *Arabidopsis* gene epistatic to the *Arabidopsis* ZMMs, of which mutants display a similar phenotype to other *A.thaliana* ZMM mutants (discussed in Osman *et al*. 2011), with a significant reduction in CO formation (Mascaisne *et al.* 2008). AtSHOC1 is required for the Class I CO formation, identified to act in the same pathway as AtMSH5 following double mutant analysis (Higgins *et al*. 2008a). AtSHOC1 is an XPF endonuclease related protein thought to be involved in the maturation of DNA intermediates, resulting in CO formation (Mascaisne *et al*. 2008). SHOC1 homologs have been identified in a number of eukaryotes, with this protein showing similarity to the yeast ZMM protein Zip2 (Chua

& Roeder 1998). XPF-related endonucleases are involved in branched-DNA structure recognition and processing, therefore owing to the resolution of recombination intermediates, such as dHJs. XPF proteins form a heterodimer with an ERCC1 protein in order to function in somatic DNA repair. AtPDT (ParTing Dancer) is an *Arabidopsis* specific protein which shares sequence similarity with the ERCC1 protein family and has been shown to play a role in meiotic recombination (Wijeratne *et al.* 2006). AtSHOC1 has been shown to interact *in-vitro* with AtPTD, allowing for the assumption to be made that SHOC1 and PTD form an XPF-ERCC1-like heterodimer in *Arabidopsis* that is required for the formation of class I COs, possibly by the resolution of dHJs (Macaisne *et al.* 2011).

Dissolution is the alternative way to process recombination intermediates, leading to NCOs. This mechanism is carried out in eukaryotes by the RTR complex comprised of a RecQ helicase, a type1A topoisomerase and the structural protein RMI1 (Thaler, & Stahl 1988; Bonnet *et al.* 2013).

Class I COs are sensitive to CO interference whereby the occurrence of one CO-designation interferes with the occurrence of another nearby CO-designation, resulting in CO patterning where COs tend to be evenly spaced. This phenomenon was first identified in *Drosophila* (King & Mortimer 1990), with the formulation of a number of models trying to account for a plausible explanation to decipher the reasons as to why and how it occurs. Such models include the polymerization model (King & Mortimer 1990), the counting model (Foss *et al.* 1993; Lande & Stahl 1993) and the mechanical stress model (Kleckner *et al*. 2004). The mechanical stress model illustrates the macroscopic mechanical properties of chromosomes enabling

the accumulation, relief and redistribution of stress, with the formation of COs redistributing mechanical stress at certain regions (Kleckner *et al.* 2004; Börner *et al.* 2004). This theory can be qualitatively modelled by analogy with a beam-film model, which is a known physical system that displays analogous behaviour (Kleckner *et al.* 2004; discussed in Zhang *et al.* 2014). The promotion of the formation of widely spaced COs by CO interference, along with CO homeostasis and interhomologue bias, a process which ensures DSBs are preferentially repaired using a homologue instead of a sister, are meiotic regulatory mechanisms that act in coordination to confer CO assurance and thus the formation of at least the obligate CO. Pachytene Checkpoint 2 (PCH2) is a hexameric ring ATPase, with homologs in a range of organisms, including *Arabidopsis* (Chen *et al*. 2013; Miao *et al.* 2013). Mutant phenotypes include defective interhomologue repair bias, timely progression of recombination, elevated CO levels and defects in CO interference, thus indicating a role for PCH2 in the regulation of meiotic CO outcomes (Börner *et al.* 2008; Joshi *et al*. 2009; Zanders & Alani 2009; Zanders *et al*. 2011; Ho & Burgess 2011; Farmer *et al*. 2012). PCH2 has been shown to bind to and remodel the axial component Hop1, the budding yeast ASY1 homologue, in the presence of ATP, displacing it from DNA thus regulating Hop1 binding (Chen *et al.* 2013). In budding yeast, Zip1 is loaded in response to pre-existing Hop1 pattern during zygotene, which confers CO placement (Börner *et al.* 2008). PCH2 promiscuously removes loaded Hop1 from the chromosome axis, by physically interacting with the protein. The maintenance of differential Hop1 localization is critical for the promotion of interhomologue repair at CO designation sites (Chen *et al*. 2013).

Pathways to Crossover formation: Class II Crossovers

Class II COs represent only 5-10% of COs in *A.thaliana* which arise from a second pathway of CO formation (Mercier *et al*. 2005). This pathway is independent of the ZMM proteins and requires the activity of the MUS81-EME1 heteroduplex (reviewed in Osman *et al.* 2011). Class II COs differ to Class I COs by the fact that the Class II pathway is independent of MSH4, and therefore has different genetic requirements, and by the fact that this pathway is not sensitive to CO interference, resulting in an uneven CO distribution in comparison to Class I CO distribution (Berchowitz *et al.* 2007; Berchowitz & Copenhaver 2010).

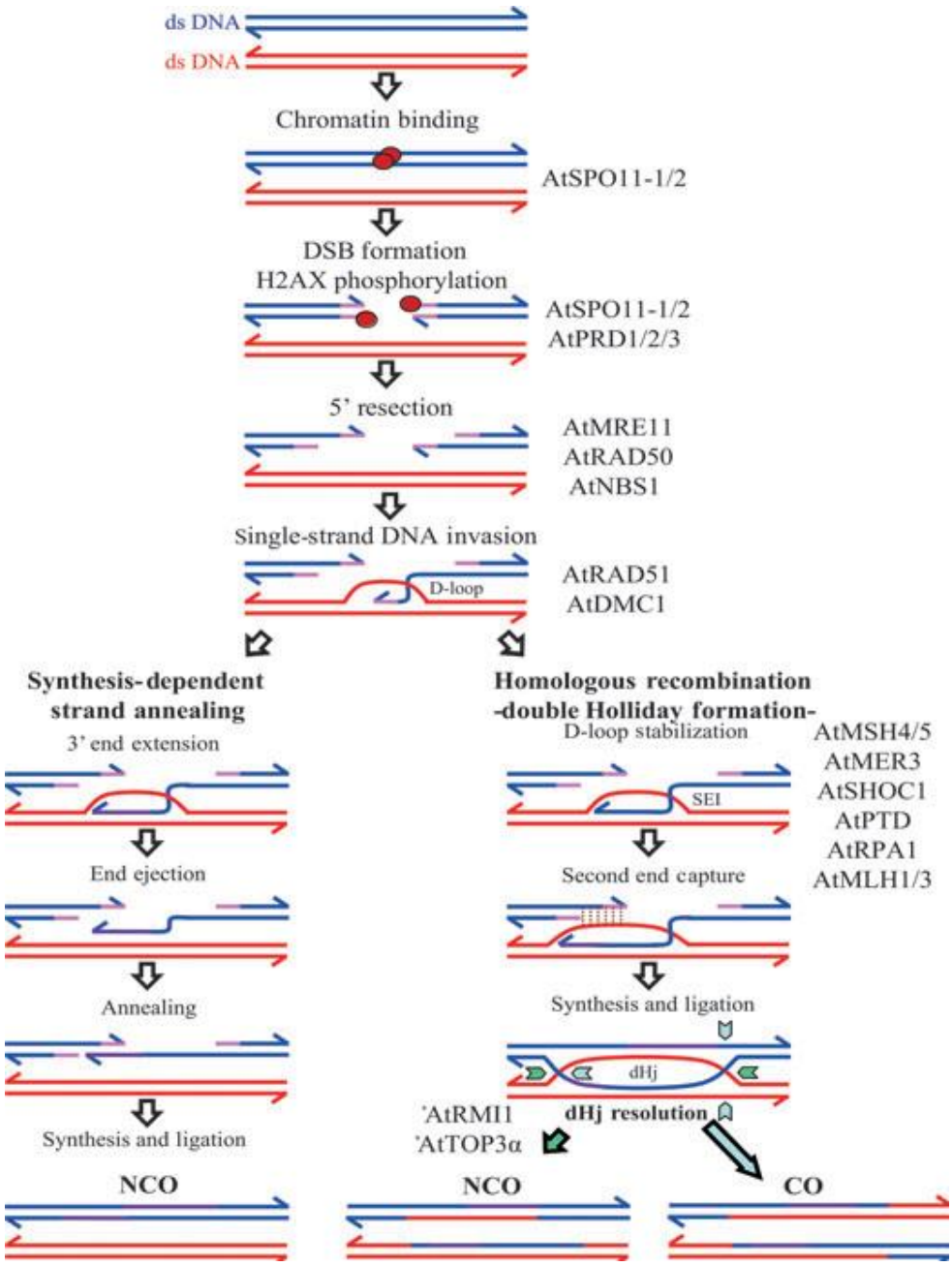

Figure 3. [Reproduced from Osman *et al.* (2011)]. Schematic diagram showing the meiotic double-strand break repair pathways. Processing of DSBs results in the strand resection of 5'ends to 3' ends. This precedes strand invasion which leads to the formation of the D-loop. A number of D-loops undergo the SDSA repair pathway, resulting in NCO formation. A portion of DNA intermediates undergo 2nd end capture, synthesis and ligation. The stabilisation of these structures leads to the formation of dHJs. Resolution of dHJs by endonuclease leads to the formation of a CO, whereas dissolution generates NCOs.

Arabidopsis thaliana: a model plant for studying meiosis.

The use of *Arabidopsis* in numerous studies investigating meiosis has provided valuable insights regarding meiotic recombination and its control. *A.thaliana* is a key experimental system utilised to increase understanding of the control of genetic COs. This is mainly due to the fact that this plant species has a relatively small genome size, of which has been sequenced (*Arabidopsis* Genome Initiative 2000), and the identification and characterization of meiotic genes in this species has been enhanced by the availability of a large selection of T-DNA insertional mutants (Mercier *et al.* 2001). In addition to this, *Arabidopsis* is considered cytogenetically amenable with synchronized meiocytes being present within the anther locules, permitting the analysis of the cytogenetically distinct stages apparent within meiosis (Armstrong *et al*. 2001). Although it is clear that there are fundamental differences in the mechanics of meiotic control between the various species analysed, analyses carried out in *A.thaliana* have provided much insight into the control of meiosis in plants, over the last decade, allowing for the generation of tools that could potentially be used to analyse processes in crop species. The fundamental knowledge obtained from *Arabidopsis* can ultimately be translated to crop species for practical application, enabling the understanding of the mechanisms in these species along with the ability to manipulate meiotic recombination in an attempt to increase the genetic variation available to plant breeders, therefore contributing to food security efforts.

Aim and Objectives.

An understanding of the networks and protein interactions controlling the formation of meiotic COs in *A.thaliana* is of great importance. This is mainly due to the potential this has on the ability to manipulate recombination pathways, allowing CO outcomes to be changed to increase available genetic variation. This investigation is being carried out in order to provide fundamental insights into the control of genetic crossover formation during meiosis in *A.thaliana.* This will be achieved by the gene cloning and subsequent protein expression and purification of both AtSHOC1 and AtASY1, in order to generate recombinant proteins to be used in antibody-based immunolocalisation studies, which will allow the dynamics of the repair process in relation to axis-remodelling to be analysed in more detail. Furthermore, a yeast two-hybrid (Y2H) system will be used to test for a direct interaction between AtASY1 and AtPCH2, as previous data suggests these proteins form a complex, with an interaction being confirmed with the yeast homologues. In addition to this, the interaction between PCH2 and a number of other key axis proteins, including AtPRD3, will be carried out, along with the mutagenesis of *PCH2*, in order to remove its ATP hydrolytic activity to determine the impact this has on possible protein interactions.

Materials and Methods

1. *A.thaliana* SHOC1 and ASY1 Recombinant Protein Production for Antibody Production.

1.1. *SHOC1:* Gene Cloning

AtSHOC1 AT5G52290.1 (see Appendix 1 for genomic sequence).

Polymerase Chain Reaction (PCR) purified SHOC1 (exon 7) (see Appendix 1 for DNA sequence) was used in subsequent steps.

1.1.2. Ligation of Blunt-end PCR Purified *SHOC1* DNA fragment into cloning vector

pCR®-Blunt (Invitrogen) – Zero Blunt® PCR Cloning Kit (Invitrogen by Life Technologies).

pCR®-Blunt vector is a 3.5kb plasmid designed for blunt-end cloning to ensure a low background of non-recombinants via the lethal *Escherichia coli ccdb* gene (Bernard *et al.* 1994).

PCR purified *AtSHOC1* exon 7 DNA fragment was cloned into pCR®-BLUNT (Invitrogen).

Table 1. Reagents and volumes for the ligation reaction of PCR purified *AtSHOC1* exon 7 DNA fragment into the blunt-end cloning vector, pCR®-BLUNT (Invitrogen).

Reagent	Volume
Purified SHOC1 exon 7 PCR product	7µl
pCR®-Blunt vector	1µl
10x T4 Ligase Buffer (New England Biolabs – NEB)	1µl
T4 Ligase enzyme (NEB)	1µl
Total volume = 10µl	

Ligation reaction was mixed by pipetting up and down and incubated at 16°C for 2h.

1.1.3. Transformation of pCR®-Blunt-*SHOC1* into competent *E.coli* DH5α cells by heat shock.

2µl pCR®-Blunt-*SHOC1* ligation mix was added to a 50µl aliquot of competent cells that had been thawed on ice for 10mins. The mixture was mixed by gently pipetting up and down, heat-shocked at 42°C for 45s and incubated at 37°C for 45mins with shaking at 200rpm, in 400µl Lysogeny Broth (LB).

50µl, 100µl and 250µl of transformed cells in LB were plated onto fresh LB agar plates with Kanamycin antibiotic selection (50µg/ml final concentration). (As a negative control, untransformed DH5α *E. coli* cells were also plated onto a Kanamycin LB agar plate to ensure antibiotic selection is efficient).

Plates were sealed with parafilm and incubated overnight (O/N) at 37°C.

1.1.4. Colony PCR

Colony PCR was carried out to clarify whether *E. coli* DH5α cells had been successfully transformed with the recombinant plasmid.

A single *E. coli* colony was used to inoculate a PCR reaction (Table 2) (this was carried out for 8 different colonies obtained from the kanamycin LB agar plates).

Table 2. Colony PCR reaction to confirm successful transformation of *E.coli* cells with pCR®-Blunt ligated with the *AtSHOC1* DNA insert.

Reagent	Volume
Sterile Distilled Water (SDW)	7.5µl
2µM primer mix (SHOC1 forward and reverse primers – see Appendix 1 for primer sequences).	5µl
GoTaq® Green Master Mix (2x) (Promega)	12.5µl
Total volume = 25µl	

A positive control was carried out for the colony PCR using DNA from previously PCR purified SHOC1 DNA fragment (6.5µl SDW, 5µl 2µM forward and reverse primer mix, 1µl Purified SHOC1 PCR product, 12.5µl GoTaq® Green Master Mix (2x)).

Table 3. PCR Programme for the colony PCR to ensure successful transformation of *E.coli* cells with the recombinant plasmid.

Steps	Temperature, Time
Initial Denaturation	95°C for 2min
Cycle –x32	
Denaturation	95°C for 30s
Annealing	60°C for 1min
Extension	73°C for 1min
Final extension	73°C for 10min
(carried out with a heated lid at 112°C) using a ThermoHybaid PCRSprint thermo-cycler.	

DNA Agarose Gel Electrophoresis:

7µl of each of the 8 PCR reactions and the positive control, with added DNA loading buffer, was ran on a 1% agarose (Sigma) gel containing 0.5µg/ml ethidium bromide, along with 1kb+ DNA Ladder (Invitrogen) at 100V for 40mins (Hybaid electrophoresis kit). The gel was visualised using a Gel-Doc XR imager using QuantityOne Software.

1.1.5. O/N Liquid Culture

4 single colonies that had been shown to have been successfully transformed with ligated pCR®-Blunt and the *SHOC1* DNA insert via colony PCR, were used to inoculate 5ml LB broth with the selective antibiotic kanamycin at a final concentration of 50µg/ml.

Launched liquid cultures were incubated O/N at 37°C with shaking at 200rpm.

1.1.6. Plasmid DNA Purification

Plasmid DNA (pCR®-Blunt ligated with *SHOC1*) was purified from the O/N liquid cultures using a Promega Wizard Plus SV Miniprep DNA Purification System (Promega) using the manufacturer's guidelines for the microcentrifuge protocol.

Purified Plasmid DNA was heated at 65°C for 10mins prior to subsequent steps.

1.1.7. Restriction Digestion

2 samples of purified pCR®-Blunt/*SHOC1* were cut with the restriction enzymes *NdeI* and *XhoI* (NEB) (Table 4).

Table 4. Restriction digest reaction to digest pCR®-Blunt/*SHOC1* with the restriction enzymes *NdeI* and *XhoI* (NEB).

Reagent	Volume
Sterile Distilled Water (SDW)	13.5µl
Buffer 4 (10x) (NEB)	2µl
Bovine Serum Albumin	0.5µl
Purified Plasmid DNA	3µl
NdeI	0.5µl
XhoI	0.5µl
Total volume = 20µl	

Plasmid DNA was digested at 37°C for 60mins.

Purified pET-21b (Novagen) expression vector (obtained from a glycerol stock of transformed DH5α E.coli cells, cultured O/N and purified using the Promega Wizard Plus SV Miniprep DNA Purification System (Promega) using the manufacturer's guidelines for the microcentrifuge protocol) was also cut with the same restriction enzymes, as shown above, to form a linear plasmid with complementary sticky ends to the SHOC1 DNA insert.

Restriction digests of pCR®-Blunt/*SHOC1*and pET-21b were visualised by DNA gel electrophoresis (as described above) on a 0.8% agarose (Sigma) gel along with uncut samples of each and 1kb+ DNA Ladder (Invitrogen).

1.1.8. Large-Scale Restriction Digest

Carried out to cut the 2x SHOC1 DNA inserts out of the pCR®-Blunt cloning vector and to linearize pET-21b expression vector to ensure complementary sticky ends.

Table 5. Large-Scale Restriction digest reaction to digest pCR®-Blunt/*SHOC1* and linearize pET-21b expression vector with the restriction enzymes *NdeI* and *XhoI* (NEB).

Reagent	Volume
SDW	51µl
Buffer 4 (10x) (NEB)	10µl
Bovine Serum Albumin	1µl
Purified Plasmid DNA	30µl
NdeI	4µl
XhoI	4µl
Total volume = 100µl	

Plasmid DNA was digested at 37°C for 90mins.

Restriction digest reactions were ran on a 0.8% agarose (Sigma) gel at 86V for 1h.

1.1.9. Gel extraction and purification of restriction digests

2x *SHOC1* DNA inserts and linearized pET-21b was extracted from the agarose gel and purified using a QIAquick Gel Extraction Kit (QIAGEN) following the manufacturer's guidelines for the microcentrifuge protocol.

Gel purified SHOC1 and pET-21b was subsequently visualised by DNA gel electrophoresis, ran on a 0.8% agarose (Sigma) gel, to ensure purity and as a

method to semi-quantify DNA to determine a concentration ratio to be used in subsequent ligation steps.

1.1.10. Ligation of *SHOC1* into pET21-b (Novagen) Expression Vector

Table 6. Reagents and volumes for the ligation reaction of *AtSHOC1* DNA fragment into pET21-b (Novagen) Expression Vector.

Reagent	Volume
Gel purified SHOC1 exon 7 restriction digest	3µl
pET21-b (Novagen) expression vector	4µl
10x T4 Ligase Buffer (NEB)	1µl
T4 Ligase enzyme (NEB)	0.5µl
SDW	1.5µl
Total volume = 10µl	

Ligation reaction was mixed by pipetting up and down and incubated at 16°C O/N.

Ligation into the protein expression vector pET-21b will generate a recombinant protein fused to a C-terminal His-tag protein.

1.1.11. Transformation of pET-21b-*SHOC1* into competent *E.coli* DH5α cells by heat shock.

2µl pET-21b-*SHOC1* ligation mix was added to a 50µl aliquot of competent that had been thawed on ice for 10mins. The mixture was mixed by gently pipetting up and down, heat-shocked at 42°C for 45 seconds and incubated at 37°C for 45mins with shaking at 200 rpm, in 500µl LB broth. *(carried out for both SHOC1 samples).*

50µl, 100µl and 250µl of transformed cells in LB broth were plated onto fresh LB agar plates with ampicillin antibiotic selection (100µg/ml final concentration). (As a negative control, untransformed DH5α *E.coli* cells were also plated onto an ampicillin LB agar plate to ensure antibiotic selection is efficient).

Plates were sealed with parafilm and incubated overnight (O/N) at 37°C.

8 single transformed colonies for both *SHOC1* samples ligated in pET-21b were restreaked onto fresh ampicillin (100 µg/ml) LB agar plates, sealed with parafilm and incubated O/N at 37°C.

1.1.12. O/N Liquid Culture

8 single colonies for each pET-21b/*SHOC1* sample, that had been restreaked, were used to inoculate 5ml LB broth with the selective antibiotic carbenicillin (synthetic ampicillin analogue) at a final concentration of 100µg/ml.

Launched liquid cultures were incubated O/N at 37°C with shaking at 200rpm.

1.1.13. Plasmid DNA Purification

Plasmid DNA (pET-21b ligated with *SHOC1*) for each *SHOC1* sample was purified from the O/N liquid cultures using a Promega Wizard Plus SV Miniprep DNA Purification System (Promega) using the manufacturer's guidelines for the microcentrifuge protocol.

Purified Plasmid DNA was heated at 65°C for 10mins prior to subsequent steps.

1.1.14. Restriction Digestion

The 2 samples of purified pET-21b/*SHOC1* were cut with the restriction enzymes *NdeI* and *XhoI* (NEB) (Table 7).

Table 7. Restriction digest reaction to digest purified pCR®-Blunt/*SHOC1* with the restriction enzymes *NdeI* and *XhoI* (NEB).

Reagent	Volume
SDW	11.5µl
Buffer 4 (10x) (NEB)	2µl
Bovine Serum Albumin	0.5µl
Purified Plasmid DNA	5µl
NdeI	0.5µl
XhoI	0.5µl
Total volume = 20µl	

Plasmid DNA was digested at 37°C for 90mins.

Restriction digests of the 2 pET-21b/*SHOC1* samples were visualised by DNA gel electrophoresis (as described above) on a 0.8% agarose (Sigma) gel, ran at 90V, along with uncut samples of each and 1kb+ DNA Ladder (Invitrogen). This was carried out to ensure that the samples contained pET-21b that had been successfully ligated with the *SHOC1* DNA insert.

1.1.15. DNA Sequencing

In order to confirm pET-21b plasmids ligated with *SHOC1* DNA inserts for both samples were in-frame and had no mutations, purified plasmid DNA was sequenced. DNA sequencing was carried out by the Functional Genomics Unit, University of Birmingham, UK, using the BigDye Terminator Sequencing v2.0 Ready Reaction Kit (PE Biosystems).

Table 8. DNA Sequencing Reaction to sequence purified plasmid DNA to confirm pET-21b plasmids ligated with *SHOC1* DNA inserts were in-frame and free from mutations.

Reagent	Volume
Purified plasmid DNA	3µl
Primer (0.8µM concentration)	3µl
SDW	4µl
Total volume = 10µl	
3 reactions were carried out, using the following primers: T7 Promoter, SHOC1 Exon 7 forward, SHOC1 Exon 7 Reverse (see Appendix 1 for sequences).	

Sequencing reactions were run out on an ABI 3700 DNA Analyser.

DNA sequences were analysed using Chromas software. The BLAST program on the National Centre for Biotechnology Information (NCBI) website (www.ncbi.nlm.nih.gov) was used to carry out homology searches.

As a result of the DNA sequencing results, only one of the pET-21b/SHOC1 samples was used for the protein expression protocol.

1.2. *ASY1*: Gene Cloning

The *Arabidopsis ASY1* gene's coding region was cloned into the expression vector pGex-6P-1 (Amersham Pharmacia Biotech), as an N-terminal fusion to glutathione S-transferase (GST) (Armstrong *et al.* 2002).

1.3. Protein Expression of SHOC1 and ASY1 Recombinant Proteins

1.3.1. Transformation of Ready-Competent *E.coli* BL21 (DE3) cells (Novagen) with pET-21b/*SHOC1* and pGex/*ASY1*

2µl of purified plasmid DNA was added to a 50µl aliquot of *E.coli* BL21 (DE3) cells. The mixture was kept on ice for 20mins prior to being heat-shocked at 42°C for 45s.

Transformed cells were mixed with 400µl LB broth and incubated at 37°C on a shaker at 200rpm, for 30mins.

Recovered transformed cells were plated onto fresh ampicillin (100µg/ml) LB agar plates, which were sealed with parafilm and incubated at 37°C O/N.

Single colonies of transformants were restreaked onto ampicillin (100µg/ml) LB agar plates, sealed with parafilm and incubated at 37°C until single colonies were visible.

1.3.2. Small-scale induced protein expression

1.3.2.1. Induction of protein expression

2 single colonies of *E.coli* BL21 cells transformed with pET-21b/*SHOC1* and 1 colony of *E.coli* BL21 cells transformed with pGex/*ASY1*, was used to inoculate 20ml prewarmed LB broth (0.5% glucose, 100µg/ml carbenicillin) in prewarmed 100ml conical flasks.

Cultures were incubated O/N at 30°C with shaking at 200rpm.

19ml prewarmed LB broth (0.5% glucose, 100µg/ml carbenicillin) was inoculated with 1ml O/N culture, in prewarmed 250ml conical flasks. Cultures were incubated at 30°C until an OD_{650} ~ 0.5 was reached.

In order to induce expression of the two SHOC1 proteins and the ASY1 protein, Isopropyl β-D-1-thiogalactopyranoside (IPTG) was added to a final concentration of 1mM (Cultures that had not been induced, referred to as uninduced, were carried out as a negative control for protein expression analysis). 0h samples were taken after induction with IPTG, for all of the cultures. 1ml of culture was removed, centrifuged for 5mins at 13k rpm, the supernatant was discarded and the resultant pellets were stored at -20°C until needed. 4h and 24h samples were also taken.

1.3.2.2. Protein Extraction from Bacterial Pellet

Pellets from 0h, 4h and 24h were thawed on ice for 20mins. Cell pellets were resuspended in 300µl Bugbuster Mastermix (Novagen) and mixed on a rotator for 20mins. The solutions were centrifuged at 13k rpm at 4°C for 15mins.

10µl of the supernatant (S/N), containing the soluble fraction of proteins, was transferred to a sterile 1.5ml microcentrifuge tube and 3µl 5 x Final Sample Buffer was added. Resultant pellets, containing the insoluble protein fraction, were resuspended in 300µl 1 x Final Sample Buffer (Tris-HCl (pH 6.8) 12.5% (v/v), SDS 2% (w/v), Glycerol, 10% (v/v), β-Mercaptoethanol 5% (v/v), Bromophenol blue 0.001% (w/v).

Soluble and insoluble protein fractions were boiled for 10mins. 10µl of the insoluble samples, 13µl of the soluble samples and 8µl ThermoScientific PageRuler Plus Prestained Protein Ladder (ThermoScientific) were loaded onto 12.5% polyacrylamide Sodium dodecyl sulphate polyacrylamide gel electrophoresis (SDS-PAGE) for further analysis, using a 3rd generation BioRad self-assembly kit. Gels were ran at 50V for 30mins to allow samples to travel through the stacker gel, following which the voltage was increased to 100V for 1.5h to allow samples to migrate though the resolving gel and for separation of the proteins to occur according to their molecular weight. SDS-PAGE gels were stained with Coomassie Blue (0.25g coomassie blue, 112.5ml methanol, 112.5 ml acetic acid (glacial), 25ml SDW) for 1h and destained (100ml methanol, 35ml acetic acid (glacial), 365ml SDW) O/N.

1.3.2.3. Large-Scale Protein Expression

Purified transformants were used to inoculate 20ml prewarmed LB broth (0.5% glucose, 100µg/ml carbenicillin), in prewarmed 100ml conical flasks. Cultures were incubated O/N at 30°C, with shaking at 200rpm.

10ml O/N culture was used to inoculate 190ml prewarmed LB broth (0.5% glucose, 100µg/ml carbenicillin), in prewarmed 2L conical flasks. Cultures were incubated at 30°C with shaking at 200rpm until an OD_{650} ~ 0.5 was reached. IPTG to a final

concentration of 1mM was added to the cultures to induce protein expression. 0h samples were taken (as described above). 24h post-induction, cultures were centrifuged using a floor centrifuge (SORVALL ® RC26) at 5k rpm for 10mins at 4°C. The S/N was discarded and resultant cell pellet was resuspended in 150ml cold lysis buffer (50mM Tris-HCL pH 8.0, 100mM NaCl, 1mM 0.5M EDTA, made up to 500ml with SDW). The resuspension was centrifuged at 5k rpm for 10mins at 4°C in order to wash the cells, and the S/N was discarded.

1.3.2.3.1. Western Blotting

Insoluble SHOC1 proteins were extracted from 0h and 24h post-induction bacterial pellets (as described previously). Protein samples were separated on a 12.5% SDS-PAGE gel and electroblotted onto Hybond C extra nitrocellulose membrane (Amersham Pharmacia Biotech). Western blots were incubated with anti-His probe (1:5000 dilution) followed by anti-mouse antibodies conjugated to horseradish peroxidase (HRP) (1:10000 dilution) (Sigma-Aldrich). ECL reagents (Amersham Pharmacia Biotech) were used to visualise the protein bands, which were subsequently detected by autoradiography.

1.3.2.4. Protein Purification

Upon induction, HISTAG-SHOC1 and GST-ASY1 recombinant proteins accumulated as insoluble inclusion bodies in E.coli BL21.

Bacterial pellets were resuspended in 40ml cold lysis buffer. 400µl 10µgml^{-1} lysozyme and 100µl of 50mM phenylmethanesulfonylfluoride (PMSF) was added and samples were incubated at 4°C for 1.5h. Following this, 26mg sodium deoxycholate and 50µl 50mM PMSF was added and the samples were incubated at 37°C for 30mins. Samples were subsequently syringed through a 0.4mm needle twice, centrifuged at 5000rpm for 20mins at 4°C and the S/N was discarded. The resultant pellet was resuspended in 20ml cold lysis buffer, syringed and centrifuged again under the same conditions. This was repeated 3x. The resulting pellet was resuspended in 5ml PBS (1x) (Sigma) and syringed.

1.3.2.4.1. Analysis of Purified Inclusion Bodies

1.3.2.4.1.2. SDS-PAGE

Purified HISTAG-SHOC1 and GST-ASY1 recombinant inclusion bodies were ran on a 12.5% polyacrylamide SDS-PAGE gel along with BSA of a known concentration for quantification of purified proteins.

1.3.2.4.1.3. Western Blot

Undiluted and diluted purified samples of both the SHOC1 and ASY1 recombinant proteins were ran on 12.5% and 10% SDS-PAGE gels, respectively, and electroblotted onto Hybond C extra nitrocellulose membrane. Western blot for SHOC1 protein was carried out as before. ASY1 western blots were incubated with anti-ASY1 antiserum (1:1000 dilution) followed by anti-rabbit antibodies conjugated to HRP (1:10000). ECL reagents were used to visualise the protein bands, which were detected by autoradiography.

1.3.2.4.1.4. Protein Quantification

Protein concentrations were quantified using BioRad assays according to the manufacturer's guidelines. 2µl, 5µl and 20µl purified inclusion bodies (resuspended in PBS) were added to PBS to make a final volume of 800µl. 200µl BioRad Stain was added to each sample, which were incubated at room temperature for 10mins. Absorbance at 595 nm was measured using a spectrophotometer (Jenway 6305). The absorbance of BSA (2.5 $\mu g \mu l^{-1}$) was used as a standard.

Rabbit polyclonal antiserum was produced against the HISTAG-SHOC1 and GST-ASY1 fusion proteins (ISL, Poole, UK).

2. Yeast Two-Hybrid Analysis of PCH2 with ASY1 and other key meiotic proteins.

Yeast Two-Hybrid Analysis was carried out using the Matchmaker™ Gold Yeast Two-Hybrid System (Clontech) according to the manufacturer's User Manual.

2.1. Gene cloning

The coding regions of *PCH2*, *ASY1, ZYP1, ASY3* and *PRD3 Arabidopsis* genes were cloned into both the pGBKT7 DNA-BD and pGADT7 AD Cloning Vectors (Clontech) and sequenced using the BigDye Terminator Sequencing v2.0 Ready Reaction Kit (PE Biosystems) by the Functional Genomics Unit, University of Birmingham, UK (see Appendix 2 for *PCH2* primer sequences).

2.2. Yeast Transformation

Yeast Transformation was carried out using the Yeastmaker™ Yeast Transformation System 2 (Clontech) according to the manufacturer's user manual.

2.2.1. Preparation of Competent Yeast Cells

Y2H Gold Yeast cells (*S.cerevisiae*) (from a glycerol stock) were aseptically spread onto YPDA (see Appendix 2 for recipe) agar plates. Incubated at 30°C, for 4 days, until single colonies became visible.

Inoculated 3ml YPDA liquid medium with a single colony (diameter >2mm) of Y2H Gold Yeast Cells. Incubated cultures at 30°C, with shaking at 200rpm, for 12h.

2x 3.5µl culture was used to inoculate 50ml YPDA liquid broth in a sterile 250ml conical flask and incubated at 30°C, with shaking at 250rpm, until OD_{600} ~ 0.5 was reached (23.5h).

Cultures were transferred into 2 sterile 50ml falcon tubes and centrifuged at 2.7x1000g for 5mins at room temperature. Resultant pellets were resuspended in 30ml SDW and centrifuged. Yeast cells were resuspended in fresh 1.5ml 1.1xTE/LiAC solution (see Appendix 2). Cell suspensions were transferred into 2

respective 1.5ml microcentrifuge tubes, centrifuged at high speed for 15s. Resultant pellet was resuspended in 600µl 1.1xTE/LiAc solution.

2.2.2. Transformation of Competent Yeast Cells

Yeastmaker Carrier DNA was denatured by boiling for 5mins and subsequently kept on ice until needed. (This was repeated prior to use).

3µl (100ng) plasmid DNA constructs, 5µl (10µgµl^{-1}) denatured Yeast Carrier DNA and 50µl competent Y2H Gold Yeast cells were combined in a pre-chilled 1.5ml sterile tube, and gently mixed by pipetting up and down. 500µl PEG/LiAc (see Appendix 2) was added.

Cells were incubated at 30°C for 30mins, mixing the cells every 10mins. 20µl DMSO was added and the mixture was pipetted up and down gently to mix. Mixture was heat-shocked at 42°C for 15mins (mixing the cells every 5mins). Cells were centrifuged at high speed for 15s. Resultant cell pellets were resuspended in 1ml YPDA broth and the cells were incubated at 30°C, with shaking at 200rpm, for 1h.

Cells were centrifuged at high speed for 15s and the resultant cell pellet was resuspended in 1ml filter-sterilized 0.9% (w/v) NaCl solution (see Appendix 2).

100µl of transformed yeast cells were spread onto SD/-Leu/-Trp (Double Dropout (DDO)) and SD/-His/-Leu/-Trp (Triple Dropout (TDO) media agar plates, to act as a control and to test interactions respectively. Plates were subsequently allowed to dry, and incubated at 30°C until colonies appeared

2.2.3. Drop Dilution of interacting proteins and the appropriate controls.

Single yeast colony used to inoculate 100µl filter-sterilized 0.9% NaCl, vortexed 1min. Diluted solution 1:10 and 1:100, vortexing each for 1min. Drop pipetted 3µl of each of the serial dilutions for interacting protein colonies and their controls onto DDO, TDO and SD/-Ade/-His/-Leu/-Trp (Quadruple Dropout (QDO)) medium agar plates. Plates were incubated at 30°C for 1.5 days.

3. Yeast Two-Hybrid Analysis of PCH2 E291Q with ASY1 and other key recombination proteins.

3.1. Site-directed Point Mutagenesis of *PCH2* gene.

Point mutagenesis of PCH2 was carried out using the Quikchange II XL Site Directed Mutagenesis Kit (Agilent Technologies) according to the protocol provided.

3.1.2. Mutagenesis Oligonucleotide Primer Design.

The online tool (Quikchange Primer design) was used to design appropriate primers for the point mutagenesis of the coding sequence of *PCH2* at the site E291 to product a mutant variant of the gene, referred to as *PCH2 E291Q* (see Appendix 2 for mutagenesis primer sequences).

3.1.3. Mutant Strand Synthesis Reaction

Carried out for pGBK-PCH2.

Table 9. Mutant Strand Synthesis Reaction for the site-directed point mutagenesis of the *AtPCH2* gene.

Reagent	Volume
10x Reaction Buffer	5µl
Plasmid DNA construct (pGBK-*PCH2*)	1.2µl (10mg)
10µM oligo primer 1	1.1µl
10µM oligo primer 2	1.1µl
dNTP mix	1µl
QuikSolution Reagent	4µl
Double-distilled water (ddH_20)	36.6µl
Total volume = 50µl	
1µ PfuUltra HF DNA Polymerase was added to the reaction.	

Reaction was subjected to the following temperature cycle (Table 10).

Table 10. PCR Programme for the mutant strand synthesis reaction for the site-directed point mutagenesis of the *AtPCH2* gene.

Steps	Temperature, Time
Initial Denaturation	95°C for 1min
Cycle –x18	
Denaturation	95°C for 50s
Annealing	60°C for 50s
Extension	68°C for 8min
Final extension	68°C for 7min
Temperature cycle carried out in a Techne TC-412 ThermoCycler Machine.	

3.1.4 *Dpn I* Digestion of the Amplification Product

1µl *Dpn I* restriction enzyme was added to the amplification reaction, mixture was centrifuged for 1min at high speed. Reaction was incubated at 37°C for 1h to digest the parental (non-mutated) dsDNA.

3.1.5. Transformation of XL10-Gold Ultracompetent Cells (Agilent).

XL10-Gold Ultracompetent cells were thawed on ice. 45µl aliquot was transferred to a pre-chilled 14ml BD Falcon polypropylene round-bottom tube. 2µl β-Mercaptoethanol (β-ME) mix (provided with the kit) was added, mixture was pipetted up and down gently to mix and cells were incubated on ice for 10mins.

2µl *Dpn I*-treated DNA was added to the cells, mixture was mixed and incubated on ice for 30mins. Mixture was heat-shocked at 42°C for 30s, and incubated on ice for 2mins. 500µl preheated filter-sterilized NZY^+ broth (see Appendix 2) was added, mixed by gently pipetting up and down. Cell mixtures were incubated at 37°C for 1h, with shaking at 200rpm.

250µl was spread onto fresh kanamycin (50µgml^{-1}) antibiotic selection agar media plates, which were incubated at 37°C until single colonies became visible (~20h).

3.1.6. O/N liquid cultures of pGBK-*PCH2 E291Q*

Inoculated 10ml LB (50µgml^{-1} Kanamycin antibiotic selection) with a single colony of transformants. Incubated culture at 37°C for 16h.

3.1.7. Plasmid DNA Extraction of pGBK-*PCH2 E291Q*

Carried out using the Promega Wizard Plus SV Miniprep DNA Purification System (Promega) using the manufacturer's guidelines for the microcentrifuge protocol. (Visualised by DNA gel electrophoresis on a 1% agarose gel).

3.1.8. DNA Sequencing of pGBK-*PCH2 E291Q*

Purified plasmid DNA was sequenced using the primers used for point mutagenesis (Appendix 2), to ensure the *pch2* coding sequence was ligated into the Y2H vector and has the correct point mutation.

3.1.9. Gene cloning of *PCH2 E291Q* from pGBK cloning vector into pGAD cloning vector.

3.1.9.1. PCR Reaction to amplify *PCH2 E291Q* Coding Sequence.

Carried out using In-Fusion Advantage PCR Cloning Kit (Clontech), following the kit protocol.

Table 11. PCR Reaction to amplify *PCH2 E291Q* Coding Sequence using In-Fusion Advantage PCR Cloning Kit (Clontech).

Reagent	Volume
Phusion HF Buffer (ThermoScientific)	4µl
10mM dNTP mix	0.4µl
10µM PCH2 Mutagenesis Primer 1	1µl
10µM PCH2 Mutagenesis Primer 2	1µl
Plasmid DNA	1µl (10µg/50µl)
DMSO	0.6µl
Phusion F 530S Enzyme (ThermoScientific)	0.2µl
Double-distilled water (ddH_20)	12.8µl
Total volume = 20µl	

Reaction was subjected to the following temperature cycle (Table 12).

Table 12. PCR Programme for the PCR reaction to amplify *PCH2 E291Q* Coding Sequence using In-Fusion Advantage PCR Cloning Kit (Clontech).

Steps	Temperature, Time
Initial Denaturation	98°C for 30s
Cycle –x35	
Denaturation	98°C for 10s
Annealing	52°C for 30s
Extension	72°C for 45s
Final extension	72°C for 10min
Temperature cycle carried out in a Techne TC-412 ThermoCycler Machine.	

3.1.9.2. Gel extraction and Purification of amplified *PCH2 E291Q* Coding Sequence.

PCR product was ran on a 1% agarose gel at 90V for 1h. Band was extracted and purified using a QIAquick Gel Extraction Kit (QIAGEN) following the manufacturer's guidelines for the microcentrifuge protocol.

3.1.9.3. Ligation of Gel Purified *PCH2 E291Q* PCR insert into linearized pGAD vector.

pGAD cloning vector was linearized by the restriction enzymes *NdeI* and *EcoRI*. (PCR primers used to amplify *PCH2 E291Q* coding sequence were designed with 15kb extensions (5') that are homologous to the ends of linearized pGAD).

Ligation of PCR insert into pGAD vector was carried out using the In-Fusion HD Cloning Kit (Clontech).

Table 13. In-Fusion Cloning reaction to ligate *PCH2 E291Q* gel purified PCR insert into pGAD vector.

Reagent	Volume
5x In-Fusion HD Enzyme Premix	2µl
Linearized pGAD	3.5µl
PCH2 E291Q gel purified PCR insert	3.5µl
Double-distilled water (ddH_20)	1µl
Total volume = 10µl	

Reaction was incubated at 50°C for 15min and then kept on ice.

3.1.10. Transformation of DH5α *E.coli* cells with pGAD-*PCH2 E291Q*

2.5µl ligation reaction was added to a 50µl aliquot of thawed cells, mixture was kept on ice for 30mins. Cells were heat-shocked at 42°C for 90s, mixed with 800µl LB and incubated at 37°C for 1h with shaking at 200rpm. Transformed cells were centrifuged at 13000rpm for 15s. Pellet was resuspended in 100µl LB.

100µl transformed cells in LB were spread on ampicillin (100µgml^{-1}) LB agar plates. Plates were incubated at 37°C until single colonies appeared.

3.1.11. Analysis of pGAD-*PCH2 E291Q* sequence.

O/N culture of transformants was launched and plasmid DNA was purified using the Promega Wizard Plus SV Miniprep DNA Purification System (Promega), using the manufacturer's guidelines for the microcentrifuge protocol. Purified plasmid DNA was sequenced to ensure only correct mutation was present.

3.1.12. Yeast Transformation

Yeast Transformation was carried out using the Yeastmaker™ Yeast Transformation System 2 (Clontech) according to the manufacturer's user manual (see previous yeast transformation of PCH2 for full protocol).

Drop dilution was carried out for any interacting proteins and the appropriate controls.

Results

1. AtSHOC1 and AtASY1 Recombinant Protein Production for Antibody Production.

In order for immunolocalisation analyses to be carried out to gain an insight into the functional roles of these proteins, recombinant AtSHOC1 and AtASY1 proteins were generated, to act as antigens for polyclonal antibody production.

1.1. *SHOC1:* Gene Cloning

Forward and reverse primers were designed to amplify a 726bp fragment of exon 7 in the *SHOC1* coding sequence (Appendix 1). The forward and reverse primers were designed to introduce restriction sites to permit ligation into expression vectors.

PCR purified *SHOC1* (exon 7) fragment was ligated into the pCR®-Blunt cloning vector, used to transform DH5α *E.coli* cells. Colony PCR was carried out using DNA obtained from the transformed bacterial colonies to ensure successful transformation (Appendix 3. Fig.1). From this, it can be seen that there is a PCR product of an amplified *SHOC1* DNA fragment of the correct size of 726bp for seven of the clones analysed, however, there is no product for the second clone. Therefore, it was deduced that 7 clones have the *AtSHOC1* coding sequence ligated into the vector.

pCR®-Blunt/*SHOC1* plasmid DNA was purified and digested using the restriction enzymes *NdeI* and *XhoI*, along with purified pET-21b expression vector DNA (Fig.4).

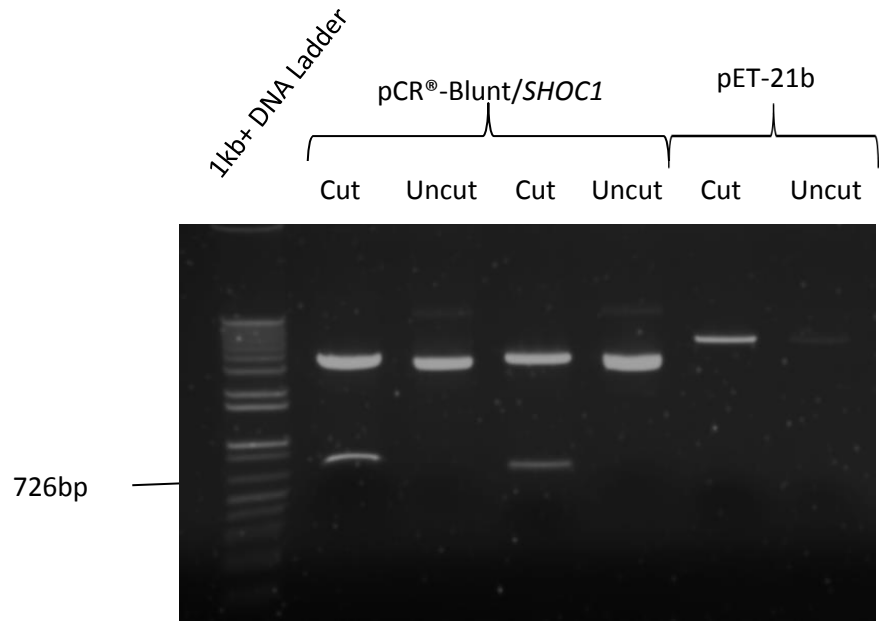

Figure 4. DNA gel electrophoresis image showing the restriction digestion of pCR®-Blunt/*SHOC1* and pET-21b expression vector, cut with the restriction enzymes, *NdeI* and *XhoI.*

The 726bp DNA insert, corresponding to the *SHOC1* fragment, was cut out of the pCR®-Blunt cloning vector for both of the clones, following digestion (Fig.4). Consequently, a large-scale restriction digestion was carried out and the digested fragments were ran on a 0.8% agarose gel. The resultant bands representing the *SHOC1* DNA insert for both of the clones, and the band corresponding to the linearized pET-21b expression vector were excised and gel purified (Appendix 3, Fig.2.).

The gel purified *SHOC1* DNA inserts were ligated into the gel purified linearized pET-21b expression vector. DH5α *E.coli* cells were transformed with the ligation mix of the two clones, and the resultant transformants were selected for by growth on ampicillin agar plates. Transformant colonies were restreaked, and O/N cultures were launched, using the ampicillin antibiotic analogue, carbenicillin.

Plasmid DNA was purified and digested, using *NdeI* and *XhoI,* to ensure pET-21b had been successfully ligated with the *SHOC1* DNA insert for both clones. It became apparent at this stage that the linearized pET-21b expression vector was of a larger size than the 5.4kb expected size, possibly due to the formation of multimers. Therefore, the *SHOC1* DNA inserts were ligated into an alternative pET-21b expression plasmid, obtained from a different glycerol stock, which had been linearized with the same restriction digests and confirmed to be of the correct size (Appendix 3, Fig.3). The second clone (Appendix 3, Fig.3) was sequenced whereby it was concluded that the *SHOC1* DNA insert had been ligated into the pET-21b plasmid vector in-frame and the construct was mutation-free.

1.2. *ASY1*: Gene Cloning

The *AtASY1* gene's coding region was cloned into the expression vector pGex-6P-1 (Amersham Pharmacia Biotech), as an N-terminal fusion to glutathione S-transferase (GST) (Work done by Armstrong *et al*.).

1.3. Protein Expression of SHOC1 and ASY1 Recombinant Proteins.

Both the pET-21b/*SHOC1* and pGEX/*ASY1* were transformed into Ready-Competent *E.coli* BL21 (DE3) cells. A small-scale test of protein induction was initially carried out with incubation temperatures of 37°C, however, although the recombinant ASY1 protein was expressed, there was no apparent induced expression of the SHOC1 recombinant protein (no data shown). Therefore, an alternative method was carried out with optimised conditions. Incubation temperatures were decreased to 30°C,

0.5% glucose was added to the LB (100µgml^{-1} carbenicillin) liquid media, and flasks and media were pre-heated prior to use.

The expression of ASY1 and SHOC1 recombinant proteins was visualised on SDS-PAGE. The ASY1 recombinant protein, with an expected size of ~90kDa, was expressed following induction with IPTG in the insoluble protein fraction only (Appendix 3, Fig.5). For the two cultures of SHOC1 recombinant protein, a band with a molecular weight of ~40kDa was revealed. This band was not present in the uninduced samples for 4h and 24h post-induction in both the insoluble and soluble protein fractions. The SHOC1 recombinant protein has an expected molecular weight of 27.95kDa, however, as the band of ~40kDa was only present in the induced samples and not in the un-induced samples of the cultures, it was assumed that this represents recombinant SHOC1. Higher expression of SHOC1 was obtained 4h post-induction when compared to that after 24h, in the soluble fraction (Appendix 3, Fig.5). Higher expression of SHOC1 for both cultures was obtained 24h after induction with IPTG than for 4h, in the insoluble fraction. Due to induced expression of ASY1and SHOC1 for both cultures, 24h post-induction in the insoluble fractions, large-scale induced expression was carried out under the same conditions as the test-induction.

Western blot analysis was carried out to detect the expression of recombinant proteins following the large-scale induction for the two SHOC1 cultures. In order to confirm that the ~40kDa protein revealed by SDS-PAGE was SHOC1, an anti-His antibody was used to detect the His-Tag fusion to the C-terminus of recombinant SHOC1 (Fig.5).

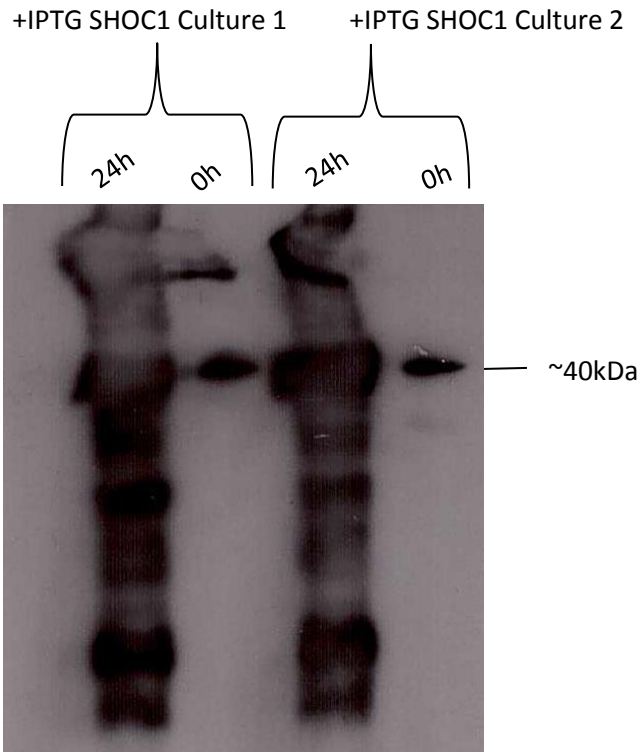

Figure 5. Detection of SHOC1 recombinant protein by western blot analysis with anti-His antibody.

The protein expressed in both cultures, following induction with IPTG, can be considered to be the recombinant SHOC1 protein as the fused His-tag was adequately detected by the anti-His antibody (Fig.5). Additionally, there is higher expression 24h post-induction when compared to that at the 0h post-induction time point (Fig.5). The expression of the ASY1 protein was only analysed by SDS-PAGE and not by western blot analysis, prior to purification.

1.3.2.4. Protein Purification

Both ASY1 and SHOC1 recombinant proteins accumulated as inclusion bodies 24h post-induction (Appendix 3, Fig.5; Fig.5). Consequently, the bacterial pellets obtained from the large-scale induction were used in the subsequent protein purification. Protein purity and semi-quantification of inclusion bodies was determined via SDS PAGE (Fig.6).

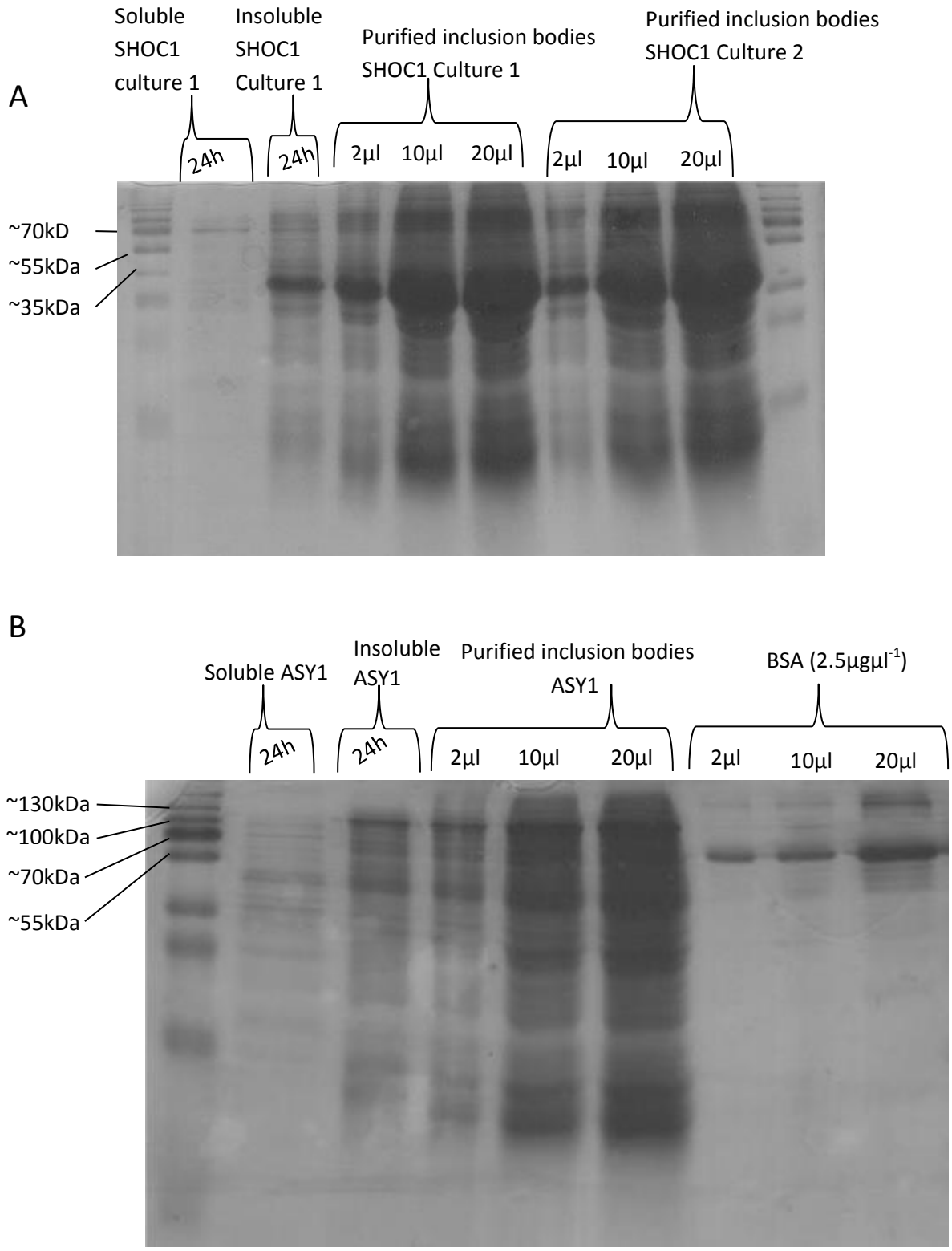

Figure 6. Coomassie blue stained SDS-PAGE gels showing varying amounts of known concentration of BSA for estimation of ASY1 and SHOC1 purified protein concentrations.

(A) Purified SHOC1 inclusion bodies from cultures 1 and 2 of varying volumes.

(B) Purified ASY1 inclusion bodies and BSA of a known concentration of varying volumes.

The large-scale induction had yielded vast concentrations of both the ASY1 and SHOC1 recombinant proteins, with the concentration for both being greater than the known concentration of BSA (2.5µgµl^{-1}). However, the purified inclusion bodies did not appear to be very pure, with the samples containing a significant amount of other proteins (Fig.6). Nevertheless, the purity of SHOC1 recombinant protein from the two samples and ASY1 recombinant protein was deemed sufficient for antibody production.

A western blot analysis (Fig.7) was carried out for the two samples of SHOC1 purified inclusion bodies and ASY1 inclusion bodies, with and without dilution. The recombinant proteins were visualised with anti-HIS and anti-ASY1antibodies, respectively.

A

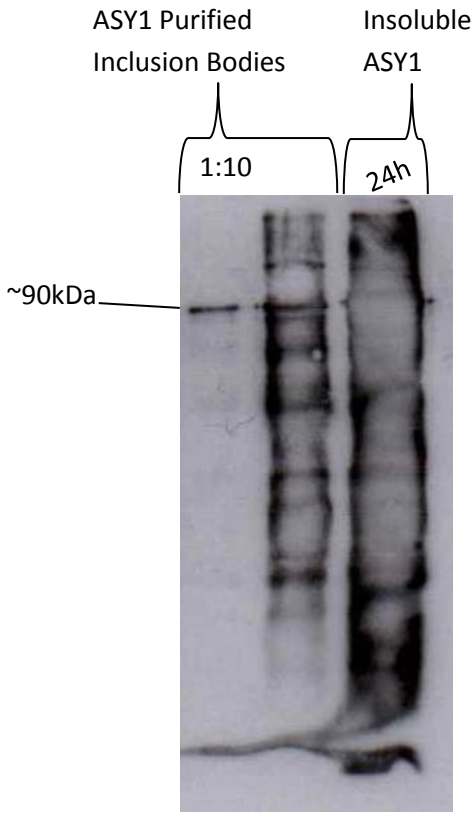

B

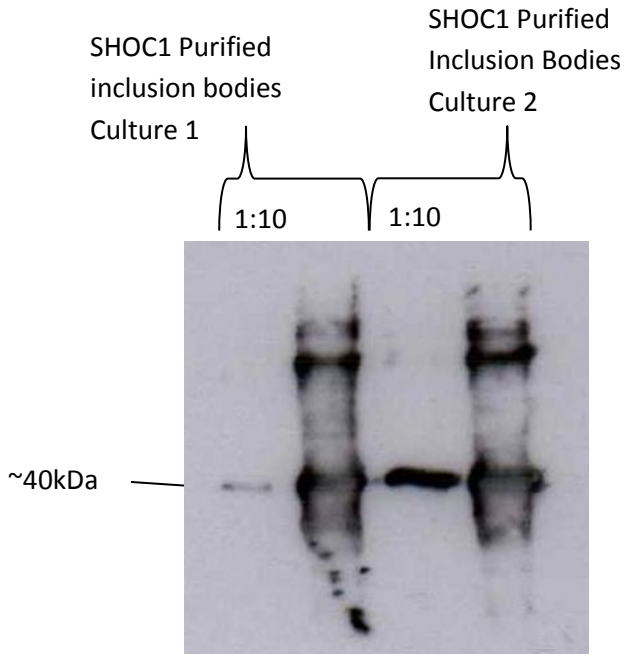

Figure 7. Detection of purified ASY1 recombinant protein (A) and purified SHOC1 recombinant protein (B) for both cultures with (1:10) and without dilution, by western blot analysis.

The ASY1 purified recombinant protein and the two samples of SHOC1 purified recombinant protein were successfully detected by western blot analysis using the appropriate antibodies (Fig.7).

In order to quantify the purified recombinant proteins in the undiluted samples, a BioRad assay was carried out with known concentrations of BSA (Table 14) (see Appendix 3 for raw data).

Table 14. Concentrations of undiluted purified recombinant proteins determined via a BioRad assay.

Recombinant Protein	Concentration ($mgml^{-1}$)
SHOC1 (Culture 1)	3.00
SHOC1 (Culture 2)	3.56
ASY1	4.34

As a result of the high concentrations determined by the BioRad assay (Table 14), the purified recombinant proteins were diluted 1:10. Rabbit polyclonal antiserum was subsequently produced against the HIS-tag-SHOC1 and GST-tag-ASY1 fusion proteins.

2. Yeast Two-Hybrid analysis of PCH2 with ASY1 and other key meiosis specific proteins.

Previous data (Franklin *et al.* Unpublished Data) has suggested that AtPCH2 forms part of a complex with AtASY1, therefore Y2H analysis will be carried out to test for a direct interaction between these two proteins and AtPCH2 with a number of key axis proteins, in order to analyse the function of this protein.

The coding sequences of the *Arabidopsis PCH2*, *ASY1, ZYP1, ASY3* and *PRD3* genes were cloned into both the pGBKT7 DNA-BD and pGADT7 AD cloning vectors, sequenced and used to transform Y2H Gold yeast cells for Y2H analysis, along with empty vectors, as their constitutive controls (Table 15). Transformed yeast cells were plated onto DDO, as a selective step to screen co-transformed cells, and TDO SD media agar plates to test for protein interactions.

Table 15. Plasmid DNA Construct Combinations Transformed into Competent Y2H Gold Yeast Cells for Yeast Two-Hybrid Analysis.

Ligated in pGAD Vector	Ligated in pGBK Vector
PCH2	***PCH2***
PCH2	**Empty vector as a negative control**
Empty vector as a negative control	***PCH2***
PCH2	***ASY1***
ASY1	***PCH2***
ASY1	**Empty vector as a negative control**
Empty vector as a negative control	***ASY1***
PCH2	***ZYP1***
ZYP1	***PCH2***
ZYP1	**Empty vector as a negative control**
Empty vector as a negative control	***ZYP1***
PCH2	***ASY3***
ASY3	***PCH2***
ASY3	**Empty vector as a negative control**
Empty vector as negative control	***ASY3***
PCH2	***PRD3***
PRD3	***PCH2***
PRD3	**Empty vector as a negative control**
Empty vector as a negative control	***PRD3***

After three days incubation at 30°C, colonies were visible for yeast transformed with the various combinations of vectors on the DDO media, with the exception for yeast transformed with the vector expressing PCH2 fused to the activating domain of the GAL4 promoter ie. pGAD-PCH2. Colonies of yeast transformed with pGAD-PCH2 constructs on the DDO media did not become visible until a total of six days incubation. Therefore, it could be deduced that the yeast transformation had been successful for these constructs, as both the pGBK and pGAD plasmid vectors were present in the cell thus permitting growth on the DDO media. Two interactions were visible, after a three day incubation period, shown by the growth of colonies on the TDO media. It was clear that pGBK-PCH2 interacted with pGAD-PCH2 and that pGAD-PRD3 interacted with pGBK-PCH2. Consequently, as the control experiment

had shown that the transformation of yeast with the pGAD-PCH2 constructs had been successful, the test plates were incubated for an additional day to allow for any possible new interactions with these constructs to become visible. However, no new interactions were revealed on the TDO medium, therefore the Y2H experiment was stopped.

Drop dilutions of yeast transformed with PCH2 (Fig.8) and PRD3 (Fig.9) constructs was carried out in order to confirm the interaction and analyse the strength, after an incubation period of 1.5 days.

A

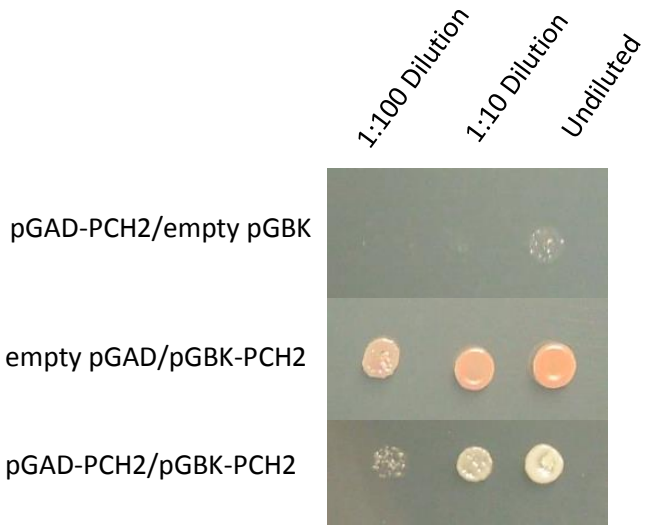

B

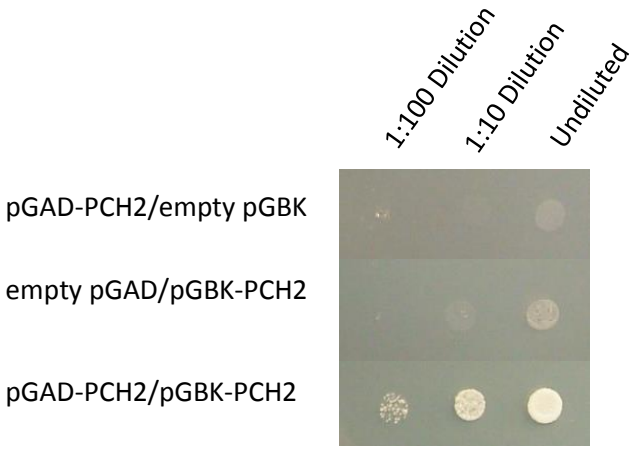

C

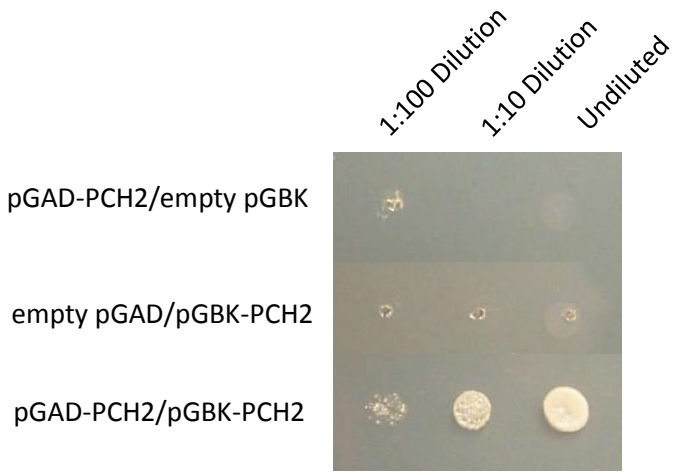

Figure 8. Yeast Two-Hybrid analysis illustrated by serial drop dilutions, showing the self-interaction of PCH2 after 1.5 days of incubation at 30°C.

(A) Control experiment of the yeast transformed with the PCH2 constructs grown on SD/-Leu/-Trp (DDO) agar media.

(B) Yeast transformed with the PCH2 constructs and negative controls grown on SD/-His/-Leu/-Trp (TDO) agar media.

(C) Yeast transformed with PCH2 constructs and negative controls grown on SD/-Ade/-His/-Leu/-Trp (QDO) agar media.

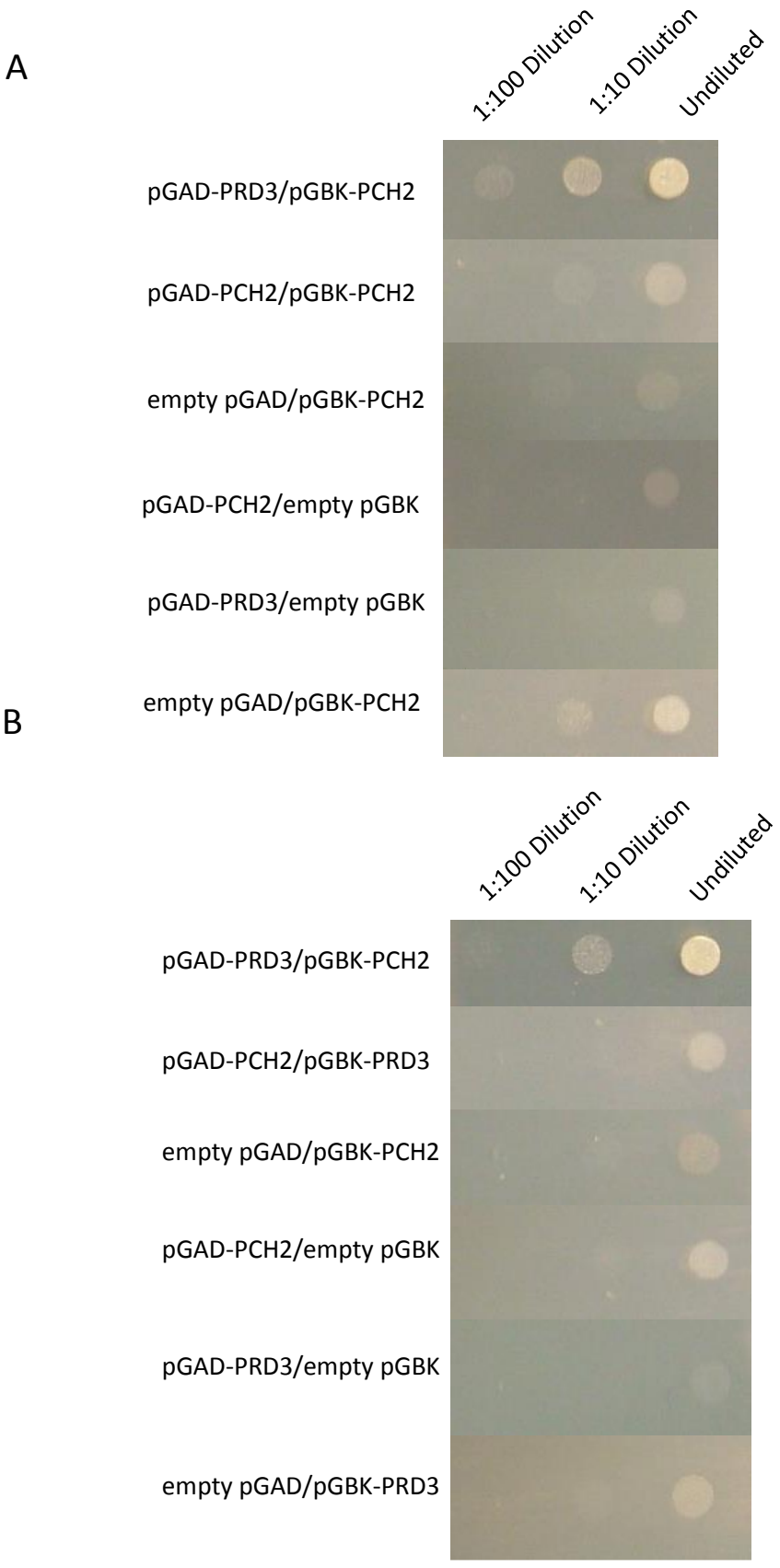

Figure 9. Yeast Two-Hybrid analysis illustrated by serial drop dilutions, showing the interaction of PRD3-PCH2 after 1.5 days of incubation at 30°C and negative controls.
(A) Yeast transformed with the PRD3 and PCH2 constructs grown on SD/-His/-Leu/-Trp (TDO) agar media.
(B) Yeast transformed with PRD3 and PCH2 constructs grown on SD/-Ade/-His/-Leu/-Trp (QDO) agar media.

PCH2 strongly self-interacts in the heterologous system, as there was substantial yeast growth on both the TDO and QDO media (Fig.8). The growth of yeast transformed with PCH2 fused to the activating domain in pGAD was slower than that observed for the yeast transformed with PCH2 fused to pGBK (Fig.8).

PCH2 was also found to interact with PRD3. When yeast was transformed with PCH2 fused with the activating domain of Gal-4 and PRD3 fused with the binding domain, there was a substantial growth on the TDO and QDO media. This suggests that pGAD-PRD3 and pGBK-PCH2 were strongly interacting in yeast cells (Fig.9).

3. Yeast Two-Hybrid analysis of PCH2 E291Q with ASY1 and other key meiotic specific proteins.

Site-directed point mutagenesis was carried out to disrupt the ATP hydrolysis activity of PCH2, as previous data showed that the interaction between the yeast Pch2 and ASY1 homologues, was stronger as a result. The mutation was achieved using primers designed to generate an amino acid substitution at site E291 in the *PCH2* coding sequence, to change a glutamic acid to a glutamine, *(PCH2 E291Q).* The *PCH2 E291Q* coding sequence, within the pGBK vector, was amplified, the PCR product was visualised on a DNA gel electrophoresis and purified (Fig.10), before ligation into the pGAD vector.

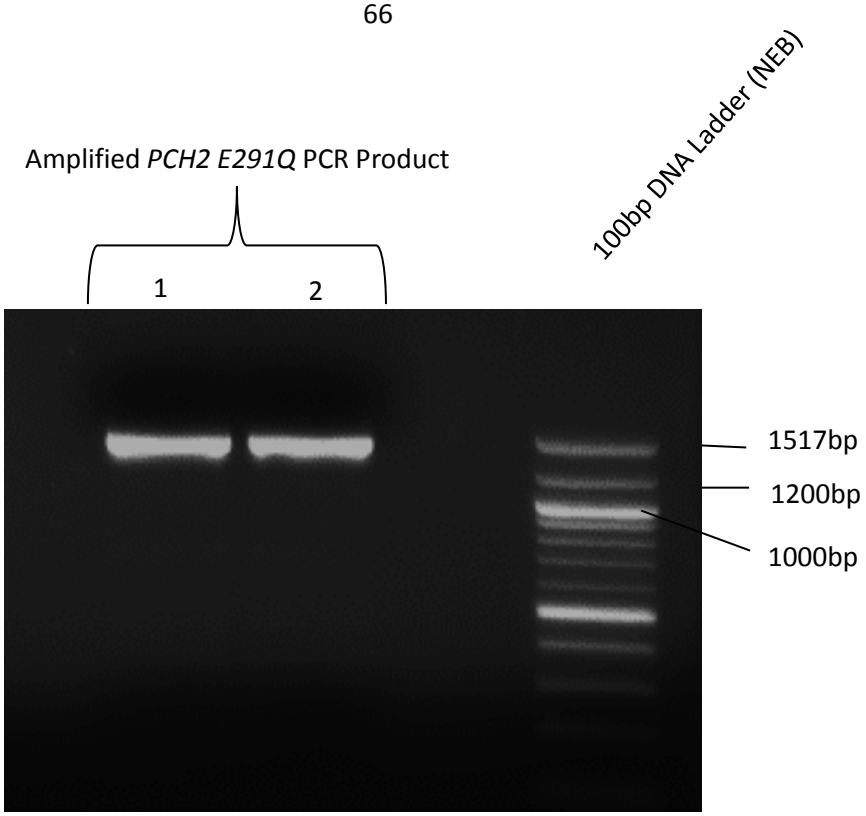

Figure 10. DNA gel electrophoresis to purify amplified *PCH2 E291Q* PCR product.

Figure 10 shows the 1,500bp gel purified amplified *PCH2 E291Q* coding sequence obtained following mutagenesis of the *PCH2* coding sequence. This PCR product was cloned into the pGAD cloning vector and used in a Y2H analysis to test for interactions (Table 16).

Table 16. Plasmid DNA Construct Combinations Transformed into Competent Y2H Gold Yeast Cells for Yeast Two-Hybrid Analysis of mutated PCH2.

Ligated in pGAD Vector	Ligated in pGBK Vector
PCH2 E291Q	***PCH2 E291Q***
PCH2 E291Q	**Empty vector as a negative control**
Empty vector as a negative control	***PCH2 E291Q***
PCH2 E291Q	***ASY1***
ASY1	***PCH2 E291Q***
PCH2 E291Q	***ZYP1***
ZYP1	***PCH2 E291Q***
PCH2 E291Q	***ASY3***
ASY3	***PCH2 E291Q***

Yeast transformed with the various constructs (Table 16) including pGAD-*PCH2 E291Q* and pGBK-*PCH2 E291Q*, was incubated at 30°C for 4 days, by which time it was apparent that the only interaction was between *PCH2 E291Q* and itself. The transformations were shown to have been successful following a screen on DDO media. The TDO plates were incubated for an additional two days in order to allow for growth of experimental yeast to see if any new interactions became apparent, however this was not the case. As a result, a drop dilution of the interacting mutated *PCH2* yeast and its corresponding controls was carried out (Fig.11).

A

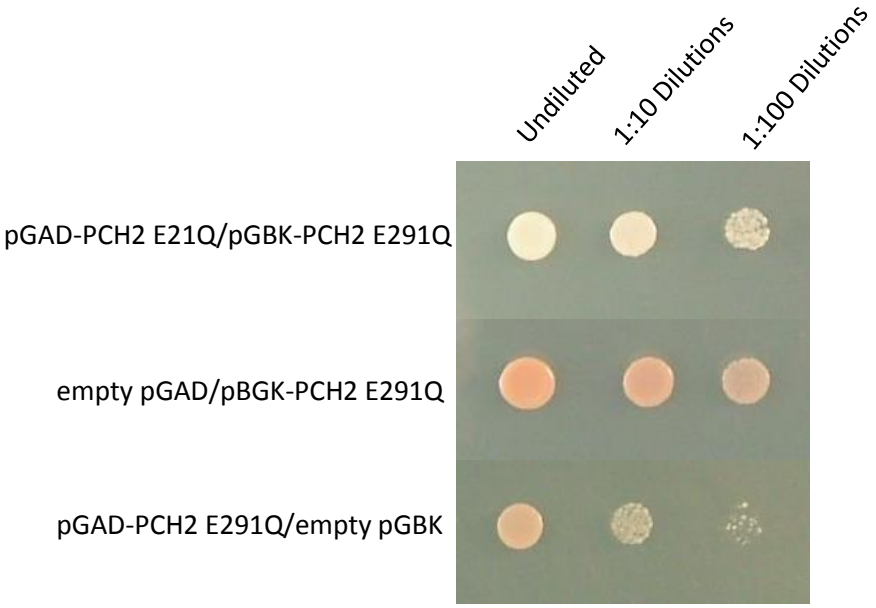

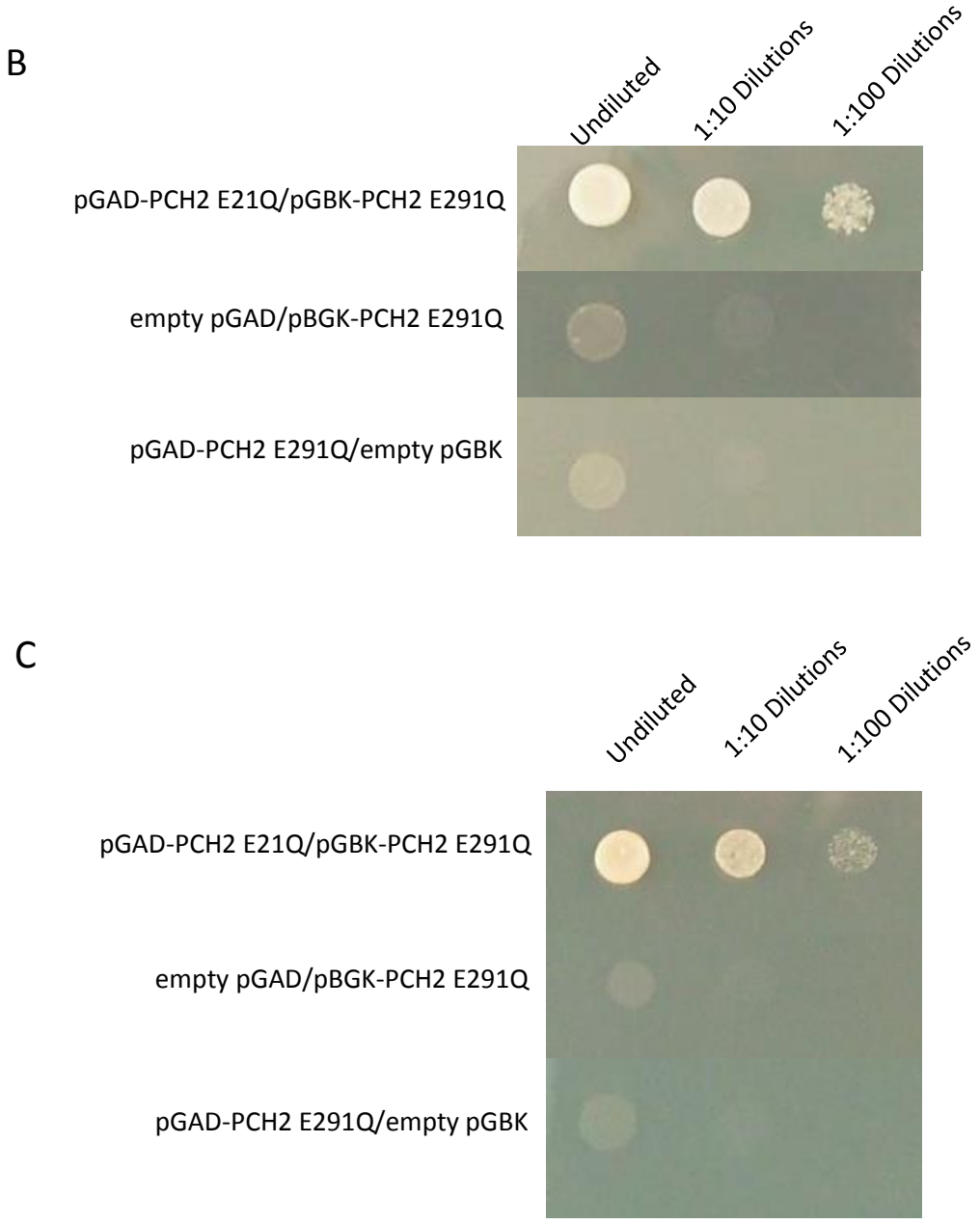

Figure 11. Yeast Two-Hybrid analysis illustrated by serial drop dilutions, showing the self-interaction of PCH2 E291Q-PCH2 E291Q after 1.5 days of incubation at 30°C.

(A) Control experiment of the yeast transformed with the PCH2 E291Q constructs grown on SD/-Leu/-Trp (DDO) agar media.

(B) Yeast transformed with the PCH2 E291Q constructs and negative controls grown on SD/-His/-Leu/-Trp (TDO) agar media.

(C) Yeast transformed with PCH2 E291Q constructs and negative controls grown on SD/-Ade/-His/-Leu/-Trp (QDO) agar media.

The yeast transformed with PCH2 E291Q-PCH2 E291Q were able to grow on TDO and QDO, however the yeast transformed with the empty vector controls did not (Fig.11). Therefore, it can be concluded that PCH2 E291Q homo-dimerises in yeast cells. As was seen with the previous Y2H with non-mutated PCH2, there appears to be slower growth of yeast when transformed with the mutated PCH2 insert fused to the activating domain of pGAD (Fig.11A). It should also be noted that the yeast appears to be slightly pinker in colour compared to that obtained when non-mutated PCH2 was analysed.

Discussion

Meiosis is essential for the life cycles of all sexually reproducing organisms. Genetic variation generated as a result of meiotic recombination is of great importance to allow for the production of novel combinations of alleles and therefore the formation of novel traits.

Numerous proteins have been identified in budding yeast, which have been implemented in the control of the meiotic events (reviewed in Roeder 1997; Zickler & Kleckner 1999; Dresser 2000). Functional analysis of these proteins as a means to decipher the control of meiotic recombination, proves beneficial as gained knowledge can ultimately be translated into crop species, in an attempt to allow for the manipulation of this process to increase genetic variation.

Homologues of the genes that encode these proteins in other eukaryotic species have been identified, as a result of the utilisation of a number of techniques (reviewed in Kumar & De Massy 2010). The identification of proteins sharing sequence homology in *A.thaliana* has proved challenging over recent years, mainly due to functional divergence of genes due to a whole genome duplication event (The Arabidopsis Genome Initiative, 2000). Functional analysis of proteins revealed via homology searches, requires extensive research and the use of numerous tools in order to confirm the roles of these proteins within meiosis.

The use of *Arabidopsis* as a model plant species to research meiotic events has increased recently with the identification of a range of meiotic mutants, enabling a method by which meiotic genes can be identified and characterised. The availability

of such meiotic mutants has enabled the ability to clone genes involved in meiosis, contributing to research on meiotic recombination in flowering plants. Nevertheless, compared to other eukaryotes, such as budding yeast, comparatively few meiotic genes have been characterised (reviewed in Osman *et al*. 2011).

The generation of recombinant proteins is a valuable process allowing for the production of antibodies that can be used for immunocytology techniques. Immunocytology represents a tool of great significance in terms of deciphering protein function and therefore control of meiotic events. Antibodies able to detect meiotic proteins, enable localisation and co-localisation studies to be carried out, thus contributing to efforts to determining protein function (discussed in Caryl *et al.* 2003; Osman *et al*. 2011).

Consequently, the cloning of the At*SHOC1* and At*ASY1* genes, and the expression and purification of the generated recombinant proteins, represented in this study, will prove valuable for insights into the functions of these meiotic proteins.

SHOC1 (*shortage in chiasmata*) was identified via the screening of *A.thaliana* meiotic mutants generated via T-DNA insertions, whereby a mutant phenotype of reduced fertility and meiotic defects was displayed (Mascaisne *et al.* 2008). A 1594 amino acid protein is encoded for by the *SHOC1* gene, of which homologues in various eukaryotes have been revealed that all comprise of the highly conserved homology domain. Similarity of this domain to the domain found within the XPF family of nucleases, inferred this protein as XPF-related with possible nuclease activity. *SHOC1* mutants analysed by chromosome spreads, revealed the generation of polyads as the products of meiosis. The potential biological function of SHOC1 was

deciphered due to a reduced number of chiasmata, and thus COs, in the *Atshoc1* mutant, compared to wild-type, which consequently affected chromosome segregation. Furthermore, SHOC1 was found to belong to the ZMM group of proteins, enabling the assumption to be made that this protein is involved in the class I pathway of CO formation, processing branched DNA intermediates to promote the generation of COs, and thus chiasmata (Macaisne *et al.* 2008).

A further insight in the function of SHOC1 was made following the identification that SHOC1 interacted with PTD, suggesting that these proteins form an XPF-ERCC1-like complex required for class I CO formation (Mascaisne *et al*. 2011).

In order to study the localisation of SHOC1 and to enhance knowledge regarding the function of this meiotic protein, the production of an antibody to permit immunolocalisation studies would prove beneficial.

The gene cloning of *SHOC1* carried out in this study, did not involve the cloning of the entire coding sequence of the gene. Instead, a small fragment of exon 7 of the gene (Appendix 1) was cloned, resulting in the expression of a truncated version of the protein. This was carried out due to the fact that previous studies (West, A. unpublished data), had cloned the entire *SHOC1* gene however, no expression of the protein was achieved. This may have been due to the fact the gene product may have been toxic, proving lethal to *E.coli* strains used to induce expression. As a result, cloning of a 726bp *SHOC1* insert from exon 7 was carried out.

Blunt-end cloning of the *SHOC1* PCR fragment into the cloning vector, pCR®-Blunt (Invitrogen), was carried out, which proves advantageous over other cloning vectors

mainly due to the inclusion of the lethal *E.coli ccdB* gene, fused to the C-terminus of LacZα, that ensures low background of non-recombinants. The *lacZα-ccdB* gene fusion is disrupted following the ligation of the blunt PCR insert, therefore only allowing for the growth of positive recombinants following transformation (Bernard *et al*. 1994). Hence, following transformation of *E.coli* DH5α cells with the *SHOC1*-pCR®-Blunt construct, it could be pre-conceived that the colonies visible had been successfully transformed with the recombinant plasmid. However, following colony PCR, it was apparent that one of the colonies analysed did not appear to have been transformed with a recombinant plasmid, as amplification of the SHOC1 DNA insert did not occur (Appendix 3, Fig.1). DNA sequencing of the *SHOC1*-pCR®-Blunt construct was not carried out following plasmid DNA purification, therefore it could not be guaranteed that the gene was free from mutation and had been ligated into the vector in-frame, in the correct orientation. However, as sequencing was carried out once the insert had been cloned into the expression vector, this did not pose too much of a problem and did not affect the reliability of the results obtained.

The pET-21b expression vector was used for the expression of the truncated SHOC1 protein, which proves a beneficial plasmid for protein production. The use of the T7 RNA polymerase within the host expression cell enables the selective induced expression of the gene of interest, with a vast majority of the cells' resources involved in the expression upon induction. Due to the polymerase gene being controlled by the lac-UVS promoter, IPTG can be used as a means to induce expression. The pET-21b plasmid is also advantageous as it confers resistance to the antibiotic, ampicillin, therefore providing a selectable marker to identify positive transformants. In this study, carbenicillin was used as an alternative for ampicillin for liquid cultures.

Carbenicillin is a synthetic analogue of ampicillin, known to be more stable, resulting in fewer satellite colonies (Basker *et al.* 1977).

The *AtASY1* coding region was ligated into the pGEX-6P-1 expression vector. This vector produced recombinant ASY1 with a fusion to a GST peptide at the N-terminus. Armstrong *et al*. (2002) produced an ASY1 protein fused to GST and found that the antibody they had produced did not cross-react with the GST component and was specific for the ASY1 component. On the basis of this, it can be thought that the antibody produced as a result of the present study, will adequately detect ASY1.

The BL21 (DE3) *E.coli* strain was used in this study as a means to induce expression of the SHOC1 and ASY1 proteins. These cells were used as they are known to aid protein production as they are deficient in protease and hence do not degrade proteins as they are generated.

Expression of both SHOC1 and ASY1 was initially carried out at 37°C, in the first test-induction. SDS-PAGE analysis revealed that no expression of SHOC1 had occurred and although ASY1 had appeared to be expressed, it was of a small quantity compared to amounts yielded in previous studies (Armstrong *et al.* 2002). As a result of this, the protocol for inducing expression was optimized. The cultures were subjected to temperatures of 30°C, glucose was added to the media and cultures were prevented from reaching stationary phase by restreaking of BL21 transformants and prevention of cold-shock. This alternative method is usually employed when the proteins expressed are sufficiently toxic. A majority of proteins involved in meiosis, bind to DNA, therefore inhibiting normal functioning of host cells. This may be the case with SHOC1. A basal level of expression is known to be sufficient enough to

prevent the establishment of plasmids and adequate growth of DE3 lysogen bacteria. Grossman *et al*. (1998) describe a method by which regulation of basal expression levels can be ensured. This is achieved through the addition of glucose to the media in which the bacteria are grown in, that prevents the metabolism of alternative carbon sources that causes a rise in cyclic adenosine monophosphate (AMP) levels, resulting in the stimulation of transcription from the lac-UV5 promoter. Preventing growth to stationary phase and addition of glucose to liquid media ensures plasmid stability by significantly decreasing basal transcription and expression levels, thus increasing expression of the target protein following induction with IPTG. SHOC1 and increased amounts of ASY1 proteins were expressed following the use of this alternative method (Appendix 3, Fig.4).

Analysis of expression of SHOC1 by both SDS-PAGE and Western Blotting revealed a band apparent, following induction with IPTG only, with a molecular weight of ~40kDa (Appendix 3, Fig.4; Fig.5). The expected molecular weight of the truncated protein was 27.95kDa. Electrophoretic migration abnormalities may be the reason for the difference in calculated and actual protein size. These abnormalities have been shown to occur with a number of other DNA processing proteins, such as AtRECQ4A (Schröpfer *et al.* 2013) and MUS81-EME1 (Geuting *et al.* 2009). Confirmation that this protein was in fact SHOC1 was achieved via western blot analysis whereby an anti-HisTag probe was used to facilitate the detection of the Histag peptide fused to the SHOC1 protein, as a result of the pET-21b expression vector (Fig.5).

The GST-ASY1 fusion protein accumulated as insoluble inclusion bodies, as the expression of this protein was identified within the insoluble fraction (Appendix 3,

Fig.5). This coincides with results obtained by Armstrong *et al*. (2002) that also found that their recombinant protein was expressed within the insoluble fraction as an inclusion body. Consequently, the HISTAG-SHOC1 fusion protein was expressed within both the soluble and insoluble fractions (Appendix 3, Fig.5). It can be seen there is a larger expression within the soluble fraction 4h post-induction with IPTG that is higher than the expression observed 24h post-induction, as indicated by the band size and intensity. Consequently, the highest level of expression in the insoluble fraction was seen 24h post-induction. Therefore, it can be proposed that the fusion protein is in a soluble form initially, however, over a period of 20h, it accumulates as inclusion bodies within the insoluble fraction.

The large-scale induced expression of both the fusion proteins produced in this study was carried out to yield the highest concentration of protein possible. Thus, proteins were extracted 24h post-induction from the bacterial pellets, and the insoluble fraction. Purification of the insoluble inclusion bodies obtained was carried out via the use of chemical detergents and the application of sheer force by syringing the proteins through a needle. This eliminated a vast amount of contaminating proteins from the sample, as seen by the reduced number of other bands on the SDS-PAGE gels (Figure 6; Appendix 3, Fig.5), and western blot analysis (Fig.7). Although this purity was deemed sufficient for antibody production, additional or alternative purification methods could have been carried out in order to attempt to purify the protein samples further to reduce the majority, if not all contaminants, as quantification of the samples by BioRad assay (Table 14) would have accounted for contaminants in addition to the target proteins. Sonication is a widely used purification method, demonstrated to purify recombinant proteins efficiently to the

point where there is a single band on a coomassie blue stained SDS-PAGE gel, as seen in the data presented by Schröpfer *et al.* (2014). Therefore, this method could have been employed which would have likely achieved purer samples. Moreover, the HisTag affinity tag fused to the SHOC1 recombinant protein could have been utilised for purification purposes, in a one-step method, under totally denaturing conditions that would also enable solubilisation of the protein (Hoffman & Roeder 1991).

The generation of both SHOC1 and ASY1 recombinant proteins, presented in this study, allowing for the production of polyclonal antibodies, will aid research into not only the functions of these specific proteins but also the functions of other meiotic proteins. Armstrong *et al.* (2002) revealed data regarding immunocytological analyses carried out using an antibody specific to an ASY1 recombinant protein, as a means to gain an understanding to the functional role of this protein within meiosis. However, although this has already been carried out, the production of an anti-ASY1 antiserum shown in the present study is of great importance mainly due to the fact that the localisation of ASY1 is used as a tool to investigate the mutant phenotype shown by chromosome behaviour, of other key meiotic proteins. For example, insights into AtSHOC1 function during meiosis, was aided by the use of anti-ASY1 antiserum, which allowed for the chromosome axes to be viewed in *Atshoc1* mutants (Mascaisne *et al*. 2008).

ASY1, otherwise referred to as *Asynaptic 1,* is a gene the mutant phenotype of which is complete failure of chromosome synapsis (Ross *et al.* 1997; Armstrong *et al.* 2002). As a result, no normal pachytene cells are prevalent, and a low residual bivalent frequency is apparent, at late diplotene, with the majority of chromosomes

revealed as univalent (Ross et al. 1997; Sanchez-Moran *et al.* 2001). Polyads, containing uneven chromosome numbers, are formed as a result of the meiotic non-disjunction, from the lack of synapsis. Using an antibody raised against recombinant ASY1, both spatial and temporal distribution was revealed via immunolocalisation analysis. The data obtained revealed that a continuous signal was present throughout leptotene and zygotene, that disappears simultaneously with desynapsis of the homologous chromosomes (Armstrong *et al*. 2002). Analysis using immunogold labelling enabled the realisation that the protein localises to discrete points, associated with the axial and lateral elements, associated with chromatin (Armstrong *et al*. 2002). Localization analyses and the mutant phenotype of ASY1, allowed for the proposal to be made that this protein had a possible function in homologous chromosome juxtaposition, defects of which results in the asynaptic phenotype identified, or the recruitment of the bases of the chromatin loops to the proteinaceous structure developed in G2 (Armstrong *et al.* 2002; Ferdous *et al.* 2012).

AtASY1 is comprised of a HORMA region over the first 250 amino acids. This domain has been identified in a number of proteins that interact directly with chromatin (Aravind & Koonin 1998), including the ASY1 yeast homologue, Hop1. A reduction in meiotic recombination is a feature prominent in yeast *Hop1* mutants (Hollingsworth & Byers 1989). Hop1 is able to bind to DNA (Hollingsworth *et al.* 1990), with suggestions that the HORMA domain may participate in DNA-binding activity (Kironmai *et al.* 1998). Hop1 has been shown to associate with the chromosome axes, with discontinuous loading initially during leptotene, which progresses to domain-like organisation that is most apparent when synapsis is complete, at

pachytene. The ZMM protein, Zip1, in budding yeast, also exhibits this domain-like organization onto the chromosomes (Börner *et al.* 2008). It is thought that CO designation dictates the loading of both Hop1 and Zip1, with Zip1 being loaded as a result of a pre-existing Hop1 pattern (Börner *et al.* 2008).

Pch2, an ATPase that couples both the binding and hydrolysis of ATP, in order to induce conformational changes on its substrates (Hanson & Whiteheart 2005), has been found to bind Hop1, in yeast. This interaction coincides with a proposed model in which the localisation of Hop1 is restricted to specific chromosomal regions, by the remodelling of the protein by Pch2. Therefore, interhomologue repair is promoted at CO designation sites, following the chromosomal organization deciphered by Pch2 (Chen *et al*. 2013). *In vitro*-binding assays using purified proteins, identified weak binding of GST tagged-Pch2 with Hop1 that were transient in the presence of ATP and would therefore prove challenging to detect *in vivo* (Chen *et al*. 2013).

As a result of these findings, a Y2H analysis was carried out in this present study, in order to test whether the *A.thaliana* PCH2 ortholog interacts with the *Arabidopsis* functional homolog of Hop1, ASY1. A number of other key meiosis specific proteins were also tested for interactions with AtPCH2, contributing to the functional analysis of this protein within the control of meiotic recombination. The results of the Y2H analysis revealed that AtPCH2 did not interact with AtASY1, as was apparent for the yeast homologues (Chen *et al.* 2013).

Subsequently, AtPCH2 was not found to interact with the Zip1 *Arabidopsis* homologue, ZYP1. This TF protein is comprised of two globular domains, separated by a coiled-coil domain (Higgins *et al.* 2005), a structure which is highly conserved

among all TF proteins identified in a wide range of eukaryotes (Meuwissen *et al*. 1992; Dong & Roeder 2000; Anderson *et al*. 2005; Schild-Prüfert *et al.* 2011). The rice (*Oryza sativa*) orthologue of PCH2, CENTRAL REGION COMPONENT 1 (CRC1), was found to interact with ZEP1, the rice ZYP1 ortholog, in Y2H assays (Miao *et al*. 2014). Therefore, the rice PCH2 homologue is thought to be a component of the SC. Although the SC is a highly conserved structure among eukaryotes, there is poor conservation at the sequence level of the components identified. As a result, difference in primary sequences between the rice and *Arabidopsis* orthologues, may be an explanation as to why interactions occur between the homologues in one species and not another.

Y2H analysis did reveal that *Arabidopsis* PCH2 self-interacts, an interaction that can be considered strong, as demonstrated by growth on both TDO and QDO media (Fig.8). Chen *et al.* (2013) found that Pch2 self-interacts in budding yeast, owing to the oligomerization of this protein into single hexameric rings that comprise of a central pore, essential for its functional role in meiosis. As a result, it can be suggested that this essential feature of PCH2 is conserved in *Arabidopsis*, due to the self-interaction observed in both the flowering plant and yeast.

Throughout the Y2H analysis, it was apparent that slower growth of yeast occurred when yeast cells were transformed with the construct whereby AtPCH2 was fused to the activating domain, compared to that observed with PCH2 fused to the binding domain (Fig.8A). This observation may be representative of the functional role of AtPCH2, in that when AtPCH2 is fused to the binding domain, the protein is bound to the GAL4 promoter and thus restricted in its capability to bind other loci within the

cell. However, when fused to the activating domain, the protein is free to bind other loci, causing damage to the yeast cells, allowing for a slower growth of the organism. As a result of this slower growth seen in this study, it proved advantageous to clone *PCH2* into both of the cloning vectors, pGAD and pGBK, as if the coding sequence would have just been ligated into the pGAD vector, the slow growth of the yeast could have enabled for the assumption to be made that the transformation had not been successful at all.

Moreover, AtPRD3 interacted with AtPCH2, when AtPCH2 was fused to the binding domain only, after 1.5 days incubation of the yeast (Fig.9). AtPRD3 is a DSB-forming factor known to function alongside SPO11 (De Muyt *et al.* 2009), interacting with AtASY1, linking break complexes to the axis (Osman *et al.* 2011; Franklin *et al.* Unpublished Data). A possible interaction between AtPRD3 and AtPCH2 provides valuable insights into the functional role of these two proteins. This interaction is consistent with that observed in rice, whereby the orthologues of PRD3 and PCH2, PAIR1 (Nonomura *et al*. 2004) and CRC1 respectively, were also found to interact, possibly forming a complex that promotes the formation of DSBs during meiotic recombination (Miao *et al*. 2013). Therefore, the formation of such complex could be conserved in *Arabidopsis*, suggesting a similar role for AtPCH2 and AtPRD3.

Mutagenesis of the AtPCH2 coding sequence in order to form the mutant variant, PCH2 E291Q, was also carried out in this study in order to further test interactions via Y2H analysis. Chen *et al.* (2013) identified that the introduction of a mutagen within the Walker B domain, is associated with a dominant negative phenotype. Mutagens within this domain are known to disrupt the ATP hydrolysis activity of an

ATPase, with no alteration to the ATP binding function (Hanson & Whiteheart 2005). Mutated Pch2 allows for an ATP-bound state whereby the interaction of the ATPase and its substrate is locked (Brosh & Matson 1995). Chen *et al*. (2013) revealed that in the presence of ATP, Pch2 with a mutation in the Walker B domain interacted strongly with Hop1, in budding yeast. The mutagenesis of Pch2 also enabled the proposal to be made that the ATP hydrolysis activity of this protein is required for the DNA-binding stimulation of Hop1 (Chen *et al*. 2013). The fact that no interaction between AtASY1 and AtPCH2 E291E was observed in this present study could indicate no conservation of the interaction between the *Arabidopsis* homologues of these two proteins. This would imply that AtPCH2 does not promote inter-homolog bias, via the remodelling of AtASY1, as reported in yeast. On the other hand, it may have been the case that the interaction in *Arabidopsis* between these two proteins is significantly weaker, and therefore could not be detected via Y2H.

As a possible interaction between AtPCH2 and AtPRD3 was shown by Y2H analysis, it would be interesting to test whether this interaction is dependent on the ATP hydrolytic activity of AtPCH2, via mutation of the ATPase, in order to analyse this interaction further.

Mutated AtPCH2 still self-interacts (Fig.11), however, it can be deduced that when compared to the yeast seen with non-mutated PCH2 (Fig.8), that the yeast is slightly more pink in colour (Fig.11). This may be due to an accumulation of adenine, hence hinting at a weaker self-interaction of PCH2 E291Q, compared to PCH2.

As a result of the data presented in this study, it was revealed that AtPCH2 and AtASY1 do not interact directly when analysed via Y2H, as was observed for their

yeast homologues (Chen *et al*. 2013). The reason for this may be due to a modification of AtASY1 required to permit the interaction, such as phosphorylation of the protein. Another possible explanation may be that the interaction seen in yeast, involves the non-classical DNA-binding domain that is found within Hop1, but is not conserved within AtASY1. AtASY1 has a SWIRM domain instead of a zinc-finger domain (Hollingsworth *et al.* 1990; Armstrong *et al*. 2002). Consequently, it may just be the case that the *Arabidopsis* homologues do not interact, suggesting an alternative function in meiotic recombination, which may be a result of the functional divergence observed by many *A.thaliana* proteins, resulting from the genome duplication event (Arabidopsis Genome Initiative 2000). Nevertheless, it is now known that AtASY1 is depleted by AtPCH2 from the axes as synapsis occurs, with this remodelling being crucial for the control of CO distribution (Franklin *et al.* Unpublished Data).

Future work regarding the data presented in this study should focus on further functional analyses of AtSHOC1, in terms of its function in the formation of Class I COs, utilising the antibody produced in this study. In addition to this, further investigations into the functional role of AtPCH2, by inferring protein-interactions should be carried out, and alternative methods should be employed, other than Y2H analyses, in order to extend the data presented. One such possible method is immunoprecipitation, whereby possible investigations into interactions between phosphorylated and non-phosphorylated forms of the AtASY1 protein could be carried out.

Conclusions

The mechanisms underpinning meiotic recombination are known to be mediated by the functions of numerous proteins, the vast majority of which are conserved between eukaryotic species. Analysis of such meiotic proteins in *A.thaliana* has increased over recent years. In this study, the production of recombinant AtASY1 and AtSHOC1, was carried out, whereby an optimized method of SHOC1 expression was established. The resultant production of antibodies, will permit immunolocalisation analyses of these and other proteins, thus providing further insights into the functional roles of proteins, allowing for a greater understanding of the control of meiotic recombination in plants. This study also indicated that AtPCH2 and AtASY1 do not interact, as displayed by their yeast homologues, thus indicating the need for further research to demonstrate possible reasons as to why this is not conserved between species. Interestingly, this study identified an interaction between AtPRD3 and AtPCH2, coinciding with an interaction identified between the rice homologues. Research regarding the control of meiotic recombination is of great importance; due to the beneficial impact this potentially has on increasing genetic variation available to plant breeders. Genetic variation that can be exploited by plant breeders is often limited by the fact that COs predominantly occur towards the ends of chromosomes and a large proportion of genes rarely recombine. Therefore, knowledge to permit the manipulation of the control of meiotic recombination would prove invaluable to enabling plant breeders to employ classical breeding techniques to select for favourable traits, hence contributing to food security efforts.

References

Albini, S.M. & Jones, G.H. (1984) Synaptonemal complex-associated centromeres and recombination nodules in plant meiocytes prepared by an improved surface-spreading technique. *Exp Cell Res.* 155 (2): 588-592.

Allers, T. & Lichten, M. (2001) Differential timing and control of noncrossover and crossover recombination during meiosis. *Cell*. 106: 47–57.

Anderson, L.K., Royer, S.M., Page, S.L., McKim, K.S., Lai, A., Lilly, M.A., & Hawley, R.S. (2005) Juxtaposition of C(2)M and the transverse filament protein C(3)G within the central region of Drosophila synaptonemal complex. *Proc. Natl. Acad. Sci. USA.* 102: 4482–4487.

***Arabidopsis* Genome Initiative** (2000) *Nature.* 408: 796-815.

Aravind, L. & Koonin, E.V. (1998) The HORMA domain: a common structural and denominator in mitotic checkpoints, chromosome synapsis and DNA repair. *Trends in Biochemical Science.* 23: 284-286.

Armstrong, S.J., Franklin, F.C. & Jones, G.H. (2001) Nucleolus-associated telomere clustering and pairing precede meiotic chromosome synapsis in Arabidopsis thaliana. *J Cell Sci.* 114 (23): 4207-4217.

Armstrong, S.J., Caryl, A.P., Jones, G.H. & Franklin, F.C.H. (2002) Asy1, a protein required for meiotic chromosome synapsis, localizes to axis-associated chromatin in Arabidopsis and Brassica. *J Cell Sci*.115 (18): 3645-3655.

Armstrong, S.J., Franklin, F.C.H. & Jones, G.H. (2003) A meiotic time-course for *Arabidopsis thaliana. Sexual Plant Reproduction*. 16: 141–149.

Bai, X., Peirson, B.N., Dong, F., Xue, C. & Makaroff, C.A. (1999) Isolation and characterization of SYN1, a RAD21-like gene essential for meiosis in *Arabidopsis*. *Plant Cell.* 11 (3): 417-430.

Barakate, A., Higgins, J.D., Vivera, S., Stephens, J., Perry, R.M., Ramsey, L., Colas, I., Oakey, H., Waugh, R., Franklin, F.C.H., Armstrong, S.J. & Halpina, C. (2014) The Synaptonemal Complex Protein ZYP1 Is Required for Imposition of Meiotic Crossovers in Barley. *The Plant Cell.* [Online] tpc.113.121269: 1-12. Available from: http://www.plantcell.org/content/early/2014/02/21/tpc.113.121269.full.pdf+html [Accessed 25th February 2014].

Basker, M.J., Comber, K.R., Sutherland, R. & Valler, G.H. (1977) Carfecillin: antibacterial activity *in vitro* and *in vivo*. *Chemotherapy.* 23 (6): 424–35.

Bass, H.W., Riera-Lizarazu, O., Ananiev, E.V., Bordoli, S.J., Rines, H.W., Phillips, R.L., Sedat, J.W., Agard, D.A. & Cande, W.Z. (2000) Evidence for the coincident initiation of homolog pairing and synapsis during the telomere-clustering (bouquet) stage of meiotic prophase. *J Cell Sci*.113 (6): 1033-1042.

Berchowitz, L.E., Francis, K.E., Bey, A.L. & Copenhaver, G.P. (2007) The role of AtMUS81 in interference-insensitive crossovers in *A.thaliana. PLoS Genet*. 3: e132.

Berchowitz, L. E. & Copenhaver, G.P. (2010) Genetic interference: don't stand so close to me. *Curr. Genomics.* 11: 91-102.

Bernard, P., Gabant, P., Bahassi, E. M., & Couturier, M. (1994) Positive Selection Vectors Using the F Plasmid *ccdB* Killer Gene. *Gene.* 148: 71-74.

Bleuyard, J.Y., Gallego, M.E. & White, C.I. (2004) Meiotic defects in the Arabidopsis rad50 mutant point to conservation of the Mrx complex function in early stages of meiotic recombination. *Chromosoma.* 113: 197–203.

Bishop, D.K. (1994) RecA homologs Dmc1 and Rad51 interact to form multiple nuclear complexes prior to meiotic chromosome synapsis. *Cell.* 79 (6): 1081-1092.

Bishop, D.K. & Zickler, D. (2004) Early decision: meiotic crossover interference prior to stable strand exchange and synapsis. *Cell.* 117 (1): 9-15.

Bonnet, S., Knoll, A., Hartung, F. & Puchta, H. (2013) Different functions for the domains of the *Arabidopsis thaliana* RMI1 protein in DNA cross-link repair, somatic and meiotic recombination. *Nucleic Acids Research.* 1-12. doi:10.1093/nar/gkt730.

Börner, G.V., Kleckner, N. & Hunter, N. (2004) Crossover/noncrossover differentiation, synaptonemal complex formation, and regulatory surveillance at the leptotene/zygotene transition of meiosis. *Cell.* 117 (1): 29-45.

Börner, G.V., Barot, A. & Kleckner, N. (2008) Yeast Pch2 promotes domainal axis organization, timely recombination progression, and arrest of defective recombinosomes during meiosis*. Proc Natl Acad Sci USA.* 105 (9): 3327-3332.

Brosh, R.M. Jr. & Matson, S.W. (1995) Mutations in motif II of *Escherichia coli* DNA helicase II render the enzyme nonfunctional in both mismatch repair and excision repair with differential effects on the unwinding reaction. *J Bacteriol.* 177 (19): 5612-5621.

Bundock, P. & Hooykaas, P. (2002) Severe developmental defects, hypersensitivity to DNA-damaging agents, and lengthened telomeres in Arabidopsis mre11 mutants. *Plant Cell*. 14: 2451–2462.

Cai, X., Dong, F., Edelmann, R.E. & Makaroff, C.A. (2003) The *Arabidopsis* SYN1 choesin protein is required for sister chromatid arm cohesion and homologous chromosome pairing. *J Cell Sci.* 116: 2999-3007.

Caryl, A.P., Armstrong, S.J., Jones, G.H. & Franklin, F.C.H. (2000) A homologue of the yeast HOP1 gene is inactivated in the Arabidopsis meiotic mutant asy1. *Chromosoma.* 109 (1-2): 62-71.

Caryl, A.P., Jones, G.H. & Franklin, F.C.H. (2003) Dissecting plant meiosis using *Arabidopsis thaliana* mutants. *Journal of Experimental Botany*. 54(380): 25-38.

Chakraborty, S. & Newton, A.C. (2011) Climate change, plant diseases and food security: an overview. *Plant Pathology*. 60: 2-14.

Chelysheva, L. (2005) AtREC8 and AtSCC3 are essential to the monopolar orientation of the kinetochores during meiosis. *Journal of Cell Science.* 118 (20): 4621-4632.

Chen, Z., Higgins, J.D., Hui, J.T.L., Li, J., Franklin, F.C.H. & Berger, F. (2011) Retinoblastoma protein is essential for early meiotic events in *Arabidopsis*. *EMBO Journal.* doi: 10.1038/emboj.2010.344.

Chen, C., Jomaa, A., Ortega, J. & Alani, E.E. (2014) Pch2 is a hexameric ring ATPase that remodels the chromosome axis protein Hop1. *PNAS*. 111 (1): E44-E53.

Chi, P., San Filippo, J., Sehorn, M.G., Petukhova, G.V. & Sung, P. (2007) Bipartite stimulatory action of the Hop2-Mnd1 complex on the Rad51 recombinase. *Genes Dev.* 21 (14): 1747-1757.

Chikashige. Y. & Hiraoka, Y. (2001) Telomere binding of the Rap1 protein is required for meiosis in fission yeast. *Curr. Biol*.11: 1618–1623.

Chikashige, Y., Tsutsumi, C., Yamane, M., Okamasa, K., Haraguchi, T. & Hiraoka, Y. (2006) Meiotic Proteins Bqt1 and Bqt2 Tether Telomeres to Form the Bouquet Arrangement of Chromosomes. *Cell.* 125 (1): 59-69.

Chua, P.R. & Roeder, G.S. (1998) Zip2, a meiosis-specific protein required for the initiation of chromosome synapsis. *Cell*. 93: 349-359.

Church, K. & Moens, P.B. (1976) Centromere behavior during interphase and meiotic prophase in Allium fistulosum from 3-D, EM reconstruction. *Chromosoma.* 56: 249–263.

Cloud, V., Chan, Y.L., Grubb, J., Budke, B. & Bishop, D.K. (2012) Rad51 is an accessory factor for Dmc1-mediated joint molecule formation during meiosis. *Science.* 337 (6099): 1222-1225.

Cole, F., Keeney, S. & Jasin, M. (2010) Evolutionary conservation of meiotic DSB proteins: more than just Spo11. *Genes & Development.* 24 (12): 1201-1207.

Cooper, J.P., Nimmo, E.R., Allshire, R.C. & Cech, T.R. (1997) Regulation of telomere length and function by a Myb-domain protein in fission yeast. *Nature*. 385: 744–747.

Couteau, F., Belzile, F., Horlow, C., Grandjean, O., Vezon, D. & Doutriaux, M.P. (1999) Random chromosome segregation without meiotic arrest in both male and female meiocytes of a dmc1 mutant of Arabidopsis. *Plant Cell.* 11: 1623–1634.

Daoudal-Cotterell, S., Gallego, M.E. & White, C.I. (2002) The plant Rad50–Mre11 protein complex. *Febs Letters.* 516: 164–166.

De Muyt, A., Vezon, D., Gendrot, G., Gallois, J.L., Stevens, R. & Grelon, M. (2007) AtPRD1 is required for meiotic double strand break formation in *Arabidopsis thaliana. EMBO J*. 26 (18): 4126-4137.

De Muyt, A., Pereira, L., Vezon, D., Chelysheva, L., Gendrot, G., Chambon, A., Laine-Choinard, S., Pelletier, G., Mercier, R., Nogue, F. & Grelon, M. (2009) A high throughput genetic screen identifies new early meiotic recombination functions in *Arabidopsis thaliana. PLoS Genet*. 5 (9): e1000654.

Ding, D-Q., Yamamoto, A., Haraguchi, T. & Hiraoka, Y. (2004) Dynamics of Homologous Chromosome Pairing during Meiotic Prophase in Fission Yeast. *Developmental Cell*. 6: 329-341.

Dong, H., & Roeder, G.S. (2000) Organization of the yeast Zip1 protein within the central region of the synaptonemal complex. *J. Cell Biol.* 148: 417–426.

Dresser, M.E. (2000) Meiotic chromosome behavior in *Saccharomyces cerevisiae* and (mostly) mammals*. Mutation Research.* 451: 107-127.

Farmer, S., Hong, E-J, E., Leung, W-K., Argunhan, B., Terentyev, Y., Humphryes, N., Toyoizumi, H. & Tsubouchi, H. (2012) Budding yeast Pch2, a widely conserved meiotic protein, is involved in the initiation of meiotic recombination. *PLos ONE.* 7 (6): e39724.

Ferdous, M., Higgins, J.D., Osman, K., Lambing, C., Roitinger, E., Mechtler, K., Armstrong, S.J., Perry, R., Pradillo, M., Cuñado, N. & Franklin, C. (2012) Inter-homolog crossing-over and synapsis in Arabidopsis meiosis are dependent on the chromosome axis protein AtASY3. *PLoS Genet.* [Online] 8 (2): e1002507. Available from: http://www.plosgenetics.org/article/info%3Adoi%2F10.1371%2Fjournal.pgen.1002507 [Accessed 25th August 2014].

Fernandez-Capetillo, O., Mahadevaiah, S.K., Celeste, A., Romanienko, P.J., Camerini-Otero, R.D., Bonner, W.M., Manova, K., Burgoyne, P. L. & Nussenzweig, A. (2003) H2AX is required for chromatin remodeling and inactivation of sex chromosomes in male mouse meiosis. *Dev Cell*. 4 (4): 497-508.

Foss, E., Lande, R., Stahl, F.W. & Steinberg, C.M. (1993) Chiasma interference as a function of genetic distance. *Genetics*. 133: 681–691.

Gallego, M.E., Jeanneau, M., Granier, F., Bouchez, D., Bechtold, N. & White, C.I. (2001) Disruption of the Arabidopsis RAD50 gene leads to plant sterility and mms sensitivity. *Plant Journal.* 25: 31–41.

Geuting, V., Kobbe, D., Hartung, F., Durr, J., Focke, M. & Puchta, H. (2009) Two distinct MUS81-EME1 complexes from *Arabidopsis* process Holliday junctions. *Plant Physiol.* 150: 1062-1071.

Grelon, M., Vezon, D., Gendrot, G. & Pelletier, G. (2001) AtSPO11-1 is necessary for efficient meiotic recombination in plants. *EMBO J.* 20 (3): 589-600.

Grossman, T.H., Kawasaki, E.S., Punreddy, S.R. & Osburne, M.S. (1998) Spontaneous cAMP-dependent derepression of gene expression in stationary phase plays a role in recombinant expression instability. *Gene.* 209: 95–103.

Gruber, S., Haering, C.H. & Nasmyth, K. (2003) Chromosomal cohesin forms a ring. Cell. 112 (6): 765–777.

Haering, C.H., Löwe, J., Hochwagen, A. & Nasmyth, K. (2002) Molecular Architecture of SMC Proteins and the Yeast Cohesin Complex. *Molecular Cell.* 9: 773-788.

Hanson, P.I. & Whiteheart, S.W. (2005) AAA+ proteins: Have engine, will work. *Nat Rev Mol Cell Biol*. 6 (7): 519-529.

Hartung, F. & Puchta, H. (2001) Molecular characterization of homologues of both subunits A (SPO11) and B of the archaebacterial topoisomerase 6 in plants. *Gene.* 271 (1): 81-86.

Heyting, C. (1996) Synaptonemal complexes: structure and function. *Curr Opin Cell Biol.* 8:389–396.

Higgins, J.D., Armstrong, S.J., Franklin, F.C.H. & Jones, G.H. (2004) The Arabidopsis MutS homolog AtMSH4 functions at an early step in recombination: evidence for two classes of recombination in Arabidopsis. *Genes & Development.* 18: 2557–2570.

Higgins, J.D., Sanchez-Moran, E., Armstrong, S.J., Jones, G.H. & Franklin, F.C. H. (2005) The Arabidopsis synaptonemal complex protein ZYP1 is required for chromosome synapsis and normal fidelity of crossing over. *Genes & Development.* 19 (20): 2488-2500.

Higgins, J.D., Vignard, J., Mercier, R., Pugh, A.G., Franklin, F.C.H. & Jones, G.H. (2008a) AtMSH5 partners AtMSH4 in the class I meiotic crossover pathway in *Arabidopsis thaliana,* but is not required for synapsis. *Plant Journal.* 55: 28–39.

Higgins, J.D., Buckling, E.F., Franklin, F.C.H. & Jones, G.H. (2008b) Expression and functional analysis of AtMUS81 in Arabidopsis meiosis reveals a role in the second pathway of crossing-over. *Plant Journal.* 54: 152–162.

Hiraoka, Y. & Dernburg, A.F. (2009) The sun rises on meiotic chromosome dynamics. *Developmental Cell.* 17: 598–605.

Ho, H-C. & Burgess, S.M. (2011) Pch2 acts through Xrs2 and Tel1/ATM to modulate interhomolog bias and checkpoint function during meiosis. *PLoS Genet.* 7 (11): e1002351.

Hochwagen, A. (2008) Meiosis. *Curr Biol.* 18 (15): R641-R645.

Hoffman, A. & Roeder, R.G. (1991) Purification of his-tagged proteins in non-denaturing conditions suggests a convenient method for protein interaction studies. *Nucleic Acids Research.* 19 (22): 6337-6338.

Holliday, R. (1964) A mechanism for gene conversion in fungi. *Genet. Res.* 5: 282-304.

Hollingsworth, N.M. & Byers, B. (1989) *Hop1*: a yeast meiotic pairing gene. *Genetics.* 121: 445-462.

Hollingsworth, N.M., Goetsch, L. & Byers, B. (1990) The *Hop1* gene encodes a meiosis-specific component of yeast chromosomes. *Cell.* 61: 73-84.

Jones, G.H & Franklin, F.C. (2006) Meiotic crossing-over: obligation and interference. *Cell*. 126: 246–248.

Joshi, N., Barot, A., Jamison, C. & Borner, G.V. (2009) Pch2 links chromosome axis remodelling at future crossover sites and crossover distribution during yeast meiosis. *PLos Genet.* 5 (7): e1000557.

Kanoh, J. & Ishikawa, F. (2001) spRap1 and spRif1, recruited to telomeres by Taz1, are essential for telomere function in fission yeast. *Curr. Biol.* 11: 1624-1630.

Keeney, S., Giroux, C.N. & Kleckner, N. (1997) Meiosis-specific DNA double-strand breaks are catalyzed by Spo11, a member of a widely conserved protein family. *Cell.* 88 (3): 375-384.

Kerzendorfer, C. (2006) The Arabidopsis thaliana MND1 homologue plays a key role in meiotic homologous pairing, synapsis and recombination. *Journal of Cell Science.* 119 (12): 2486-2496.

King, J.S. & Mortimer, R.K. (1990) A polymerization model of chiasma interference and corresponding computer simulation. *Genetics.* 126: 1127–1138.

Kironmai, K.M., Muniyappa, K., Freidman, D.B., Hollingsworth, N.M. & Byers, B. (1998) DNA-binding activities of Hop1 protein, a synaptonemal complex component from *Saccharomyces cerevisiae*. *Molecular and Cell Biology.* 18: 1424-1435.

Kleckner, N. (2006) Chiasma formation: chromatin／axis interplay and the role(s) of the synaptonemal complex. *Chromosoma.* 115: 175–194.

Kleckner, N., Zickler, D., Jones, G.H., Dekker, J., Padmore, R., Henle, J. & Hutchinson, J. (2004) A mechanical basis for chromosome function. *Proc Natl Acad Sci U S A.* 101: 12592–12597.

Klein, F., Mahr, P., Galova, M., Buonomo, S.B.C., Michaelis, C., Nairz, K. & Nasmyth, K. (1999) A Central Role for Cohesins in Sister Chromatid Cohesion Formation of Axial Elements, and Recombination during Yeast Meiosis. *Cell.* 98 (1): 91-103.

Kumar, R. & De Massy, B. (2010) Initiation of Meiotic Recombination in Mammals. *Genes.* 1 (3): 521-549.

Kurzbauer, M.T., Uanschou, C., Chen, D. & Schlogelhofer, P. (2012) The recombinases DMC1 and RAD51 are functionally and spatially separated during meiosis in Arabidopsis. *Plant Cell.* 24 (5): 2058-2070.

Lande, R. & Stahl, F.W. (1993) Chiasma interference and the distribution of exchanges in Drosophila melanogaster. *Cold Spring Harb Symp Quant Biol.* 58: 543–552.

Lam, W.S. (2005) Characterization of *Arabidopsis thaliana* SMC1 and SMC3: evidence that AtSMC3 may function beyond chromosome cohesion. *Journal of Cell Science.* 118 (14): 3037-3048.

Lee, J.Y. & Orr-Weaver, T.L. (2001) The molecular basis of sister-chromatid cohesion. *Annu. Rev. Cell Dev. Bio.* 17: 753-777.

Lee, C.Y., Conrad, M.N. & Dresser, M.E. (2012) Meiotic chromosome pairing is promoted by telomere-led chromosome movements independent of bouquet formation. *PLoS Genet.* 8 (5): e1002730.

Li, W.X., Chen, C.B., Markmann-Mulisch, U., Timofejeva, L., Schmelzer, E., Ma, H. & Reiss, B. (2004) The Arabidopsis AtRAD51 gene is dispensable for vegetative development but required for meiosis. *Proceedings of the National Academy of Sciences, USA.* 101: 10596–10601.

Link, J., Leubner, M. Schmitt, J., Göb, E., Benavente, R., Jeang, K-T., Xu, R. & Alsheimer, M. (2014) Analysis of Meiosis in SUN1 Deficient Mice Reveals a Distinct Role of SUN2 in Mammalian Meiotic LINC Complex Formation and Function. *PLOS*

GENETICS. [Online] 10(2): e1004099. Available from: http://www.plosgenetics.org/article/fetchObject.action?uri=info%3Adoi%2F10.1371%2Fjournal.pgen.1004099&representation=PDF [Accessed 24th August 2014].

Loidl, J. (1990) The initiation of meiotic chromosome pairing: the cytological view. *Genome.* 33 (6): 759-778.

Lynn, A., Soucek, R., & Börner, G.V. (2007). ZMM proteins during meiosis: Crossover artists at work. *Chromosome Res*. 15: 591–605.

Macaisne, N., Novatchkova, M., Peirera, L., Vezon, D., Jolivet, S., Froger, N., Chelysheva, L., Grelon, M. & Mercier, R. (2008) SHOC1, an XPF endonuclease-related protein, is essential for the formation of class I meiotic crossovers. *Current Biology.* 18: 1432–1437.

MacQueen, A.J., Phillips, C.M., Bhalla, N., Weiser, P., Villeneuve, A.M. & Dernburg, A.F. (2005) Chromosome Sites Play Dual Roles to Establish Homologous Synapsis during Meiosis in *C. elegans. Cell.* 123 (6): 1037-1050.

Martini, E., Diaz, R.L., Hunter, N. & Keeney, S. (2006) Crossover homeostasis in yeast meiosis. *Cell.* 126: 285–295.

Mercier, R., Grelon, M., Vezon, D., Horlow, C. & Pelletier, G. (2001) How to characterize meiotic functions in plants? *Biochimie.* 83: 1023-1028.

Mercier, R., Jolivet, S., Vezon, D., Huppe, E., Chelysheva, L., Giovanni, M., Nogué, F., Doutriaux, M.P., Horlow, C., Grelon, M. & Mézard, C. (2005) Two

meiotic crossover classes cohabit in *Arabidopsis:* one is dependent on Mer3, whereas the other one is not. *Current Biology.* 15: 692–701.

Meuwissen, R.L.J., Offenberg, H.H., Dietrich, A.J.J., Riesewijk, A., van Iersel, M., & Heyting, C. (1992) A coiled-coil related protein specific for synapsed regions of meiotic prophase chromosomes. *EMBO J*. 11: 5091–5100.

Miao, C., Tang, D., Zhang, H., Wang, M., Li, Y., Tang, S., Yu, H., Gu, M. & Chenga, Z. (2013) CENTRAL REGION COMPONENT1, a Novel Synaptonemal Complex Component, Is Essential for Meiotic Recombination Initiation in Rice. *The Plant Cell.* 25: 2998–3009

Mimitou, E.P. & Symington, L.S. (2009) DNA end resection: Many nucleases make light work. *DNA Repair.* 8 (9): 983-995.

Moses, M.J. (1956) Chromosomal structures in crayfish spermatocytes. *J Cell Biol*. 2:215–218.

Nasmyth, K. (2001) Disseminating the genome: joining, resolving, and separating sister chromatids during mitosis and meiosis. *Annu. Rev. Genet.* 35: 673–745.

Neale, M.J., Pan, J. & Keeney, S. (2005) Endonucleolytic processing of covalent protein-linked DNA double-strand breaks. *Nature.* 436: 1053–1057.

Nimmo, E.R., Pidoux, A.L., Perry, P.E., & Allshire, R.C. (1998) Defective meiosis in telomere-silencing mutants of *Schizosaccharomyces pombe. Nature.* 392: 825–828.

Nonomura, K.I., Nakano, M., Fukuda, T., Eiguchi, M., Miyao, A., Hirochika, H., & Kurata, N. (2004) The novel gene *HOMOLOGOUS PAIRING ABERRATION IN RICE MEIOSIS1* of rice encodes a putative coiled-coil protein required for homologous chromosome pairing in meiosis. *Plant Cell*. 16: 1008–1020.

Novak, I., Wang, H., Revenkova, E., Jessberger, R., Scherthan, H. & Höön, C. (2008) Cohesin SMC1β determines meiotic chromatin axis loop organization. *The Journal of Cell Biology.* 180 (1): 83-90.

Ober, E.S., Bloa, M.L., Clark, C.J.A., Royal, A., Jaggard, K.W. & Pidgeon, J.D. (2005) Evaluation of physiological traits as indirect selection criteria for drought tolerance in sugar beet. *Field Crops Research.* 91: 231-249.

Osman, K., Higgins, J.D., Sanchez-Moran, E., Armstrong, S.J. & Franklin, F.C.H. (2011) Pathways to meiotic recombination in *Arabidopsis thaliana. New Phytologist.* 190: 525-544.

Page, S.L. & Hawley, R.S. (2003) Chromosome choreography: the meiotic ballet. *Science.* 301: 785-789.

Page, S.L. & Hawley, R.S. (2004) The genetics and molecular biology of the synaptonemal complex. *Annual Review of Cell and Developmental Biology.* 20: 525–558.

Petronczki, M., Siomos, M.F. & Nasmyth, K. (2003) Un Ménage à quatre: the molecular biology of chromosome segregation in meiosis. *Cell.* 112: 423-440.

Prieto, I., Suja, J.A., Pezzi, N., Kremer, L., Martínez-A, C., Rufas, J.S. & Barbero, J.L. (2001) Mammalian STAG3 is a cohesin specific to sister chromatid arms in meiosis I. *Nature Cell Biol.* 3: 761–766.

Puizina, J., Siroky, J., Mokros, P., Schweizer, D. & Riha, K. (2004) MRE11 deficiency in Arabidopsis is associated with chromosomal instability in somatic cells and SPO11-dependent genome fragmentation during meiosis. *Plant Cell.* 16: 1968–1978.

Reider, C.L. & Salmon, E.D. (1998) The vertebrate cell kinetochore and its role during mitosis. *Trends Cell Biol*. 8: 310-318.

Reider, C.L. & Cole, R. (1999) Chromatid cohesion during mitosis: lesson from meiosis. *J. Cell Sci.* 112: 2607-2613.

Rockmill, B., Sym, M., Scherthan, H. & Roeder, G.S. (1995) Roles for two RecA homologs in promoting chromosome synapsis. *Genes Dev.* 9: 2684–95.

Roeder, G.S. (1997) Meiotic chromosomes: it takes two to tango. *Genes and Development.* 11: 2600-2621.

Ross-Macdonald, P. & Roeder, G.S. (1994) Mutation of a meiosis-specific MutS homolog decreases crossing over but not mismatch correction. *Cell.* 79: 1069–1080.

Ross, K. J., Fransz, P., Armstrong, S. J., Vizir, I., Mulligan, B., Franklin, F. C. H. & Jones, G. J. (1997) Cytological characterisation of four meiotic mutants of *Arabidopsis* isolated from T-DNA transformed lines. *Chromosome Res.* 5: 551-559.

San Filippo, J., Sung, P. & Klein, H. (2008) Mechanism of Eukaryotic Homologous Recombination. *Annual Review of Biochemistry.* 77 (1): 229-257.

Sanchez-Moran, E., Armstrong, S.J., Santos, J.L., Franklin, F.C.H. & Jones, G.H. (2001) Chiasma formation in *Arabidopsis thaliana* accession Wassileskija and in two meiotic mutants. *Chromosome Research.* 9: 121-128.

Sanchez-Moran, E., Santos, J.L., Jones, G.H. & Franklin, F.C.H. (2007) ASY1 mediates AtDMC1-dependent interhomolog recombination during meiosis in Arabidopsis. *Genes Dev.* 21 (17): 2220-2233.

Scherthan, H. (2001) A bouquet makes ends meet. Nature Reviews Molecular Cell Biology. 2: 621-627.

Schild-Prüfert, K., Saito, T.T., Smolikov, S., Gu, Y., Hincapie, M., Hill, D.E., Vidal, M., McDonald, K., & Colaiácovo, M.P. (2011) Organization of the synaptonemal complex during meiosis in *Caenorhabditis elegans. Genetics.* 189: 411–421.

Schröpfer, S., Kobbe, D., Hartung, F., Knoll, A. & Puchta, H. (2013) Defining the roles of the N-terminal region and the helicase activity of RECQ4A in DNA repair and homologous recombination in Arabidopsis. *Nucleic Acids Research.* [Online] 42 (4): 1-14. Available from: http://nar.oxfordjournals.org/content/early/2013/10/29/nar.gkt1004.full [Accessed 8th February 2014].

Sebastian, J., Ravi, M., Andreuzza, S., Panoli, A.P., Marimutha, M.P.A. & Siddiqi, I. (2009) The plant adherin *AtSCC2* is required for embryogenesis and sister-

chromatid cohesion during meiosis in Arabidopsis. *The Plant Journal.* [Online] 59 (1): 1-13. Available from: http://onlinelibrary.wiley.com/doi/10.1111/j.1365-313X.2009.03845.x/pdf [Accessed 24th August 2014].

Shimanuki, M., Miki, F., Ding, D.Q., Chikashige, Y., Hiraoka, Y., Horio, T. & Niwa,O. (1997). A novel fission yeast gene, kms1^{+}, is required for the formation of meiotic prophase-specific nuclear architecture. *Mol. Gen. Genet.* 254: 238–249.

Shinohara, M., Oh, S.D., Hunter, N. & Shinohara, A. (2008) Crossover assurance and crossover interference are distinctly regulated by the zmm proteins during yeast meiosis. *Nature Genetics*. 40: 299–309.

Shroff, R., Arbel-Eden, A., Pilch, D., Ira, G., Bonner, W.M., Petrini, J.H., Haber, J.E. & Lichten, M. (2004) Distribution and dynamics of chromatin modification induced by a defined DNA doublestrand break. *Curr Biol.* 14 (19): 1703-1711.

Siaud, N., Dray, E., Gy, I., Gerard, E., Takvorian, N. & Doutriaux, M.P. (2004) BRCA2 is involved in meiosis in Arabidopsis thaliana as suggested by its interaction with DMC1. *EMBO Journal.* 23: 1392–1401.

Snowden, T., Acharya, S., Butz, C., Berardini, M. & Fishel, R. (2004) hMSH4-hMSH5 recognizes Holliday junctions and forms a meiosis-specific sliding clamp that embraces homologous chromosomes. *Molecular Cell.* 15: 437–451.

Stacey, N.J., Kuromori, T., Azumi, Y., Roberts, G., Breuer, C., Wada, T., Maxwell, A., Roberts, K. & Sugimoto-Shirasu, K. (2006) Arabidopsis SPO11-2 functions with SPO11-1 in meiotic recombination. *The Plant Journal.* 48 (2): 206-216.

Storlazzi, A., Xu, L.Z., Schwacha, A. & Kleckner, N. (1996) Synaptonemal complex (SC) component Zip1 plays a role in meiotic recombination independent of SC polymerization along the chromosomes. *Proceedings of the National Academy of Sciences, USA.* 93: 9043–9048.

Sym, M., Engebrecht, J.A. & Roeder, G.S. (1993) ZIP1 is a synaptonemal complex protein required for meiotic chromosome synapsis. *Cell.* 72 (3): 365-378.

Tesse, S., Storlazzi, A., Kleckner, N., Gargano, S. & Zickler, D. (2003) Localization and roles of Ski8p protein in Sordaria meiosis and delineation of three mechanistically distinct steps of meiotic homolog juxtaposition. *Proc Natl Acad Sci U S A*. 100 (22): 12865-12870.

Thaler, D.S. & Stahl, F.W. (1988) DNA double-chain breaks in recombination of phage lambda and of yeast*. Annu. Rev. Genet*. 22: 169-197.

Tiang, C-L., He, Y. & Pawlowski, W.P. (2012) Chromosomes Organization and Dynamics during Interphase, Mitosis and Meiosis in Plants. *Plant Physiology.* 158 (1): 26-34.

Tsubouchi, T. & Roeder, G.S. (2005) A synaptonemal complex protein promotes homology-independent centromere coupling. *Science*. 308: 870–873.

Tsubouchi, H. & Roeder, G.S. (2002) The Mnd1 Protein Forms a Complex with Hop2 To Promote Homologous Chromosome Pairing and Meiotic Double-Strand Break Repair. *Molecular and Cellular Biology.* 22 (9): 3078-3088.

Uanschou, C., Siwiec, T., Pedrosa-Harand, A., Kerzendorfer, C., Sanchez-Moran, E., Novatchkova, M., Akimcheva, S., Woglar, A., Klein, F. & Schlogelhofer, P. (2007) A novel plant gene essential for meiosis is related to the human CtIP and the yeast COM1⁄SAE2 gene. *EMBO Journal*. 26: 5061–5070.

Uhlmann, F. & Nasmyth, K. (1998) Cohesion between sister chromatids must be established during DNA replication. *Current Biology.* 8 (20): 1095-1101.

van Heemst, D. & Heyting, C. (2000) Sister chromatid cohesion and recombination in meiosis. *Chromosoma.* 109: 10-26.

Vignard, J., Siwiec, T., Chelysheva, L., Vrielynck, N., Gonord, F., Armstrong, S.J., Schlogelhofer, P. & Mercier, R. (2007) The interplay of RecA-related proteins and the MND1-HOP2 complex during meiosis in Arabidopsis thaliana. *PLoS Genet.* 3 (10): 1894-1906.

von Wettstein, D., Rasmussen, S.W, & Holm, P.B. (1984) The synaptonemal complex in genetic segregation. *Annu Rev Genet*.18:331–411.

Waterworth, W.M., Altun, C., Armstrong, S.J., Roberts, N., Dean, P.J., Young, K., Weil, C.F., Bray, C.M. & West, C.E. (2007) NBS1 is involved in DNA repair and plays a synergistic role with ATM in mediating meiotic homologous recombination in plants. *Plant Journal.* 52: 41–52.

Wijeratne, A.J., Chen, C.B., Zhang, W., Timofejeva, L. & Ma, H. (2006) The *Arabidopsis thaliana PARTING DANCERS* gene encoding a novel protein is required

for normal meiotic homologous recombination. *Molecular Biology of the Cell.* 17: 1331–1343.

Yamamoto, A., West, R.R., McIntosh, J.R. & Hiraoka, Y. (1999) A cytoplasmic dynein heavy chain is required for oscillatory nuclear movement of meiotic prophase and efficient meiotic recombination in fission yeast. *J.Cell Biol.* 145: 1233-1249.

Zalevsky, J., MacQueen, A.J., Duffy, J.B., Kemphues, K.J. & Villeneuve, A.M. (1999) Crossing over during Caenorhabditis elegans meiosis requires a conserved MutS-based pathway that is partially dispensable in budding yeast. *Genetics*. 153: 1271–1283.

Zamariola, L., De Strorme, N., Tiang, C.L., Armstrong, S.J., Franklin, F.C. & Geelan, D. (2013) SGo1 but not SG02 is required formaintenance of centromrere cohesion in *Arabidopsis thaliana* in meiosis. *Plant Reprod*. 26 (13): 197-208.

Zanders, S. & Alani, E. (2009) The pch2Delta mutation in baker's yeast alters meiotic crossover levels and confers a defect in crossover interference. *PLos Genet.* 5 (7): e1000571.

Zanders, S., Sonntag Brown, M., Chen, C. & Alani, E. (2011) Pch2 modulates chromatid partner choice during meiotic double-strand break repair in *Saccharomyces cerevisiae. Genetics.* 188 (3): 511-521.

Zickler, D. & Kleckner, N. (1999) Meiotic chromosomes: integrating structure and function. *Annu Rev Genet.* 33: 603-754.

Zhang, L., Liang, Z., Hutchinson, J. & Kleckner, N. (2014) Crossover Patterning by the Beam-Film Model: Analysis and Implications. *PLoS Genet.* 10 (1): e1004042. doi:10.1371/journal.pgen.1004042.

Appendix 1.

SHOC1 AT5G52290.1: Genomic Sequence (6202bp)

ATGCGAACTCGATTTCTCAACATCGATTACTTCTCTACTCCACCTTCTCACGTATTTGAAACCCTAGGCTTCCTCAATCTTCCGGCTCCTGATAATTTCCCGGC
ACCCATCGTCTACAACGGAGAAGAAGACCGTCTCCGATTTGGCTCGATCGAAAATGTTAGTATCCCTATCGGAAATTTGCCTATTGAAGCTGCTTTGTCGAA
GTTCCTTTCCGACGTGGTTCCCGACCGCGTCAGTGTGGACTATCGAGTTTTTGAAATCGACGACTCTTCGCTCGGAGTTTATTACTCAGACGAGGTAAAGTT
CCTTCGATCTAGATATTATCAGTTCCTGGAGGTGAAATTTCGAATTTCCTGAGTCTCGCTGACTGTTTCTGTCAACGGTCCTTTGTTTCTTATAGTGAGATTGGT
TGTAGATTTTTCGAAATTTGTGGTGTGTTTTCTCAGTTTCCATTTCTGATTGTTGCTTAGATCTTATATTCATACTTGGGTTGGAAATTTTGGTAGCTTAAGCGAAT
CTTACCGGAGTTTGAAAACCGAAGTTATGATCTATTTGCAGAAGGATGACGGAGATGCCATTGCGGATAAAGCTACACCTAAAATTATTGAGTTGGAGACTC
CAGAGTTGGATTTTGAGATGGTATTGCTCAAGCTGTGTAAGCATTGTACTAATTGAACTAGTTCAGCTTTTTCTTTTTCATTGCGAGATAAAGCATCTTTTGATAT
ACAGGAGAACAAGCTCTTATGCACGAGTGAGGATCATCTCCAATGTTTCTCTGAAGTTCTAGAGATCAAAAATGACCCGGTAAATCCCTGAGTTGATTTTAGT
TGGCACACACAACAGTAGTTTTTGCTTTTGCTGTAGAGTGGTAGAGCTGGTTCCTGTTCTTGGCATCATCTGATTTTAGCTAGTCTTCTTATTGCAGGTTAAATA
TGAGGGGTCAGATATTATCCTGCAGAACTCAAAGGACATTCAAGAGCAGATTTATTCTGTTGATTACATTCCTTCTGATTACTTTACAGAGAACAACACTTCTG
TAGCAGAAAATGAATGCTTCCGCAAGATTCAACCATGGTTCAAAGATGCCAGATTTCCCCTTCTAGAAGTGGATGAAGTAAACTTGAGCGAACTATCAAGCT
TATCTGTGCTTGATAAAGTATTTACTGTTCTTGAGACGATTGAACCCCAAGACACTAATGCAGGGAGTTCTCTCATTATCAATTCTAAGGAGCTTATAGGCTCA
AAGGATTATGATCTATTGGATGTACTCTCTACGGATTGCTATTTGAACAAGAGTGGCCAATCTGATGTGGTACCAGAGGATGAATTTTCTGAAATGGATATAGT
GACTATCCTGGAAATATCAAATGCTGAGGAATTTCAGGGAAAGGTGGCTGTACCAGTAACTTATGAGGAATTCCAGATCCTGGATGTGGATATCTCTGATGT
TTTTGATATCTTCCTTTGTCTTCAAAAAGCCATTGAACCAGAAATCTGTTACGGTATGTTCAGTAAAGAGATGAACTTCAAGGATTTCGATGAATTAGTTGTCAG
TTCCGAACTTGCCTTCACAGATGATGCCTTCAAGTCTTTGCCTACTCCTATTTTACATGATTATGAGATGACAAGATCTCTGGAGCTCATTTATGAGGATGTTTT
GTCAAAGATCAAGCCTCAATCCTTGTCTGCCTCAAATGACATATACTTGCCGTGGAACCTTCTTGAGGAAAGAAACCACAACCATTGTGATTATCCGTTTGAA
GAAATAGTTACATTCAACATTGATTATAACTGGGAAGCTTCAGAAGGAGACAAATGGGTTTATGATTTCATTTTCTCTGAAGATGCTTTCTGCGAGCCACTTGT
AGAGAAATGCACTGAACCTTTCTATGGTATATCTAACCTTGATGAGCATGCTCCTGTTAATACTTCGCATGGGTTATTGGAAAACCCTTTCCAAAAAACAGGA
GCAAGGGATTGTGCAGTGGATGATAATGCTAAGAAGGCTACGCTGTTGTTCAAATCAATGTCTGCTTTTGATGACTTAACCTTTTTCATGGATCCGAAGAAGG
CTGTGATTGAAGATAATCTCGAGTCTAGAGTCGAAGCTGCTAAGACTACCAACCATAAATGTATGTCTATTGACTCGAAGGCTTCATGTAGATCTGGTGGTAT
GCACCCAAACCCGAAGACAGAGGAAATGATACTTCACAGTGTGCGCCCTTCAGAAAATATTCAGGCTCTTGTTGGGGAATTTGTGAAGAGCTATTTAACTCT
TGTGAAGGATGAATCAGAGAATTTATCAGAAGATAAACTTAAGTTACTCAGCATATCTAAAGGAAAGCTTATTGACTGCATAAGAAAGGCAAATGTCCACAAA
ACACAGTTGGCGGATGATAAGACTTTCACGTTTGCATTACTATTAGCAATTAAACAGATGACATGGTATATGTGTTTCTTCGGTATCCATGTGGCATATATCTAT
CTTAACAAGGTATGTCGAAGCTCAAATCCCATGAAGATAGGATTGCACACCCTCTACTCAGCAGTTGAAACAGAACACAAATCAGATGAGACAGACATCAC
AAGATCACATCCATCACTAGCTGTTATCCAGGGGATTTTACAGTCAGAATTTGCCCGGGGGAACTCCAAAGCATTACTTTTGGCTGAGAAAGTGTTTTGGTC
CTCGCTGAAGAGGCTACTGATGTCCATGGGGTTATCTTACAATGACCTCAACAGTCCCTCCCCAAGTGGAAATCGACCAAATGTTCATGAAGCCATAGAACT
TGGTTTCCTGCCGATTTCAGACTGTCTAATTATCTCTTACGAGTGAGTATTATTTCTTCCTATAGCCATATCCTCATTATCAATGATCATAGCTTTTCACAGTTGA
ATTTTTTGGGAACTAGAAAGGGAACCAAAGAATTGATATATTGCGGCCTGAAAAGCATTTTCAGTCTTTTAGCATGGTGATTGTAAGAGATACCACAAAATGTT
GTTACTTCTCTGCTCGTGAAATTGCTGCATTATTGTTCTTTGCATGCTAAAACATAGCTTTATCGATTCTTTGTTCAATATCTTTTAGTGAAATTGTCTTTTGGGAG
TAGTTAAGCTAACTAGTCCTTTCTTTTTCATCTAAGGCAAATTTCTCCATCTTTTCCTGTGGAGAATTTCAGCGTCATTGTAGAATATGGAGGTCCAAATGCCTC
GCCCAGATATTCTTTTCCTTCAAAGTTGGATTCCTTTCCTTCCTTTCATTTCATAAAAGTGGAGCTGGATATGCCCAGTGCATGCGGGCAACTCTGTGCAGGT
GTTACAGTACCTTATAGTCTCAAAATGATAAAGGTGAGAAACATTCAACCTTTTCTTACAAGTTATATTGGTAGATTGTATATTACGATGGAAGAGTCTGTGTGA
AGGGTTCAAATTCAGAGCAGTAGATCAATCTGTATCACAAATAGTACTTTCATGAGCATATGATCTTGATTGGTTTTGCAACACTGAAAATTATGCAAGTTTAA
CATTAGTATGTACTTTAACCTAAAATTGTGTTGTCACATCAGTGGTATTCACGTTTATTCCATAACTGCATATTTTGAACGCTTTGTTTGAATATGTTCCAGAATAT
GCAGATACGAGAACCTATGTACACTATTATCTCTTTTGTAGGGAGACGAAGTTGAGACGAAAACTGGGTGGTTGGAAGAAGTGTTGAACTTTGTTCCACTTG
AAAAAGTGTGTTATGCAGGATCTTCCGAAACCACAAATGAATCTGAATTTATCTCCATGCCTCAAGAATCTGAAAGAAAACGTGGGATAATTGAACAGGGTCT
CTCTGACCAAAGATCTGTGATTGTTGTGAACACAAAAACTGTCGATAAGGAGATGATCATATCCAGAAGAAGTACATACCAGAAGGTGTTAGCAATGGAAAA
AGAAGGAGTGCAAGTTGTGGAGCGCGATTCAGATCTACCTGTGGACCTGATGTTAAGTCCTGCAGTTTGCCTACTCTGGTATGATAGTGAAACTGTTAGTAA
GAAGTCGGCTGCAACTATTGGTACTTCCTCAAGTTCACTTTCATGGATTGGAGATATCGCAACTAATGTTTTGACGTCATTGAGTTTCAGTTTCAGCACTTGCA
TTATGGTAAATTCCACCAAACTTTGCTTTTTGCCGTTCTTTTGTGGGAACGTTGCAGTATATATGTGGACCTTTCACTTTAAGAATCATCTTCTATTATTTTTGCTA
ATTTGATGATTACAAACTTACTAGATGTTTAATACTCACTCATATACTAAAGTCTCTGCAACATTTTCTTCTAAACTGTAGACTGAGTCCAGAGAACTTAAAGAA
CGATTGTTATTTTTCGTACAGGTTTTTGAGGGGGAACCCGCCTTCCTGGCTGCCGTAATGGACTCCTCTGATGAACTGTATGCAGCAGCTGGTAGCCTAGGA

ATCAGTTTACAGATGTTTTGCTCATCGTCAGCTAATCTCACGGATGAAATTATATTGAAGTGTATCAAATCTTCTGTTAAGTTGTCCAAACTCCATGTCAAAATG
CCCGAGTCAGAATCTCTAGCAGAATCATTTCTCACCAAGTTTCCTTCCGTGAATCCACTCACAGCTCAAGTAATTCTGTCATCTTCTGGGTCACTTCTCGAATT
CATGAAGCTCCCACATAAAAGCAAGGTTGAAAGGACGCAAAAGTATCATGTACCTGAAGAGAGTGTTGATCTATTCAGTTCAGTATGCAGATACGGAGCAA
GGGAGGACTCCAGATCTGTAATGACAGACAGCTCTTCTTCGGTATCTTCTGGACCTGACTCAGACACACACCATGTCAGTGTCCATTCTGGCTCAAAAAAGA
AACAGTACATTGCTGAGAAAGATGAGATAGATATGGACGACTTGGTGCATTTTTCTCCCTCGATAGAATTTGCTGATACACAGCTCAAGTCTTCTGGGGATTT
CCAACTTGATGATTCTTGGTCATCGAAAGATCATGAGATCTTTCATTTTGACCCTGTCACTGAATTCTCAGATGCACCTTTCAAACCTTCTGGGATCAGTCATC
CCAATGACTCTTGGCCGTCTAAAGATCCTGAGAGATTTGACAAGAAGTCAGGACCTGGTTCATCATCAAAGGACACATTTTGGGAGAAAGATCAGCCTGATT
TTTCAGTGGAGGACAGTCTTCCTGGAATTCCTGAATTAGAAGATTGGAGTTTCCCAGTTAAAGACAAATTCATGAGCCAGAACAGAGGATGTAAATTTCCGGT
GATGAGAGATTTTAACTTGCATGACAATAGGAACTCGGAGAATTTCATCGCAGACTACAAAGGTGAAGTAATTGACAGAGCTGATAAGTATCTCGAGGAAGA
CTTCCCGCCTTCTCCTGGTTATAATAGGTTTGCTCGAATAGTTTCTGATGTTAATGAAGAGGAACTTCCAAGAAAATCAAAATCTTCAAGGAAGTTATCTTTCTT
TGGATCTCTCCAGCCTAACTTCCCAAAGGCGGCTGACATCGACTCGAGTTCTGAAAGATACGCCACTGAGAAAGATTCAAAATATGATAACAACACTTCTTT
GCGTGGCTATGCTGATAACTATCCAGCAAAACGCCAAAGGACCCTTTTGGAGGAGGTCTTAACACGAAGATCTGCAGTTCCAACAACAGAGCTTCCATTTA
GAGAAGAAATATCACATTTTGGTGGATCTCCACTATCAAACGCAATCCGTTCTTCAAATCAAGTACAAAGTTCTCCTTGGACGGTTGATTTCCTTAACAGAGTT
CGAGAAAGAAGCAGAGCAAGGAAACAACAACAATCTCTTCCTTCTTATGCTTCTCCACCTAGTTTGGAGACTCCAGGGAACATAAAGAAAGCTAATACCAA
GAGAAAGAGTCCATCCATACTCGAGTTTTTCAAGTATAAAGGAGGCAACAAACTTCAAGAAGAGAAGAGGCAGAAGCGGTCAAAGAATTCTTCAGCCTCAC
CAAAAAACGAGAGATTTTACTCGCCTCTTAAGTCATGCACACCAATTGATAAGCGAGCAAAACAGGTATTCATTATATATGATCCCTATAGAAGTGAGATTTGT
TCATACCGTTGATTTCTTTAACATCTTTTTTTTTTCATTCCAGTCTCTATCTTACACAGCGAATGGAACTGGCCAAACAAAACTTGTATGGAAGTAA

***SHOC1* (exon 7) AT5G52290.1: DNA Sequence** (1686bp) (highlighted = fragment amplified by designed forward and reverse primers).

Proposed antibody size = 726bp

GTTTTTGAGGGGGAACCCGCCTTCCTGGCTGCCGTAATGGACTCCTCTGATGAACTGTATGCAGCAGCTGGTAGCCTAGGAATCAGTTTACAGATGTTTTGC
TCATCGTCAGCTAATCTCACGGATGAAATTATATTGAAGTGTATCAAATCTTCTGTTAAGTTGTCCAAACTCCATGTCAAAATGCCCGAGTCAGAATCTCTAGC
AGAATCATTTCTCACCAAGTTTCCTTCCGTGAATCCACTCACAGCTCAAGTAATTCTGTCATCTTCTGGGTCACTTCTCGAATTCATGAAGCTCCCACATAAAA
GCAAGGTTGAAAGGACGCAAAAGTATCATGTACCTGAAGAGAGTGTTGATCTATTCAGTTCAGTATGCAGATACGGAGCAAGGGAGGACTCCAGATCTGTA
ATGACAGACAGCTCTTCTTCGGTATCTTCTGGACCTGACTCAGACACACACCATGTCAGTGTCCATTCTGGCTCAAAAAAGAAACAGTACATTGCTGAGAAA
GATGAGATAGATATGGACGACTTGGTGCATTTTTCTCCCTCGATAGAATTTGCTGATACACAGCTCAAGTCTTCTGGGGATTTCCAACTTGATGATTCTTGGTC
ATCGAAAGATCATGAGATCTTTCATTTTGACCCTGTCACTGAATTCTCAGATGCACCTTTCAAACCTTCTGGGATCAGTCATCCCAATGACTCTTGGCCGTCTA
AAGATCCTGAGAGATTTGACAAGAAGTCAGGACCTGGTTCATCATCAAAGGACACATTTTGGGAGAAAGATCAGCCTGATTTTTCAGTGGAGGACAGTCTTC
CTGGAATTCCTGAATTAGAAGATTGGAGTTTCCCAGTTAAAGACAAATTCATGAGCCAGAACAGAGGATGTAAATTTCCGGTGATGAGAGATTTTAACTTGCA
TGACAATAGGAACTCGGAGAATTTCATCGCAGACTACAAAGGTGAAGTAATTGACAGAGCTGATAAGTATCTCGAGGAAGACTTCCCGCCTTCTCCTGGTTA
TAATAGGTTTGCTCGAATAGTTTCTGATGTTAATGAAGAGGAACTTCCAAGAAAATCAAAATCTTCAAGGAAGTTATCTTTCTTTGGATCTCTCCAGCCTAACTT
CCCAAAGGCGGCTGACATCGACTCGAGTTCTGAAAGATACGCCACTGAGAAAGATTCAAAATATGATAACAACACTTCTTTGCGTGGCTATGCTGATAACTA
TCCAGCAAAACGCCAAAGGACCCTTTTGGAGGAGGTCTTAACACGAAGATCTGCAGTTCCAACAACAGAGCTTCCATTTAGAGAAGAAATATCACATTTTGG
TGGATCTCCACTATCAAACGCAATCCGTTCTTCAAATCAAGTACAAAGTTCTCCTTGGACGGTTGATTTCCTTAACAGAGTTCGAGAAAGAAGCAGAGCAAG
GAAACAACAACAATCTCTTCCTTCTTATGCTTCTCCACCTAGTTTGGAGACTCCAGGGAACATAAAGAAAGCTAATACCAAGAGAAAGAGTCCATCCATACTC
GAGTTTTTCAAGTATAAAGGAGGCAACAAACTTCAAGAAGAGAAGAGGCAGAAGCGGTCAAAGAATTCTTCAGCCTCACCAAAAAACGAGAGATTTTACTC
GCCTCTTAAGTCATGCACACCAATTGATAAGCGAGCAAAACAG

SHOC1 **Exon 7 Primers Used to Amplify DNA fragment (Sequence 5' to 3').**

Forward - cc/catatg/TCACTTCTCGAATTCATGAAG
Reverse - cc/CTCGAGATACTTATCAGCTCTGTC

T7 Promoter Primer Used for DNA Sequencing (Sequence 5' to 3').

TAATACGACTCACTATAGGG

Appendix 2.

PCH2 **internal sequencing primers (5' - 3')**

PCH2 Primer 1: GGTTACTACGTTATGCTGGG
PCH2 Primer 2: AACTACTGCTATTGATGTTGC

YPDA Media Recipe

2.5g Yeast Extract
5g Bactopeptone
5g Glucose
Made up to 250ml with SDW, stirred with a magnetic stirrer until dissolved. Adjusted pH to 6.5 using kOH.
Added adenine hemisulfate to a final concentration of 120µgml^{-1} (3.75ml 0.2% adenine hemisulfate).

1.1x TE/LiAc Solution (Reagents provided in Clontech Transformation Kit)

1.1ml 10x TE Buffer
1.1ml 1M LiAc (10x)
Total volume bought to 10ml with SDW.

PEG/LiAc (polyethylene glycol 3350/lithium acetate) solution (Reagent provided in Clontech Transformation Kit)

8ml 50% PEG 3350

1ml 10X TE buffer

1ml 1M LiAc

Total volume = 10ml

0.9% (w/v) NaCl Solution

0.9g NaCl was dissolved in 100ml of SDW and filter-sterilized.

Sequences of the Oligonucleotide Primers Used for the Point Mutagenesis of *PCH2* (5' to 3').

1. CTGGTATTTGTTTTGATCGATCAGGTAGAAAGTCTTGCTGCTGCT
2. AGCAGCAGCAAGACTTTCTACCTGATCGATCAAAACAAATACCAG

NZY$^+$ Broth Recipe (per liter)

10g NZ amine (casein hydrolysate)

5g yeast extract

5g NaCl

Bought to a final volume of 1L with SDW.

pH adjusted to pH 7.5 using NaOH.

Autoclaved.

12.5ml filter-sterilized 1M $MgCl_2$

12.5ml filter-sterilized 1M $MgSO_4$

20ml 20% (w/v) filter-sterilized glucose

Appendix 3.

Results:

SHOC1 gene cloning

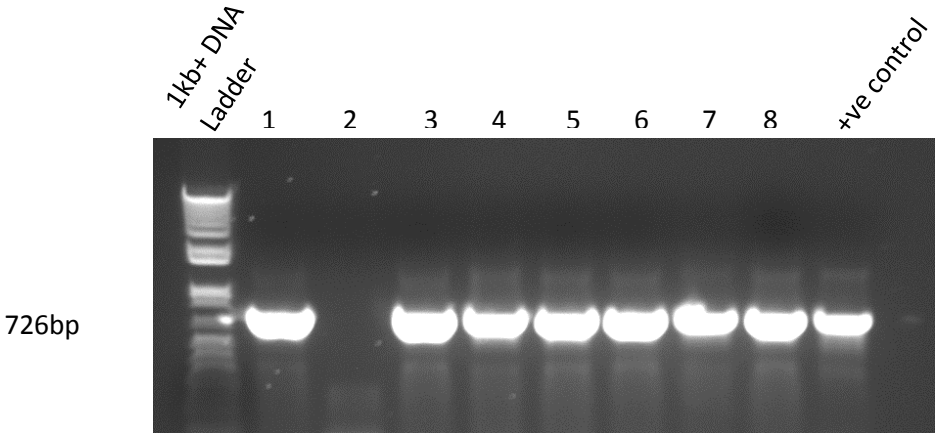

Figure 1. DNA Gel electrophoresis image illustrating a 726bp *SHOC1* DNA fragment amplified by colony PCR for 8 clones transformed with pCR®-Blunt/*SHOC1* and a positive control of PCR purified *SHOC1* DNA insert.

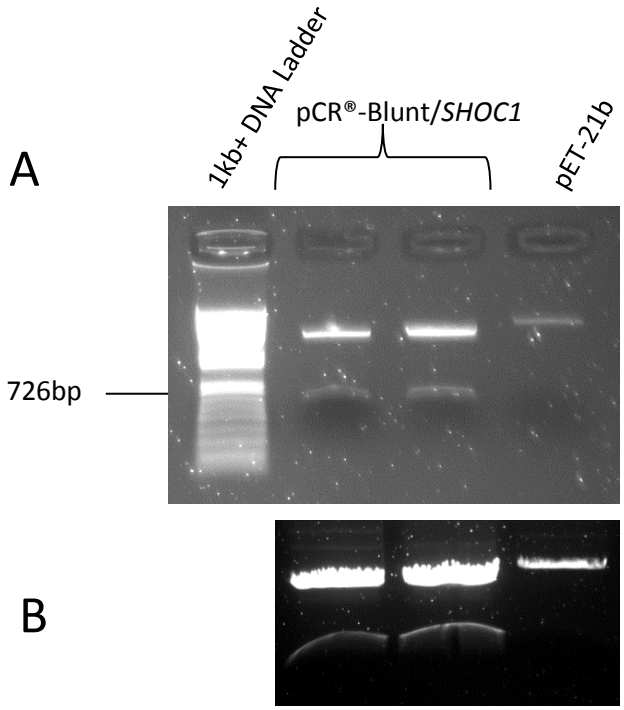

Figure 2. Large-Scale Restriction Digest of pCR®-Blunt/*SHOC1* and pET-21b and gel extraction of *SHOC1* inserts and linearized pET-21b.

(A) DNA gel electrophoresis image showing confirmation that large-scale restriction digest with *NdeI* and *XhoI* had successfully cut out the two *SHOC1* DNA inserts from pCR®-Blunt cloning vector following the loading of 3µl into a 0.8% agarose gel.

(B) DNA electrophoresis gel depicting the bands representing the two *SHOC1* DNA inserts and the pET-21b expression vector to be extracted from the gel and purified.

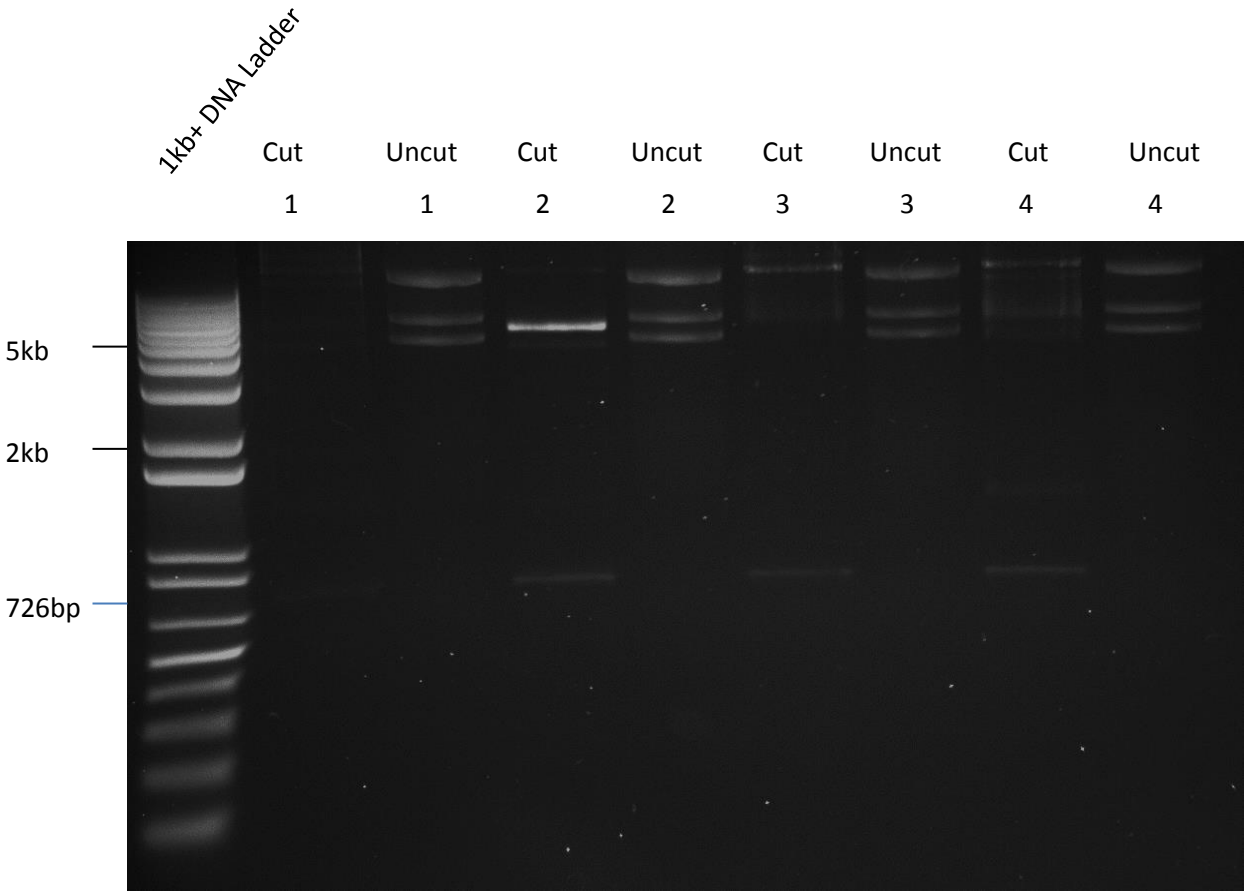

Figure 3. DNA Gel Electrophoresis image showing the restriction digests of four pET-21b/*SHOC1* clones, both cut with the restriction enzymes *NdeI* and *XhoI,* and uncut samples.

Protein Expression of SHOC1 and ASY1 Recombinant Proteins.

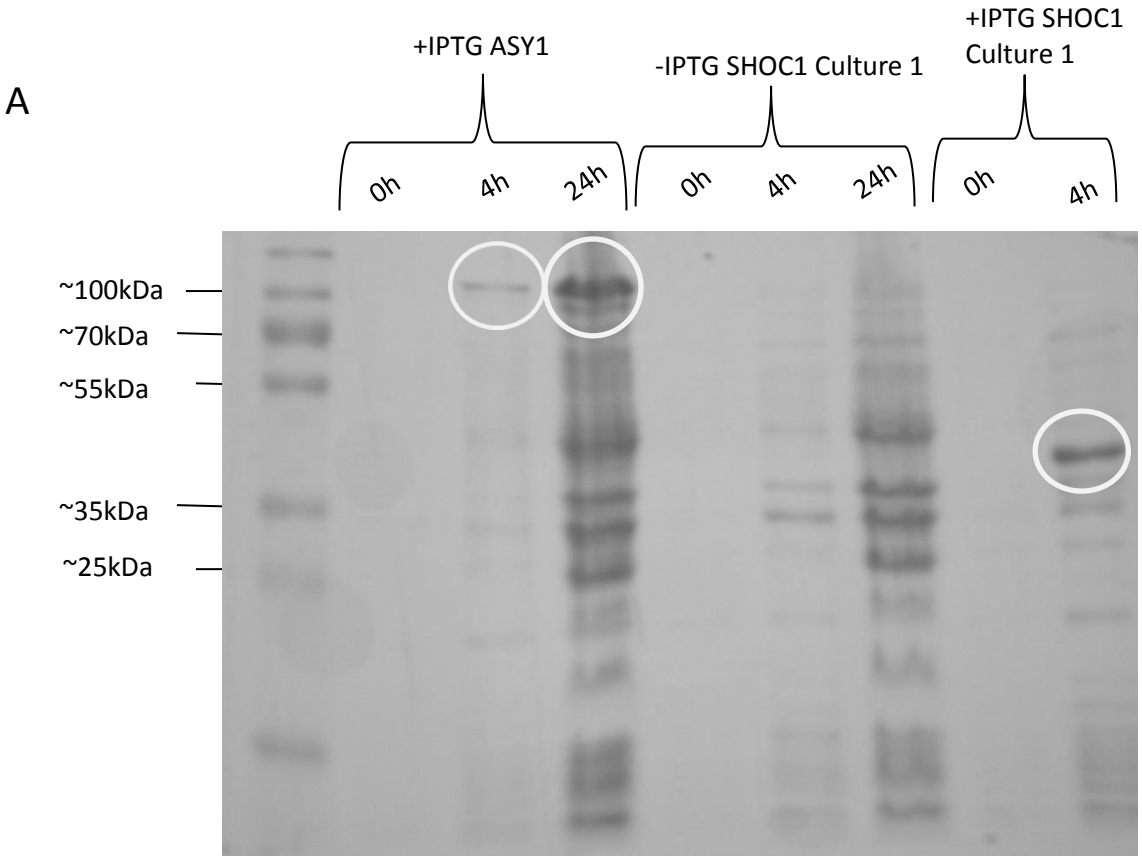

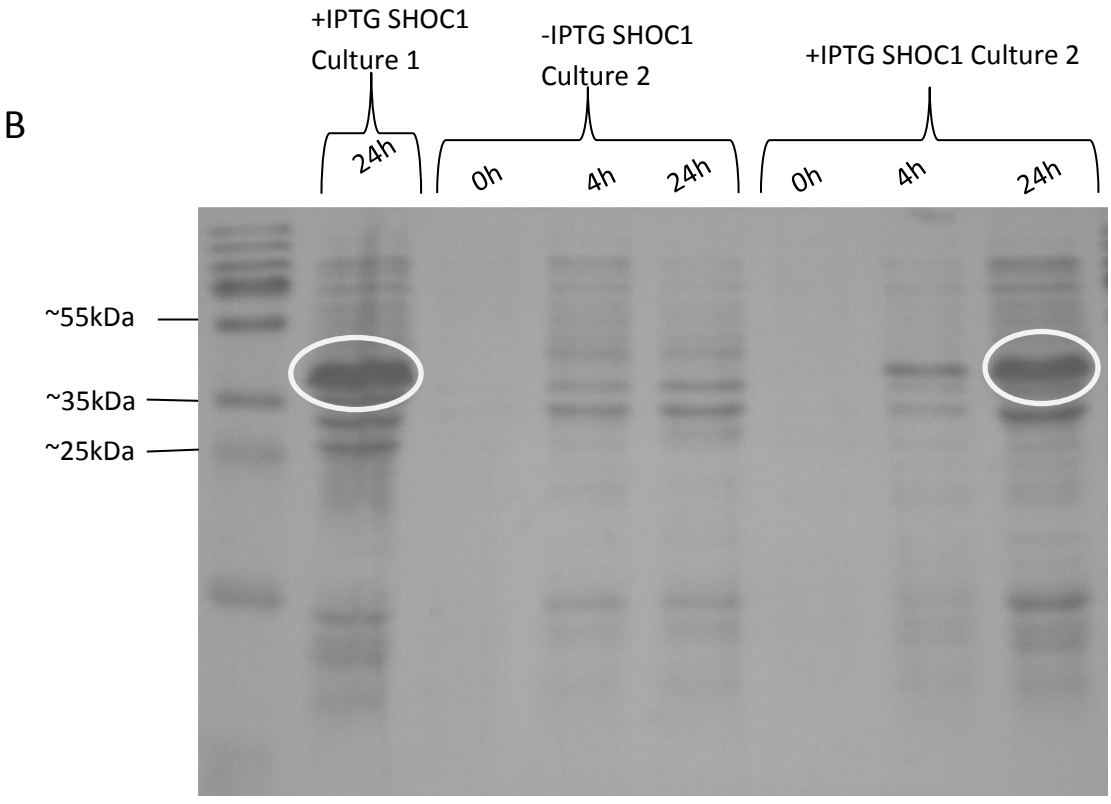

C

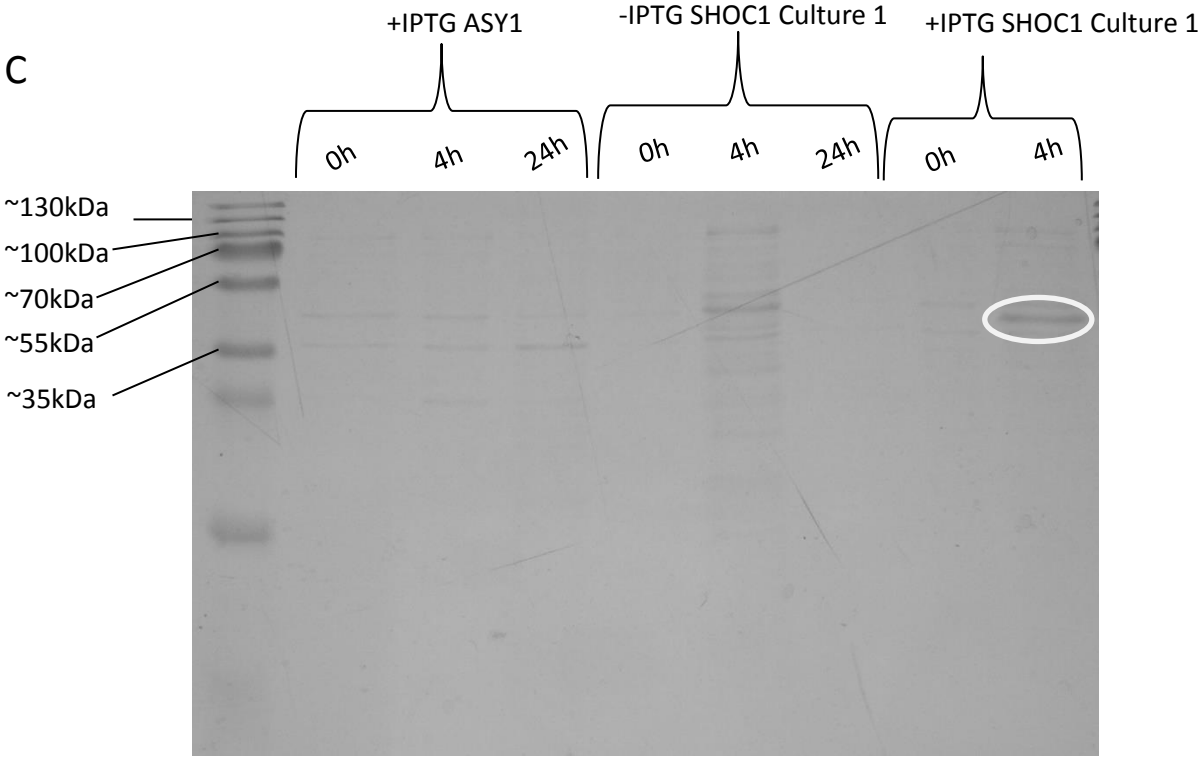
+IPTG ASY1
-IPTG SHOC1 Culture 1
+IPTG SHOC1 Culture 1
0h
4h
24h
0h
4h
24h
0h
4h
~130kDa
~100kDa
~70kDa
~55kDa
~35kDa

D

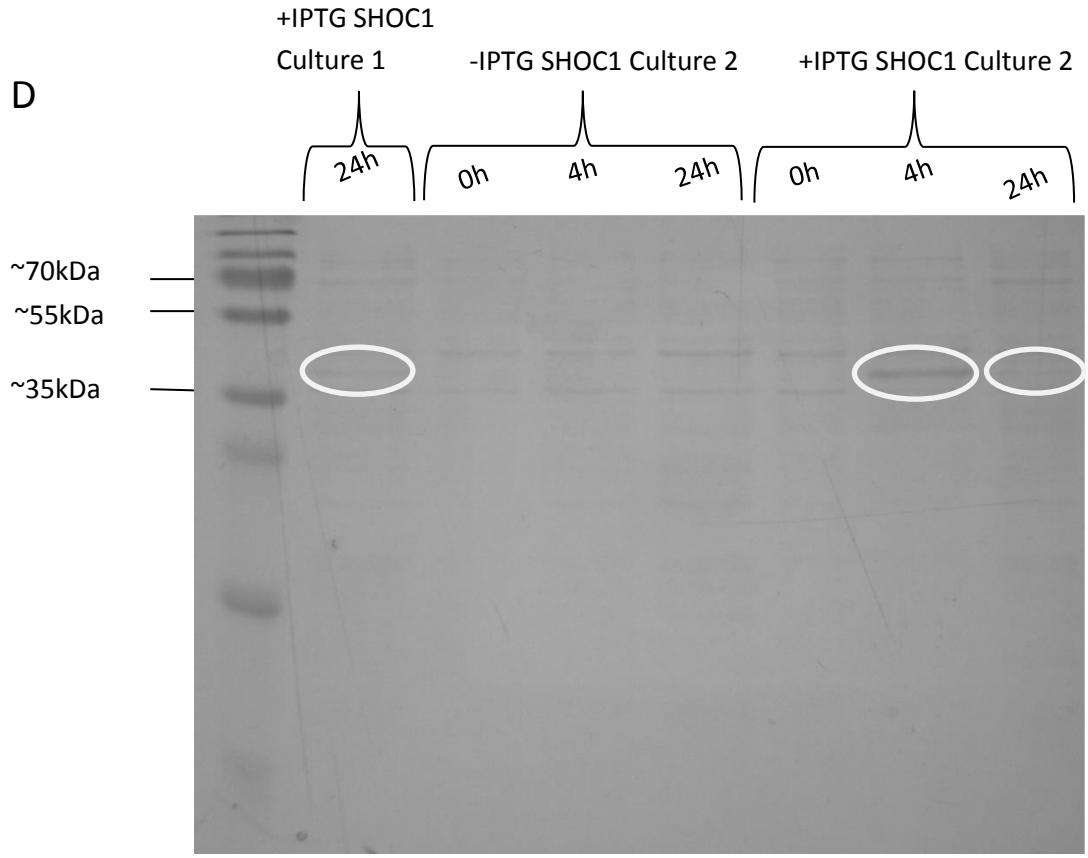
+IPTG SHOC1
Culture 1
-IPTG SHOC1 Culture 2
+IPTG SHOC1 Culture 2
24h
0h
4h
24h
0h
4h
24h
~70kDa
~55kDa
~35kDa

Figure 4. Detection via SDS-PAGE of ASY1 and SHOC1 recombinant proteins to validate expression upon induction with IPTG.

(A) Coomassie blue staining of the SDS-PAGE gel revealed that ASY1 (circle) of ~90kDa was expressed upon induction and is present within the insoluble fraction 4h and 24h post-induction with IPTG. SHOC1 protein of ~90kDa is present 4h post-induction in the insoluble fraction for culture 1.

(B) Coomassie blue staining of the SDS-PAGE gel revealed that the ~90kDA SHOC1 protein is expressed 24 post-induction in the insoluble fraction for culture 1 and both 4h and 24h post-induction with IPTG for culture 2.

(C) Coomassie blue staining of the SDS-PAGE gel revealed that ASY1 is not expressed in the soluble fraction. SHOC1 protein of ~90kDA is present within the soluble fraction for culture 1 4h post-induction with IPTG.

(D) Coomasssie blue staining of the SDS-PAGE gel revealed that SHOC1 protein of ~90kDa is expressed in the soluble fraction 24h post-induction for culture 1 and both 4h and 24hh post-induction with IPTG for culture 2.

BioRad Assay Raw Data

Table 1. Absorbance at 595nm of the recombinant ASY1 and SHOC1 proteins, using 2.5µgµl^{-1} BSA as a standard.

Recombinant Protein	Replicate	**Volume**		
		2µl	5µl	20µl
SHOC1 Culture 1	1	0.015	0.129	0.638
	2	0.016	0.135	0.490
	Average	**0.0155**	**0.132**	**0.564**
SHOC1 Culture 2	1	0.035	0.192	0.655
	2	0.118	0.191	0.638
	Average	**0.0765**	**0.1915**	**0.669**
ASY1	1	0.080	0.209	0.827
	2	0.096	0.269	0.807
	Average	**0.088**	**0.239**	**0.817**
BSA (Standard)	1	0.031		
	2	0.063		
	Average	**0.047**		

Calculations:

As 2µl BSA at a known concentration of 2.5µgµl^{-1} was used as a standard, the standard concentration of a volume of 2µl was 5µg.

SHOC1(1):

(0.564/0.047) x 5µg = 60µg in 20µl

Therefore, there is 15mg in 5ml purified inclusion bodies so the protein sample if of a concentration of 3mgml^{-1}.

SHOC1(2):

(0.669/0.047) x 5µg = 71.17µg in 20µl

Therefore, there is 17.8mg in 5ml purified inclusion bodies so the protein sample if of a concentration of 3.56mgml^{-1}.

ASY1:

(0.817/0.047) x 5µg = 86.91µg in 20µl

Therefore, there is 21.7mg in 5ml purified inclusion bodies so the protein sample if of a concentration of 4.34mgml^{-1}.

UNIVERSITY OF BIRMINGHAM

Investigating the regulatory effects of *N*-acyl-homoserine lactones and hormone networks on spore germination in the model bryophyte *Physcomitrella patens*.

by

Amy Whitbread

A thesis submitted to the University of Birmingham as part requirement for the degree of Master of Research in Molecular and Cellular Biology.

School of Biosciences

University of Birmingham

Abstract

Understanding the mechanisms underlying key evolutionary transitions is of great importance due to the potential this offers to manipulate such mechanisms in crop species, contributing to efforts to ensure food security. *Physcomitrella patens,* the model bryophyte, has recently emerged as a powerful system for investigating plant development and evolution. This study investigates the effects of hormone networks and *N*-acyl-homoserine lactones, on the control of spore germination, which is currently not sufficiently understood compared to the analogous process in seed plants. The results of this study demonstrate that specific molecules show specific responses, with unsubstituted and longer acyl-HSLs having more potent increasing effects on spore germination overall. A negative effect on spore germination was shown for mutants lacking the initial enzyme in the gibberellin synthesis pathway, *ent*-kaurene synthase. This study also demonstrates significantly increased spore germination rates in a DELLA-deficient mutant line, which lacks the negative regulator of the gibberellin signalling pathway. Therefore, this study provides novel data suggesting the presence of a DELLA-mediated GA signalling pathway in moss, challenging previous evidence that the hormonal pathway was acquired following the evolution of the bryophyte lineage.

Acknowledgements

I would like to thank everyone that supported me whilst I was both carrying out the research in the lab and writing this thesis.

I would firstly like to thank my superviser, Dr Juliet Coates, for her continued support and guidance throughout the project and most importantly for providing me with such an interesting project to carry out in the first place.

I would also like to express my gratitude to Eleanor Vesty for providing training and for her exceptional guidance and support throughout completion of the project.

Finally, I would like to say a huge thank you to Susan Bradshaw for being a great help to me whilst I was working in the lab, with helping me to find my way around within the initial few days and for her consistent kindness towards me.

Table of Contents

List of Tables and Figures

Appendix 1

List of Abbreviations

ABA	Abscisic Acid
Acyl-HSL	*N*-acyl-homoserine lactone
BCD	Spore germination media
bp	Base pairs
C3	Third carbon position
C4-HSL	*N*-Butyryl-L-homoserine lactone
C6-HSL	*N*-Hexanoyl-L-homoserine lactone
C8-HSL	*N*-octanoyl-L-homoserine lactone
C10-HSL	*N*-Decanoyl-L-homoserine lactone
C12-HSL	*N*-Dodedcanoyl-L-homoserine lactone
cDNA	Complementary Deoxribonucleic Acid
CPS/KS	*Physocmitrella patens ent*-kaurene synthase (Copalyl Synthase/Kaurene Synthase)
ddH_2O	Double deionized water
DNA	Deoxyribonucleic Acid
GA	Gibberellin
GA_9-Methyl Ester	Gibberellin A9 Methyl Ester
gDNA	Genomic Dexoyribonucleic Acid
GDDP	geranylgeranly diphosphate
GID1	GIBBERELLIN-INSENSITIVE DWARF 1
KO	Knockout Mutant
LB	Luria Broth
NEB	New England Biolabs
OH	Hydroxyl Group
oxo	Ketone Group
PCD	Programmed Cell Death
PCR	Polymerase Chain Reaction
QS	Quorum-Sensing
RNA	Ribonucleic Acid
RT-PCR	Reverse-Transcription Polymerase Chain Reaction
SDW	Sterile Distilled Water
STDEV	Standard Deviation
SEM	Standard Error of the Mean

TF	Transcriptional Factor
Wt	Wild-type

Introduction

The transition from unicellularity to multicellularity confers one of the most important steps throughout evolution (reviewed in Grosberg & Strathmann 2007). This evolutionary transition was key in the development of present life on earth, enabling the colonisation of land by plants and the formation of the earth's ecosystems, climate and atmosphere.

The transition to multicellarity arose independently multiple times throughout evolutionary history, with frequent origins within the plant/algal lineage (Bonner 2000; Kaiser 2001). One of the key advantages of being multicellular is increased size, which constitutes to successful avoidance of predators (Bell 1985). An example of this can be observed with *Scenedesmus acutus*, a freshwater green algae. This species can live either as unicells or become 'multicellular', increasing its size by colony formation (Van den Hoek *et al.* 1995). This transformation has been shown to be induced following exposure of *S.acutus* cultures to water from cultures of a known predator of the species, *Daphnia* (Lürling & Van Donk 2000). This mechanism of increasing its size through 'multicellularity' enables the algae to avoid predation by becoming too large for consumption and additionally by using gravity to move their position lower within the water. Furthermore, multicellularity is also advantageous as biological complexity can be increased via the generation of new biological structures (discussed in Ratcliff *et al*. 2011), enabling the formation of an internal environment protected by an outer layer of external cells (Gerhart & Kirschner 1997).

It is apparent why multicellularity frequently arose from unicellular ancestors, however little is known regarding the mechanisms underlying how this phenomenon

actually occurred (Herron *et al.* 2009). Understanding the ecology and physiology of transitional forms is proving challenging due to extinction and thus only fossil evidence being available (Herron & Michod 2008). Nonetheless, numerous genes and epigenetic modifications of patterns of gene expression that are required for the development of multicellular organisms, have also been shown to exist within unicells (Shapiro 1998; Bonner 2000; Kaiser 2001; Miller & Bassler 2001; Lachmann *et al.* 2003; Keller & Surette 2006; Merchant *et al.* 2007; Prochnik *et al.* 2010; Richter & King 2013). Consequently, it may be the case that the evolution of multicellularity occurred from mechanisms already utilised by their unicellular ancestors, as a means to recognise self from non-self and interact with other organisms within their environment.

The ability to understand how multicellularity arose is of great significance due to the potential this offers to manipulate such mechanisms in order to provide social benefit. Considerable efforts are currently being made to ensure food security, which has recently emerged as a crucial target for the 21st century (reviewed in Godfray *et al.* 2010). The need to enhance food production is highlighted by the fact that by the year 2050 the global population is estimated to increase to 9 billion, heightening the importance to ensure increasing food demand is met. Moreover, limitations of arable land and space raise pressures on the need to generate sustained crop yield improvements, as well as inevitable adverse effects as a result of climate change (reviewed in Chakraborty & Newton 2011). Therefore, one such effort to contribute to ensuring food security is that of understanding multicellularity in order to ultimately generate a means to modify the mechanisms involved. In doing this, ecosystems

could be manipulated in such a way to maximise their useful potential to improve crop yields.

In addition to understanding the transition to multicellularity, understanding more regarding the transition from an aquatic environment to a terrestrial one also offers the potential to increase productivity of plants. For example, in order to adapt to life on land, plants had to overcome numerous obstacles, including that of a limited water supply. Mechanisms involving drought-resistance evolved enabling successful colonisation of land. Understanding this process offers the potential to manipulate plants, particularly crop species, in order to increase their drought-tolerance, thus contributing to efforts to ensure food security. Therefore, an understanding of plant development and tracing evolutionary history to increase knowledge on the key transitional events that occurred is of great importance.

***Physcomitrella patens*: a model system to understand plant development and evolution.**

The model bryophyte moss species, *Physcomitrella patens*, is increasingly being used for research regarding plant evolution and development. The recent availability of the genome (Rensing *et al*. 2008) makes this model plant system the only primitive plant to have its genome completely sequenced, thus proving significant for studies aiming to understand the molecular biology of evolution (reviewed in Prigge & Bezanilla 2010). Furthermore, due to the key position of *P.patens* within evolutionary history, this ancient plant is considered an early stage in the transition to terrestrial life from an aquatic one. Hence, this species represents a powerful tool for

understanding land plant evolution and the key transitions that took place (discussed in Delaux *et al.* 2012).

Additionally, there are numerous other advantages associated with using *P.patens* as a research tool. Firstly, efficient gene targeting (Kammerer & Cove 1996; Schaefer & Zryd 1997) in this species enables the manipulation of genes and the generation of knockout mutants, thus allowing for reverse genetic approaches to be carried out (Reski 1998). The simple morphology and rapid generation time of *Physcomitrella* is also advantageous as it allows for ease of culturing, in addition to vegetative propagation being easily achieved at any developmental stage (reviewed in Prigge & Bezanilla 2010). Finally, a vast majority of the key developmental gene families found in flowering plants have been identified to be conserved in the genome of *P.patens*, adding to the potential of further understanding land plant evolution and development by studying this model system (Rensing *et al.* 2008; Prigge & Bezanilla 2010).

P.patens is commonly found colonising banks exposed by decreasing water levels (Hodgetts 2010), developing in late summer from spores, as an ephemeral species (Cove 2005). The moss is largely distributed in temperate regions (Rensing *et al*. 2009), however the strain commonly used for research purposes was obtained from Gransden Wood, Cambridgeshire and is known as the ‘Gransden’ isolate (Cuming 2011).

Mosses, alongside hornworts and liverworts, are a group of plants collectively known as the bryophytes. These non-vascular plants, made the transition onto land approximately 470 million years ago, and hence have accumulated a number of adaptations through evolution, in order to overcome the stresses associated with

habituating a terrestrial environment (Prigge & Bezanilla 2010). One such adaptation was the generation of a desiccation-resistant structure, the sporophyte, analogous to the seed structure produced by the more recent lineage of land plants, the spermatophytes (Delaux *et al.* 2012).

Bryophytes share a common life cycle which is characterised by a specific alternation of generations (see Fig.1). In bryophytes, the haploid gametophyte is the dominant generation, unlike vascular plants, and constitutes the large, green part of the plant. The diploid generation is the sporophyte, which produces a large number of haploid spores via meiosis. Germination of an imbibed spore occurs when protonema, a filamentous structure, protrudes through the spore coat. Protonemal filaments are comprised of two cell types, chloronemata and caulonemata. Chloronema emerges initially, which is characterised by large numbers of chloroplasts and perpendicular walls, followed by the differentiation of the cells into the faster growing cell type, caulonema. Additional chloronemal cells are formed following further branching of the protonemal filaments, by tip growth of their subapical cells, generating side branches. Maturation of the plant coincides with the transition of these side branches to form meristematic buds, known as gametophyte initials. The shoot of this dimorphic plant, the gametophore, is then produced from these initials, enabling the generation of the complex structures such as the phylloids, rhizoids and reproductive organs. *Physcomitrella* is a monoecious species, therefore both the antheridia (male) and archegonia (female) are produced within the same individual plant, at the top of a single gametophore. The production of biflagellate spermatozoids occurs within the antheridia, which require moist conditions for motility. Due to *P.patens* being self-compatible, once the spermatozoids enter the archegonia, fertilisation occurs

producing the diploid generation, the sporophyte, a spore capsule associated with a short seta. Following maturation, which can be observed with a darkening in colour, the spore capsule breaks enabling the distribution of the haploid spores for the generation of new individual plants (Engel 1968; Cove 2005; Prigge & Bezanilla 2010).

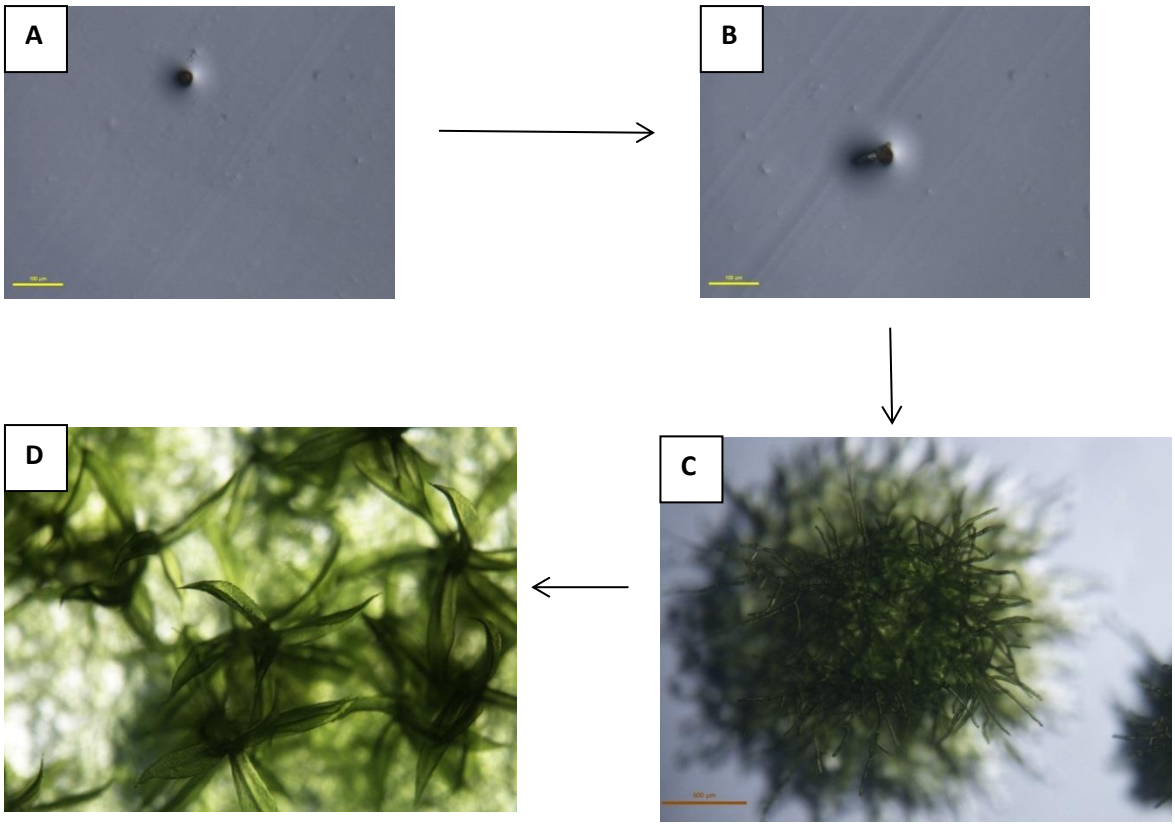

Figure 1. Diagram showing real-life images of the key stages within the life cycle of *Physcomitrella patens.* A) Imbibed haploid unicellular spore. B) Germinated spore with protruding protonemal filaments from the spore capsule. C) Protonemata with side branch formation from chloronemal filaments. D) Adult plant comprised of leafy shoot-like gametophyte tissue. [Images: Whitbread, A. (2014)].

Antheridia and archegonia are generated as a result of shorter light periods and decreased temperatures (Hohe *et al.* 2002), with sporophyte formation also being triggered by these conditions (Cove *et al.* 2005). To ensure survival and reproductive

success of the plant, the timing of germination of the spore is critical, in order to allow for favourable conditions. The timing is primarily controlled by the formation of the desiccation-resistant structure itself, as with seeds in non-vascular plants. Seed germination is also known to be controlled by a number of hormonal and environmental factors (reviewed in Holdsworth *et al.* 2008), however little is known regarding the regulatory mechanisms that are responsible for determining the timing of spore germination in ancient lineages of plants, such as the bryophytes. Nevertheless, previous studies have implied conservation of some of these regulatory mechanisms between the two different types of dispersal units, even though they arise from different developmental stages and vary in ploidy (discussed in Sabovljević *et al.* 2014).

Gibberellins and Abscisic Acid: Hormones known to affect plant growth and development.

Gibberellins (GAs) are a group of plant growth regulators (PGRs), established as key players in the germination of seeds in vascular plants (reviewed in Sabovljević *et al.* 2014). These *ent*-kaurene derived phytohormones have also been identified to be involved in cell expansion, flower induction, antheridia formation (discussed in Hooley 1994) and spore germination in the non-seed vascular fern lineage (Weinberg & Voeller 1969), as well as a number of other processes.

The role of gibberellins in *Arabidopsis* seed germination has been studied extensively, where it has been shown by numerous functional genomic approaches, that inhibition of endogenous GA biosynthesis and detection, results in seed germination inhibition (Koornneef & van der Veen 1980; Gallardo *et al.* 2002;

Voegele *et al.* 2011). The GA signalling pathway in vascular plants initiates with the binding of bioactive GAs to the GIBBERELLIN INSENSITIVE DWARF 1 (GID1) receptor. The perception of GA, through a conformational change of the receptor molecule, enables the GA-induced degradation of the transcriptional repressor DELLA protein (Dill *et al.* 2004; discusses in Wang & Deng 2014).

Conflicting results has contributed to a lack of understanding regarding the roles of GAs within bryophytes. Although ubiquitous in vascular plants, and over 100 identified within the genomes of numerous bacteria, fungi and plants (Gomi & Matsuoka 2003), it is becoming increasingly evident that land plant bioactive GAs are not present within bryophytes (Anterola & Shanle 2008).

The GID1-like (GLP1) and DELLA proteins in *P.patens* share only limited homology with those found in *Arabidopsis* (Vandenbussche *et al.* 2007), with no interaction between these proteins being shown in the bryophyte (Yasamura *et al*. 2007). With no documented phenotype of DELLA deficient *P.patens* mutant strains, and no detectable growth responses to GA, it has been suggested that there is no GA signalling in moss and that this process evolved later in land plant evolution (Yasamura *et al*. 2007).

In spite of this, it is apparent that GA-like substances are present within mosses (Ergün *et al*. 2002), with Anterola & Shanle (2008) indicating that a GA-like biosynthesis pathway is present within *P.patens*, which may be indicative of a similar pathway observed in vascular plants. The bifunctional *ent*-kaurene synthase (Copalyl Synthase/Kaurene Synthase (CPS/KS), the initial enzyme in the GA synthesis pathway, was identified in *P.patens* by Hayashi *et al.* (2006), whereby

functional analysis of a *cps* mutant suggested no apparent role of the enzyme in spore germination. However, the use of AMO-1618, an inhibitor of gibberellin and *ent*-kaurene biosynthesis in angiosperms, on *P.patens* spores identified a potential role of gibberellin-like compounds for germination. Decreased rates of spore germination was observed with AMO-1618, the effects of which were reduced upon exogenous application of *ent*-kaurene, thus suggesting the potential need for the gibberellin precursor *ent*-kaurene for spore germination (Anterola *et al.* 2009). Following the recent availability of the complete genome sequence of *P.patens* (Rensing *et al.* 2008), the identification of putative genes involved in the biosynthesis pathway of GA and the subsequent functional analyses, via the generation of knockout mutants, should increase current understanding of the roles of GA/GA-like phytohormones in moss, particularly in terms of the control of spore germination.

The regulation of seed germination is known to be tightly regulated by the antagonistic interactions between GA and another phytohormone, abscisic acid (ABA), with GA promoting germination whilst suppression being a result of high ABA levels (reviewed in Kucera *et al.* 2005). ABA is a ubiquitous compound, identified in a vast number of taxa, shown to exhibit a range of functional roles (discussed in Savovljević *et al.* 2014). With regards to seed germination, increased levels of ABA have been shown to result in suppression of germination, and therefore maintenance of primary seed dormancy, of which can be overcome by increased levels of GA (Kucera *et al.* 2005). Biosynthetic pathways of ABA have been shown to be encoded for by the genome of *P.patens* (Rensing *et al.* 2008), with ABA playing a vital role with the response to stresses caused by drought, salt and osmolarity, by improving tolerance (Cuming *et al*. 2007; Khandelwal *et al*. 2010). Consequently, the ABA-

biosynthetic pathway may represent an evolutionary adaption to the stresses imposed on ancient plants, which made the transition onto land.

Jasmonates, brassinosteroids and ethylene are additional phytohormones known to be implicated in the regulation of growth and development in flowering plants (Steber & McCourt 2001; Linkies & Leubner-Metzger 2012), alongside ABA and GAs (reviewed in Sabovljević *et al.* 2014). As a reduced number of these hormone signalling pathways, and therefore their corresponding extensive interactions, are implicated in moss morphogenesis, analysing hormone signalling pathways in *P.patens* represents a beneficial means to gain a thorough understanding of the complex interactions, many of which may have arisen since the divergence of the bryophyte lineage. Moreover, due to the lack of knowledge regarding the control of spore germination in moss, functional analysis of the various hormones and analysing the interactions between them may provide beneficial insights into the regulation of this process.

_N_-acyl-homoserine lactones: Quorum-sensing molecules shown to induce responses in plants.

In addition to phytohormones, other chemical compounds have been found to effect plant growth and development. *N*-acylated derivatives of $_{L}$-homoserine lactones (acyl-HSLs) are quorum-sensing (QS) signal molecules, produced by gram-negative bacteria species, that have been extensively studied with regards to plant responses (Mathesius *et al.* 2003; Ortiź-Castro *et al.* 2008; von Rad *et al*. 2008; Schikora *et al.* 2011; Bai *et al.* 2012; Schenk *et al.* 2012). QS is a mechanism employed by bacteria in order to respond to population cell density, via the regulation of the expression of

specific gene sets (Cha *et al*. 1998). By the production and detection of these small, diffusible chemical signal molecules, bacteria are able to monitor their surroundings and respond accordingly (Cha *et al.* 1998). Acyl-HSLs are termed autoinducers as perception by bacteria, not only generates a specific response, but it also induces the production of additional acyl-HSLs, by a positive feedback-type system (González & Venturi 2013).

Acyl-HSL QS systems utilise a synthase protein component, which catalyses the synthesis of the signal molecules within the bacterium, and is generally a homolog of the LuxI protein found within the Lux operon. A transcriptional factor (TF) that shares homology with LuxR is responsible for the subsequent detection of acyl-HSLs and thus the generation of a beneficial response. Specific responses are produced following the perception of a local quorum, upon which a physiologically relevant threshold concentration of acyl-HSLs has been reached, indicating an increase in the local bacterium population size (Whitehead 2001). This results in the interaction of the signal molecules with the cognate TF and hence the transcription of specific gene sets, in a coordinated manner (Fig.2) (discussed in Scott *et al.* 2005).

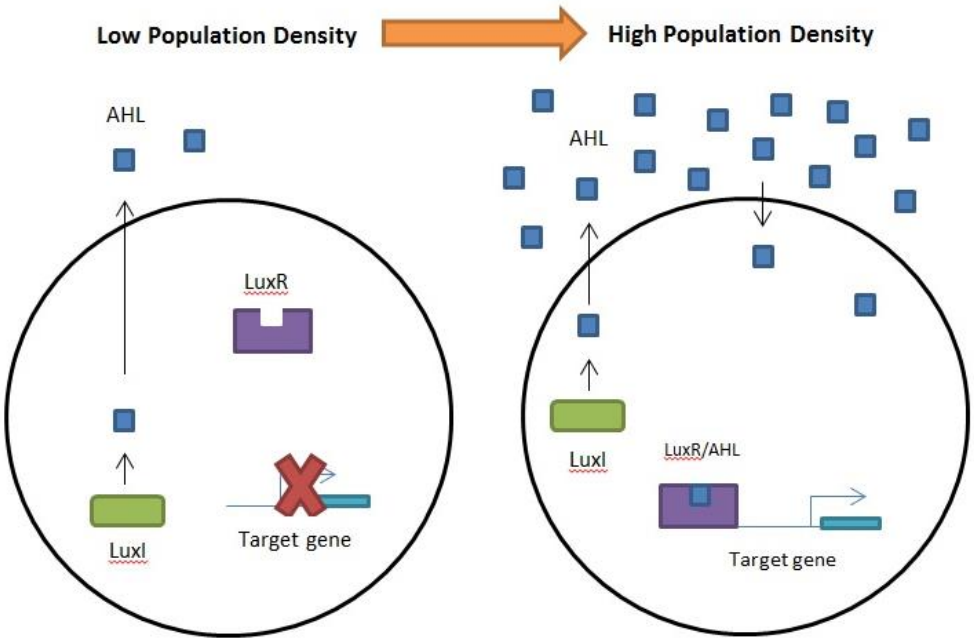

Figure 2. [Modified from Choudhary & Schmidt-Dannert 2010]. A schematic diagram representing the acyl-HSL (AHL) mediated QS system in gram-negative bacteria.

Autoinductor synthases, homologs of the LuxI, catalyse the synthesis of acyl-HSL signal molecules. At low population densities, the concentration of acyl-HSLs is low. At high population densities, and high acyl-HSL concentrations, a threshold is achieved indicating the presence of a local quorum. The signal molecules interact and activate the LuxR transcription factor homolog and the resultant complex mediates the transcription of target gene sets to permit the generation of a response.

A number of different acyl-HSLs can be synthesised by a single gram-negative bacterial species, as a result of various LuxI homologs encoded for by their genome (Kock *et al.* 2005), however, these all share a conserved principal structure. All acyl-HSLs comprise of a homoserine lactone moiety with an associated acyl side chain (Scott *et al.* 2005). Variation between the acyl-HSL molecules arises from differing lengths of the acyl side chain, which can range from four carbons to a maximum of 18. In addition to this, at the third carbon position (C3), different substitutions can also occur whereby the molecule can either be unsubstituted (*N*-acyl-HSL), contain a

ketone group (oxo) or a hydroxyl group (OH). These differences between the various synthesised acyl-HSL molecules, contributes to specificity whereby certain variations result in specific gene sets being transcribed (Scott *et al.* 2005).

Bacteria employ acyl-HSL mediated QS for intercellular communication, hence why acyl-HSLs are produced in high concentrations (OD_{600} 0.5) during biofilm and colony formation. This system enables the bacteria to essentially work together rather than independently, thus allowing for responses to be generated in concert to enhance the effect required. A diverse range of gene systems have been shown to be regulated by acyl-HSL mediated QS, by a range of gram-negative bacterial species across a spectrum of genera (Cha *et al*. 1998; Pierson *et al*. 1999; Winas *et al*. 1999; Loh *et al*. 2002; Whitehead *et al*. 2002; von Bodman *et al*. 2003; Zheng *et al.* 2003; Ramey *et al*. 2004). Gene systems that are responsible for the formation of biofilms (Dickschat 2010) and plant and animal disease-causing virulence factors (Rad *et al* 2008) are just two examples of the many that are regulated by this mechanism.

A number of plant-associated bacterial species have been shown to utilise QS systems and synthesise acyl-HSLs (Cha *et al.* 1998). Although this may predominantly be used as a means for the bacteria to communicate between themselves, it has become increasingly apparent that acyl-HSLs can mediate biocommunication between the microbes and the eukaryotic plant hosts as well, representing inter-kingdom interaction.

The perception of bacteria, and other microorganisms, by plants is of significant importance in terms of monitoring their surroundings and thus being able to respond accordingly to enhance their chances of survival (Schenk *et al*. 2014). The ability of

eukaryotic plants to detect the chemical QS molecules may have occurred as a result of the coevolution of the microbes with their specific host. The perception of acyl-HSLs by plants may provide them with an evolutionary advantage over their associated microbial community, especially if the bacteria are pathogenic species, as it may enable the plants to detect increasing population numbers and alter the QS outcome (Palmer *et al.* 2014). For example, plants may produce anti-QS molecules and use quorum quenching as a response to a detected local quorum, via the perception of acyl-HSLs. As a result, the plant is able to intersect the QS signal, preventing transcription of specific gene sets, thus averting the synthesis of virulence factors by pathogenic bacteria, for instance (Manefield *et al.* 2002; Koh *et al.* 2013).

A number of studies have been carried out analysing the effects of bacterial QS molecules on plants, with some implying that perception of these induces a primed state of the plant (Schenk *et al*. 2014). A study testing the interactions between tomato (*Solanum lycopersicum*) and *Serratia liquefacians*, provided the initial indication that acyl-HSLs have a functional involvement in plant immunity. The results of this study showed that *S.lycopersicum* became resistant to *Alternaria alternata*, a pathogenic fungal species, following the growth of wild-type *S.liquefacians*, whereas no induced resistance occurred following the growth of a corresponding AHL-deficient mutant (Schuhegger *et al.* 2006). Consequently, additional studies have been carried out whereby it has been deduced that interactions between microbes and plants can induce local defence mechanisms (Schenk *et al.* 2014). In the model plant system, *A.thaliana*, resistance against both bacterial and fungal pathogens was observed following the exogenous application of synthetic acyl-HSLs (Schenk *et al*. 2014).

However, it is not just immunity that is a response of plants to the QS signal molecules. Several reports have shown acyl-HSL application on plants can modify protein profiles by inducing changes in gene expression, altering the formation of roots (Mathesius *et al.* 2003; Ortiź-Castro *et al.* 2008; Rad *et al.* 2008; Shikora *et al.* 2011; Schenk *et al.* 2012), including the promotion of adventitious root growth (Bai *et al.* 2012). A large number of studies have been carried out regarding the rhizosphere of plants and the interactions of microbes, due to the natural association of bacteria with these structures. Plant-growth-promoting bacteria have been shown to employ QS systems which aid with the colonisation of the rhizosphere, thus providing benefit for both bacteria and host plant (Lugtenberg et al. 2001; Savka et al. 2002). The ecology of rhizosphere bacterial populations on *S.lycopersicum* has been shown to be modulated by acyl-HSLs produced by bacteria a significant distance away, able to be perceived by signal diffident bacteria, owing to the movement of the compounds through the rhizosphere via diffusion (Pierson *et al*. 1998; Steidle *et al.* 2001). Furthermore, Joseph & Phillips (2003) demonstrated the potential beneficial effects on the physiology of plants by the by-products of acyl-HSL degradation. Exogenous application of homoserine lactones, and homoserine, the degradation products of acyl-HSLs, was carried out on bean roots. The effects observed represented a plant-microbe interaction whereby both the rhizosphere-associated bacteria and the host plant benefited. A significant increase in the conductance of stomata was observed, owing to higher transpiration rates and therefore enhanced mineral nutrient availability for growth promotion of the plant and the associated acyl-HSL producing bacteria.

Plant-produced compounds, such as strigalactones and alkamides, share structural similarity to the bacteria-generated acyl-HSL molecules. Consequently, it can be thought as not surprising that these QS molecules impose effects on the growth and development of plants, as both alkamides and strigalactones are known to induce a number of morphological responses, including changes in root architecture (Ortiź-Castro *et al.* 2008).

Biotechnological applications involving acyl-HSLs and QS systems are currently of much interest, due to the potential beneficial impacts on society. Manipulating the formation of biofilms by bacteria, in order to prevent the occurrence of plant and animal diseases, is one such area of interest. Acyl-HSL molecules, or derivatives of, are being targeted as potential antimicrobials as a means to aid with the prevention of harmful diseases caused by pathogenic bacteria (reviewed in Jayaraman & Wood 2008). Furthermore, in order to control gene expression in plants, the lactone-inducible system employed by bacteria for QS has been investigated in terms of introducing an efficient inducible system within plants themselves, which may prove beneficial in terms of translating this knowledge to crop species in order to contribute to efforts to ensure food security. An inducible system was introduced into *P.patens,* whereby the receptor QS component of *Agrobacterium tumefaciens* was translationally fused to the TF, VP16, activation domain. Following application of acyl-HSL molecules, the resultant transcriptional regulator was shown to induce gene expression in the moss, whilst not affecting endogenous gene expression (You *et al.* 2006). Bioengineering plants themselves to synthesise acyl-HSL molecules is also an application that has been investigated, whereby it was found that engineering plants to express the synthase genes, enabled the production of acyl-HSLs, which

were freely diffusible across plant membranes (Scott *et al*. 2005). As a result of these possible applications, increasing current knowledge on plant responses to acyl-HSLs is of great significance.

Aim and Objectives.

An understanding of the regulatory mechanisms imposed on spore germination in the model bryophyte, *P.patens*, is of great importance. This is mainly due to the potential this has on enhancing current understanding of the mechanisms that may have evolved as a result of the colonisation of land by plants, whilst providing insights into transitions to multicellularity. This investigation is being carried out in order to provide fundamental insights into the control of spore germination of *P.patens,* by both hormone signalling networks and QS signalling molecules, which have both shown to induce physiological changes in more evolutionary recent vascular plants. This will be achieved by carrying out numerous spore germination assays whereby gibberellin, abscisic acid and acyl-HSLs will be exogenously added to the medium in order to determine the effects these potentially have on spore germination and the interactions between these that may also have an impact on the regulation of germination. In addition to this, *P.patens* wild-type spore germination will be compared to that observed with mutants lacking proteins within the gibberellin pathways. This will be carried out in order to gain a higher understanding of the effect of gibberellin on spore germination and thus provide crucial insights into the evolutionary history of the hormonal signalling pathway.

Materials and Methods.

SPORE GERMINATION ASSAYS.

P.patens Tissue Culture.

All tissue culture techniques were carried out under sterile conditions.

Gransden wild type *P.patens* gametophyte and protonemal tissue was cultured on BCD media (250mgl^{-1} $MgSO_4.7H_2O$, 250mgl^{-1} KH_2PO_4 (pH6.5), 1010mgl^{-1} KNO_3, 12.5mgl^{-1} $FeSO_4.7H_2O$, 0.001% Trace Element Solution [0.614mgl^{-1} H_3BO_3, 0.055mgl^{-1} $AlK(SO_4)_2.12H2O$, 0.055mgl^{-1} $CuSO_4.5H_2O$, 0.028mgl^{-1} KBr, 0.028mgl^{-1} LiCl, 0.389mgl^{-1} $MnCl_2.4H_2O$, 0.055mgl^{-1} $CoCl_2.6H_2O$, 0.055mgl^{-1} $ZnSO_4.7H_2O$, 0.028mgl^{-1} KI and 0.028mgl^{-1} $SnCl_2.2H_2O$) with 0.8% agar (Sigma-Aldrich) or as BCD liquid cultures, at 22°C under a 16h light regime (65µmoles/m_2/s or 4810 LUX; 36W Cool white fluorescent tubes). Additional 1mM $CaCl_2$ and 5mM ammonium tartrate was supplemented upon generation of protonemata, whilst BCD media used for the growth of gametophore was supplemented with only 1mM $CaCl_2$.

P.patens Induced Sporulation.

Cultured protonemal and gamtetophyte tissue was homogenised for 1 minute at 19,000rpm, using a polytron tissue tearer (IKA® T25 digital Ultra-Turrax), and used to cover the surface of a moist sterile peat plug (Jiffy Products UK). The homogenate covered peat plugs were placed in Magenta pots (Sigma) and exposed to a temperature of 22°C under a 16h light regime. Following successful generation of gametophore tissue over the entire surface (~3-4 weeks), the plugs were exposed to a lower temperature of 15°C under short day conditions (8h light and 16h dark; 50µmoles/m_2/s or 3996 LUX, 36W cool fluorescent tubes) to promote production of reproductive structures (~3-4 weeks). 1-2ml SDW was added to the base of the plug prior to the plugs being incubated back at 22°C for 1-2 weeks, in order to allow for the generation of sporophytes. Sterile forceps were used to harvest mature (dark brown) sporophytes from the plugs, using a Nikon SMZ645 dissecting microscope. Harvested sporophytes were left at room temperature for 1-2 weeks to dry before

being stored within sterile 2ml eppendorf tubes, in the dark at room temperature for future use.

Spore Germination Assays.

A ratio of at least three mature, dried sporophytes per ten petri dishes was used for assays, with sporophytes being of similar age and level of maturity (time post-harvest).

Sterilisation and release of spores from sporophytes.

Using sterile forceps and a Nikon SMZ645 dissecting microscope, gametophyte tissue was removed from the sporophytes, in addition to the foot and seta, with the sporophyte capsules only being used in subsequent steps. The sporophyte capsules were divided into groups of small numbers within sterile 2ml eppendorf tubes, and sterilised. 1ml 25% Parazone^{TM} bleach was added to the sporophytes, and the tubes were placed on a rotator for 10 minutes. Following removal of the bleach, 1ml sterile distilled water (SDW) was added to wash the spores, and the tubes were placed on the rotator for 10 minutes. This washing step was carried out a further two times, and the resultant sterilised spores were released from the sporophyte capsules, via the application of a mechanical pressure, in 1ml SDW.

Plating of Sterilised Spores.

Spore solutions were transferred to a falcon tube (15ml/50ml/round-bottomed) and diluted with SDW to permit 500µl to be plated on each petri dish. Sterile cellophane discs (A.A. Packaging Limited) were laid over the surface of BCD (supplemented with additional 5mM $CaCl_2$ and 5mM ammonium tartrate) agar. 500µl spore solution was plated, with the solution being resuspended by pipetting up and down three times beforehand to ensure even distribution of spores across all plates. Plates were allowed to dry before being sealed with Micropore^{TM} tape and either stored in the dark at 4°C for a short period of time before being transferred, or incubated directly at 22°C with a 16h light regime, to induce spore germination.

Exogenous hormone/chemical treatment to spores.

A volume of the hormone/chemical solutions to be analysed, was added to 1ml SDW in order to obtain a desired final concentration following the addition to the molten BCD agar media, prior to pouring it into the petri dishes. The same volume of solvent for each plate was ensured, and a solvent-only negative control was used for each hormonal/chemical assay.

Spore Germination Assay Data Collection.

A Leica compound microscope, with a total magnification of 40x (10x eyepiece; 4x objective lens), was used to observe and count plated spores, every 1-3 days, until the assay was deemed to be finished. The percentage of germinated spores for each plate was recorded, with a minimum of 200 spores being counted in total. A minimum of 2 technical replicates of each plate was carried out and the resultant average germination % was determined, with the standard deviation (STDEV) and standard error of the mean (SEM) being calculated using the functions available on Microsoft Excel. Spores were determined germinated following the observation of spore coat deformity and subsequent protonemal filament tissue growth.

For some assays, biological replicates were carried out with fresh media and spores of a different level of maturity (different post-harvest date) to those previously used.

Table 1. Information regarding the mutant bacterial extract and the corresponding wild-type and the *P.patens* mutants analysed in this present study.

Mutant bacterial extract and corresponding wild-type
Bacterial species: *Serratia plymuthica* **Mutant**: Referred to in study as AHL-deficient *Serratia* mutant (*S.plymuthica* C48). Only produces short-chain *N*-acyl-homoserine lactones; deficient in long-chain *N*-acyl-HSLs. **Source of extracts**: Liu Xiaguang, University of Nottingham, England. **Reference**: **Xiaoguang, L., Mohammed, B., Yingxin, M., Müller, H., Ovadis, M., Eberl, L., Berg, G. & Leonid, C.** (2007) Quorum-sensing signalling is required for production of the antibiotic pyrrolnitrin in a rhizospheris biocontrol strain of *Serratia plymuthica*. *FEMS Microbial Lett.* 270: 299-305.
***P.patens* mutants**
CPS/KS Mutants **(Genotypes analysed in present study)** 1) CPS/KS Disruption Mutant 2) CPS/KS Knockout Mutant (PBK3-e) **Source**: Henrik Toft Sorensen *et al*. (Denmark)
PpDellaA Mutant **Genotype:** Deficient in the DELLA A protein involved in the giberellin signalling pathway. **Source:** Nick Harberd *et al*. (Oxford, England)

Statistical Analysis.

Statistical analysis of the data was carried out via the application of a two-tailed student's T-Test, with two-sample assumed unequal variance, performed using the function on Microsoft Excel. Statistical analysis was carried out for each experimental array of data, at each time point, with that of the corresponding control data set. A *p*-value of <0.05 resulted in the conclusion that the data sets being analysed were statistically significantly different.

P.PATENS RNA EXTRACTION FOR TRANSCRIPTOME SEQUENCING BY JGI (Trizol Protocol).

RNA extraction carried out under sterile, RNase-free conditions.

Re: moss, CPS/KS came from Henrik Toft Sorensen's lab in Denmark, and the PpDellaA came from Nick Harberd's lab in Oxford.

RNA was extracted from dry spores (~250 harvested sporophytes), imbibed spores (spores from ~250 sporophytes in liquid BCD for ~14-16h) and germinating spores (spores from ~250 sterilised sporophytes plated at high density on BCD agar medium, incubated at 22°C (16h light) until >60% germination observed).

Imbibed spores were centrifuged in a 5415D Eppendorf Microcentrifuge for 30s at 10,000 x g and the BCD was removed.

Germinating spores were obtained from plates by scraping with a sterile microspatula and transferred to RNase-free microcentrifuge tubes.

P.patens spore material (dry, imbibed and germinating) was immediately froze in liquid nitrogen and homogenised either by using balls in a ball mill for 1min at 30Hz, or a micropestle.

1ml Trizol was added to the homogenised tissue, in a fume hood and material was subsequently vortexed until resuspended. Solutions were incubated at room temperature for 5 minutes to allow the dissociation of nucleoprotein complexes, centrifuged for 10 minutes at 12,000 x g at 4°C, and the resultant supernatant transferred to a sterile 1.5ml microcentrifuge tube. 200µl chloroform (0.2ml per initial ml of Trizol) was added, solutions were vortexed for 15s and incubated at room temperature for 2.5 minutes. Solutions were centrifuged for 15 minutes at 12,000 x g at 4°C until clear phase separation. Upper aqueous phase was transferred into a sterile 1.5ml microcentrifuge tube and 500µl isoproponal was added, solution was resuspended by pipetting up and down. Solutions were incubated at room temperature for 10 minutes, centrifuged for 10 minutes at 12,000 x g at 4°C and the

resultant supernatant was discarded. Visible white pellet was washed by adding 1ml 75% ethanol and centrifuging for 5 minutes at 7,500 x g at 4°C. The supernatant was removed and the pellet was air-dried at room temperature. Dry pellet was dissolved in 100µl RNase-free water and incubated for 10 minutes at 55°C. RNA samples were analysed using ND-1000 Nanodrop to determine concentration and purity.

RNA Clean-Up with QIAGEN RNeasy Mini Kit, using a modified version of the manufacturer's protocol.

350µl Buffer RLT + β-mercaptoethanol (10%) was added to 100µl extracted RNA sample. 250µl 100% ethanol was added to the RNA and solution was mixed by pipetting up and down. 700µl of the sample was transferred to an RNeasy mini spin column placed in a 2ml collection tube, and centrifuged for 15s at 8,000 x g. Flow-through was discarded.

DNase digestion. 350µl Buffer RW1 was added to the RNeasy spin column which was centrifuged for 15s at 8,000 x g. Flow-through was discarded and spin column was placed into a new 2ml collection tube. 10µl DNase 1 stock solution (lyophilized DNase 1 dissolved in 550µl RNase-free water, mixed by inversion and divided into aliquots for storage at -20°C) was added 70µl Buffer RDD and mixed by inverting gently and centrifuged briefly to collect residual liquid. 80µl DNase solution was added to the RNeasy spin column, directly. Samples were incubated at room temperature for 15 minutes. 350µl Buffer RW1 was added to the spin column and the samples were centrifuged for 15s at 8,000 x g and the flow-through was discarded.

RNA clean-up. 500µl buffer RPE was added to the RNeasy spin column and was centrifuged for 15s at 8000 x g. The flow-through was discarded and the spin column was carefully placed into a new 2ml collection tube. An additional 500µl Buffer RPE was added to the RNeasy spin column and the sample was centrifuged for 2 min at 8,000 x g. Flow-through was discarded and the spin column was placed into a new 2ml collection tube and was centrifuged for 1 minute at 8,000 x g. RNeasy spin column was placed into a sterile 1.5ml RNase-free microcentrifuge tube. 30µl pre-heated (37°C) RNase-free water was added directly onto the column membrane and

the sample was centrifuged for 1 minute at 8,000 x g to elute the RNA. Eluate was re-eluted through the spin column as an attempt to increase obtained yield, and centrifuged for another 1 minute at 8,000 x g. RNA samples were analysed again using a ND-1000 Nanodrop. RNA samples were stored at -80°C.

P.PATENS RNA PREPARATIONS FOR TRANSCRIPT ANALYSIS OF MUTANTS AND REVERSE TRANSCRIPTION - POLYMERASE CHAIN REACTION (RT-PCR), FOR GENE EXPRESSION ANALYSIS.

RNA extractions were conducted using the BIOLINE ISOLATE II RNA PLANT KIT.

RNA was extracted from dry spores, imbibed spores and germinating spores, in addition to the vegetative material; colony tissue (entire *P.patens* plant), gametophyte (obtained by cutting from a plug prior to the production of reproductive structures) and protonemal tissue. RNA was extracted according to the manufacturer's guidelines for both of the kits used, with the exception that pre-heated (37°C) RNase-free water was used for the elution of the RNA, and the eluate was re-eluted to increase yield. RNA samples were analysed using a ND-1000 nanodrop and samples were stored at -80°C.

RT-PCR

RT-PCR was carried out on 20ng RNA using the BIOLINE MyTaq^{TM} One-Step RT-PCR Kit according to the product manual guidelines, in a TC-412 TECHNE Thermocycler, with the following gene-specific primers

Table 2. Gene-specific primer sequences for RT-PCR.

Gene	Primer Type	Primer Nucleotide Sequence (5' -> 3')	Expected Fragment size
Tubulin	Forward	TGTGCTGTTGGACAATGAG	438bp
Tubulin	Reverse	ACATCAGATCGAACTTGTG	
Ent-kaurene Synthase (CPS/KS)	Forward	CACAGACTTCCGATACCCATGG	521bp
Ent-kaurene Synthase (CPS/KS)	Reverse	GCCTTGGCATCTTCCATCATCG	

Table 3. RT-PCR Reaction Components for a 25µl reaction.

Reagent	Volume
2x MyTaq One-Step Mix	12.5µl
Forward Primer (10µM)	1µl
Reverse Primer (10µM)	1µl
Reverse Transcriptase	0.25µl
RiboSafe RNase Inhibitor	0.5µl
DEPC-H_20	Up to 20µl
Template (20ng)	5µl 4ngµl^{-1}
Total Volume = 25µl	

Table 4. RT-PCR Program [Reproduced from the BIOLINE Product Manual].

Cycles	Temperature	Time	Notes
1	45°C	20min	Reverse transcription
1	95°C	1min	Polymerase activation
40	95°C 60°C 72°C	10s 10s 30s	Denaturation Annealing Extension

GENOTYPE ANALYSIS.

DNA EXTRACTION

DNA was extracted from *P.patens* protonemal tissue using a BIOLINE ISOLATE II Plant DNA Kit, according to the manufacturer's protocol.

PCR

PCR was carried out on extracted DNA samples, using the BIOLINE MyTaq™ Red Mix, according to the product instructions, using the following gene-specific primers.

Table 5. Gene-specific primer sequences for PCR.

Gene	Primer Type	Primer Nucleotide Sequence (5' -> 3')	Expected Fragment size
Tubulin	Forward	TGTGCTGTTGGACAATGAG	752bp
Tubulin	Reverse	ACATCAGATCGAACTTGTG	

Table 6. PCR Reaction.

Reagent	Volume
MyTaq Red Mix, 2x	12.5µl
Forward Primer (20µM)	0.5µl
Reverse Primer (20µM)	0.5µl
DNA Template	Volume added to dilute DNA to 100ng.
Water (ddH_20)	Volume added to make a final reaction volume of 25µl.
Final Volume = 25µl	

The standard PCR cycling programme was carried out, as advised in the product manual, in a TC-412 TECHNE Thermocycler, using an annealing temperature of 50.15°C, 30 cycles of the denaturation/annealing/extension set and a final extension of 10 minutes. The PCR reactions were subsequently stored at 4°C until needed.

GEL ELECTROPHORESIS.

DNA (gDNA and cDNA) and RNA samples were visualised and analysed by gel electrophoresis. Gel Loading Buffer (6x) (New England Biolabs) was added to each sample, and subsequently loaded onto a 1% agarose (Web Scientific Iberose, High Specification Agarose) gel containing 0.5μgml^{-1} ethidium bromide, using a gel electrophoresis kit (Appleton Woods) and a Hoefer EPS 2A200 power supply.

The gel was visualised using a Gel-Doc XR imager using QuantityOne Software.

Results

Spore Germination Assays.

Germination of *P.patens* imbibed spores was determined following the observation of spore coat deformation and hence a less spherical appearance, due to protruding protonemal filaments, which give rise to the generation of a protonemal colony (Fig.3). From Figure 3 (A, B), it can be seen that a spore increases subtly in diameter and becomes more spherical in appearance following imbibition. Figure 3C represents the apparent deformation of the spore coat, as a result of the protruding protonemal filament. In this present study, germinating spores are said to have been those whereby a protonemal filament is visible, either by the reduction in the spherical appearance of the spore coat, or by the presence of a protruding filament(s) or the clear formation of a protonemal colony. Therefore, spores shown in C-J of Figure 3 are considered to have germinated.

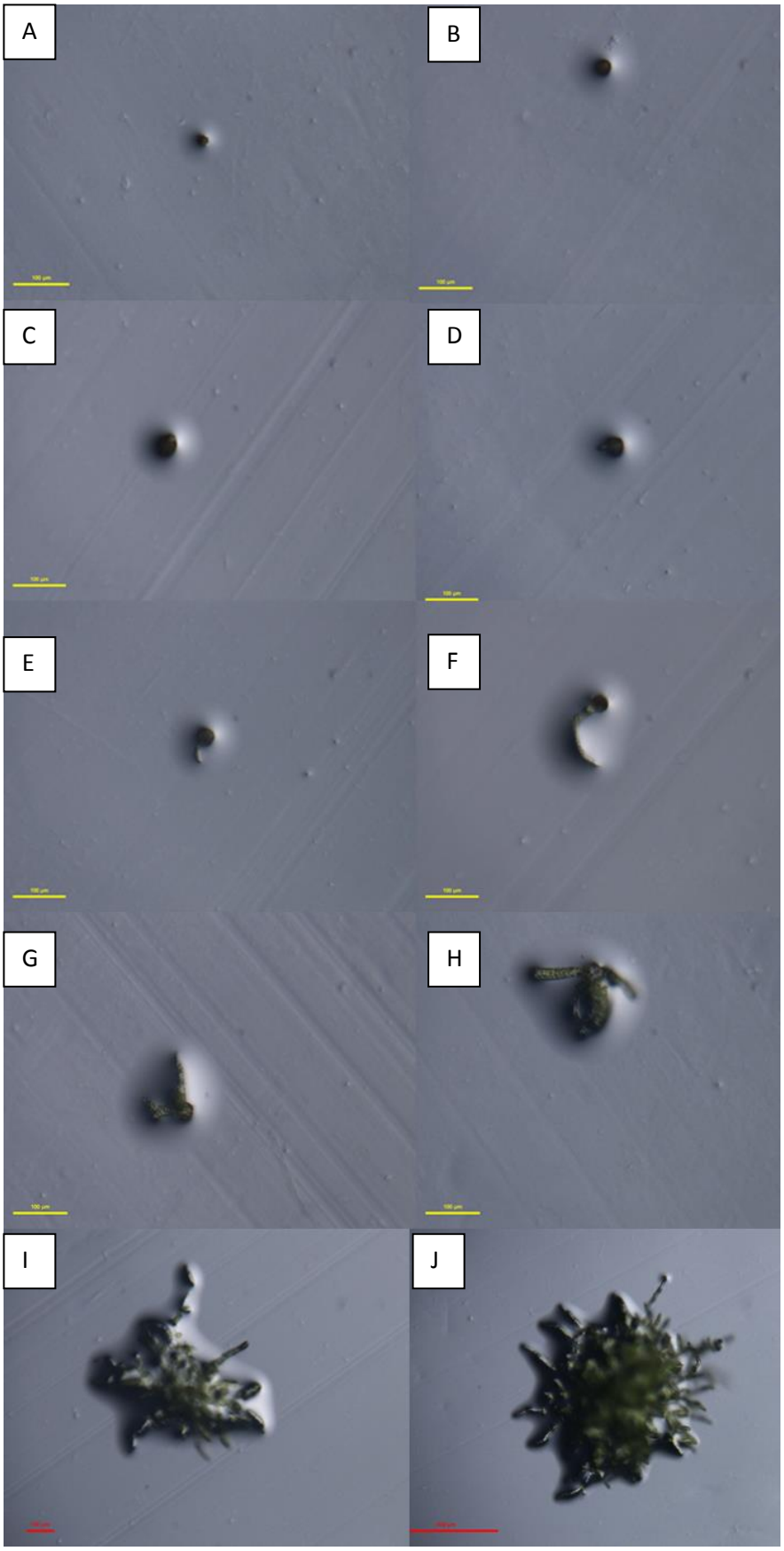

Figure 3. *Physcomitrella patens* spore germination. A-J represent the morphological changes that occur as a result of the germination process. (A) Dry spore. (B) Imbibed spore. (C) Deformation of spore coat. (D) Protrusion of protonemal filament. (E, F) Growth of protruding protonemal filament. (G) Protrusion of multiple protonemal filaments. (H, I, J) Formation of a protonemal colony and subsequent growth.

Initial germination of wild-type *P.patens* spores was shown to vary greatly between different spore batches, as seen from the data presented in this study, in addition to the rate of germination. This variation can be seen in Figure 4 whereby two different Wt spore batches were plated on BCD agar medium at the same time. It can be seen that spores that were harvested from the plugs the earliest (blue), showed an increased rate of germination compared to those harvested 13 days later (green), with some data points showing a highly significant increase, such as that for day 10.

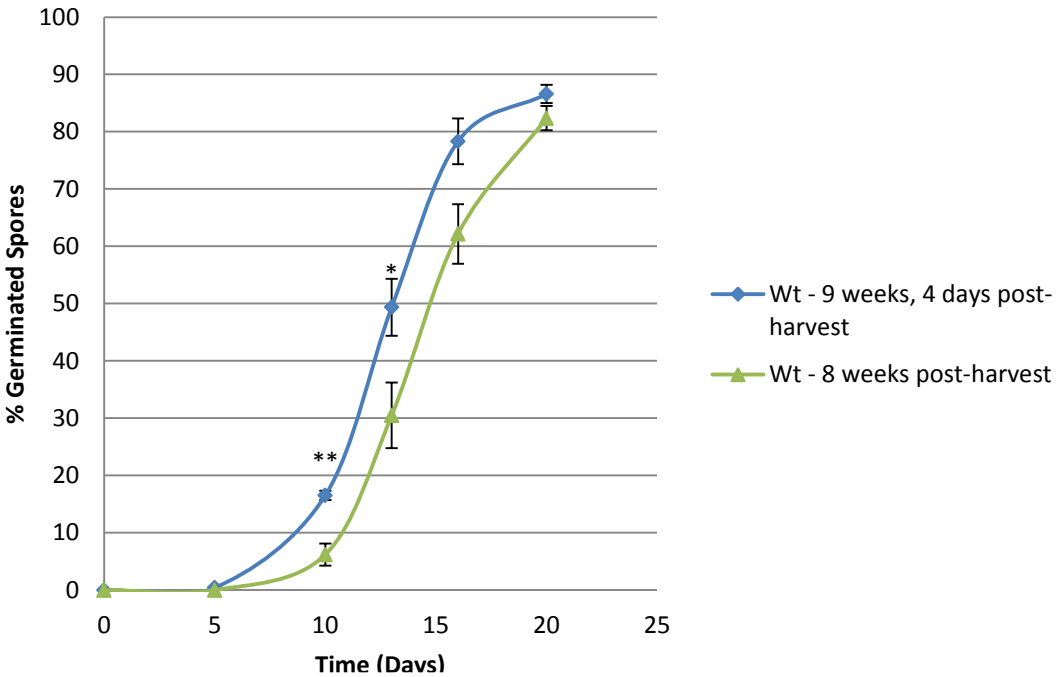

Figure 4. Spore germination assay indicating the germination rate of 2 different batches of wild-type *P.patens* spores with 1 week and 4 days difference between the dates in which the sporophytes were harvested, showing a higher rate for the older spores analysed. Statistical analysis - Student's T-Test (* = $p < 0.05$, ** = $p < 0.01$). Error bars = ± SEM.

For the germination assays presented in this study, wild-type spores were used to obtain negative control data when compared to data shown by mutant spores. Due to the possible variation between spores harvested at different times, for all assays

presented in this study, spores of the same or very similar (i.e. within 1-2 days) age (post-harvest) were used.

Analysing the effects of *N*-acyl-homoserine lactones of different substitution states at C3 and different chain lengths on *P.patens* spore germination.

10nM Synthetic Panel

In order to determine whether AHLs have an effect on spore germination, synthetic AHLs of different substitution states at carbon 3 (C3) and of varying carbon chain lengths were analysed, initially at a concentration of 10nM, as this had previously been found to be physiologically relevant (Coates et al. Unpublished Data). A panel of all of the substitution states and carbon chain lengths was tested on wild-type spores of the same age (5 months post-harvest).

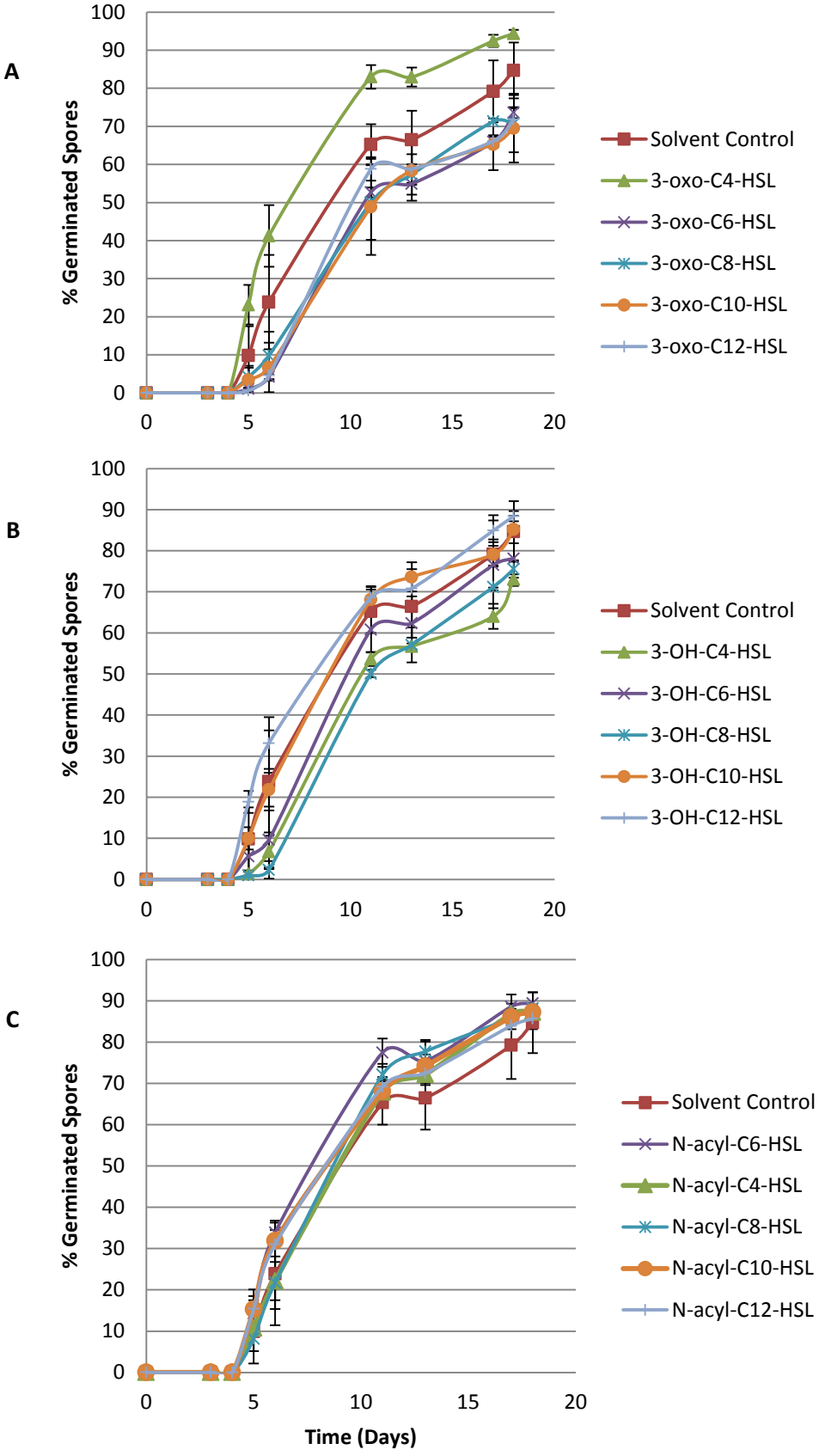

Figure 5. Spore germination assay indicating the germination rate of 15 day old (post-harvest) wild-type *P.patens* spores when grown on BCD media supplemented with 10nM synthetic AHLs of varying substitution states and chain lengths. Highest promotional effects shown by 3-oxo-C4-HSL. Statistical analysis - Student's T-Test (* = $p < 0.05$, ** = $p < 0.01$). Error bars = ± SEM.

Figure 5 (see also Fig.A1.1.) indicates the germination rate of 15 day old (post-harvest) Wt *P.patens* spores when supplemented with 10nM synthetic AHLs of varying chain lengths and substitution states at C3. It must be noted with this assay that the data obtained showed that the solvent- (methanol-) only control slightly promoted germination compared to that observed with the negative BCD-only control; however this promotion was not seen to be statistically significant over any of the time points (data not shown). A substitution state of oxo at C3 of chain length C4 can be seen to have the most promotional effects on spore germination compared to that observed with the solvent-only control, throughout the entire assay, although not statistically significant. On the other hand, the following synthetic AHLs at a final concentration of 10nM were found to show slightly lower levels of germination; 3-oxo-C6-HSL, 3-oxo-C8-HSL, 3-oxo-C10-HSL, 3-oxo-C12-HSL, 3-OH-C4-HSL, 3-OH-C6-HSL and 3-OH-C8-HSL. Therefore, it can be said that with the exception of 3-oxo-C4-HSL, the 3-oxo-HSLs had lower percentages of germination at each time point, and a lower rate.

In terms of the 3-OH-HSLs, it can be seen from Figure 5 (and Fig.A1.3) that the shorter chain molecules had a slight inhibitory effect on spore germination. However, the longer chains, C10 and C12, could be said to slightly promote germination with 3-OH-C10-HSL showing the same rate as the control experiment up until day 13, whereupon the germination rate increases during the log phase. 3-OH-C12-HSL also demonstrates promotional effects throughout the entire assay, albeit the increased rate is not statistically significant.

On the other hand, the *N*-acyl-HSLs were shown to have the most potent affect overall on spore germination, (Fig.5; Fig.A1.1), with all of the carbon chain lengths showing an increased average rate of germination during the log phase at day 17 (Fig.6).

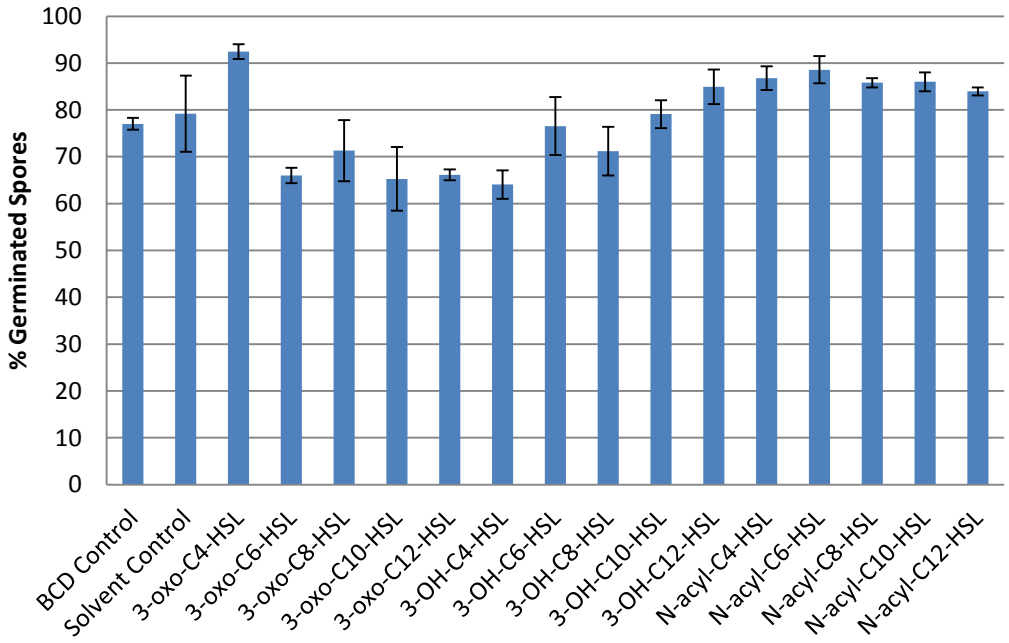

Figure 6. Graph illustrating the percentage of spore germination for spores grown on BCD media supplemented with the different AHL molecules at a final concentration of 10nM, and the relevant controls, at day 17 of the assay, showing significant promotion by all of the unsubstituted HSLs and 3-oxo-C4-HSL. Statistical analysis - Student's T-Test (* = $p < 0.05$, ** = $p < 0.01$). Error bars = ± SEM.

When the AHLs were substituted with OH and HSL, it is apparent that the chain lengths C10 and C12 were consistently more potent in terms of promoting spore germination.

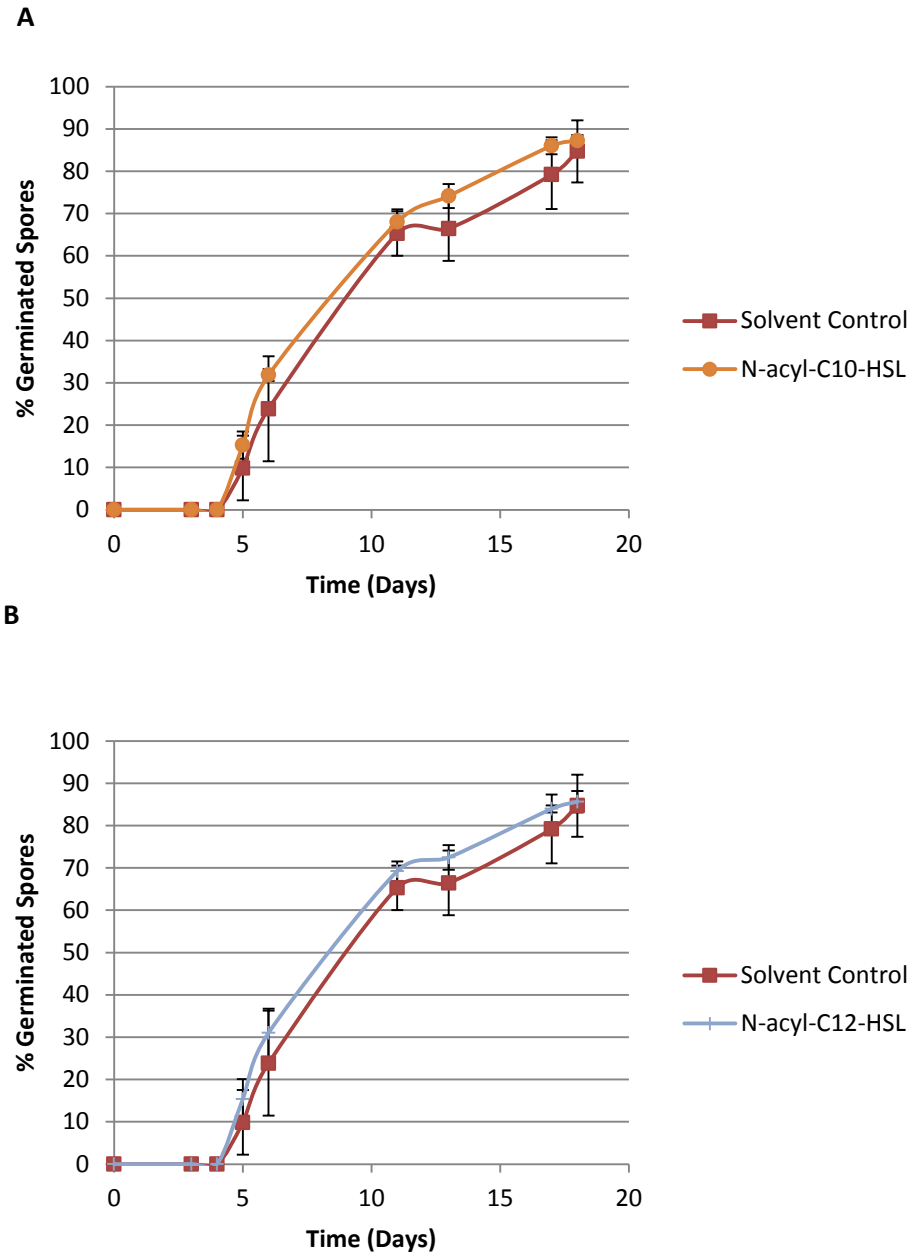

Figure 7. *P.patens* spore germination when spores were grown on BCD medium supplemented with 10nM synthetic N-acyl-HSLs of carbon chain lengths C10 (A) and C12 (B), compared to that of the solvent-only control, demonstrating promotion for both chain lengths. Statistical analysis - Student's T-Test (* = $p < 0.05$, ** = $p < 0.01$). Error bars = ± SEM.

N-acyl-HSLs, C10 and C12, in length show slightly increased germination compared to that shown by the solvent-only control (Fig.7). As a result of the promoting effects on spore germination of the long chain (C10, C12) 3-OH-HSLs and *N*-acyl-HSLs, at a final concentration of 10nM, the effects of the C10 and C12 AHLs at a range of

concentrations was analysed in order to ascertain a concentration at which these effects are more potent.

Long chain (C10) Synthetic AHL Assays at a range of concentrations.

AHL molecules of chain length C10 were exogenously added to the BCD media on which spores that had been harvested two months previously, were grown on. In order to ascertain which concentrations optimised the promoting effects on spore germination, of the different substitution states of AHLs, four different concentrations were used: 2nM, 10nM, 0.1µM and 1µM.

A

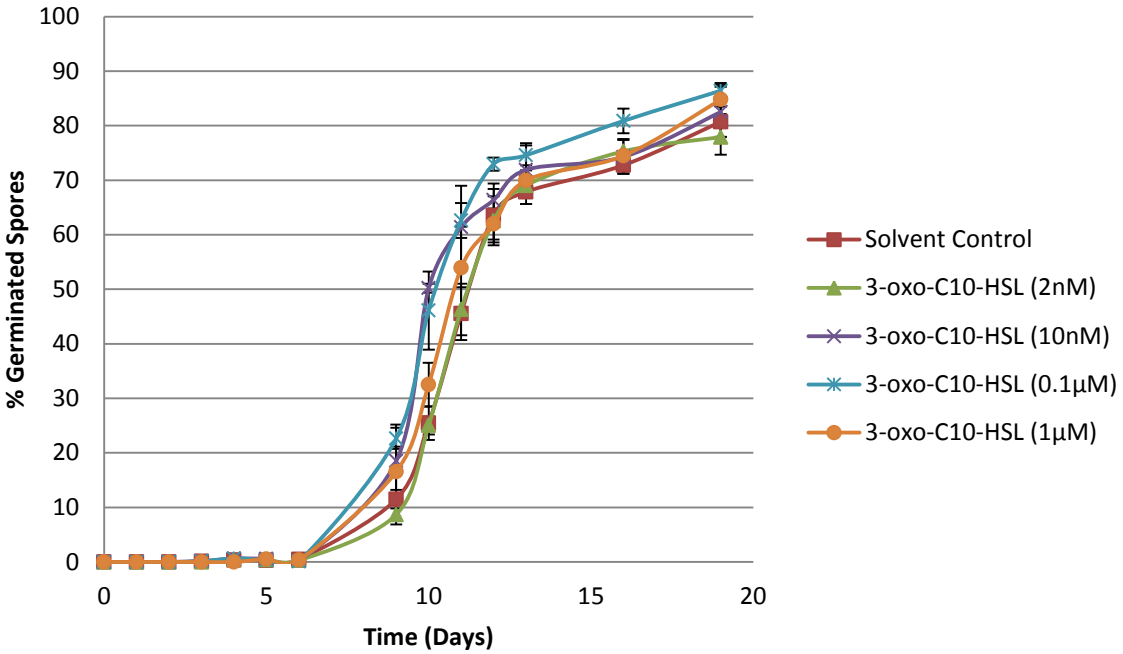
100
90
80
70
60
50
40
30
20
10
0
% Germinated Spores
0
5
10
15
20
Time (Days)
Solvent Control
3-oxo-C10-HSL (2nM)
3-oxo-C10-HSL (10nM)
3-oxo-C10-HSL (0.1µM)
3-oxo-C10-HSL (1µM)

B

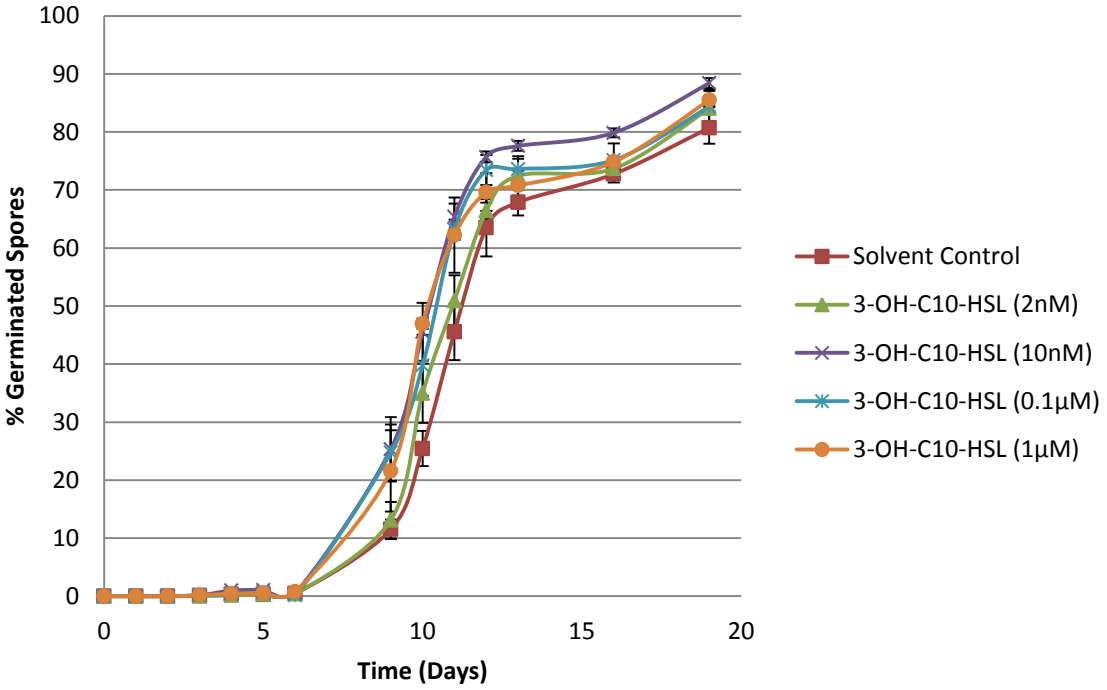
100
90
80
70
60
50
40
30
20
10
0
% Germinated Spores
0
5
10
15
20
Time (Days)
Solvent Control
3-OH-C10-HSL (2nM)
3-OH-C10-HSL (10nM)
3-OH-C10-HSL (0.1µM)
3-OH-C10-HSL (1µM)

C

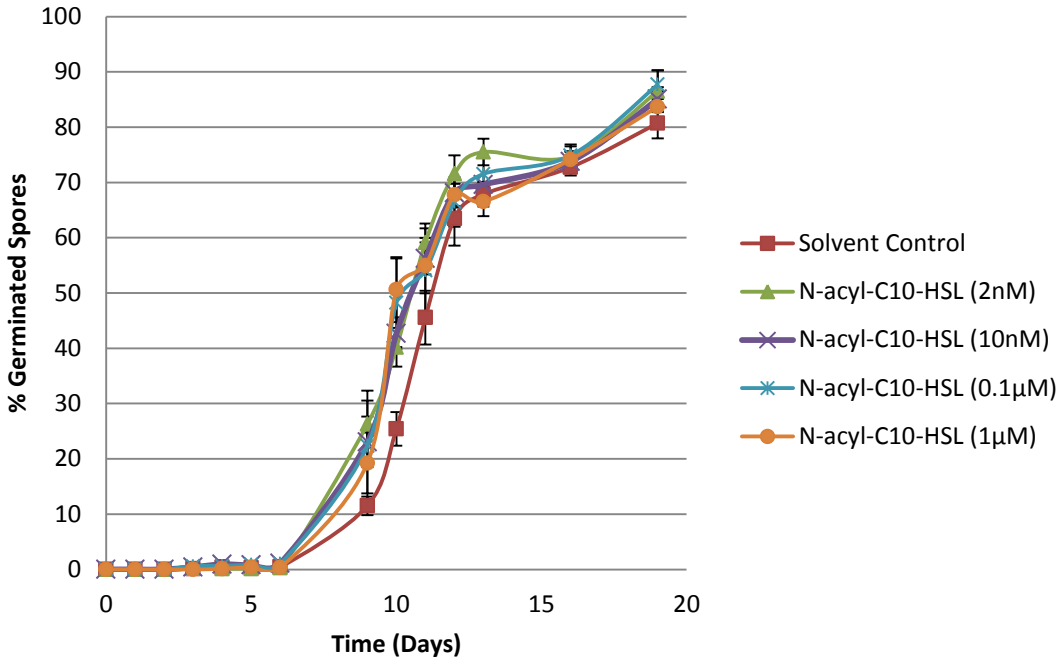

Figure 8. *P.patens* spore germination when spores were grown on BCD medium supplemented with synthetic *N*-acyl-HSLs of carbon chain lengths C10 at concentrations 2nM, 10nM, 0.1µM and 1µM, compared to that of the solvent-only control. A) 3-oxo-C10-HSLs. B) 3-OH-C10-HSLs. C) *N*-acyl-C10-HSLs. Most of the HSLs show an increased rate of germination compared to that of the control, although not a significant promotion. Error bars = ± SEM.

The majority of the substituted and non-substituted acyl-HSLs show an increased spore germination rate compared to that observed for the solvent-only control, at the different concentrations analysed (Fig.8). It can be deduced that 3-oxo-C10-HSLs show a slight increase at concentrations of 10nM and 1µM, whilst at a concentration of 2nM the rate could be said to be slightly lower than that shown by the solvent-only control, indicating no increase in spore germination. It is apparent that the 3-oxo-C10-HSLs show the most potent increased rate of spore germination at a concentration of 0.1µM (Fig.8A).

On the other hand, spore germination rate was observed to be slightly increased by the addition of 3-OH-C10-HSLs at all of the 4 concentrations used (Fig.8B), with the most promotion at 10nM (Fig.9).

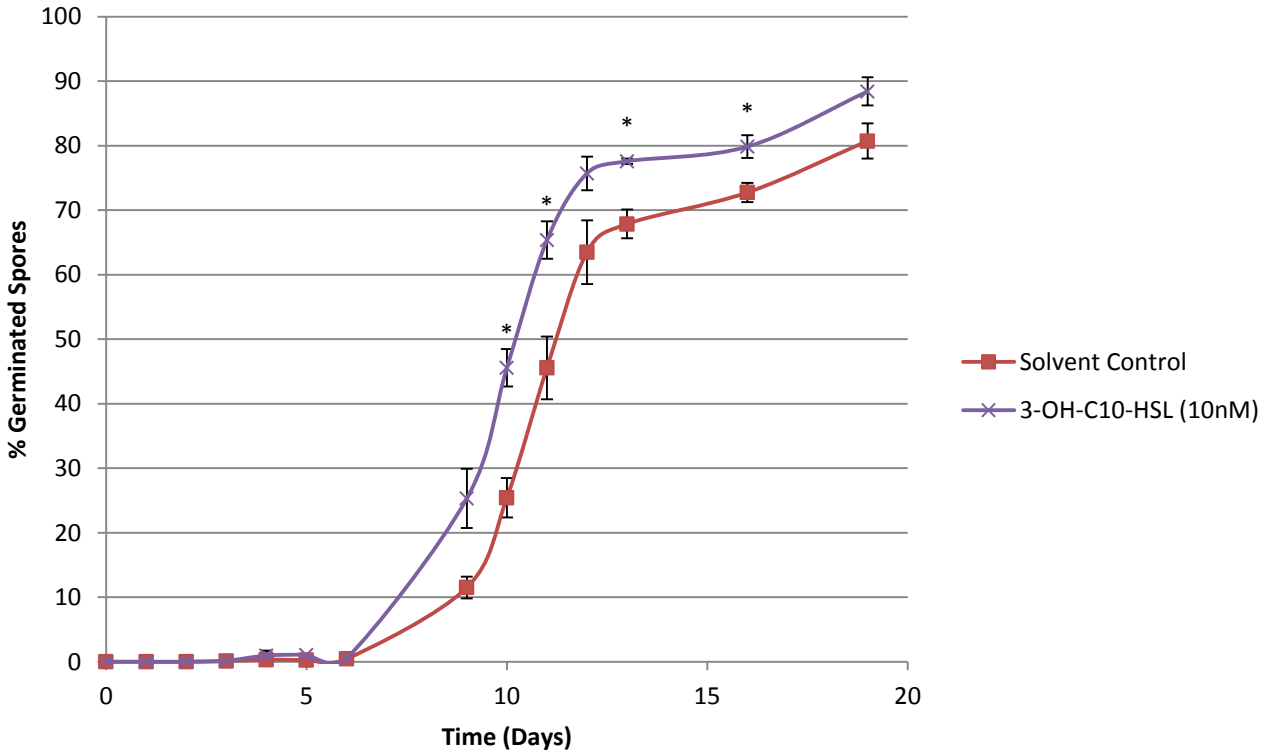

Figure 9. *P.patens* spore germination when spores were grown on BCD medium supplemented with synthetic 3-OH-C10-HSL at a concentration of 10nM compared to that of the solvent-only control. 3-OH-C10-HSL at 10nM showed significant promotion of germination rate, compared to that of the control, over 4 individual time points. Statistical analysis - Student's T-Test (* = $p < 0.05$, ** = $p < 0.01$). Error bars = ± SEM.

The synthetic AHL substituted with an OH group at C3, of chain length C10, adequately increased spore germination rate, with four of the data points being shown to be statistically significant, compared to the negative control (Fig.9).

Furthermore, *N*-acyl-C10-HSLs slightly increased spore germination rate at all of the concentrations used, at a similar level (Fig.8C).

Long chain (C12) Synthetic AHL Assays at a range of concentrations.

The following assay involved analysing the effects of exogenously added synthetic AHLs of different substitution states and length of C12, at different concentrations, to BCD medium in which spores of 2 months old (post-harvest) were grown on.

A

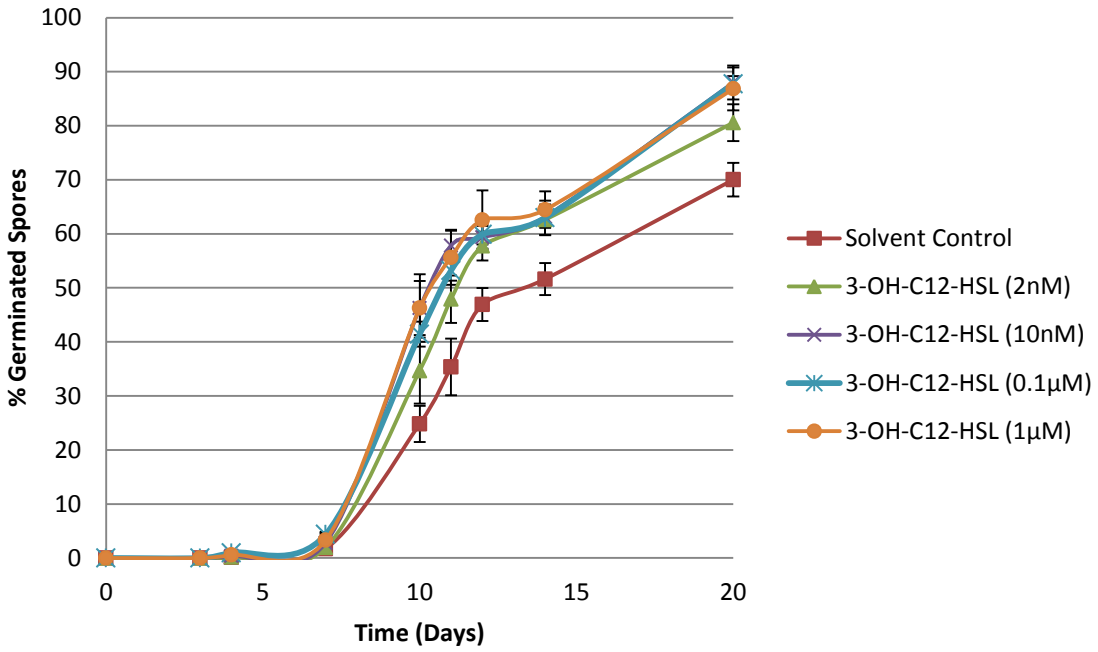

B

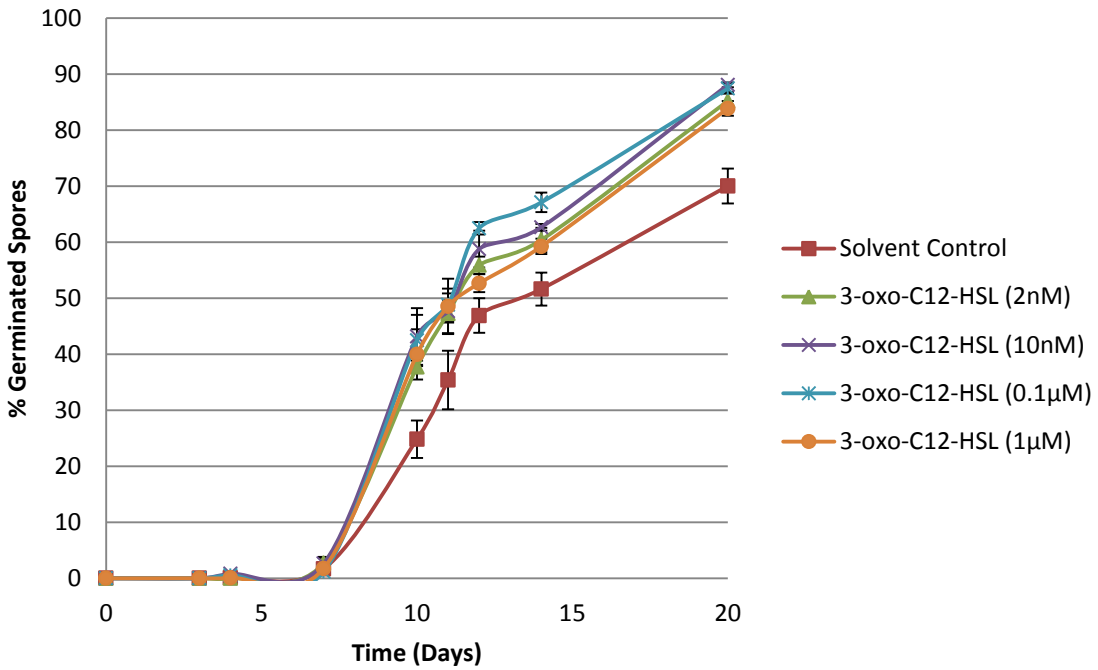

C

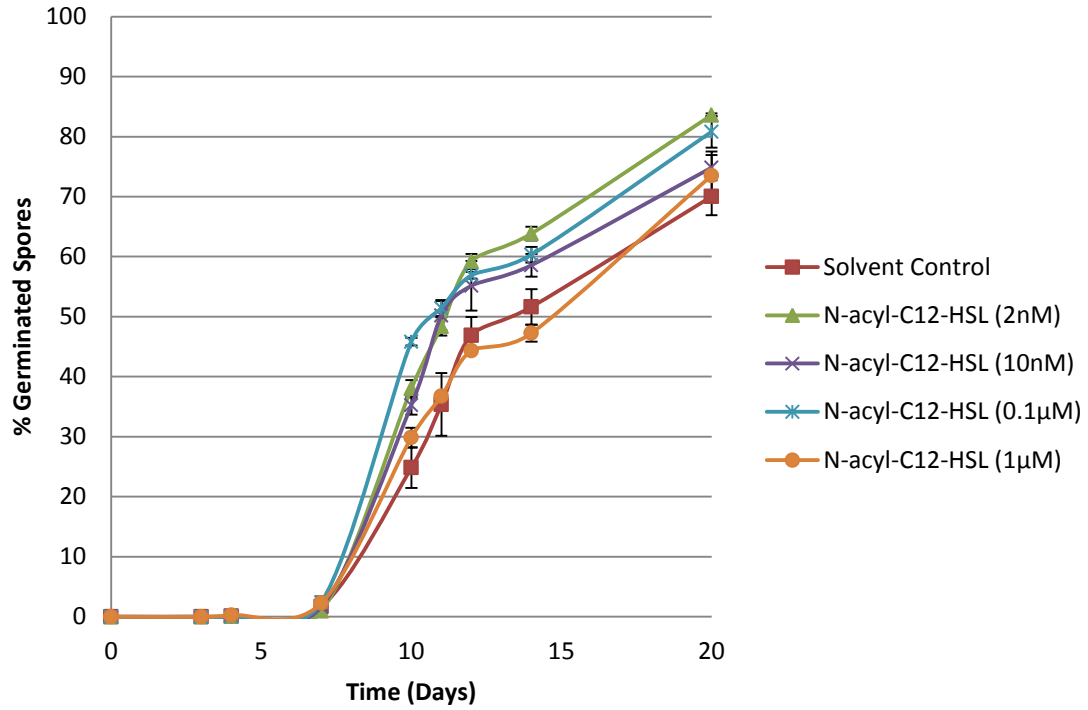

Figure 10. *P.patens* spore germination when spores were grown on BCD medium supplemented with synthetic *N*-acyl-HSLs of carbon chain lengths C12 at concentrations 2nM, 10nM, 0.1µM and 1µM, compared to that of the solvent-only control, showing that promotional effects of the different substituted C12-HSLs varies with varying concentrations. A) 3-oxo-C10-HSLs. B) 3-OH-C10-HSLs. C) N-acyl-C10-HSLs. Error bars = ± SEM.

3-oxo-C12-HSLs increase spore germination at all of the four concentrations used (Fig.10A). This increase appears to be dose-dependent in the fact that as the concentration is increased from 2nM to 0.1µM, the rate of germination increases slightly. However, at a concentration of 1µM, spore germination appears to be increased but to a lesser extent compared to that observed with the other three concentrations.

With regards to the 3-OH-C12-HSLs, it appears that these too all increase spore germination at the concentrations used in this assay (Fig10.B). At the highest concentration of 1µM, it can be seen that spore germination is promoted the most, when compared to that observed by the solvent-only control.

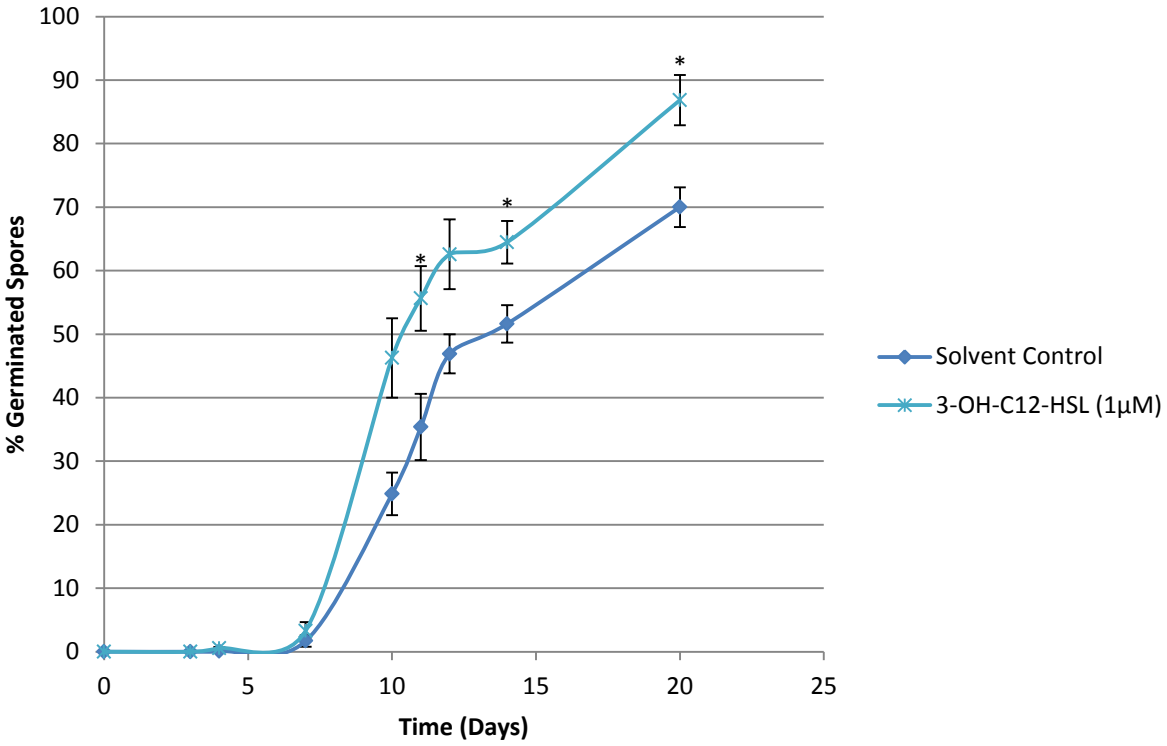

Figure 11. *P.patens* spore germination when spores were grown on BCD medium supplemented with synthetic 3-OH-C10-HSL at a concentration of 1µM compared to that of the solvent-only control. Significant increased germination can be seen at three individual time points, highlighting the promotional effect of 3-OH-C12-HSL at this concentration. Statistical analysis - Student's T-Test (* = $p < 0.05$, ** = $p < 0.01$). Error bars = ± SEM.

The extent of this promotion on spore germination is exemplified in Figure 11, whereby it can be seen that 3-OH-C12-HSLs at a concentration of 1µM significantly increased germination percentage at three different time points analysed.

Nevertheless, the *N*-acyl-C12-HSLs at a concentration of 1µM, promote spore germination very little (Fig.10C). However, it can be seen that these molecules show an increased rate of germination at the lower concentrations, with the most potent effect being observed at 2nM.

0.1µM Synthetic Panel

As a result of the data presented in both Figures 8 and 10, it can be seen that at a concentration of 0.1µM, all of the substitution states of the AHLs have a positive effect on spore germination, to some extent. Therefore, the AHL molecules with both the short and long chain lengths were analysed at a final concentration of 0.1µM, as this concentration was deemed adequate for all of the longer chained AHLs as a whole, with 2 month old (post-harvest) wild-type spores.

A

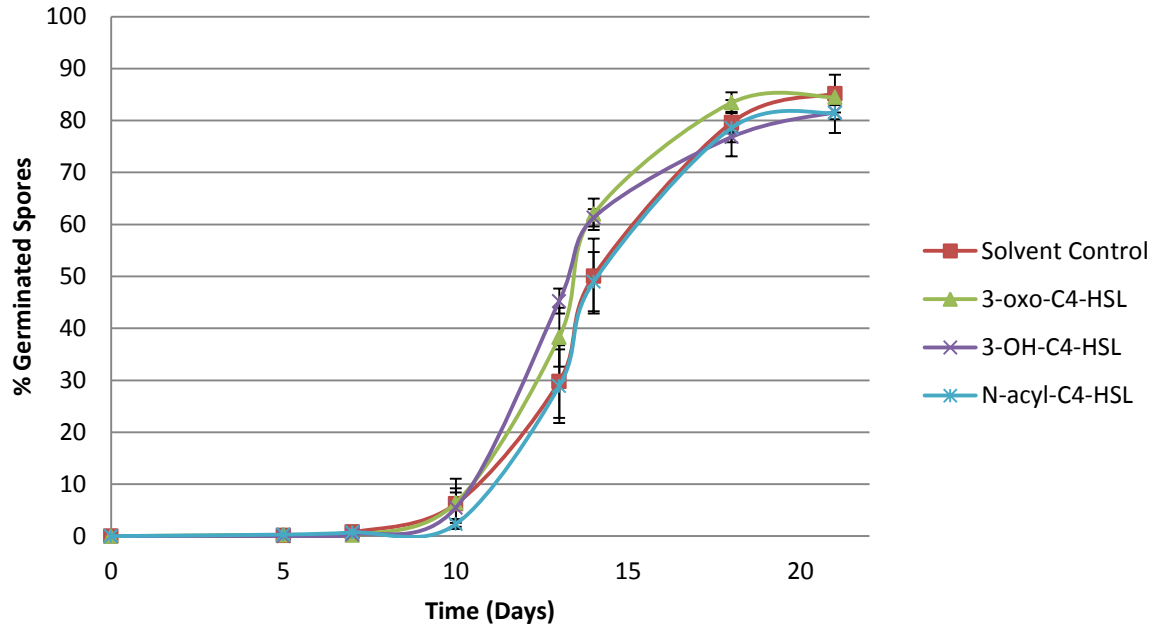

B

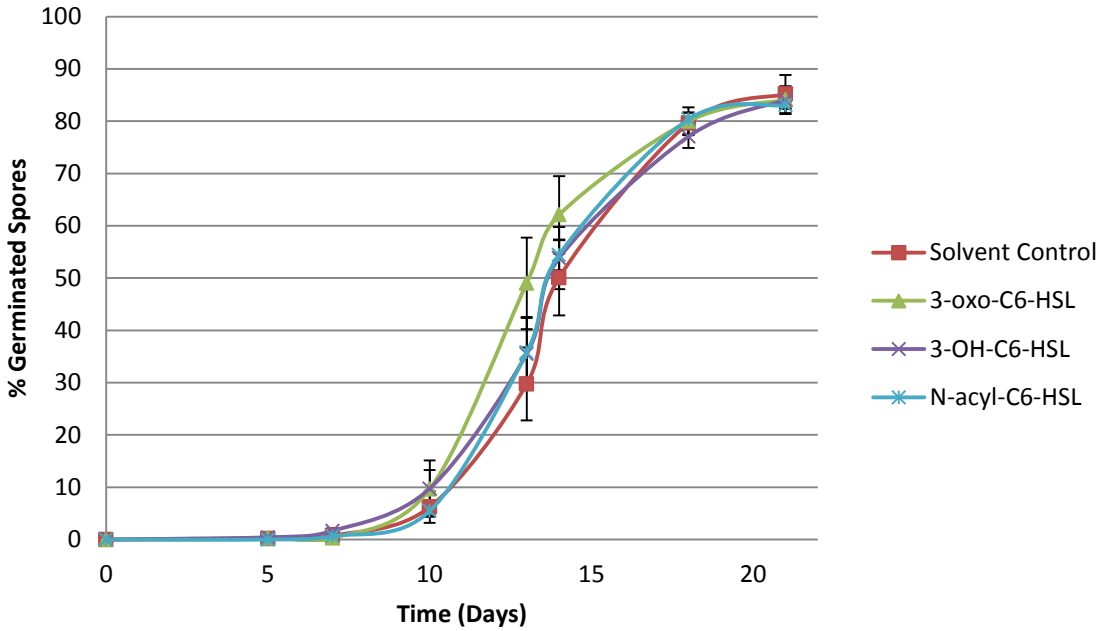
100
90
80
70
60
50
40
30
20
10
0
% Germinated Spores
0
5
10
15
20
Time (Days)
Solvent Control
3-oxo-C6-HSL
3-OH-C6-HSL
N-acyl-C6-HSL

C

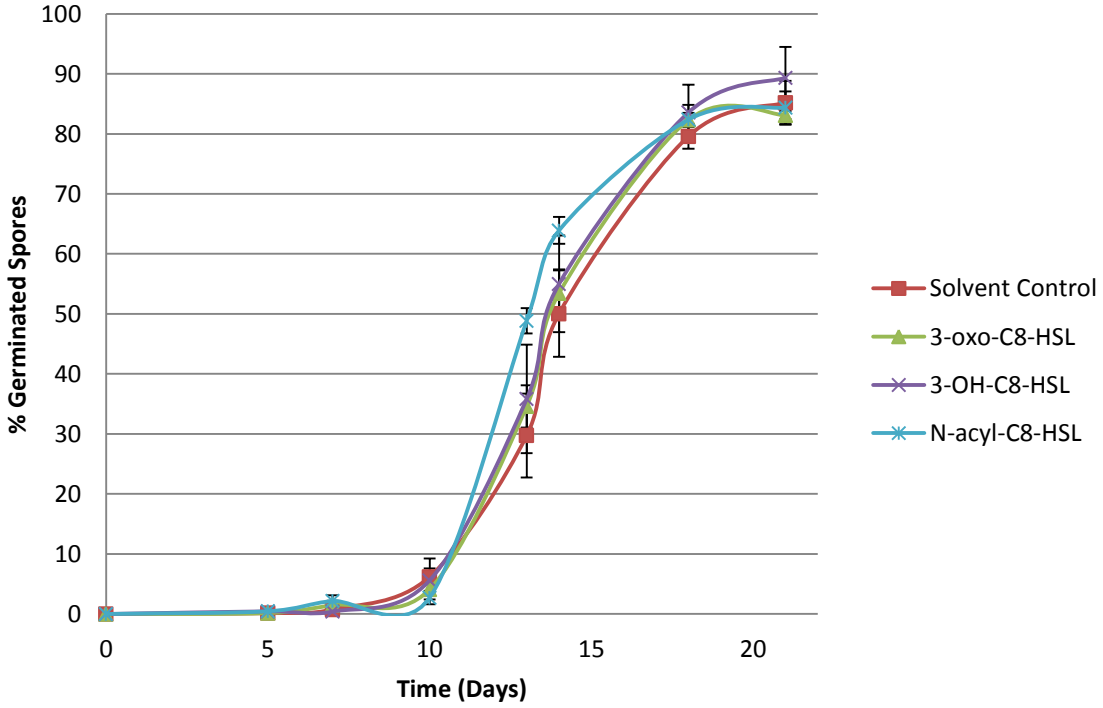
100
90
80
70
60
50
40
30
20
10
0
% Germinated Spores
0
5
10
15
20
Time (Days)
Solvent Control
3-oxo-C8-HSL
3-OH-C8-HSL
N-acyl-C8-HSL

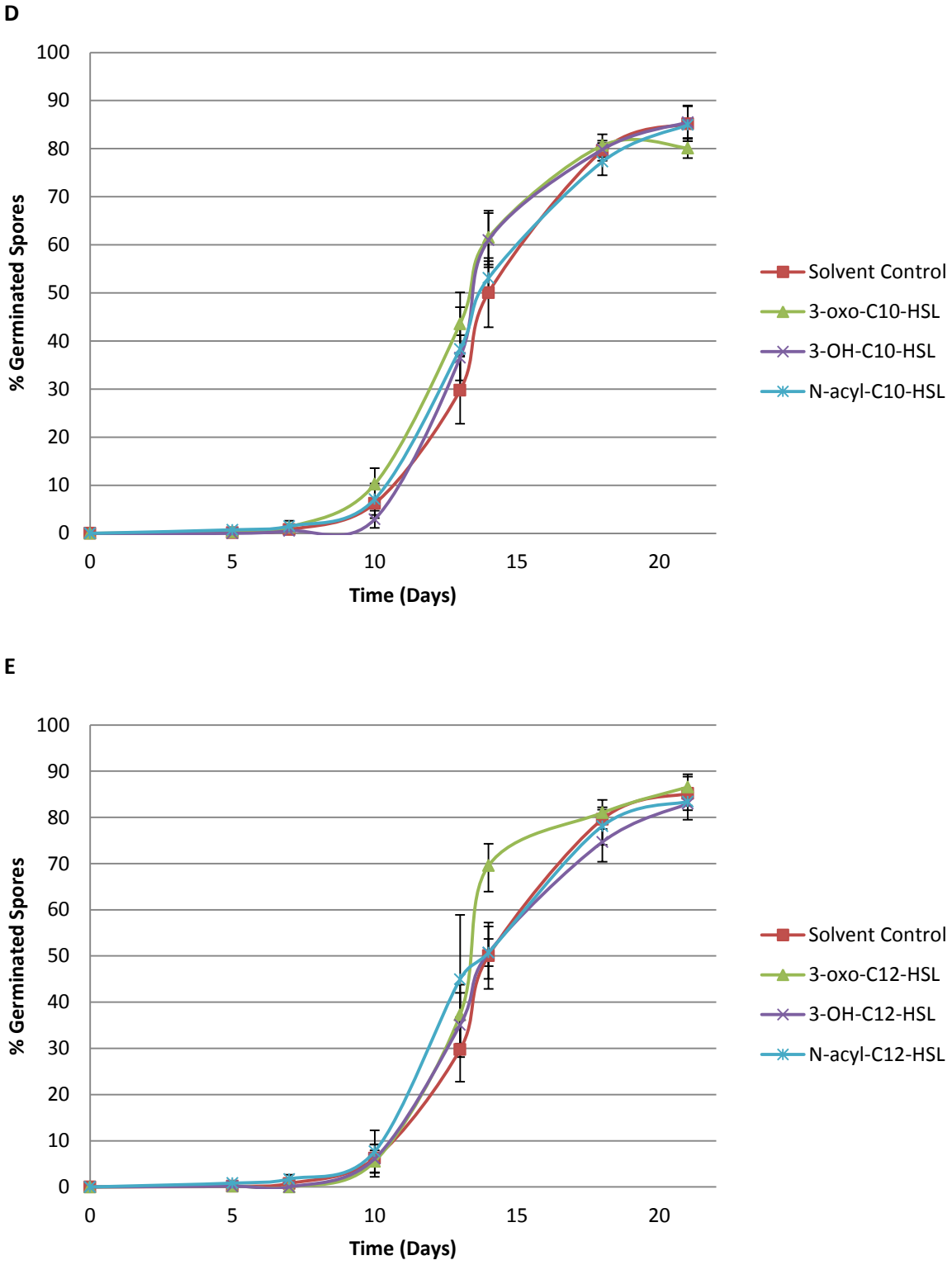

Figure 12. Spore germination assay indicating the germination rate of 2 month old (post-harvest) wild-type *P.patens* spores when grown on BCD media supplemented with 0.1µM synthetic AHLs of varying substitution states and chain lengths, showing no or very low increased germination rates. Error bars = ± SEM.

The majority of the different substituted AHLs of varying chain lengths very slightly promote spore germination at 0.1µM (Fig.12). The increased promoting effects observed from the AHLs at a concentration of 10nM (Fig.5), is not apparent at 0.1µM. For instance, 3-oxo-C12-HSL shows the same germination rate as observed for the solvent-only control, up to a point, whereby there is then an increase in the rate over a short period of time, however the rate then goes to stationary phase and matches that seen for the negative control by day 20. Initially, on day 7, 3-oxo-C12-HSL and 3-OH-C12-HSL even showed significantly decreased germination. For the C10 and C12 *N*-acyl-HSLs, it can be seen that there is an initial promotional effect on the rate of germination, however as the germination rate comes to the end of the log phase and into the stationary phase, the rate of germination becomes lower than that seen with the negative control.

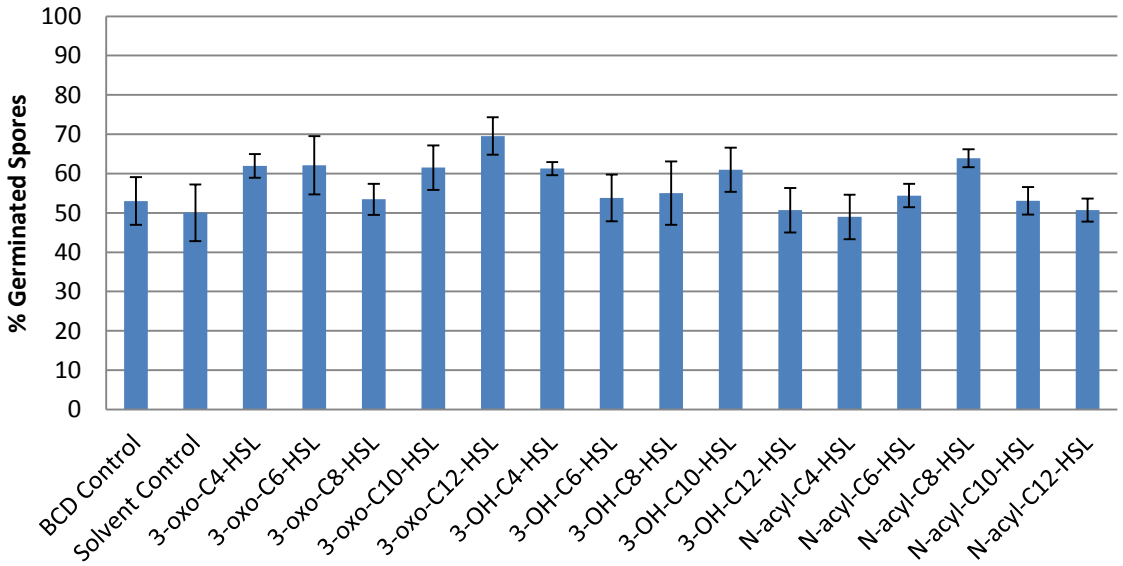

Figure 13. Graph illustrating the percentage of spore germination for spores grown on BCD media supplemented with the different AHL molecules at a final concentration of 0.1µM, and the relevant controls, at day 14 of the assay. C10 and C12 3-oxo-HSLs showed increased germination compared to the shorter chains of this substitution state. Statistical analysis - Student's T-Test (* = $p < 0.05$, ** = $p < 0.01$). Error bars = ± SEM.

Figure 13 illustrates the percentage of germination observed at a single time point, day 14, for each of the different treatments and the relevant controls. From this, it can be seen that the slight increase observed is not statistically significant. It is apparent however, that for the 3-oxo-HSLs, the two longer chained molecules of C10 and C12 in length, have a higher percentage of germination than the shorter chained molecules, however this effect is not observed for the 3-OH-HSLs or the *N*-acyl-HSLs.

Long Chain (C10 and C12) Synthetic AHLs at a concentration of 0.1µM on older (post-harvest) P.patens spores.

Due to the only subtle promoting effects, if any, of the long chain AHL molecules at 0.1µM on spores 2 months of age (post-harvest) (Fig.12), the same analysis was carried out with older spores that were 8 months post-harvest, to test the hypothesis that younger spores may be slightly insensitive to the effects of AHLs.

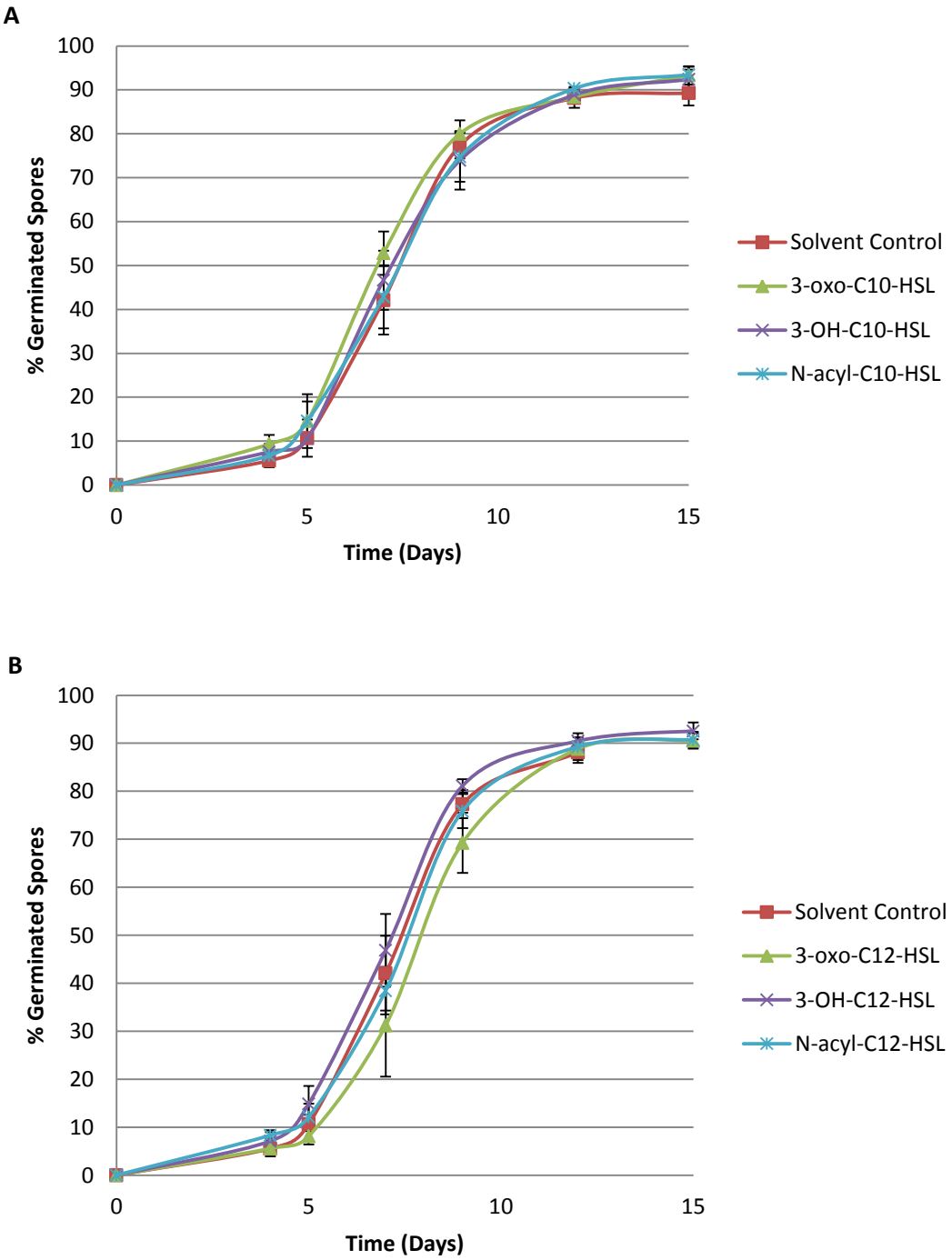

Figure 14. Spore germination assay indicating the germination rate of 8 month old (post-harvest) wild-type *P.patens* spores when grown on BCD media supplemented with 0.1µM synthetic AHLs of varying substitution states and long chains. A) C10. B) C12. Error bars = ± SEM.

The long chain AHL molecules at a final concentration of 0.1µM, within BCD media of which 8 month old (post-harvest) spores were grown on; do not show much promotional effects on the rate of germination (Fig.14). It can be seen that for 3-oxo-

C10-HSL there is a slight increase, however for the C12 3-oxo-HSL, the rate of germination is actually lower than that observed for the solvent-only control. On the other hand, 3-OH-C10-HSL shows a similar germination rate as for the control whereby there is a small increase seen for the C12 equivalent. Furthermore, for both the C10 and C12 *N*-acyl-HSLs the germination rate was very similar to that seen for the solvent-only control with only a very subtle increase seen for the longer chain *N*-acyl-HSL (Fig.14.).

Abscisic Acid Rescue with C10 and C12 Synthetic AHLs at a concentration of 0.1µM.

From the results obtained previously within this study, it was deduced that AHLs of C12 in length, have overall a slightly more potent promoting effect on spore germination than the shorter chains. As a result, the C12 AHLs at 0.1µM were exogenously added to BCD medium on which 2 month old (post-harvest) spores were plated on, in addition to ABA at concentrations of 5µM and 10µM. This was carried out in order to test whether the promoting effects observed for the C12 AHLs were sufficient enough to rescue and therefore overcome, the inhibitory effects already known for ABA.

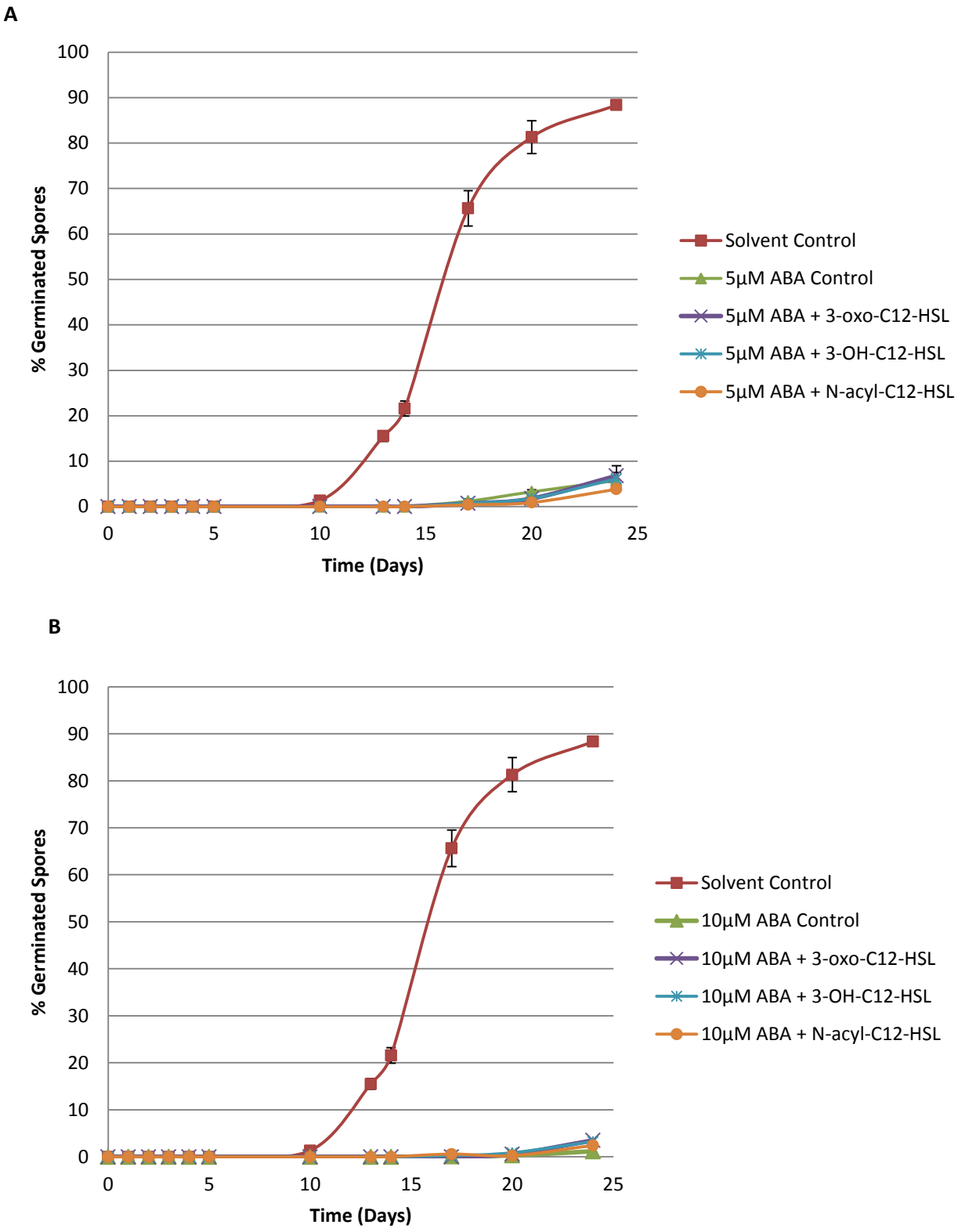

Figure 15. Spore germination assay indicating the germination rate of 2 month old (post-harvest) wild-type *P.patens* spores when grown on BCD media supplemented with 0.1µM synthetic C12 AHLs of varying substitution states and Abscisic Acid (ABA). A) 5µM ABA. B) 10µM ABA. The reduced germination caused by the ABA application at both concentrations, was not rescued by any of the C12-HSLs. Error bars = ± SEM.

It can be clearly seen that the initial germination observed for the spores occurred at day 10, for the solvent-only control (Fig.15). The C12 AHLs were not shown to rescue the inhibitory effect of ABA at a concentration of 5µM on spore germination at all, with the 3-oxo-C12-HSL and the *N*-acyl-C12-HSL showing a slightly lower germination rate than that shown for the 5µM control (Fig.15A). On the other hand, all three of the AHL variants displayed a very slight increased germination rate, when added to medium containing ABA, than the 10µM ABA control (Fig.15B). However, it can be seen that overall the AHL molecules did not rescue spore germination, as the rates were still remarkably lower than that shown by the solvent-only control.

The effects of natural AHL molecules secreted by a Serratia bacterial species when compared to an AHL-deficient mutant.

The following assay involved adding the extracts secreted by *Serratia* bacterial species (Wt) to the BCD medium, at a dilution of 1:50, in order to determine the effects of natural AHLs secreted by the bacteria. The extracts of an AHL-deficient mutant were also added for comparison (extracts prepared by Xiaguang Liu, Univ of Nottingham). As the extracts were within Luria Broth (LB) media, an LB-only control was used, in addition to a BCD-only control to ensure the spores used show ‘normal’ germination.

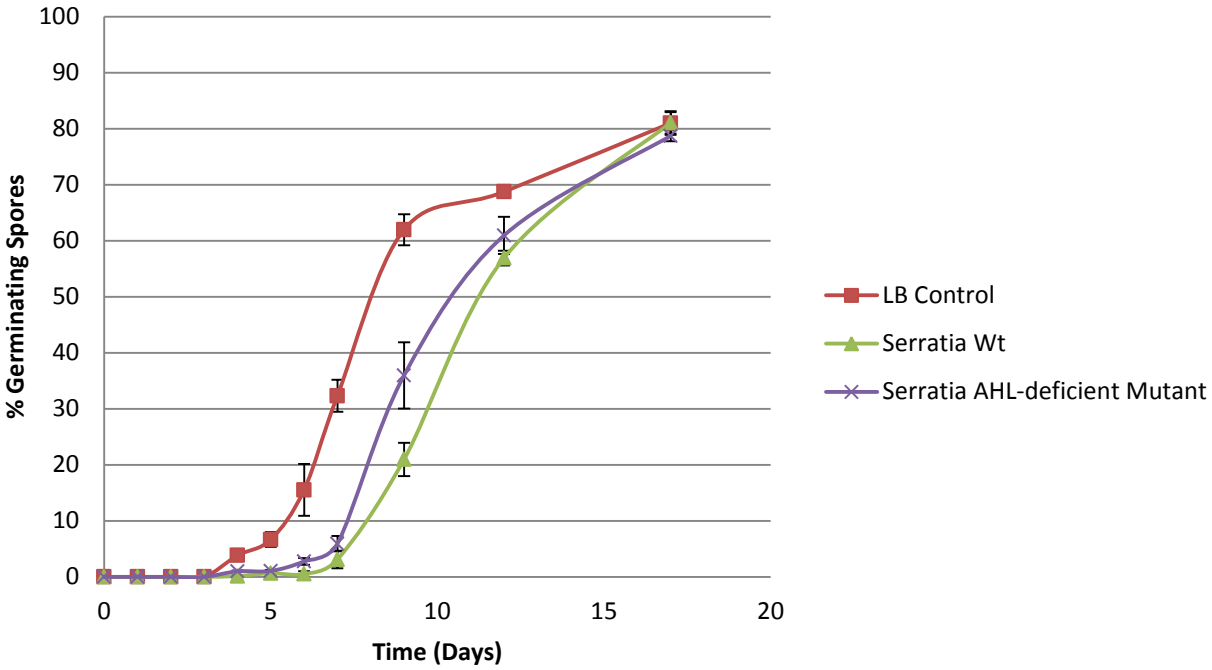

Figure 16. Analysing the effects of natural AHL molecules secreted by Serratia bacterial species, compared to the extract produced by an AHL-deficient mutant, on *P.patens* spore germination. Both the Serratia extracts showed a decreased rate of germination compared to that observed for the LB-only control, with an even lower rate shown for the Wt extract than for the AHL-deficient mutant extract. Error bars = ± SEM.

The LB control data did not show any effects of adding LB to the BCD medium, as there was no statistically significant difference between the spore germination observed between the LB-only control and the BCD control (data not shown). It can be seen from Figure 16 that both the extracts from both the Wt and mutant Serratia bacteria showed a decreased rate of germination compared to that shown by the LB-only control. The Serratia Wt extracts also show a reduced rate of germination compared to that shown by the spores that were grown on medium containing the extracts secreted by the AHL-deficient Serratia mutants. Therefore, this data does not show that the natural AHL molecules secreted by Serratia bacteria have a promoting effect on *P.patens* spore germination

Analysing the effects of gibberellin and abscisic acid and their respective pathways, on spore germination.

The Effect of Gibberellins on P.patens Spore Germination.

To analyse the effect of GA on spore germination and to ascertain whether 1µM GA_9-methyl ester could rescue the effects of 5µM and 10µM ABA, when exogenously added to BCD media, the following assay was carried out with spores 2 months of age (post-harvest).

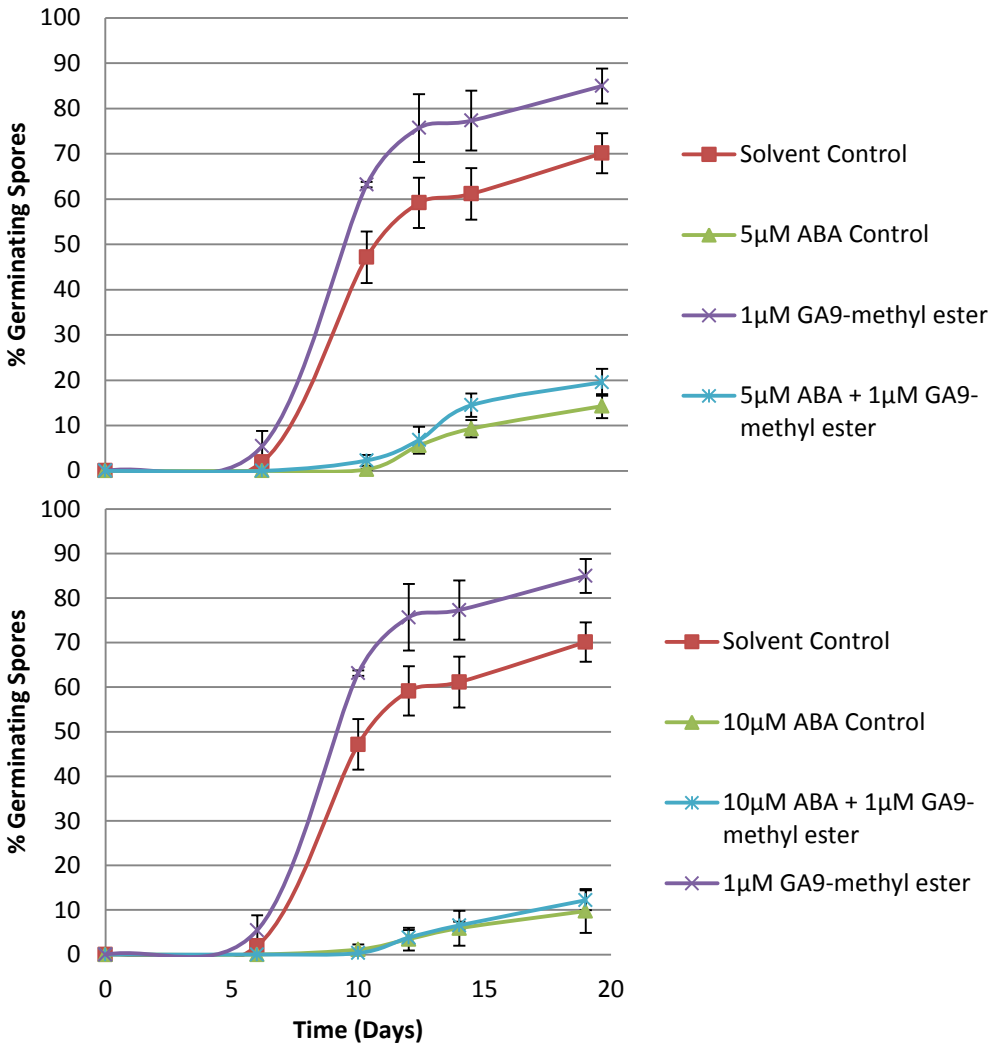

Figure 17. 5µM and 10µM ABA rescue with 1µM GA_9-methyl ester on *P.patens* spore germination. Application of GA_9-methyl ester showed increased germination rates, although no rescue of the inhibitory effects of ABA at both concentrations was seen. Error bars = ± SEM.

The addition of 1µM GA_9-methyl ester to the BCD medium, increases the germination rate of the spores, compared to that seen with the solvent-only control (Fig.17). However, this difference was not found to be statistically significant when analysed by the Student's T-test. The inhibitory effects on spore germination of both 5µM and 10µM can also be seen by Figure 17, as the germination observed is much lower than that seen for the negative control. However, when 1µM GA_9-methyl ester is also added to the medium, in addition to ABA at the two concentrations, there is a slight increase in the rate of germination compared to when ABA is present on its own. Nevertheless, even with the addition of GA_9-methy ester, it can still be seen that the rate of germination and level of germination is still very low compared to that observed for the solvent-only control and the GA_9-methyl ester control.

As a means to analyse the effects of the gibberellin pathway protein, *ent*-kaurene synthase (CPS/KS), on *P.patens* spore germination, an assay was carried out looking at two different CPS/KS mutants. One of the mutants was produced via disruption within the gene and the other mutant was a complete gene knockout (PBK3-e). The spore germination rates of the mutants were compared against Wt spores, of similar age (2 months post-harvest). For the complete gene knockout CPS/KS mutant, the Wt spores used in the assay were of the exact same age whereas for the disruption mutant, the Wt spores were harvested one day after the mutant spores.

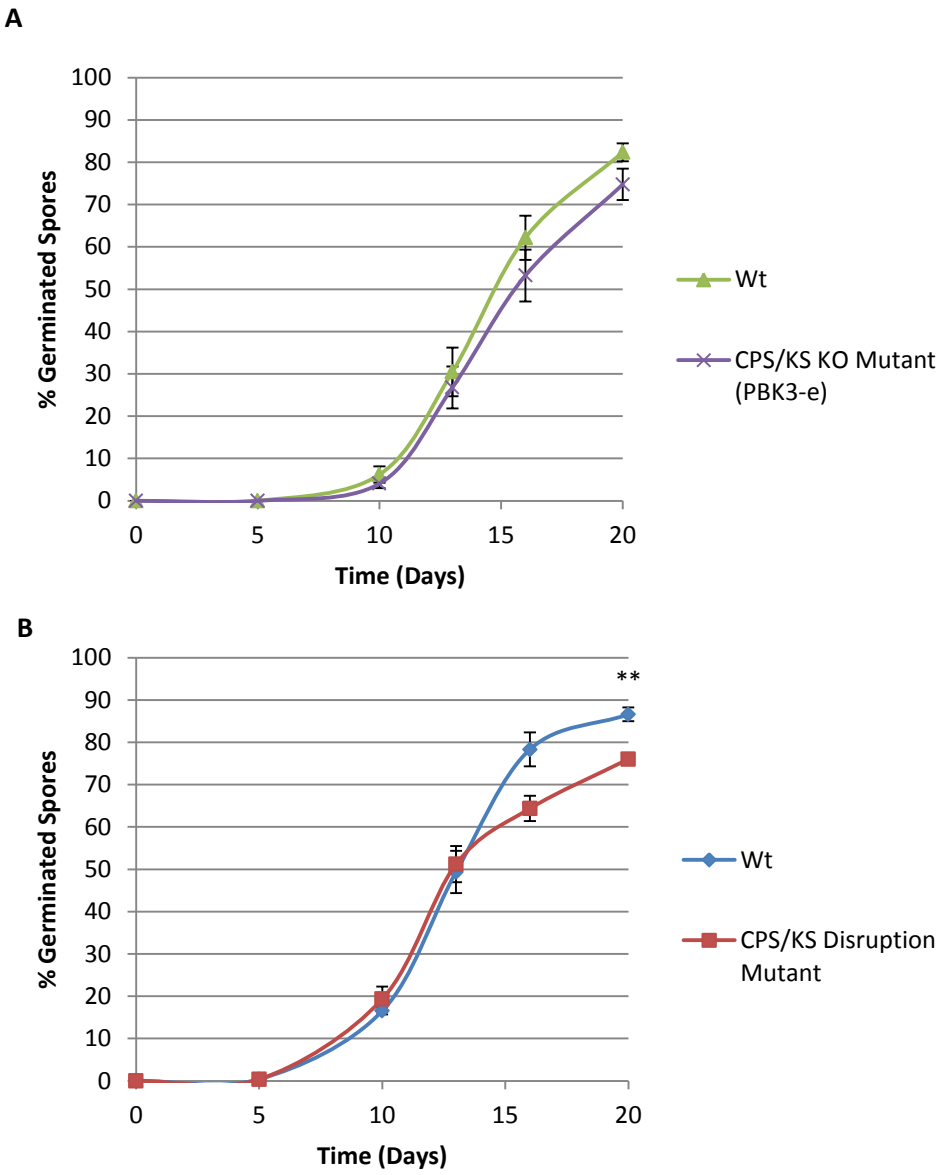

Figure 18. Analysis of the effects of gibberellins on *P.patens* spore germination by comparing wild-type germination to that observed from two CPS/KS mutant plants. A) A complete knockout mutant. B) A mutant created by a disruption in the gene. Slightly decreased germination rates were shown for the CPS/KS KO mutant throughout the entire assay, whilst decreased rates were only seen following day 14, for the disruption mutant, with a significant decreased rate at day 20. Statistical analysis - Student's T-Test (* = $p < 0.05$, ** = $p < 0.01$). Error bars = ± SEM.

The germination rate observed for the CPS/KS KO mutant can be seen to be very slightly lower than that shown for the corresponding wild-type spores, for all of the data points, once germination had been initiated (Fig.18A). However, this was not statistically significant at any time point. On the other hand, the germination rate for the CPS/KS disruption mutant can be seen to be very similar to that for the wild-type,

although once the majority of spores (~50%) had germinated, there is a slight decrease in the rate of germination, to the point whereby at day 20 the Wt germination percentage is very statistically significantly higher than that for the mutant.

CPS/KS Mutant Genotyping: RNA transcript and DNA gene analysis.

RNA Extraction and RT-PCR.

RNA was extracted from protonemal tissue for both the CPS/KS mutants (disruption mutant and the KO mutant (PBK3-e)), the Wt in which the mutants were produced from (CPS/KS Wt) and another Wt, as an additional control.

Table 7. RNA quantity and quality extracted from protonemal tissue of the CPS/KS mutants and wild-types, obtained using an ND-1000 Nanodrop.

SAMPLE	ng/µl	260/280	260/230
Wt	383.4	2.19	1.75
CPS/KS Wt	404.75	2.21	1.79
CPS/KS Disruption Mutant	244.3	2.12	1.27
CPS/KS KO (PBK3-e)	334.5	2.21	1.11

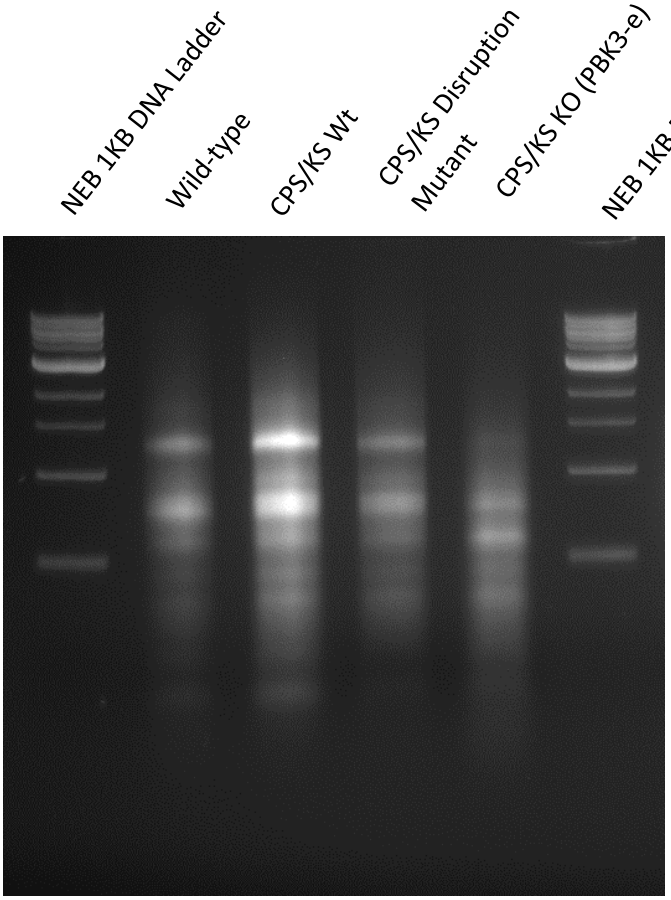

Figure 19. Gel electrophoresis image showing the RNA extracted from protonemal tissue of the CPS/KS mutants and the respective wild-types, using the BIOLINE ISOLAT II PLANT RNA KIT. RNA quantity and quality for all samples is sufficient, although RNA from the CPS/KS KO mutant looks slightly degraded.

From Table 7 it can be seen that the quality and quantity of the RNA extracted from the protonemal tissue of both the two CPS/KS mutants and the wild-types, is sufficient for subsequent analysis with RT-PCR, in order to genotype the mutants. However, it can be said that the RNA for the CPS/KS KO mutant is slightly degraded, from gel electrophoresis (Fig.19).

The extracted RNA was used for RT-PCR, using both tubulin primers as a control and CPS/KS primers designed to amplify a small fragment of the cDNA produced from the transcript of the CPS/KS gene.

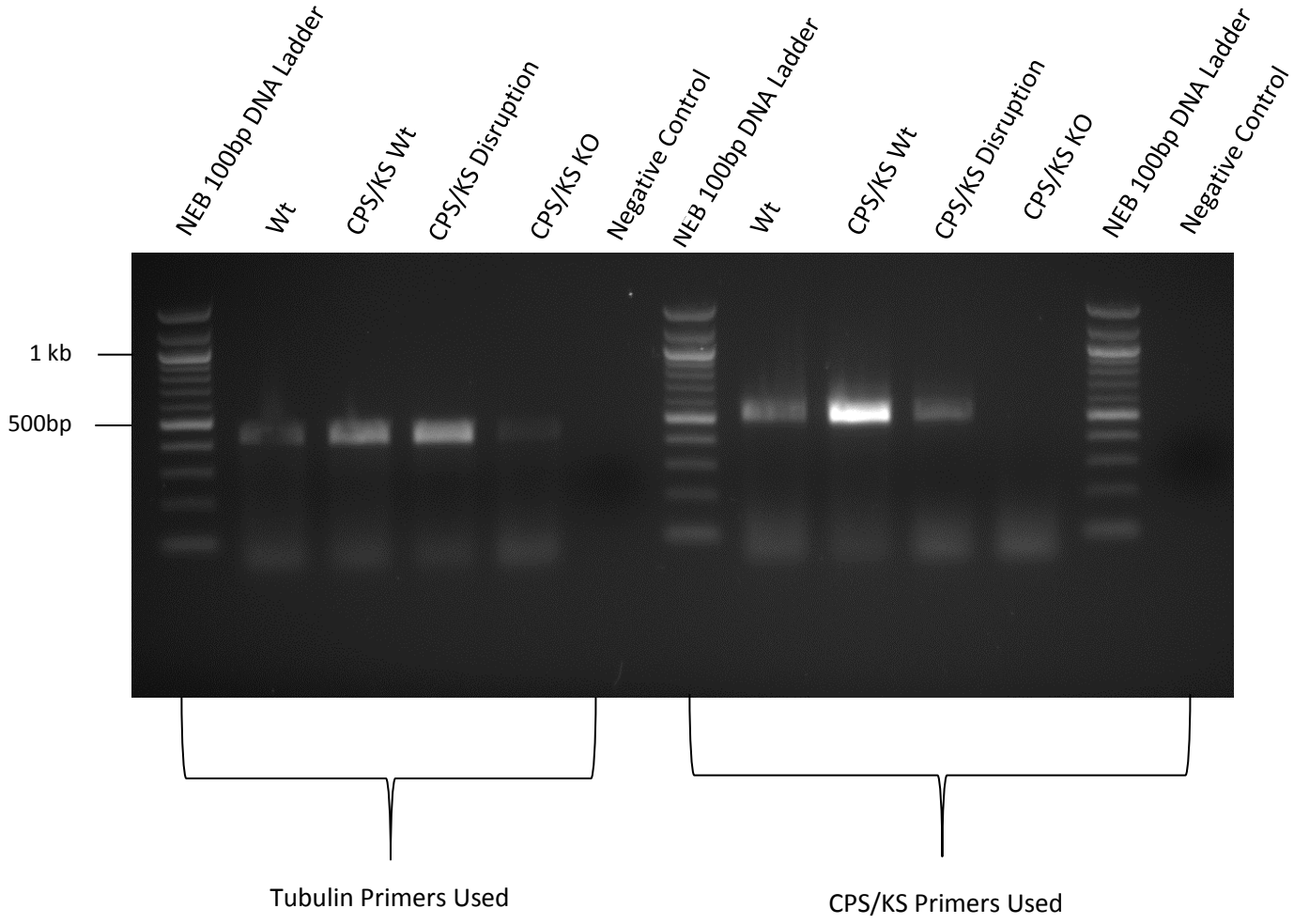

Figure 20. Gel electrophoresis image showing the results of the RT-PCR analysis for the genotyping of CPS/KS mutants to confirm the presence of cDNA produced by the transcript of the gene. A band representing the tubulin fragment can be seen for all of the RNA samples, although a lower quantity can be seen for the CPS/KS KO mutant sample. The CPS/KS fragment is present within the two Wt control samples and the disruption CPS/KS mutant, but not for the KO mutant.

The results of the RT-PCR analysis are depicted in Figure 20, whereby it can be seen that the two wild-type protonemal *P.patens* samples and the two CPS/KS mutant samples, show a band of the correct size for the expected tubulin cDNA

fragment, at ~438bp. Although the RNA that had been extracted was quantified and supposedly 20ng of each sample was used in the reactions, it can be seen that the tubulin fragments amplified are of varying concentrations, according to the brightness of the bands present on the gel. It can be seen that for the Wt sample and the CPS/KS KO sample, that the bands for these PCR reactions are relatively fainter compared to the bands for the other two samples, indicating a lower quantity or quality of RNA used, highlighting the slightly degraded CPS/KS KO RNA sample. The negative control, whereby no RNA template was used in the reaction, can be seen to have not produced any cDNA, therefore showing that there is no contamination within the reaction, thus increasing the reliability of the results obtained for the other reactions with the tubulin primers.

Furthermore, it can be seen that when the CPS/KS primers were used within the RT-PCR reaction, that cDNA was amplified for both of the Wt samples, as expected, as there is a band shown on the gel at the correct expected size of the fragment of ~521bp (Fig.20). Additionally, it can be seen that there is a band for the CPS/KS disruption mutant, although there is not a band for the complete KO mutant, thus suggesting that mRNA transcript is not being transcribed in this mutant plant.

DNA Extraction and PCR for genotyping the cps mutants.

DNA was extracted from 100mg protonemal tissue of two wild-type plants, and the two mutant variants and quantified using an ND-1000 nanodrop (Tab.7).

Table 8. DNA quantity and quality extracted from protonemal tissue of the CPS/KS mutants and wild-types, obtained using an ND-1000 Nanodrop.

SAMPLE	ng/µl	260/280	260/230
Wt	26.3	1.91	2.06
CPS/KS Wt	3.70	1.98	0.86
CPS/KS Disruption Mutant	14.75	1.90	2.51
CPS/KS KO (PBK3-e)	58.5	1.84	2.31

Table 8 shows the quantity and purity of the DNA extracted. It can be seen from this that the quantity is fairly low, and for the CPS/KS Wt sample in particular, the purity is not very high. However, the DNA extracted is sufficient for genotyping, therefore 100ng DNA was used as templates in 25µl PCR reactions, with no DNA template being added for the negative control. The PCR was only carried out with tubulin primers designed to amplify a fragment of tubulin gDNA.

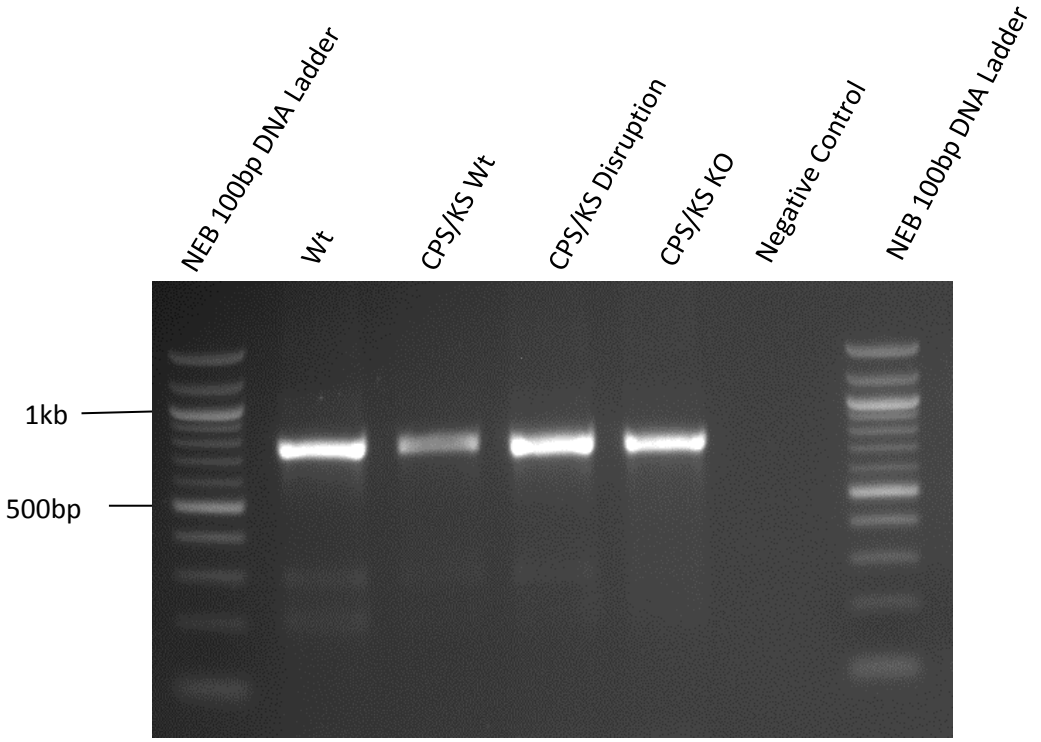

Figure 21. Gel electrophoresis image showing the results of the PCR analysis for the genotyping of CPS/KS mutants to confirm the presence of gDNA of a fragment of the tubulin gene. Tubulin fragment was amplified for all of the samples, both Wt and mutant.

The samples analysed, both Wt and mutants, show a band present of the correct fragment size of ~752bp, indicating the presence of tubulin gDNA (Fig.21.). Therefore, it shows that the DNA extracted is of sufficient quality to be used for subsequent analysis with primers designed to amplify a fragment or the entire CPS/KS gene, for complete genotyping of the mutant variants.

Analysing the effect of the gibberellin signalling pathway protein DELLA homologue on *P.patens* spore germination.

A comparison of the germination of *DELLAa* Wt spores and spores in which were mutants of the Della A proteins (*dellaa*) was carried out. Spores of corresponding ages (10 days post-harvest) were used for both *DELLAa* and *dellaa* spores and 5 replicates were analysed.

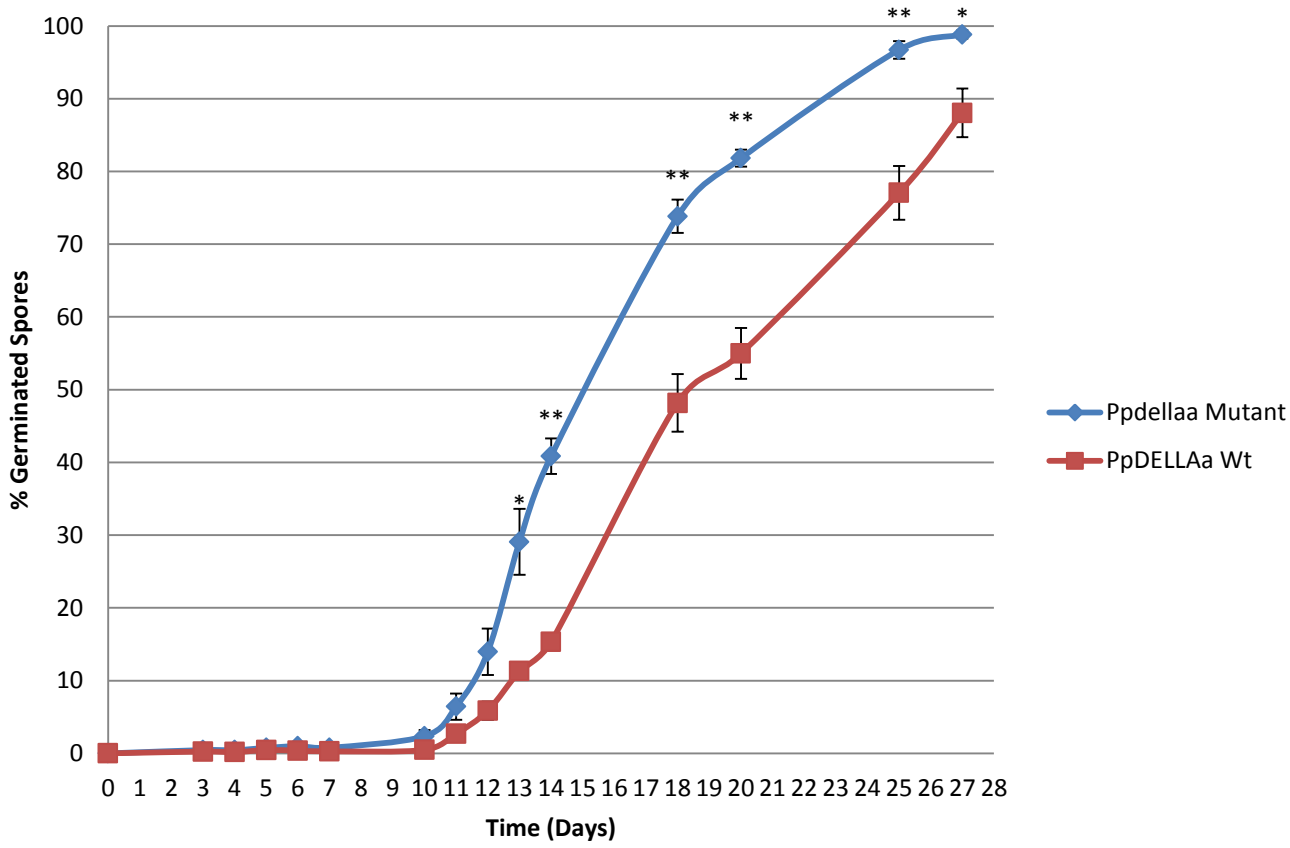

Figure 22. Analysis of the effects of gibberellins on *P.patens* spore germination by comparing wild-type germination to that observed from a *Ppdellaa* mutant plant. *Ppdellaa* deficient mutant spores showed highly significantly increased germination rates the respective Wt. Statistical analysis - Student's T-Test (* = $p < 0.05$, ** = $p < 0.01$). Error bars = ± SEM.

Spore germination rate is significantly increased for the spores that are unable to produce Della A proteins, the *dellaa* mutants, compared to that observed for the Wt spores (Fig.22). This increase in germination rate can be seen to be statistically significant for six of the data points obtained, therefore indicating a significant increase and a positive effect on spore germination.

P.patens **RNA Extraction for Transcriptome Sequencing by JGI.**

RNA was extracted from spores during various stages of the germination process, using the trizol method, in order to provide RNA for the sequencing of the transcriptome (to be carried out by the US department of Energy Joint Genome Institute as part of a collaborative project headed by Stefan Rensing).

Table 9. Quality and quantity of the RNA extracted, via the trizol method after the Qiagen clean-up, from *P.patens* material at differential germination stages, for the sequencing of the transcriptomes, obtained by an ND-1000 nanodrop.

Replicate	Sample	ng/μl	260/280	260/230
1	Dry Spores	134.4	1.87	1.18
	Imbibed Spores 1	42.5	1.86	0.97
	Imbibed Spores 2	97.13	1.80	0.92
	Germinating Spores	47.43	1.55	0.60
2	Dry Spores	11.25	1.93	0.88
	Imbibed Spores	7.9	1.81	0.26
	Germinating Spores 1	14.9	2.15	1.26
	Germinating Spores 2	1856.6	2.21	2.53
	Germinating Spores 3	624.5	2.21	2.47

The RNA quality and quantity extracted using the trizol method with the Qiagen clean-up process, is not consistent between replicates (Tab.9). As a result, it was decided to extract the RNA for the sequencing of the transcriptome, with the BIOLINE ISOLATE II PLANT RNA Kit instead, with the necessary controls of protonemal tissue that had been grown on BCD medium.

Table 10. Nanodrop data of the RNA extracted for the sequencing of the transcriptome of various *P.patens* tissue material, using the BIOLINE ISOLATE II PLANT RNA KIT.

Technical Replicate	Samples and biological replicates	ng/µl	260/280	260/230
1	Colony Tissue 1	58.05	2.12	1.91
	Colony Tissue 2	232.3	2.20	2.28
	Colony Tissue 3	232.6	2.13	1.99
	Colony Tissue 4	67.95	2.14	1.83
	Dry Spores	139.6	2.13	1.95
	Gametophyte	116.9	2.12	2.14
2	Dry Spores	194.4	2.18	2.15
	Imbibed Spores	107.1	2.20	1.90
	Early Germinating Spores 1	631.8	2.20	2.19
	Early Germinating Spores 2	763.2	2.16	2.05
	Late Germinating Spores 1	465.2	2.16	1.95
	Late Germinating Spores 2	454.25	2.21	2.34
	Protonemal 1	366.7	2.23	2.45
	Protonemal 2	409.0	2.20	2.05
	Protonemal 3	483.7	2.17	2.25
	Gametophyte	35.65	2.04	1.38
3	Dry Spores	173.4	2.18	1.92
	Imbibed Spores	203.9	2.22	1.44
	Gametophyte 1	45.7	2.22	1.34
	Gametophyte 2	96.9	2.17	1.91
4	Dry Spores	265.2	2.06	0.89
	Imbibed Spores	96.8	2.21	0.49
	Germinating Spores	554.8	2.19	1.32
	Protonemal 1	948.3	2.25	1.55
	Protonemal 2	668.8	2.24	2.06
	Gametophyte 1	68.62	2.16	1.26
	Gametophyte 2	58.8	2.11	1.94

Table 10 shows that in general, the quality of RNA extracted is of a high standard from most of the different tissue types used. It can be seen that for the 260/280 ratios, all of the RNA samples extracted were above 2 in value.

Discussion

Analysing spore germination and the possible regulatory networks that are employed to control the timing of this process, in *P.patens*, represents a powerful tool for gaining an understanding of land-plant evolution.

Throughout this study, spore germination was characterised by the observation of protruding protonemal filament through the spore coat (Fig.3). In doing this, it was ensured that all of the results were consistent and reliable, as the distinction between ungerminated and germinated spores was the same. It is apparent that in some studies, germination is characterised differently (discussed in Glime 2007), therefore initial germination and rates may differ between studies. It is imperative that a standard means of determining germination is established and used by all researchers, in order to prevent any conflicting results being published that may hinder the collaborative effort to increase current understanding.

For this study, spores of various ages (post-harvest) were used. From Figure 4, it can be seen that two Wt spore batches of different ages showed significantly different rates of germination. This difference did however decrease over time, with the germination percentage of the younger spores showing to increase to just below the levels observed for the older spores. It is known that different spore batches do exhibit varying germination rates to one another. However, Coates *et al.* (Unpublished data) emphasise that there is no correlation between the germination rates and initial germination of spores with age. Nevertheless, it has to be noted that in some instances, variation between spores of different ages does occur, hence the reason as to why throughout all assays, spores of corresponding ages were used to

ensure eradication of this variation. As moss in an ephemeral species, spores are known to initiate germination when environmental conditions are favourable, so theoretically all spores should germinate at the same time and rate, unless an additional regulatory mechanism is being employed. Nonetheless, spore batch variation may be utilised as a strategy for survival. All spores for this investigation were subjected to identical environmental conditions, however, as numerous environmental factors are known to affect germination (Coates *et al*. unpublished data), slight variations within an assay may have contributed to differences observed. In addition to this, sporophytes are harvested from the plugs when they are deemed mature, i.e. dark brown in colour. Therefore, it is only based on observational means whether the sporophytes are mature, hence, sporophytes harvested on the same day may still differ in maturity levels. As a way to try to reduce possible issues regarding this, for each assay more than 2 sporophytes were used, with a ratio of 3 sporophytes worth of spores for each ten petri dishes.

Acyl-HSLs have an effect on *P.patens* spore germination, with longer chain, unsubstituted molecules showing the most potent positive effect.

Numerous physiological effects, as a result of altered gene expression profiles, on plants have been reported by the presence of the QS signal molecules, acyl-HSLs (Mathesius *et al*. 2003; Ortiź-Castro *et al*. 2008; Rad *et al.* 2008; Shikora *et al.* 2011; Schenk *et al*. 2012). As a result, an investigation was carried out in order to determine whether molecules, of varying acyl-chain lengths (4-12C) and substitution states, showed any apparent effects on the germination of *P.patens* spores.

Initially, the acyl-HSLs were added at a final concentration of 10nM, based on previous unpublished data by Coates *et al*. For this assay (Fig.5), it was noted that the solvent-only control, whereby the highest amount of methanol used was added, showed a subtle increased rate of germination, compared to that observed for the BCD-only control (data not shown). Although, the addition of methanol is thought to inhibit spore germination rather than promote it, this highlighted the importance of including a solvent-only control in each of the assays whereby solutions had been made up with a substance other than water. In doing this, it ensures that the germination rates are being analysed just on the basis of the added compounds, rather than the variation that may be incurred by the added solvent. However, the BCD control is still of great significance as it is used as a means to determine that the spores are behaving in an expected manner and therefore acting as a control to assure the data is reliable. Moreover, from figure 5, it can be seen that there was an apparent decrease in the germination percentage of the spores for a number of the different treatments. A decrease in germination numbers cannot occur, as germination is notably an irreversible process. Nevertheless, due to a minimum of 200 spores being counted for each plate, it may have been the case that a different part of the plate was counted than was counted previously, whereby less germination had taken place, due to chance or environmental factors (such as the position of the light source in relation to that part of the plate). Therefore, in order to gain a more representative germination percentage, a higher number of spores should have been counted to reduce inaccuracies.

However, in terms of the effects of acyl-HSLs at a concentration of 10nM, from figure 5 it can be seen that the addition of 3-oxo-C4-HSL (an acyl-HSL substituted with a

ketone group, of 4 carbons in acyl side-chain length) promoted germination rate, compared to that observed for the control and for the other acyl-HSLs, although not statistically significantly. It may be the case that acyl-HSLs of a shorter chain length are able to enter plant cells via simple diffusion, whereby longer molecules require active transport to gain entry into plant cells. As spore germination, following imbibition, is an active process itself (Glime 2007), spores may not expend additional energy on transporting molecules through their cell plasma membranes, as a compromising cost-benefit approach. Nonetheless, it can be seen that the unsubstituted and 3-oxo-acyl-HSL short chained molecules did not show the same promotional effects as 3-oxo-C4-HSL, so this may not be a reasonable explanation. Furthermore, apart from the C4-HSL, the other ketone substituted HSLs showed a lower rate of germination than the other substitutions, therefore implying that is it not the effect of the HSL being substituted with a ketone group that confers the promotional effects observed.

Alternatively, for the 3-OH-HSLs, the shorter chains showed a reduced rate of germination, compared to that observed for the control. The longer chains, however, show a slightly increased rate, suggesting that the long chain OH-HSLs promote and have an opposite effect to that seen with the shorter chain molecules. As this study only used acyl-HSLs with a maximum acyl-side chain length of 12 carbons, it would have been interesting to investigate whether this promotional effect is more potent with increasing chain length. Furthermore, the unsubstituted HSLs all appeared to show promotion of spore germination (Fig.6), however, as with the OH-HSLs, it was the longer chains 10 and 12 carbons in length, which showed the most potent promotion (Fig.7), as also observed for previous data obtained by Coates *et al.*

(Unpublished Data). Ortiź-Castro *et al.* (2008) examined the effects of acyl-HSLs on root architecture of the vascular model plant, *A.thaliana.* The result of which determined that the most bioactivity was observed for medium-long molecules, with side-chains 10 carbons in length, showing the most potent bioactivity, whereby increased root hair formation was noted. Additionally, this study found that at higher concentrations, the effect was amplified, suggesting the effect was dose–dependent. However, the concentrations used in this study was substantially higher than 10nM, with concentrations used ranging from 12-192μM on a multicellular root rather than a unicellular spore.

As it was deciphered that acyl-HSLs with a longer acyl side-chain length were found to have more potent effects on plants in previous studies, and with the unsubstituted and hydroxyl substituted HSLs at 10nM (Fig.7) in this current investigation, the longer molecules of C10 and C12 were used in an assay to analyse the effects of concentrations of these molecules on spore germination. For these analyses, four different concentrations were used (2nM, 10nM, 0.1μM and 1μM). From figures 8 and 10, it can be seen that there is not a single concentration whereby all of the various acyl-HSLs showed potent increased germination rates, suggesting that each variation has a particular concentration whereby it induces a greater effect. It is apparent that the different substituted molecules and the C10 and C12 molecules all differ in the effect they have on spore germination between the concentrations, with some showing increased germination rate at one concentration, whilst another showed a decreased rate at the same concentration. An example of this can be seen with 3-OH-HSL, where the C10 variant was most potent at 10nM (Fig.9), whereby the C12 equivalent showed the highest germination promotion at 0.1μM (Fig.11). Bai *et*

al. (2012) found that 3-oxo-C10-HSL at a concentration of 100nM showed an increased effect at promoting adventitious root growth in mung bean. From Figure 9, it can be seen that at 0.1μM (100nM) 3-oxo-C10-HSL also had the greatest effect on promoting spore germination. Thus suggesting that at this concentration, this particular acyl-HSL variant greatly induces plant responses, in both non-seed and seed plants. Bai *et al*. (2012) also reported that at concentrations greater than 100nM, 3-oxo-C10-HSL inhibited adventitious root growth. The inhibition of spore germination was not observed in this present study, however with 3-oxo-C12-HSL, it can be seen that above 0.1μM, the promotion was not as potent as at the lower concentrations (Fig.10). *N*-acyl-C12-HSL also showed this effect, however the greatest rate of spore germination was shown at 2nM and consequently the effect was decreased at higher concentrations (Fig.10). Therefore it can be suggested that the acyl substituted variant is the most potent one in this family.

Accordingly, it can be concluded that the different acyl-HSLs have a specific concentration at which they have a greater effect on promoting spore germination in *P.patens*, with some even showing no promotion to even a very slight decrease at certain concentrations, whilst promoting at others. Coates *et al*. (unpublished data) showed that strong inhibition occurs when concentrations above 5μM are used, although this may have been due to the high solvent volume as well. It may be the case that unicellular spores are just highly sensitive to these compounds.

As all of the acyl-HSLs appeared to at least slightly promote spore germination at a concentration of 0.1μM, to some extent, and the fact that Bai *et al.* (2012) showed that this was the most potent concentration for 3-oxo-C10-HSL for promoting

adventitious root growth, all of the acyl-HSLs were analysed at this concentration to determine the effects of the varying substitution states and chain lengths (Fig.12). From this it could be seen that the majority did show increased rates of spore germination, however no significant promotion was observed. 3-oxo-C12-HSL and 3-OH-12-HSL were shown to initially have a negative effect on spore germination but then show increasing rates of the later germinating spores. On the other hand, the opposite was shown for *N*-acyl-C12-HSL, whereby initial promotion was observed, up a point, whereby the effect was then reduced so that the percentage of germinated spores at a single time point was lower than that observed for the solvent-only control. From figure 13, it can be seen that the longer oxo-HSLs showed an increased germination percentage, than the shorter ones. Therefore, it can be thought that at this concentration, the longer oxo substituted molecules are more potent than the shorter chains, in which had a greater effect at the lower concentration of 10nM (Fig.5).

As the spores used to analyse the effects of acyl-HSLs thus far had been relatively young (<2months post-harvest), the C10 and C12 length HSLs were used at a concentration of 0.1μM, to ensure that younger spores are not insensitive to the effects of acyl-HSLs, hence as to the reason why the promotional effects at this concentration are not significant. However, it was apparent this was not the case, as only a slight increase was observed, as seen with younger spores (Fig.14). In some instances, such as with 3-oxo-C10-HSL, there was a decreased promotional effect to that shown in previous assays, at this concentration. However, this may be a result of spore batch variation further highlighting the importance of repeating assays with spores of varying ages.

All of the assays in this present study have shown that not all of the acyl-HSLs variants have the same promotional effects on spore germination. Analysis of the *A.thaliana* transcriptome, following application of three different acyl-HSL molecules, showed that specific responses occurred with each one, highlighting the fact that plants do react differently to each type (Schenk *et al*. 2014). As acyl-HSLs are produced by bacteria, and can be perceived by plants possibly as a result of coevolution to enhance reproductive fitness, it could be the case that either a negative, positive or neutral effect on spore germination is a result of the plant responding to the particular bacteria in which produces that specific acyl-HSL variant. For example, as mutual bacterial species are present within *P.patens'* natural environment, no effect on spore germination may occur following perception of some of the molecules, as no benefit will be conferred to the moss as a result. Mathesius *et al.* (2003) carried out proteome analysis with two ketone substituted acyl-HSLs of different chain lengths, and showed that around 150 proteins were differentially accumulated as a result, providing evidence that specificity with regards to the acyl-HSL molecules and the responses generated by plants exists. Subsequently, in order to determine which specific acyl-HSLs have a greater effect on promoting spore germination, a transcriptome analysis of *P.patens* treated with the various molecules should be carried out.

Schenk *et al.* (2014) also reported that saturation of the response system to acyl-HSLs occurs, whereby the molecules only have a limited time to act. It was shown that when acyl-HSLs were applied to plants for a period of 3 weeks or longer, that no significant alterations in phenotype was observed. This may be a possible explanation as to why the results in this present study were not showing consistent

positive effects on spore germination. As some of the spores used in the assays displayed a late initial germination time and subsequent slow germination rate (even for the control), the spores may become unresponsive to the molecules prior to an effect being made.

An analysis of the responses of *A.thaliana* to both acyl-HSLs and their subsequent by-products following degradation was carried out by Palmer *et al.* (2014). This study not only showed that seedling growth was significantly altered in an acyl-chain length dependent manner, but also that the observed effects were a result of the aminolysis of the molecules by an enzyme encoded for by the plant's genome. The enhanced growth observed of the seedlings was found to be a result of the acyl-HSLs stimulating ethylene production, which promoted seedling growth. As the hormone ethylene has been shown to inhibit spore germination in *Physcomitrella* (Coates *et al.* unpublished data), it can be said that this response to acyl-HSLs of promoting the production of this hormone is not conserved in the more ancient moss lineage as no positive effect on spore germination would have been observed. If it is in fact the degradation products of acyl-HSLs that are responsible for observed plant responses, the shorter chain C4-HSLs should show the most potent effects on spore germination, as these have the highest degradation rates (Yates *et al.* 2002; Hmelo & Van Mooy 2008). Nevertheless, although this was observed at a concentration of 10nM for the 3-C4-oxo-HSL (Fig.5), this was not consistently seen. From this study, it could be said that the unsubstituted acyl-HSLs show consistently increased spore germination rates, in particular the longer chain molecules (C10 and C12). *N*-acyl-HSLs are notably less stable than substituted molecules, thus coinciding with Palmer *et al.* (2014); these molecules may show more potent effects on *P.patens,* due to

them being degraded into their corresponding by-products faster, which are responsible for inducing the response.

ABA has been identified to carry out functional roles in *P.patens*, regarding tolerance to stress (discussed in Takezawa & Komatsu 2011). Coates *et al.* (unpublished data) showed that ABA inhibits spore germination, although not completely as seen with seed germination, by similar mechanisms carried out to initiate desiccation tolerance responses. In order to determine whether acyl-HSLs interact with the ABA hormonal signalling pathway, and thus can rescue the inhibitory effects of ABA, the C10 and C12 molecules were used in conjunction with both 5μM and 10μM ABA in an assay. From figure 15, it can be seen that the longer chain acyl-HSLs of varying substitution states was not able to rescue the inhibitory effects of ABA, with only a slight increase shown to that observed for the ABA-only controls, particularly for the higher concentration of the hormone. Therefore, this data suggests that the acyl-HSLs at 0.1μM concentration, do not rescue the effect of ABA and that the QS molecules do not interact with ABA signalling pathways. As specific acyl-HSLs are more potent at specific concentrations, as shown previously, it may be the case that the effect of ABA may be reduced more upon addition of the acyl-HSLs at a concentration whereby they are known to exhibit an increased effect. In addition to this, a lower concentration of ABA should also be analysed as the data shows it is very potent on moss spores.

Thus far, only synthetic acyl-HSLs have been analysed. Therefore, the extracts of an acyl-HSL producing bacterial species of *Serratia* and an AHL-deficient mutant, was added to the BCD medium to analyse the effects of naturally occurring acyl-HSL

molecules. From this analysis (Fig.16), it can be seen that a negative effect on spore germination was observed, compared to that seen by the control. This may have been a result of the effects of other molecules that had been secreted by the bacteria, as this effect was observed for both the Wt and AHL-deficient extracts, with an even lower rate of germination being shown for the Wt extracts whereby the acyl-HSLs should have been present. It is not known which specific acyl-HSLs were produced by the bacteria and at which concentrations these molecules were present. Schuhegger *et al*. (2006) found that acyl-HSLs produced by *Serratia liquefacians* induced resistance to a fungal pathogen, in the seed tomato plant species. Therefore, if the same effect occurs on *P.patens*, no change in spore germination would be observed. In order to expand upon the analysis of naturally bacterial synthesised acyl-HSLs on moss spore germination, the molecules could be purified as to ensure no other compounds within the bacterial extracts are conferring any effect. There is great biotechnological interest in the cultivation of beneficial plant-growth-promoting bacteria, therefore the effects of the acyl-HSLs produced by a range of gram negative bacterial species is of significant importance (Lugtenberg *et al*. 2001; Savka *et al.* 2002).

Gibberellins positively affect *Physcomitrella* spore germination.

In order to examine the regulatory effects of a GA-like pathway in moss, an assay was carried out to determine whether a GA derivative can rescue the inhibitory effects of ABA, as shown in seed plants. In seed plants, there is definite interaction between ABA and GA signalling pathways, whereby ABA biosynthesis is down-regulated, in an antagonist manner, upon the presence of GA, in order for seed

germination to be promoted (Holdsworth *et al.* 2008). Therefore, representing a regulatory mechanism whereby the timing of seed germination can be sufficiently controlled. GA_9 methyl-ester is a bioactive gibberellin found within *P.patens,* (Hayashi *et al.* 2010) however this gibberellin is not found to be active in the seed plant *Arabidopsis* (Talon *et al.* 1990). GA_9 methyl ester does have a positive effect on spore germination, compared to the rate observed for the solvent-only control, as seen with seeds (Fig.17). However, unlike in seed plants, GA application is not able to rescue the inhibitory effects of ABA. Nevertheless, there is a very subtle increase in the rate of germination compared to the ABA-only controls, although this is not to the same level observed for the solvent only control. If the assay was continued for a longer period of time, it would be interesting to see whether the germination rate would be increased further, more than that of the ABA-only control, to reach a higher germination percentage, indicating cross-talk between the hormonal pathways, as seen in seed plants. It can be seen from figure 17, that the increased rate of germination is higher with the lower ABA concentration. This could be said to have occurred as there is already less ABA present, therefore the endogenous levels of ABA within the moss, do not have to be lowered as much in order for GA to promote germination. Finkelstein *et al*. (1994) indicate that different *Arabidopsis* seed batches have varying sensitivity levels to ABA, thus this may also be the case with spores therefore this assay should be carried out with spores of different batches to enable a definite conclusion to be made regarding the effects of the interactions between GA and ABA. Different concentrations of the two hormones should also be investigated to ensure that the concentrations used are not an issue as to why GA was not able to fully rescue the inhibitory effects of ABA. In seed germination, it is a balance of the

two hormones which regulates germination (Holdsworth *et al*. 2008), thus the balance of the two hormones may need to be modified to enable sufficient regulation to be observed in spore germination. Furthermore, ABA does not completely inhibit spore germination in *P.patens*, as spore germination still occurs albeit at a substantially reduced rate (Fig.17).

Ent-kaurene is an intermediate precursor from which GA is synthesised from (Olszewski *et al*. 2002; Yamaguchi 2008). The synthesis of *ent*-kaurene is a result of the sequential cyclisation steps of geranylgeranly diphosphate (GGDP) by net-copalyl disphosphate synthase (CPS) (Sun & Kamiya 1994) and *ent*-kaurene synthase (KS) (Yamaguchi *et al.* 1996; 1998). Subsequent oxidisation of *ent*-kaurene results in the formation of the bioactive GAs. In *Physcomitrella,* CPS/KS is the initial enzyme in the GA-biosynthesis pathway, as opposed to the two observed in vascular plants (Chen *et al*. 2011). Hayashi *et al.* (2010) suggest that a diterpene metabolite from *ent*-kaurene may be utilised by *P.patens* as a regulator of development, as *ent*-kaurene was also shown to have an effect on the differentiation of protonemal tissue from chloronemata to caulonemata. The effects of a disruption PpCPS/KS mutant was also analysed in terms of spore germination by Hayashi *et al*. (2010), whereby no apparent effect was observed. However, as only a single time point was analysed, and not the overall rate, the data may not indicate a reduced germination rate and thus may not be deemed accurate or representative. Figure 18 shows the results of a spore germination assay whereby a *P.patens* CPS/KS KO and disruption mutant were analysed compared to the Wt of similar age (post-harvest). A negative effect on the rate of spore germination was observed with the complete KO mutant, suggesting a role for *ent*-kaurene in the germination of spores, as with seeds. On the other hand,

only the later germinating spores were shown to have a reduced rate of germination for the disruption mutant, with a significantly decreased germination percentage seen at day 20, compared to that of a Wt a day older in age. It can also be seen that the initial germination of this mutant line, showed a minor increased rate, however, as the Wt used was not of the exact age as the mutant line, this may be a result of variation observed between spore batches, as discussed previously, rather than due to the lack of CPS/KS in the mutant. The negative effect on spore germination demonstrated in this study, coincides with the germination phenotype for *cps* mutants by both Anterola *et al*. (2009) and Coates *et al.* (Unpublished data), whereby different spore batches were used, thus suggesting a role for *PpCPS* in germination. Therefore, gibberellin-related compounds, notably *ent*-kaurene, may be implicated in moss spore germination, in addition to other developmental processes.

As a means to ensure the mutant lines in the PpCPS/KS mutant assay were in fact deficient of the mRNA transcript of the gene and therefore did not produce the cDNA, mutant genotyping was carried out with RNA extracted from the mutant protonemal tissue, and the respective wild-types. From figure 20, it can be seen that there is a band indicating the presence of a partial CPS/KS transcript for the CPS/KS disruption mutant. This may be due to the fact that the primers used were designed to amplify a fragment of the CPS/KS transcript, and not the whole transcript. Therefore, the part that was amplified is present within the disruption mutant, although it may have been shifted downstream, however the disruption would ensure the resultant translated protein would not be functional, as demonstrated by the results of the phenotypic analysis in figure 19. On the other hand, the complete KO mutant does not appear to

have CPS/KS cDNA and can therefore be assured to not be able to synthesise *ent*-kaurene, hence subsequent phenotypic analysis can be deemed reliable.

Additionally, DNA was successfully extracted from different samples of protonemal tissue, from the wild-type and the two CPS/KS mutants, in order to confirm the absence of the gene. It can be seen from table 8 however, that a relatively lower yield of DNA was extracted than was for RNA (Table 7), although 100mg of wet tissue was used for both. The use of commercial kits for extracting DNA has been known to yield slightly lower amounts than other available more labour-intensive protocols, with the possible degradation of DNA (Santella 2006). Whole genome amplification could have been carried out in order to increase the amount of DNA (Santell 2006), however, the yields obtained were considered adequate for genotyping for this purpose. The extracted DNA was subjected to PCR analysis, with primers designed to amplify a fragment of the tubulin gene. As can be seen from figure 21, the tubulin gene is present within all of the extracted DNA samples, for both the wild-types and the mutants, and is absent in the negative control. Thus, the DNA extracted could be used with primers designed to amplify the gDNA of the CPS/KS gene, for complete mutant analysis, for future studies. Although an additional control of a reverse transcriptase negative reaction should have been carried out as an additional way to ensure reliability of the results.

GAs are known to be imperative for seed germination to occur (Koorneef & van der Veen 1980), however it can be seen from figure 17 that this is not the case with spore germination, as germination still occurs in the absence of GA, just to a lesser

extent. Hence, GA and GA-related compounds may have a modulatory role on spore germination rather than a regulatory one (Coates *et al*. unpublished data).

A DELLA-mediated GA signalling pathway in moss may regulate developmental processes, including spore germination.

The subsequent assay involved determining the possible hormone regulatory mechanisms involved in spore germination of *P.patens,* an area in which is currently not well understood compared to that of seed germination. Seed germination is known to be regulated by the GID1-SLEEPY-DELLA protein gibberellin signalling pathway. The DELLA protein indirectly regulates GA synthesis by repressing the action of GA when not present. The presence of GA enables the interaction between the DELLA protein and the GA-bound GID1 receptor, which results in DELLA degradation thus allowing for GA action to take place (Claeys *et al.* 2014). Two putative DELLA proteins have been identified to be encoded for by the genome of *P.patens*, DELLA A and DELLA B, that probably arose from a gene duplication event. However, at the sequence level, the genes of these proteins appear to be highly divergent to the orthologues identified within flowering plants (Yasamura *et al.* 2007). There is no apparent interaction between the GID1-like receptor (GLP1) and DELLA protein in *Physcomitrella* (Yasamura *et al.* 2007), with the moss being thought to predate the evolution of the classical gibberellin signalling pathway characterised in more recent plant lineages (Hirano *et al*. 2008). However, Yasamura *et al.* (2007) tested this interaction with GA_3, a bioactive GA found in vascular plants, rather than a GA known to be active in the early-evolving land plant (Hayashi *et al.* 2010). Developmental effects following GA-application in *P.patens,* similar to those

observed in vascular plants, have not been found to occur (Decker *et al.* 2006) leading to the general conception that there is no GA-signalling pathway in moss and that it developed later in evolutionary history (Yasamura *et al*. 2007). The DELLA-like protein found in moss is thought to carry out an alternative function as opposed to acting as a GA-regulatory repressor (Vandenbussche *et al*. 2007).

In this study, we analysed the phenotype of a PpDellaA mutant with regards to spore germination. It can be seen from figure 22, that there is a significant increase in the rate of spore germination in the absence of DELLA A, compared to the Wt, with a slightly faster initial germination observed as well. This data coincides with data obtained by Coates *et al.* (Unpublished data) whereby different spore batches were analysed. Consequently, these results suggest for the first time that increased spore germination is likely to be the phenotype of Ppdella mutants, implying that the DELLA proteins may be involved in a moss developmental process that may also be regulated by the presence of GA.

Due to the limited homology between the GA-signalling proteins in *P.patens* and *Arabidopsis*, it has been proposed that the molecular onset of the pathway may have evolved in *Physcomitrella* (Vandenbussche *et al.* 2007). As a result, the apparent DELLA-mediated GA-like signalling pathway in *P.patens* may represent a modified, more ancient version of that observed in vascular plants today.

Transcriptome data may increase our understanding of the hormone signalling pathways and their regulatory effects, in moss.

RNA was extracted from tissue of various stages throughout the lifecycle of *P.patens*, in particular stages associated with spore germination, in order for transcriptome data to be obtained. From tables 9 and 10, it can be seen that the RNA extracted with the commercial kit is of higher yield and purity that that obtained from the trizol method, which may be due to RNase contamination and subsequent degradation of the RNA with the trizol method, as it was a more time-consuming method. Isolation by Trizol was carried out for the majority of the samples in the collaborative project, nevertheless, it may just be the case that this method is not as efficient with extracting RNA from spores. It can be seen from table 10, that the RNA extracted from gametophyte tissue was of a lower yield than that extracted from the other moss tissues. This may be due to this particular tissue type having rigid cell walls in which made the tissue harder to homogenise sufficiently. However, with this extracted RNA and the transcriptome analysis that will be carried out, a detailed understanding of the protein profiles during the various stages of spore germination can be gained, whereby the proposed involvement of the various hormonal signalling pathways, and their crosstalk, will be apparent. Thus, this represents a crucial step in increasing knowledge on spore germination and its control in *P.patens.*

Conclusions

Current understanding of the control of spore germination is much less than that for the analogous seed germination, observed in vascular plants. This study provides insights into the possible effects on spore germination of the model bryophyte *P.patens,* of both the bacterial quorum-sensing signal molecules, *N*-acyl-homoserine lactones, and the two hormones known to antagonistically regulate seed germination, gibberellin and abscisic acid. From this study, it was observed that the different substituted acyl-HSL molecules, of varying chain lengths, do not all show a ubiquitous effect on spore germination. Different variants show different effects on the rate of spore germination, at different concentrations. Unsubstituted acyl-HSLs showed the most potent increasing effects on spore germination at a range of concentrations, with the longer chains showing the greatest promoting effects overall. The data in this study shows that gibberellins and abscisic acid do affect *Physcomitrella* spore germination rate, similarly to that observed in seed plants, although to a lesser extent. This study provides novel data that suggests the presence of a DELLA-mediated gibberellin signalling pathway in moss, contradicting the widely accepted dogma that such pathway evolved after the bryophyte lineage. This investigation therefore provides a comprehensive analysis of the possible mechanisms that control the timing of spore germination, and the evolution of these, thus providing beneficial insights that may aid with future efforts to ensure food security.

References

Anterola, A. & Shanle, E. (2008) Genomic insights in moss gibberellin biosysnthesis. *The Bryologist.* 111: 218-230.

Anterola, A., Shanle, E., Mansouri, K., Schuette, S. & Renzaglia, K. (2009) Gibberellin precursor is involved in spore germination in the moss *Physcomitrella patens. Planta.* 229 (4): 1003-1007.

Bai, X., Todd, C., Desikan, R., Yang, Y. & Hu, X. (2012) N-3-Oxo-Decanoyl-L-Homoserine-Lactone Activates Auxin-Induced Adventitous Root Formation via Hydrogen Peroxide- and Nitric Oxide-Dependent Cyclic GMP Signalling in Mung Bean. *Plant Physiology*. 158 (1): 725-736.

Bell, G. (1985) The origin and early evolution of germ cells as illustrated in the Volvocales. In: *The Origin and Evolution of Sex,* eds. Halvorson, H. & Monroy, A. pp. 221-256. New York: Liss.

Bonner, J.T. (2000) *First-Signals: The Evolution of Multicellular Development.* Princeton, NJ. Princeton Univ. Press. 146pp.

Cha, C., Gao, P., Chen, Y-C., Shaw, P.D. & Ferrand, S.K. (1998) Production of Acyl-Homoserine Lactone Quorum-Sensing Signals by Gram-Negative Plant-Associated Bacteria. *MPMI.* 11(11): 1119-1129.

Chakraborty, S. & Newton, A.C. (2011) Climate change, plant diseases and food security: an overview. *Plant Pathology.* 60: 2-14.

Chen, F., Tholl, D., Bohlmann, J. & Pichersky, E. (2011) The family of terpene synthases in plants: a mid-size family of genes for specialized metabolism that is highly diversified throughout the kingdom. *The Plant journal: for cell and molecular biology.* 66 (6): 212-229.

Chong, T., Koh, C., Sam, C., Choo, Y., Yin, W. & Chan, K. (2012) Characterization of Quorum Sensing and Quorum Quenching Soil Bacteria Isolated from Malaysian Tropical Montane Forest. *Sensors*. 12 (4): 4846.

Choudary, S. & Schmidt-Dannert, C. (2010) Applications of quorum sensing in biotechnology. *Appl Microbiol Biotechnol.* **86: 1267-1279.**

Claeys, H., De Bodt, S. & Inzé, D. (2014) Gibberellins and DELLAS: central nodes in growth regulatory networks. *Trends in Plant Science.* 19 (4): 231-239.

Cove, D. (2005) The moss *Physcomitrella patens. Annu. Rev. Genet.* 39: 339-358.

Cuming, A. (2011) Molecular Bryology: mosses in the genomic era. *Field Bryology.* 103: 9-13.

Cuming, A.C., Cho, S.H., Kamisugi, Y., Graham, H. & Quatrano, R.S. (2007) Microarray analysis of transcriptional responses to abscisic acid and osmotic, salt and drought stress in the moss, *Physcomitrella patens. New Phytol*. 176: 275-287.

Decker, E.L., Frank, W., Sarnighausen, E. & Reski, R. (2006) Moss systems biology en route phytohormones in Physcomitrella development. *Plant Biol (Stuttg).* 8 (3): 397-405.

Delaux, P-M., Nanda, A. K., Mathé, C., Sejalon-Delmas, N. & Dunand, C. (2012) Molecular and biochemical aspects of plant terrestrialization. *Perspective in Plant Ecology, Evolution and Systematics.* 14 (1): 49-59.

Dickschat, J. (2010) Quorum sensing and bacterial biofilms. *The Royal Society of Chemistry*. 27 (3): 343-369.

Dill, A., Thomas, S.G., Hu, J., Steber, C.M. & Sun, T.P. (2004) The Arabidopis F-box protein SLEEPY1 targets gibberellin signalling repressors for gibberellin-induced degradation. *Plant Cell*. 16: 1392-1405.

Engel, P.P. (1968) Induction of biochemical and morphological mutants in moss *Physcomitrella patens. Am. J. Bot.* 55: 438.

Ergün, N., Topcuogul, S.F. & Yildiz, A. (2002) Auxin (indole-3-acetic acid), gibberellin acid (GA_3), abscisic acid (ABA) and cytokinin (zeatin) production by some species of mosses and lichens. *Turk J. Bol.* 26: 13-18.

Finkelstein, R.R. (1994) Mutations at two new Arabidopsis ABA response loci are similar to the abi3 mutations. *The Plant Journal.* 5: 765-771.

Gao, M., Teplitski, M., Robinson, J.B. & Bauer, W.D. (2003) Production of substances by *Medicago truncatula* that affect bacterial quorum sensing. *Mol. Plant Microbe Interact*. 16: 827–834.

Gerhart, J. & Kirschner, M. (1997) *Cells, Embryos, and Evolution: Toward a Cellular and Development Understanding of Phenotypic Variation and Evolutionary Adaptability.* Oxford, UK: Blackwell Sci. 642pp.

Glime, J. M. (2007) *Bryophyte Ecology*. Volume 1. Physiological Ecology. Ebook sponsored by Michigan Technological University and the International Association of Bryologists. [Online] Available from : http://www.bryoecol.mtu.edu/ [Accessed 20th July 2014].

Godfray, H.C.J., Beddington, J.R., Crute, R., Haddad, L., Laurence, D., Muir, J.F., Pretty, J., Robinson, S., Thomas, S.M. & Toulmin, C. (2010) Food Security: The Challenge of Feeding 9 Billion People. *Science.* 327 (5967): 812-818.

Gomi, K. & Makato, M. (2003) Gibberellin signalling pathway. *Current Opinion in Plant Biology*. 6 (5): 489-493.

González, J. & Venturi, V. (2013) A novel widespread interkingdom signaling circuit. *Trend in Plant Science*. 18 (3): 167-174.

Grosber, R.K. & Strathmann, R.R. (2007) The Evolution of Multicellularity: A Minor Major Transition? *Annu. Rev. Ecol. Evol. Syst.* 38: 621-654.

Hayashi, K., Kawalde, H., Notomi, M., Sakigi, Y., Mutsuo, A. & Nozaki, H. (2006) Identification and functional analysis of bifunctional ent-kaurene synthase from the moss *Physcomitrella patens*. *FEBS LETTERS.* 580: 6157-6181.

Hayashi, K-I., Horie, K., Hiwatashi, Y., Kawaide, H., Yamaguchi, S., Hanada, A., Nakashima, T., Nakajima, M., Mander, L.N., Yamane, H., Hasebe, M. & Nozaki, H. (2010) Endogenous Diterpenes Derived from *ent*-Kaurene, a Common Gibberellin Precursor, Regulate Protonema Differentiation of the Moss *Physcomitrella patens. Plant Physiol.* 153 (3): 1085-1097.

Herron, M.D., Hackett, J.D., Aylward, F.O. & Michod, R.E. (2009) Traiassic origin and early radiation of multicellular volvocine algae. *Proc. Natl. Acad. Sci. USA.* 106: 3254-3258.

Herron, M.D. & Michod, R.E. (2008) Evolution of complexity in the volvocine algae: Transitions in individuality through Darwin's eye. *Evolution.* 62: 436-451.

Hirano, K., Nakajima, M., Asano, K., Nishiyama, T., Sakakibara, H., Kojima, M., Katoh, E., Xiang, H., Tanahashi, T., Hasebe, M., Banks, J.A., Ashikari, M., Kitano, H., Ueguchi-Tanaka, M. & Matcuoka, M. (2007) The GID1-mediated gibberellin perception mechanism is conserved in the lycophyte *Selaginella moellendorfii* but not in the bryophyte *Physcomitrella patens*. *Plant Cell*. 19: 3058–3079.

***Hmelo*, *L*. & *Van Mooy*, B.** (2008) *Kinetic constraints* on *acylated homoserine* lactone –based sensing in *marine environments*. *Aquatic Microbial Ecology*. *54*:*127-133.*

Hodgetts, H. (2010). *Aphanorrhegma patens* (*Physcomitrella patens*), spreading earth-moss. In: Atherton, I., Bosanquet, S. & Lawley, M. *Mosses and Liverworts of Britain and Ireland: a Field Guide.* British Bryological Society. p. 567.

Hohe, A., Rensing, S.A., Mildner, M., Lang, D. & Reski, R. (2002) Day length and temperature strongly influence sexual reproduction and expression of a novel MADS-box gene in the moss *Physcomitrella patens*. *Plant Biol.* 4: 595-602.

Holdsworth, M.J., Bentsink, L. & Soppe, W.J.J. (2008) Molecular networks regulating Arabidopsis seed maturation, after-ripening, dormancy and germination. *New Phytologist.* 179: 33-54.

Hooley, R. (1994) Gibberellins: perception, transduction and responses. *Plant Molecular Biology*. 26: 1529-1555.

Jayaraman, A. & Wood, T.K. (2008) Bacterial Quorum Sensing: Signals, Circuits, and Implications for Biofilms and Disease. *Annual Review of Biomedical Engineering.* 10: 145-167.

Joseph, C. M. & Phillips, D. A. (2003) Metabolites from soil bacteria affect plant water relations. *Plant Physiol. Biochem*. 41: 189-192.

Kaiser, D. (2001) Building a multicellular organism. *Annu. Rev. Genet.* 35: 103-123.

Kammerer, W. & Cove, D.J. (1996) Genetic analysis of the effects of re-transformation of transgenic lines of the moss *Physcomitrella patens.* Mol. Gen. Genet. 250: 380-382.

Keller, L. & Surette, M.G. (2006) Communication in bacteria: an ecological and evolutionary perspective. *Nat. Rev. Microbiol.* 4: 249-258.

Khandelwal, A., Cho, S.H., Marella, H., Sakata, Y., Perroud, P.F., Pan, A. & Quatrano, R.S. (2010) Role of ABA and AB13 in desiccation tolerance. *Science.* 327: 546.

Koch, B., Liljefors, T., Persson, T., Nielsen, J. Kjelleberg, S. & Givskov, M. (2005) The LuxR receptor: the sites of interaction with quorum-sensing signals and inhibitors. *Microbiology*. 151 (11):3589-3602.

Koh, C., Sam, C., Yin, W., Tan, L., Krashnan, T., Chong, Y. & Chan, K. (2013) Plant Derived Natural Products as Sources of Anti-Quorum Sensing Compounds. *Sensors.* 13 (1): 6217-6229.

Koornneef, M. & van der Veen, J.H. (1980) Induction and Analysis of Gibberellin Sensitive Mutants in *Arabidopsis thaliana* (L.) Heynh. *Theor. Appl. Genet*. 58: 257-263.

Kucera, B., Cohn, M.A. & Leubner-Metzger, G. (2005) Plant hormone interactions during seed dormancy release and germination. *Seed Sci. Res.* 15: 281-307.

Lachmann, M., Blackstone, N.W., Haig, D., Kowald, A., Werren J.H. & Wolpert, L. (2003) *Group report: Cooperation and conflict in the evolution of genomes, cells, and multicellular organisms.* See Hammerstein 2003, pp 327-356.

Linkies, A. & Leubner-Metzger, G. (2012) Beyond gibberellins and abscisic acid: how ethylene and jasmonates control seed germination. *Plant Cell Rep.* 31: 253-270.

Liu, F., Bian, Z., Jia, Z., Zhao, Q. & Song, S. (2012) The GCR1 and GPA1 participate in promotion of Arabidopsis primary root elongation induced by *N*-acyl-homoserine lactones, the bacterial quorum-sensing signals. *Mol. Plant Microbe Interact.* 25: 677–683.

Loh, J., Pierson, E. A., Pierson, L. S., Stacey, G. & Chatterjee, A. (2002) Quorum sensing in plant-associated bacteria. *Curr. Opin. Plant Biol.* 5: 285-290.

Lürling, M. & Van Donk, E. (2000) Grazer-induced colony formation in *Scensdesmus*: Are these costs to being colonial? *Oikos*. 88: 11-118.

Lugtenberg, B. J. J., Dekker, L. & Bloemberg, G. V. (2001) Molecular determinants of rhizosphere colonization by *Pseudomonas*. *Annu. Rev. Phytopathol.* 39: 461-490.

Manefield. M., Rasmussen, T.B., Henzter, M., Andersen, J.B., Steinberg, P., Kjelleberg, S. & Givskov, M. (2002) Halogenated furanones inhibit quorum sensing through accelerated LuxR turnover. *Microbiology.* 148: 1119–1127.

Mathesius, U., Mulders, S., Gao, M., Teplitski, M., Caetano- Anolles, G., Rolfe, B.G., & Bauer, W.D. (2003) Extensive and specific responses of a eukaryote to bacterial quorum-sensing signals. *Proc. Natl. Acad. Sci. USA.* 100: 1444–1449.

Merchant, S.S., Prochnik, S.E., Vallon, O., Harris, E.H., Karpowicz, S.J., Witman, G.B., Terry, A., Salamov, A., Fritz-Laylin, L.K., Maréchal-Drouard, L., Marshall, W.F., Qu, L.H., Nelson, D.R., Sanderfoot, A.A., Spalding, M.H., Kapitonov, V.V., Ren, Q., Ferris, P., Lindquist, E., Shapiro, H., Lucas, S.M., Grimwood, J., Schmutz, J., Cardol, P., Cerutti, H., Chanfreau, G., Chen, C.L., Cognat, V., Croft, M.T., Dent, R., Dutcher, S., Fernández, E., Fukuzawa, H., González-Ballester, D., González-Halphen, D., Hallmann, A., Hanikenne, M., Hippler, M., Inwood, W., Jabbari, K., Kalanon, M., Kuras, R., Lefebvre, P.A., Lemaire, S.D., Lobanov, A.V., Lohr, M., Manuell, A., Meier, I., Mets, L., Mittag, M., Mittelmeier, T., Moroney, J.V., Moseley, J., Napoli, C., Nedelcu, A.M., Niyogi, K., Novoselov,

S.V., Paulsen, I.T., Pazour, G., Purton, S., Ral, J.P., Riaño-Pachón, D.M., Riekhof, W., Rymarquis, L., Schroda, M., Stern, D., Umen, J., Willows, R., Wilson, N., Zimmer, S.L., Allmer, J., Balk, J., Bisova, K., Chen, C.J., Elias, M., Gendler, K., Hauser, C., Lamb, M.R., Ledford, H., Long, J.C., Minagawa, J., Page, M.D., Pan, J., Pootakham, W., Roje, S., Rose, A., Stahlberg, E., Terauchi, A.M., Yang, P., Ball, S., Bowler, C., Dieckmann, C.L., Gladyshev, V.N., Green, P., Jorgensen, R., Mayfield, S., Mueller-Roeber, B., Rajamani, S., Sayre, R.T., Brokstein, P., Dubchak, I., Goodstein, D., Hornick, L., Huang, Y.W., Jhaveri, J., Luo, Y., Martínez, D., Ngau, W.C., Otillar, B., Poliakov, A., Porter, A., Szajkowski, L., Werner, G., Zhou, K., Grigoriev, I.V., Rokhsar, D.S. & Grossman, A.R. (2007) The Chlamydomoas genome reveals the evolution of key animal and plant functions. *Science.* 318 (5848): 245-250.

Miller, M.B. & Bassler, B.L. (2001) Quorum sensing in bacteria. *Annu. Rev. Microbiol.* 55: 165-199.

Olszewski, N., Sun, T.P. & Gubler, F. (2002) Gibberellin signaling: biosynthesis, catabolism, and response pathways. *Plant Cell (Suppl).* 14: S61–S80.

Ortíz-Castro, R., Martínez-Trujillo, M., & López-Bucio, J. (2008) *N*-acyl-L-homoserine lactones: a class of bacterial quorum-sensing signals alter post-embryonic root development in *Arabidopsis thaliana*. *Plant Cell Environ.* 31: 1497–1509.

Palmer, A.G., Seneschal, A.C., Mukherjee, A., Ané, J-M. & Blackwell, H.E. (2014) Plant Responses to Bacterial *N*-Acyl $_{L}$-Homoserine are Dependent on Enzymatic

Degradation to $_{L}$-Homoserine. *ACS Chem. Biol.* [Online] DOI: 10.1021/cb500191a. Available from: http://pubs.acs.org/doi/pdf/10.1021/cb500191a [Accessed 17th July 2014].

Pierson, E. A., Wood, D. W., Cannon, J. A., Blachere, F. M. & Pierson, L. S., III. (1998) Interpopulation signaling via *N*-acylhomoserine lac- tones among bacteria in the wheat rhizosphere. *Mol. Plant-Microbe Interact.* 11: 1078-1084.

Pierson, L. S., III, Wood, D. W. & von Bodman, S. B. (1999) Quorum sensing in plant-associated bacteria. Pages 101-116 in: *Cell-Cell Signaling in Bacteria*. G. M. Dunny & S. C. Winans, eds. American Society for Microbiology Press, Herndon, VA, U.S.A.

Prigge, M. J. & Bezanilla, M. (2010) Evolutionary crossroads in developmental biology: *Physcomitrella patens. Development*. 137: 3535-3543.

Prochnik, S.E., Umen, J., Nedelcu, A.M., Hallmann, A., Miller, A.M., Nishii, I., Ferris, P., Kuo, A., Mitros, T., Fritz-Laylin, L.K., Hellsten, U., Chapman, J., Simakov, O., Rensing, S.A., Terry, A., Pangilinan, J., Kapitonov, V., Jurka, J., Salamov, A., Shapiro, H., Schmutz, J., Grimwood, J., Lindquist, E., Lucas, S., Grigoriev, I.V., Schmitt, R., Kirk, D. & Rokhsar, D.S. (2010) Genomic Analysis of Organismal Complexity in the Multicellular Green Alga *Volvox carteri. Science.* 329 (5988): 223-226.

Rad, U., Klein, I., Dobrev, P., Kottova, J., Zazimalova, E., Fekete, A., Hartmann, A., Schmitt-Kopplin, P. & Durner, J. (2008) Response of *Arabidopsis thaliana* to N -

hexanoyl- DL -homoserine- lactone, a bacterial quorum sensing molecule produced in the rhizosphere. *Planta*. 229 (1): 73-85.

Ramey, B. E., Koutsoudis, M., von Bodman, S. B. & Fuqua, C. (2004) Biofilm formation in plant-microbe associations. *Curr. Opin. Microbiol.* 6: 602-9.

Ratcliff, W.C., Denison, R.F., Borello, M. & Travisano, M. (2011) Experimental evolution of multicellularity. *PNAS.* 109 (5): 1595-1600.

Rensing, S., Lang. D., Zimmer, A.D., Terry, A., Salamov, A., Shapiro, H., Nishiyama, T., Perroud, P.F., Lindquist, E.A., Kamisugi, Y., Tanahashi, T., Sakakibara, K., Fujita, T., Oishi, K., Shin-I, T., Kuroki, Y., Toyoda, A., Suzuki, Y., Hashimoto, S., Yamaguchi, K., Sugano, S., Kohara, Y., Fujiyama, A., Anterola, A., Aoki, S., Ashton, N., Barbazuk, W.B., Barker, E., Bennetzen, J.L., Blankenship, R., Cho, S.H., Dutcher, S.K., Estelle, M., Fawcett, J.A., Gundlach, H., Hanada, K., Heyl, A., Hicks, K.A., Hughes, J., Lohr, M., Mayer, K., Melkozernov, A., Murata, T., Nelson, D.R., Pils, B., Prigge, M., Reiss, B., Renner, T., Rombauts, S., Rushton, P.J., Sanderfoot, A., Schween, G., Shiu, S.H., Stueber, K., Theodoulou, F.L., Tu, H., Van de Peer, Y., Verrier, P.J., Waters, E., Wood, A., Yang, L., Cove, D., Cuming, A.C., Hasebe, M., Lucas, S., Mishler, B.D., Reski, R., Grigoriev, I.V., Quatrano, R.S. & Boore, J.L. (2008) The Physcomitrella genome reveals evolutionary insights into the conquest of land by plants. *Science.* 319 (5859): 64-69.

Rensing, S.A., Land, D. & Zimmer, A.D. (2009) Comparative Genomics. In: *Annual Plant Reviews.* Volume 36: The Moss (eds. Knight, C.D., Perroud, P.-F. & Cove, D.J.), Wiley-Blackwell, Oxford, UK.

Reski, R. (1998) Physcomitrella and Arabidopsis: the David and Goliath of reverse genetics. *Trends in Plant Science*. 3 (6): 209-210.

Richter, D.J. & King, N. (2013) The genomic and cellular foundations of animal origins. *Annual Review of Genetics.* 47: 509-537.

Sabovljević, M., Vujičić, M. & Sabovljević, A. (2014) Plant growth regulators in bryophytes. *Botanica SERBIA. 38* (1): 99-107.

Savka, M. A., Dessaux, Y., Oger, P. & Rossbach, S. (2002) Engineering bacterial competitiveness and persistence in the phytosphere. *Mol. Plant-Microbe Interact.*15: 866-874.

Schefer, D.G. & Zryd, J.P. (1997) Efficient gene targeting in the moss *Physcomitrella patens. Plant Journal.* 11: 1195-1206.

Schenk, S.T., Stein, E., Kogel, K.H., & Schikora, A. (2012) Arabidopsis growth and defense are modulated by bacterial quorum sensing molecules*. Plant Signal. Behav.* 7: 178–181.

Schenk, S.T., Hernández-Reyes, C., Samans, B., Stein, E., Neumann, C., Schikora, M., Reichelt, M., Mithöfer, A., Becker, A., Kogel, K-H. & Schikora, A. (2014) *N*-acyl-Homosering Lactone Primes Plants for Cell Wall Reinforcement and Induces Resistance to Bacterial Pathogens via the Salicyclic Acid/Oxylipin Pathway.

The Plant Cell. [Online] Available from: http://dx.doi.org/10.1105/tpc.114.126763 [Accessed 17th July 2014].

Schikora, A., Schenk, S.T., Stein, E., Molitor, A., Zuccaro, A., & Kogel, K.H. (2011) *N*-acyl-homoserine lactone confers resistance toward biotrophic and hemibiotrophic pathogens via altered activation of AtMPK6. *Plant Physiol.* 157: 1407–1418.

Schuhegger, R., Ihring, A., Gantner, S., Bahnweg, G., Knappe, C., Vogg, G., Hutzler, P., Schmid, M., Van Breusegem, F., Eberl, L., Hartmann, A., & Langebartels, C. (2006) Induction of systemic resistance in tomato by N-acyl-L-homoserine lactone-producing rhizosphere bacteria. *Plant Cell Environ.* 29: 909−918.

Santella, R.M. (2006) Approaches to DNA/RNA Extraction and Whole Genome Amplification. *Cancer Epidemiol Biomarkers Prev.* 15: 1585.

Scott, R.A., Weil, J., Le, P.T., Williams, P., Fray, R.G., von Bodman, S.B. & Savka, M.A. (2005) Long- and Short- Chain Plant-Produced Bacterial *N*-Acyl-Homoserine Lactones Become Components of Phyllosphere, Rhizosphere and Soil. *MPMI.* 19(3): 227-239.

Shapiro, J.A. (1998) Thinking about bacterial populations as multicellular organisms. *Annu. Rev. Microbio.* 52: 81-104.

Steber, C.M. & McCourt, P. (2001) A Role for Brassinosteroids in Germination in Arabidopsis. *Plant Physiology.* 125 (2): 763-769.

Steidle, A., Sigl, K., Schuhegger, R., Ihring, A., Schmid, M., Gantner, S., Stoffels, M., Riedel, K., Givskov, M., Hartmann, A., Langebartels, C., & Eberl, L. (2001) Visualization of N-acylhomoserine lactone- mediated cell-cell communication between bacteria colonizing the tomato rhizosphere. *Appl. Environ. Microbiol.* 67: 5761–5770.

Sun, T.P. & Kamiya, Y. (1994) The Arabidopsis *GA1* locus encodes the cyclase *ent*-kaurene synthetase A of gibberellin biosynthesis. *Plant Cell.* 6: 1509–1518.

Takezawa, D. & Komatsu, K. (2011) ABA in bryophytes: how a universal growth regulator in life became a plant hormone? *J Plant Res.* 124: 437-453.

Talon, M., Koornneef, M. & Zeevaart, J.A.D. (1990) Endogenous gibberellins in *Arabidopsis thaliana* and possible steps blocked in the biosynthetic pathways of the semidwarf *ga4* and *ga5* mutants. *Proc Natl Acad Sci USA.* 87: 7983–7987.

Van den Hoek, E., Mann, D.G., Jahns, H.M. (1995) *Algae: An Introduction to Phycology.* Cambridge, UK: Cambridge Univ. Press. 623pp.

Vandenbussche, F., Fierro, A.C., Wiedemann, G., Reski, R. & Van Der Straeten, D. (2007) Evolutionary Conservation of Plant Gibberellin Signalling Pathway Components. *BMC Plant Biology.* 7: 65. [Online] Available from: www.biomedcentral.com/content/pdf/1471-2229-7-65.pdf [Accessed 18th July 2014].

Voegele, A., Linkies, A., Müller, K. & Leubner-Metzger, G. (2011) Members of the gibberellin receptor gene family *GID_1 (GIBBERELLIN INSENSITIVE $DWARF_1$)* play

distinct roles during *Lepidium sativum* and *Arabidopsis thaliana* seed germination. *Journal of Experimental Botany.* 62 (14): 5131-5147.

von Bodman, S. B., Bauer, W. D. & Coplin D. L. (2003) Quorum sensing in plant-pathogenic bacteria. *Annu. Rev. Phytopathol.* 41: 455-482.

von Rad, U., Klein, I., Dobrev, P.I., Kottova, J., Zazimalova, E., Fekete, A., Hartmann, A., Schmitt-Kopplin, P., & Durner, J. (2008) Response of *Arabidopsis thaliana* to N-hexanoyl-DL-homoserine- lactone, a bacterial quorum sensing molecule produced in the rhizosphere. *Planta*. 229: 73–85.

Wang, Y. & Deng, D. (2014) Molecular basis and evolutionary pattern of GA-GID1-DELLA regulatory mode. *Mol Genet Genomics*. 289: 1-9.

Weinberg, E.S. & Voeller, B.R. (1969) Induction of fern spore germination. *PNAS.* 64 (3): 835-842.

Whitehead, N. A., Barnard A. M. I., Slater, H., Simpson N. J. L. & Salmond, G. P. C. (2001) Quorum sensing in gram-negative bacteria. *FEMS (Fed. Eur. Microbiol. Soc.) Microbiol. Rev.* 25: 365-404.

Whitehead, N. A., Byers, J. T., Commander, P., Corbett, M. J., Coulthurst, S. J., Everson, L., Harris, A. K. P., Pemberton. C. L., Simpson, N. J. L., Slater, H., Smith, D. S., Welch, M., Williamson, N. & Salmond, G. P. C. (2002) The regulation of virulence in phytopathogenic *Erwinia* species: Quorum sensing, antibiotics and ecological considerations. *Antonie Leeuwenhoek.* 81:223-231.

Winans, S. C., Zhu, J. & More, M. I. (1999) Cell density-dependent gene expression by *Agrobacterium tumefaciens* during colonization of crown gall tumors. Pages117-128 in: *Cell-Cell Signaling in Bacteria.* G. M. Dunny & S. C. Winans, eds. ASM Press.

Yamauchi, T., Oyama, N., Yamane, H., Murofushi, N., Schraudolf, H., Pour, M., Furber, M. & Mander, L.N. (1996) Identification of antheridiogens in *Lygodium circinnatum* and *Lygodium flexuosum. Plant Physiol*. 111: 741–745.

Yamaguchi, S. (2008) Gibberellin metabolism and its regulation. *Annu Rev Plant Biol*. 59: 225–251.

Yamane, H., Satoh, Y., Nohara, K., Nakayama, M., Murofushi, N., Takahashi, N., Takeno, K., Furuya, M., Furber, M. & Mander, L.N. (1988) The methyl ester of a new gibberellin, GA73: the principal antheridiogen in *Lygodium japonicum. Tetrahedron Lett.* 29: 3959–3962.

Yao, J., Chang, C., Salmi, M.L., Hung, Y.S., Loraine, A. & Roux, S. (2008) Genome-scale cluster analysis of replicated microarrays using shrinkage correlation coefficient. *BMC Bioinformatics.* [Online] Available from: http://www.ncbi.nlm.nih.gov/pmc/articles/PMC2459189/pdf/1471-2105-9-288.pdf [Accessed 19th July 2014].

Yasmura, Y., Crumpton-Taylor, M., Fuentes, S. & Harberd, N.P. (2007) Step-by-step acquisition of the gibberellin-DELLA growth regulatory mechanism during land-plant evolution. *Current Biology.* 17: 1225-1230.

Yates, E.A., Philipp, B., Buckley, C., Atkinson, S., Chhabra, S.R., Sockett, R.E., Goldner, M., Dessaux, Y., Camara, M., Smith, H. & Williams, P. (2002) *N*-acyl homoserine lactones undergo electrolysis in a pH, temperature-, and acyl chain length-dependent manner during growth in *Yersinia pseudotuberculosis* and *Pseudomonas aeruginosa*. *Infection and Immunity.* 70: 5635-5646.

You, Y-S., Marella, H., Zentalla, R., Zhou, Y., Ulmasov, T., Ho, T-H.D. & Quatrano, R.S. (2006) Use of Bacterial Quorum-Sensing Components to Regulate Gene Expression in Plants. *Plant Physiology*. 140: 1205-1212.

Zheng, D. H., Zhang, S., Carle, S., Hao, G., Holden, M. R. & Burr, T. J. (2003) A *luxR* homolog, *aviR,* in *Agrobacterium vitis* is associated with induction of necrosis on grape and a hypersensitive response on to- bacco. Mol. *Plant-Microbe Interact*. 16: 650-658.

Appendices

Appendix 1.

P.PATENS SPORE GERMINATION ASSAYS.

Analysing the effects of *N*-acyl-homoserine lactones of different substitution states at C3 and different chain lengths on *P.patens* spore germination.

10nM Synthetic AHL Panel:

A

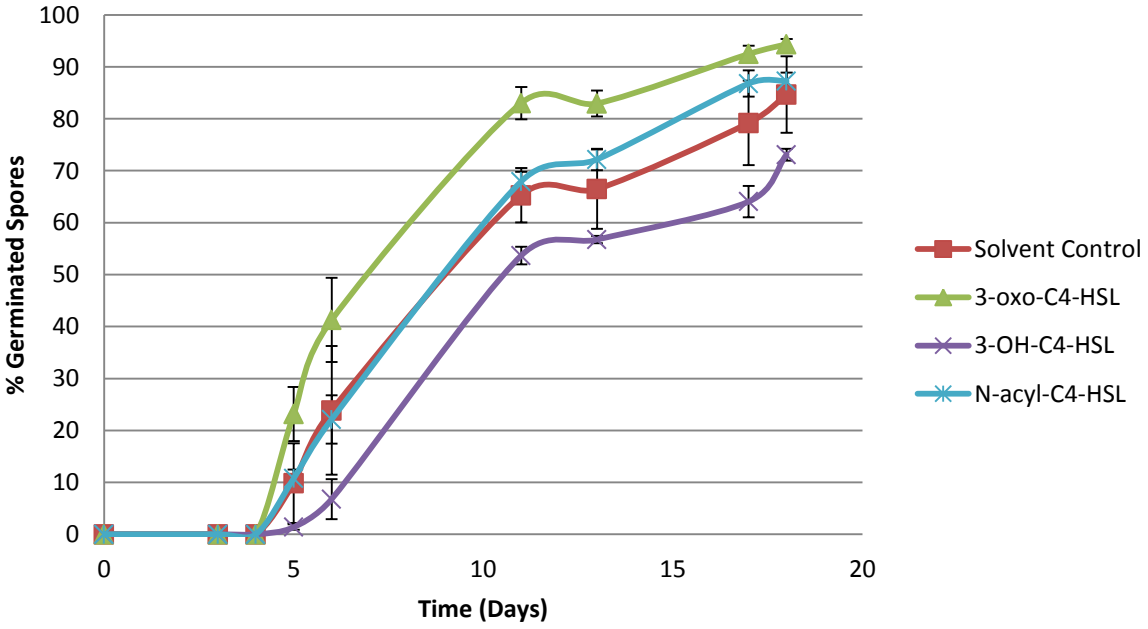

B

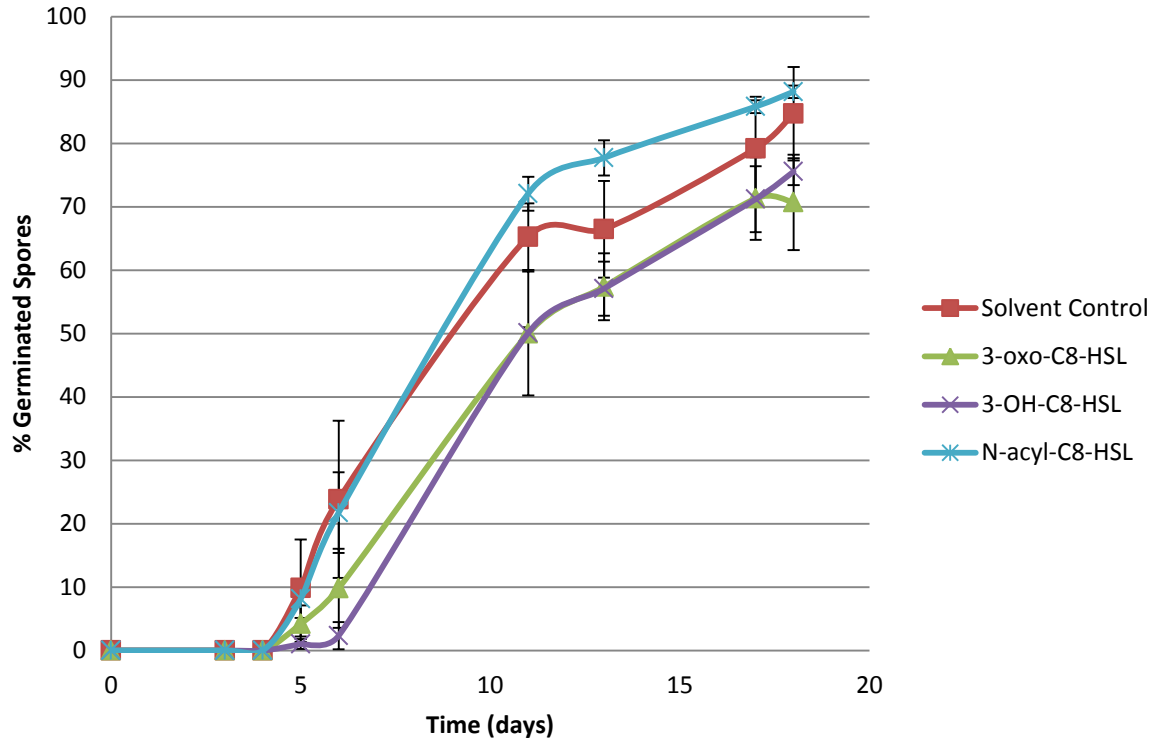
100
90
80
70
60
50
40
30
20
10
0
% Germinated Spores
0
5
10
15
20
Time (days)
Solvent Control
3-oxo-C8-HSL
3-OH-C8-HSL
N-acyl-C8-HSL

C

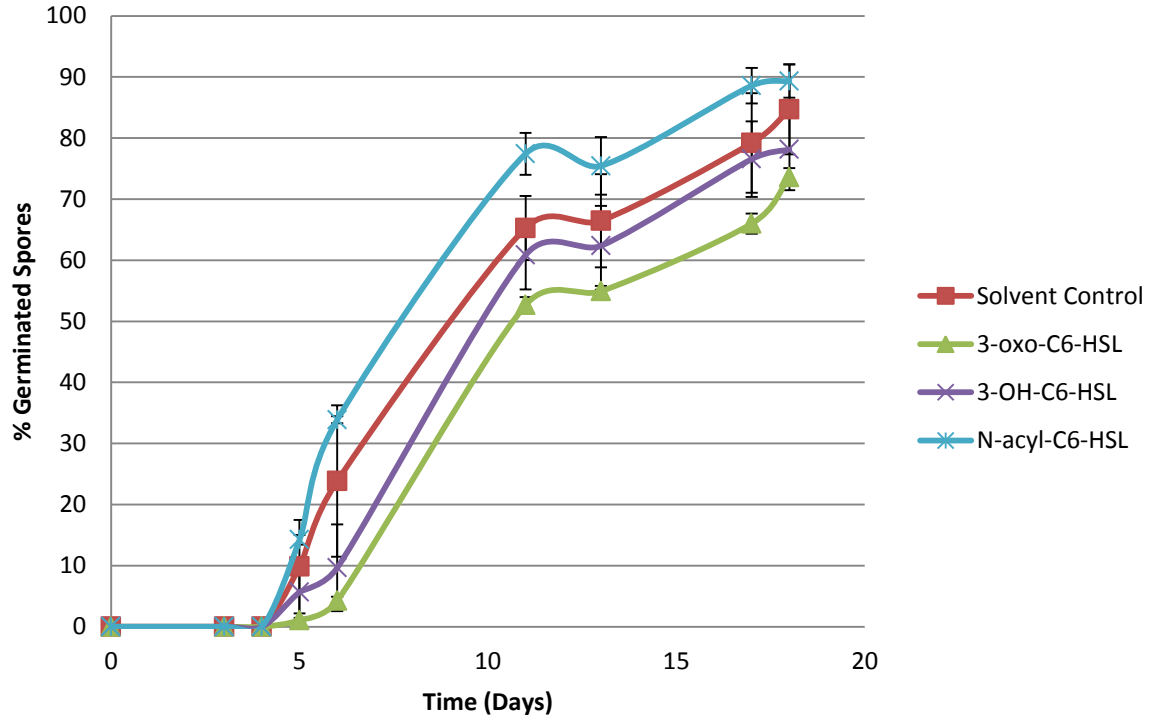
100
90
80
70
60
50
40
30
20
10
0
% Germinated Spores
0
5
10
15
20
Time (Days)
Solvent Control
3-oxo-C6-HSL
3-OH-C6-HSL
N-acyl-C6-HSL

D

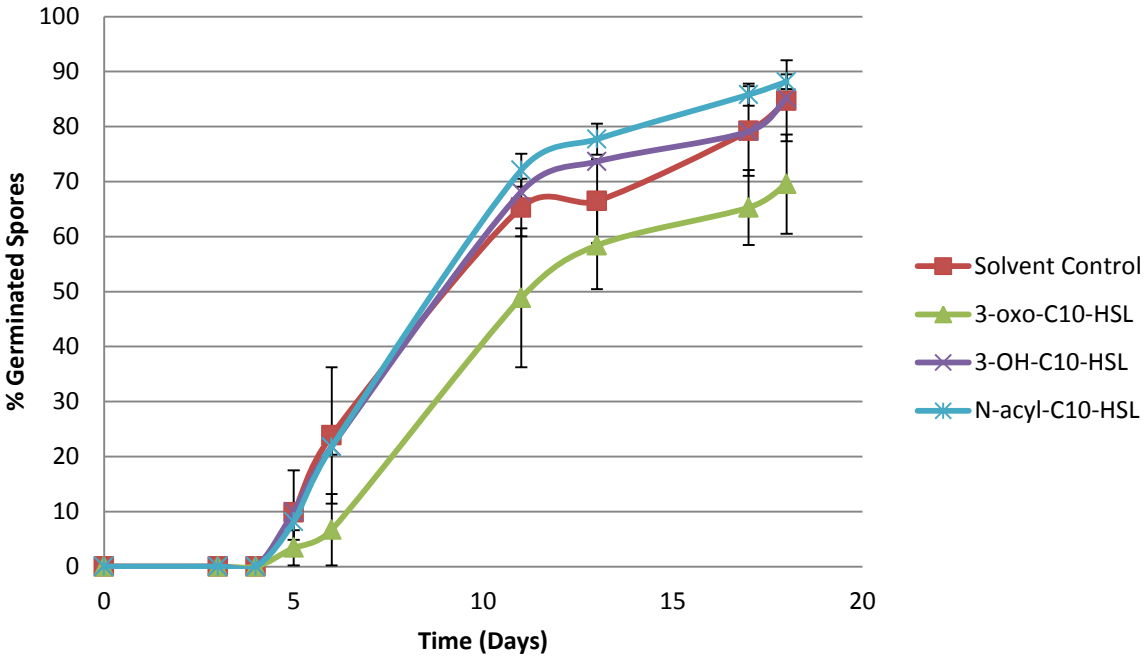

E

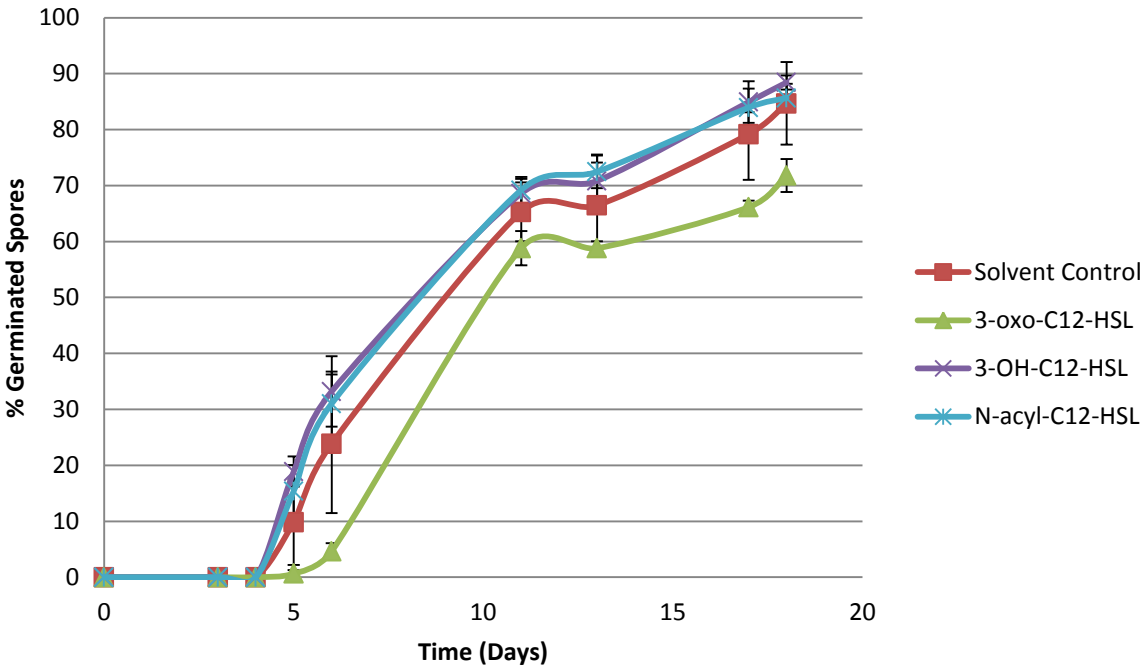

Figure A1.1. Spore germination assay indicating the germination rate of 15 day old (post-harvest) wild-type *P.patens* spores when grown on BCD media supplemented with 10nM synthetic AHLs of varying substitution states and chain lengths. A) C4. B) C6. C) C8. D) C10. E) C12. Error bars = ± SEM.